University of Bath

University of Bath

PHD

Analysis of post-harvest physiological deterioration in cassava transformed with anti-oxidant genes

Mahmod, Nor

Award date:
2015

Awarding institution:
University of Bath

[Link to publication](#)

Analysis of Post-Harvest Physiological Deterioration in Cassava Transformed with Anti-oxidant Genes

Nor Hasima Mahmod

A thesis submitted for the degree of Doctor of Philosophy

University of Bath

Department of Biology and Biochemistry

February 2015

Signed:

Nor H. Mahmod

ACKNOWLEDGEMENTS

This thesis is dedicated to my dad.

ABBREVIATIONS

APX	ascorbate peroxidase
ATPase	adenosine triphosphatase
BAP	6-benzylamino purine
BSA	bovine serum albumin
CAT	catalase
cDNA	complementary DNA
CIAT	Centro Internacional de Agricultura Tropical
CTAB	cetyltrimethyl ammonium bromide
DAB	diaminobenzidine
DAF	days after fertilisation
DAH	days after harvest
DAP	days after planting
DIG	digoxigenin
DM	dry matter
DMSO	dimethyl sulfoxide
DNA	deoxyribonucleic acid
dNTP	deoxynucleotide triphosphate
DW	dry weight
EDTA	ethylene diamine tetraacetic acid
ETH	Swiss Federal Institute of Technology
FAO	Food and Agriculture Organisation
FAOSTAT	FAO statistical database
FEC	friable embryogenic callus
FW	fresh weight
GAR	galacturonic acid reductase
GCS	gamma glutamyl cysteine synthetase
H_2O_2	hydrogen peroxide
Ha	hectare
HEPES	N-2-hydroxyethylpiperazine ethanesulfonic acid
HNL	hydroxynitrile lyase
MES	2-(N-morpholino) ethanesulfonic acid
MV	methyl viologen
NBT	nitro blue tetrazolium
PAL	phenylalanine ammonia-lyase
PCD	programmed cell death
POX	peroxidase
PPD	post-harvest physiological deterioration
PVC	polyvinyl chloride
PVP	polyvinyl pyrrolidone
qPCR	quantitative real-time polymerase chain reaction
RNA	ribonucleic acid
RNAi	ribonucleic acid interference
ROS	reactive oxygen species
SDS	sodium dodecyl sulfate
SOD	superoxide dismutase
SSC	saline sodium citrate
SYBR	Synergy Brands
TAE	tris-acetate EDTA
TCA	trichloroacetic acid
U	unit
USDA	United States Department of Agriculture
UTR	untranslated region
WT	wild-type

ABSTRACT

Cassava is the sixth most important food crop in the world, where it is the staple food for over 500 million people. Its ability to grow on marginal soil conditions and under minimal care makes cassava a vital 'food security' crop for resource-poor farmers. However, cassava production is constrained by post-harvest physiological deterioration (PPD), a storage root disorder characterised by vascular streaking and discolouration of parenchymal tissue. PPD, which renders the roots unpalatable and unmarketable, leads to significant yield loss in global cassava production.

The cause of PPD is not yet fully understood but accumulation of reactive oxygen species (ROS) has been observed in the harvested storage root. It is hypothesised that the ROS, which is triggered by wounding during harvesting, is not modulated due to deficiencies in the ROS-detoxifying system in cassava roots, causing oxidative stress to occur, which then leads to symptom formation. To investigate this, transgenic cassavas containing five separate anti-oxidant genes were studied– superoxide dismutase (SOD), ascorbate peroxidase (APX), catalase (CAT), gamma glutamyl cysteine synthetase (GCS) and galacturonic acid reductase (GAR). Each gene was controlled by a root-specific promoter, Patatin, which is also wound-inducible.

A high percentage of single-insert lines were recovered, which retained the outward phenotype of WT cassava. While this enabled comparative PPD assessment between the transgenics and the WT, this was complicated by the challenge of reproducibly measuring PPD in greenhouse-grown plants. Therefore, a reliable assay to measure PPD in greenhouse-grown samples was developed and a robust method to assess the symptoms with high confidence was devised. Scopoletin, a fluorescent compound was initially tested as an alternative PPD marker but was dismissed as it did not correlate well with PPD symptom development.

Overexpression of anti-oxidant genes was observed in selected lines – between 4- to 5-fold increase of relative transcriptional level was achieved in fresh roots and up to 20-fold was achieved in transgenic roots that had been harvested after 24 hours. However, as the increase did not alter the activity of anti-oxidant enzymes, the transgenic cassava plants generally exhibited similar levels of tolerance to oxidative stress and PPD as the WT plants. This result may be partly due to the difficulty of producing sufficient numbers of replicates for analysis, the behaviour of the Patatin promoter in cassava, and the complexity of anti-oxidant responses. Hence, while this thesis has clarified aspects of the PPD response in cassava and the role of anti-oxidant genes in it, it has not been able to identify definitive means to control the problem through altering the expression of individual genes.

CONTENTS

CHAPTER 1

Introduction

1.1   Cassava– History and distribution

Cassava (*Manihot esculenta* Crantz) is a member of *Manihot* genus, which consists of 98 different species. The other names for cassava include tapioca (Asia), mandioca (Brazil), manioc (French-speaking) and yuca (Spanish-speaking). This plant belongs to the wide-ranging Euphorbiacea family, sharing it with other crops like castor bean and rubber plant. Archaeological evidence suggest that cassava was domesticated between 2000-4000 BC (Fauquet and Fargette, 1990) in South American region. The modern cassava that exists today is thought to be originated from its wild ancestors *M. esculenta* subsp. Flabellifolia and *M. esculenta* subsp. Peruviana (Allem, 1999, Roa et al., 2000) but the exact location of its domestication was a topic of dispute. A number of places including Mexico and Peru were suggested but analyses based on molecular markers such as SNPs (single nucleotide polymorphisms) and SSR (simple sequence repeat) concluded that cassava was likely to have been domesticated in the southern Amazon basin in Brazil (Olsen, 2004, Leotard et al., 2009).

Expansion of cassava began in 16th century when the Portuguese sailors brought cassava to the West Africa through the Congo basin. There it was accepted as a valuable subsistence crop, but cassava only spread throughout Africa two centuries later after it was separately introduced in the east coast of Africa. Cassava was transported to India in the 17th century, marking its establishment in Asia. However, its dissemination to the rest of the continent was not clear because cassava was already found in the Philippines and Indonesia by that time, to which it had possibly been brought by the Mexicans and the Portuguese, respectively (Cock, 1982).

Cassava distribution is restricted to the tropics due to its adaptation to warm climate. Although it can tolerate up to 38°C, growth is favoured under an annual mean temperature of 25-29°C. Temperature of 10°C and below sufficiently inhibits cassava growth, which explains why it is not found in the temperate zones. It also favours lowlands but can occur at 1500 m above sea level. The approximate geographical limitations for naturally occurring cassava are 30°N and 30°S, but cultivation is normally located in between 20°N and 20°S (Cock, 1985).

1.2   Morphology and growth of cassava plants

Cassava is a diploid plant with chromosome number n=36. It has diverse morphology between cultivars which indicates the occurrence of high interspecific hybridisation. In general, cassava can grow either as a shrub or a small tree with stem height between 2-4 meters (Figure 1.1). The stem grows either singly or by forming sympodial branches. Primary branching occurs di-, tri- or tetrachotomously while secondary branching is most likely induced by flowering (Cock et al., 1979). Surrounding the stem or branch are palminate-shaped leaves consisting of uneven numbers of lobes. The leaves are connected to the stem by petioles which also vary from dark purple to light green.

Figure 1.1 Cassava plant morphology (a) One year old cassava plants grown in a trial farm in Uganda (b) A close-up of cassava leaf (b) Typical healthy cassava storage roots.

As the cassava plant matures it develops starch-filled storage roots. Depending on cultivars and agricultural practices, one cassava plant can produce 5-10 vertical roots weighing up to 3 kg FW per root. Generally the roots are cylindrical with lengths up to 1 meter and diameter reaching 10 cm (Jansson et al., 2009).

1 = Periderm
2 = Sclerenchyma
3 = Cortical parenchyma
4 = Phloem
5 = Cambium
6 = Storage parenchyma
7 = Xylem vessel
8 = Fibers
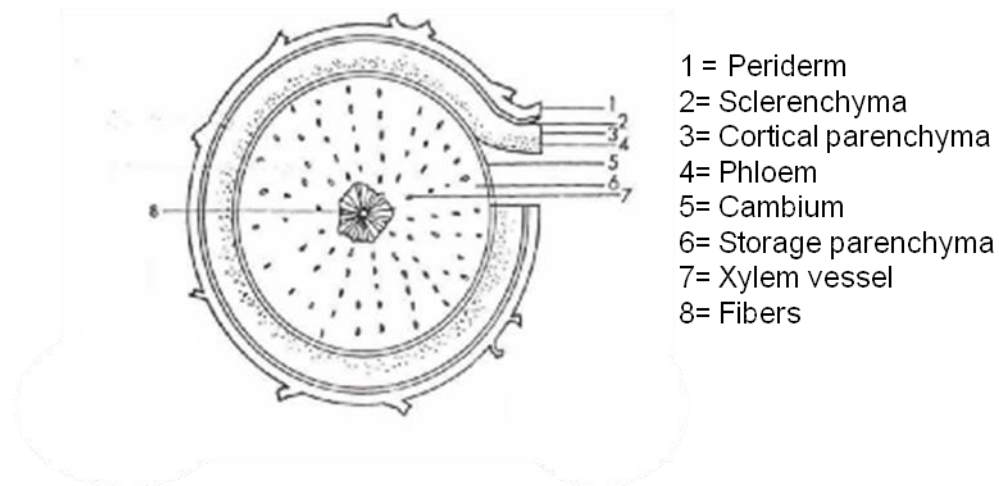
Figure 1.2 Diagram of cassava storage root labelled according to its section.

Anatomically, the storage root is not a true tuber but either taproot or adventitious root thickened with starch which functions as carbohydrate reserve (Lebot, 2009). Therefore, unlike yam or potato, it lacks propagative function. The root largely consists of xylem-dispersed storage parenchyma which is the edible part of the root (Figure 1.2). The colour of the parenchyma tissue, which varies from white, light yellow and light pink, is an important morphological descriptor. The storage parenchyma is protected by a peel layer consisting of cortical parenchyma, sclerenchyma and periderm. The centre of the root is filled with tough xylem vessels which often are discarded prior to processing. Some cultivars have cortical parenchyma layer that can be easily removed so peeling can be done by hand.

Cassava is grown primarily for the storage root. It is propagated using stem cuttings (or stakes) rather than by seeds. The stakes, which is normally obtained from the preceding harvest are cut to 25–30 cm long and buried in the ground vertically to induce sprouting. Under optimum growth conditions emergence takes place about 14 days after planting (DAP) while conversion of fibrous to storage roots occurs from 60-90 DAP. This is followed by dry matter accumulation which occurs at the highest rate between 180 and 300 DAP promoting thickening of storage roots (Alves, 2002). Within this time frame cassava is best harvested. Although mechanisation has been introduced, traditional harvesting is still practiced which involve loosening the soil with hoe and manually pulling off the roots from the ground.

1.3 Cassava as crop

The cassava root is rich in carbohydrate, of which starch is a major constituent. The carbohydrate content in cassava is approximately twice that of other staples, with 38 g per 100 g FW edible portion against 17 and 23 g in potato and rice respectively (Source: USDA). Today, more than 500 million people in the tropics depend on cassava as a source of calorie intake making it the fifth most important crop in the world. Its production is low compared to other food crops, but has been steadily increased in the past 20 years (Figure 1.3). In 2012, the cassava total world production was 269 metric tonnes, an increase of approximately 25% from 2006. Currently, the leading producers of cassava are African countries, contributing 55% of the total production, of which 35% is produced in Nigeria. The other important cassava producers are Asia (33%) and South America (10%) (Source: FAOSTAT).
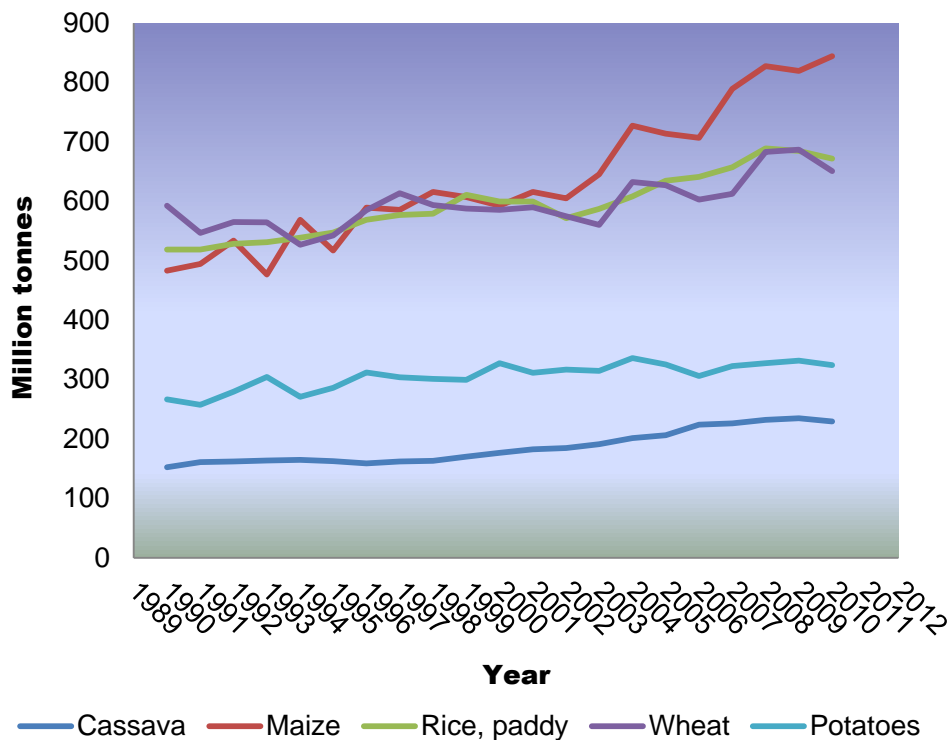
Figure 1.3 Trends in global production of the world's important food crops. Graph constructed based on data collected from FAOSTAT.

For centuries, cassava played an important role in ensuring food security in Africa. It can withstand a long periods of drought and grow on nutrient-deficient soil that may no longer suitable for other crops. Fertilisation is required but not necessary if grown on a freshly cleared forest soil (Jorge, 2008). Generally, after the formation of storage roots, cassava is relatively strong and can survive with minimal husbandry. Interestingly, cassava can be kept unharvested for up to several years making it a suitable famine reserve crop. However, prolonged growth leads to lignifications that turn the roots tough and woody. The hardiness features of cassava are attractive to the third world countries where modern agriculture is too expensive to practice. Generally, yield depends on cultivars, soil and agricultural practice. Between 5 to 20 tonnes/ha is commonly achieved under poor cultivation, while 60 tonnes/ha is achievable under the best cultivation methods (Zhang et al., 2003a).

Cassava, particularly in the processed form has an important role in the world trade with Thailand as the leading exporter. Cassava-based animal feed in the form of dried chips and pellets are exported to European countries while flour and starch are exported to Japan, Taiwan and China. Fresh cassava trade remains in Africa but it is currently expanding to developed countries due to migration of cassava consumers (Rees, 2012).

Recently, cassava is being promoted for bioethanol production due its high starch content, especially in China. Cassava conversion rate to bioethanol (L/tonne) is low when compared to other crops like maize, wheat and rice but it has the highest annual bioethanol yield (L/ha/year), mainly because more yield is obtained per cultivation area (Wang, 2002). Cassava bioethanol yield is comparable to a high-sugar crop like sugarcane yet more economical as it requires 6.6 tonne cassava storage root but 13.5 tonne sugarcane to produce 1 tonne of bioethanol (Jansson et al., 2009). The potential benefits of cassava as the new bioethanol crop are not only economic, but also environmental as high-quality arable land is not essential for its production, this quality land can then be reserved for high-quality food crops.

1.4 Cassava as food

Although the storage root is an excellent caloric source, its consumption is associated with two major problems; malnutrition and cyanide toxicity. Cassava is deficient in protein, vitamins and minerals. The typical composition is presented in Table 1.1. Other than that, it contains anti-nutrients such as phytic acid that bind to minerals reducing their absorption (Marfo et al., 1990).

Table 1.1 The average composition of cassava roots and leaf in g/100 g dry matter (DM). The root and leaf composition is adapted from Rees et al. (2012) and Wobeto et al. (2006). Asterisk indicates composition in mg/kg DM.

Composition	Whole roots	Leaf
Carbohydrate	89	15.9
Lipid	1.0	19.4
Protein	2.5	35.90
Fibre	4.5	23.63
Calcium	0.125	0.98
Zinc	0.0034	52.4*
Manganese	0.0038	157.97*
Phosphorus	0.1	0.33
Iron	0.0022	225.60*
Ascorbate	0.39	0.14**

Consumption of cassava is strongly associated with high incidences of vision impairment and weakened immune system, especially in children. To address this, tremendous effort is being taken to fortify the cassava roots with precursor of vitamin A and other micronutrients (Njoku et al., 2011). In many African countries, cassava leaf is consumed as a side dish to fulfil the dietary requirement. The leaf is not only an excellent protein substitute but also is high in minerals like zinc, iron, manganese, and calcium.

Apart from the seeds, all cassava plant organs contain cyanogens. Cyanogens can exist as cyanogenic glycosides (linamarin), cyanohydrins and free cyanide. Based on the content of cyanogens deposited in the storage roots, cassava is divided into 'sweet' and 'bitter' cultivars. Those contain between 100-500 mg/kg fresh weight (FW) cyanogens are considered as bitter cassava while those contain less 100 mg/kg FW cyanogens are considered as sweet cassava. Sweet cassava, as a crop, is more common in its place of origin (South America) while the bitter cassava became more adaptable in Africa where predators are more prevalent. The concentration of cyanogens in raw cassava roots is lethal to most predators and toxic to humans.

According to the Food and Agriculture Organization (FAO) cyanogens above 10 mg/kg DW is not safe for human consumption, thus processing to remove the cyanide prior to consumption is a must.

For generations the cyanide released from cyanogens has been removed through various methods including chopping, vigorous washing, soaking, pounding, boiling, drying and fermenting or combination of these methods. For example 'fufu' which is a common staple in West Africa is prepared by cutting cassava root into small pieces before soaking in water. The root is then dried and pounded into a dough-like consistency and it is boiled prior to consumption. Fufu prepared from bitter cassava may require additional treatment including 3-5 days fermentation to facilitate removal of cyanide. Another cassava-based dish called 'garri' is granular flour made from gelatinised fresh cassava. This dish is most popular in Ghana, Sierra Leon and Nigeria. A similar product to garri called 'farinha' is consumed in South America particularly in Brazil. To make garri, cassava root is grated and fermented in a jute sack. After a few days the sack is pressed to remove excess fluid before the resultant product is toasted to promote gelatinisation.

Each step employed in the preparation of 'edible' cassava product serves to remove considerable amounts of cyanogenic compound. Soaking in large volumes of water solubilise cyanogens while pounding rupture plant cells releasing linamarase, an enzyme that breaks down linamarin to glucose and acetocyanohydrin (Oke, 1994). Drying inactivates linamarase which prevent the accumulation of acetocyanohydrin (Mlingi and Bainbridge, 1994), while fermentation further removes cyanogens through the hydrolysis of linamarin by certain lactic acid bacteria (Giraud et al., 1992). By comparison, garri has more total cyanogens removed than fufu and this associated with volatilisation of free cyanide when cassava is toasted at high temperature at the end of the process.

1.5 Constraints in cassava production

1.5.1 Pests and diseases

The potential of cassava is recognised but its production is hindered by many factors. Insects including cassava mealy bug (*Phanacoccus manihoti*), whitefly (*Bemisia tabaci*), green and red spider mites (*Mononychellus tanajoa, Tetranychus telarius*), African grasshopper (*Zonocerus variegatus*) and burrower bug (*Cyrtomenus bergi*) are important pests of cassava (Bellotti et al., 1999). However, two major threats for growing cassava which have been given major emphasis by cassava research community are cassava mosaic disease (CMD) and cassava brown streak disease (CBSD).

CMD which has caused serious losses in many parts of Africa, India and Sri Lanka is caused by Begomovirus from the Geminiviridae family. The virus is also known as cassava mosaic virus (CMV). Being characterised by its geographical occurrence, currently, there are several distinct species of CMV. Some known examples include Africa Cassava Mosaic Virus (ACMV), East Africa Cassava Mosaic Virus (EACMV) and South Africa Cassava Mosaic Virus (SACMV) (Fauquet and Fargette 1990). The disease can be transmitted to healthy cassava plants by a whitefly vector (*Bemisia tabaci*) or through infected stem cuttings. In general, cassava plant affected by CMD has stunted growth with chlorotic mosaic symptoms in the leaf lamina. There are two types of mosaic namely 'green mosaic' and 'yellow mosaic' where the latter is more severe and easily identified than the former. Although both exhibit mottling of the leaves, severe chlorosis in the case of yellow mosaic often causes leaf tissue damage and leaf falling, which then leads to plant stunting due to reduced photosynthetic activity. Nevertheless, CMD is not characterised by stem or root symptoms though reduction in yield is common. The overall loss caused by CMD was estimated to be 19 million tonnes costing 1.9-2.7 billion dollars annually (Legg and Fauquet, 2004).

Another virus-related disease detrimental to cassava is cassava brown streak disease (CBSD). The causal agents of CBSD are Ipomovirus from the Potyviridae family and the Ugandan Cassava Brown Streak Virus (UCBSV) which recently claimed to be a distinct virus species (Mbanzibwa et al., 2011). CBSD mainly occurs in the East African countries like Tanzania and Mozambique. It has caused substantial yield losses, yet is less studied because it is less widespread (Hillocks and Jennings, 2003). Unlike CMD, CBSD-affected plants exhibit lesion/streak of stem and necrosis of storage roots with little leaf intervenal chlorosis. Therefore, it is not easily detectable unless the storage roots are harvested or the brown streak on the stem becomes apparent. Moreover,

CBSD rarely causes growth distortion and the leaf symptoms only appear when it matures. Necrosis of the storage roots is characterised by formation of hard, yellow or brown rot surrounding xylem vessels fibre which render the roots unfit for consumption.

Progress has been made in tackling the diseases to ensure production of the best quality cassava roots, including generating transgenic cassava with low susceptibilities to the diseases (Vanderschuren et al., 2007) but this does not guarantee delivery of the same quality roots. The healthiest cassava root, as harvested, is prone to a physiological disorder which affects its storability. It is known as post-harvest physiological deterioration (PPD).

1.5.2 Post-harvest physiological deterioration (PPD)

PPD is spoilage of storage roots characterised by browning of the parenchyma tissue and vascular streaking (Figure 1.4). Depending on cultivar, PPD can occur as early as 24 hours after harvest rendering the roots unpalatable and unmarketable. Rapid occurrence of PPD presents a major constraint for commercialisation of cassava, especially as the distance and time between production and market is increasing due to the expansion cassava cultivation area and increased urbanisation (Beeching, 2001).
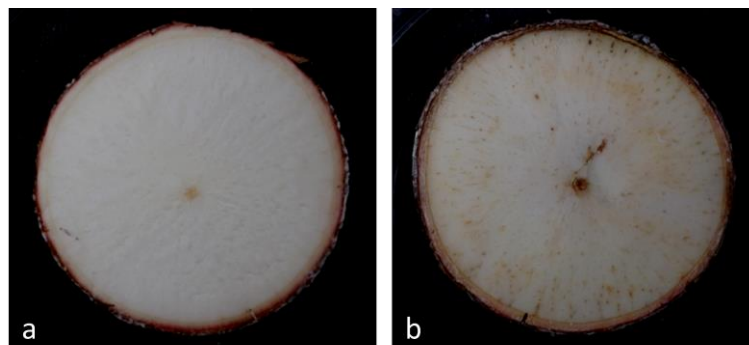
Figure 1.4 Discoloration of parenchyma tissue in cassava undergoing PPD. Cross section of (a) fresh cassava root and (b) deteriorated cassava root 72 hours after harvest. Roots were obtained from local supermarket.

Early understanding of PPD relied upon observation of the conditions that prevent its occurrence. For example, PPD was suggested to be enzymatic in nature as treatment of roots with high temperature (53°C) prior to storage inactivated PPD, while refrigeration (0-5°C) inhibited the development of PPD (Averre, 1967). The role of oxygen was proposed based on the observation that storage roots left covered in

plastic bags deteriorated slower than those uncovered (Hirose and Data, 1984) because of lower concentrations of oxygen. Supporting this is the observation that PPD was delayed in roots immersed in water and that roots with an intact periderm were less discoloured than those that had been peeled (Marriott et al., 1978).

PPD is a high energy-requiring process involving synthesis of proteins and enzymes. This was demonstrated when the application of protein synthesis inhibitor cycloheximide to wounded cassava tissue prevented the occurrence of PPD to a certain extent (Uritani et al., 1984). Correspondingly, a number of independent studies reported apparent increase in peroxidases, polyphenol oxidase, catalase, beta-1-3-glucanase and pectin methyl esterase (Rickard and Gahan, 1983, Isamah et al., 2003, Owiti, 2009). Also observed was high activity of acid invertase catalysing sucrose breakdown and ATPase (Isamah, 2004, Uritani et al., 1984).

The biochemical process of PPD is not fully understood but presumably is the consequence of cell damage due to wounding because the site damaged by wounding normally exhibits greater PPD symptom. Interestingly, although wounded tissue promotes the entry of pathogens and PPD often is followed by microbial spoilage, PPD itself is not pathological in nature. This is concluded based on the failure to isolate microbes from roots already showing PPD symptoms (Hirose et al., 1983) and inability to prevent PPD using fungicides and bactericides (Noon and Booth, 1977). Generally, spoilage by microbes is readily distinguishable from PPD, as the former is accompanied by decay and an unpleasant smell. Because PPD takes place before microbial spoilage it is also termed as primary deterioration while microbial spoilage is termed as secondary deterioration.

Study of the biochemical and enzyme profiles of deteriorating root samples facilitates further understanding about PPD. Roots that had been harvested for 24 hours have an increased ethene concentration, which is a characteristic signal in transduction pathway leading from injury. Especially in the site where injury is introduced, the increase is remarkable (Hirose et al., 1984). Parallel to this, there is an increase in respiration (Marriott et al., 1978) and activity of the entry enzyme for formation of various stress metabolites in the phenylpropanoid pathway, phenylalanine ammonia lyase (PAL) (Uritani, 1999). Such responses are expected as they are the typical wound response in plants. Ethene is a phytohormone that is commonly released, it has diverse signalling functions including in wounding, while the increase of respiration could be a result of blockage of xylem vessels due to formation of phenolic compounds resulted from increased PAL activities (Yokotani et al., 2004). However, comparison of

metabolic changes of wounded cassava to sweet potato revealed some distinctive features of cassava deterioration. For example, although both root tissues showed noticeable increases in PAL, a lesser amount of polyphenols were measured in cassava than in sweet potato. Similarly, lignin (for wound sealing) did not adequately form in wounded cassava even though peroxidase which is involved in the formation of lignin had enhanced activity in both roots (Uritani, 1999, Rickard and Coursey, 1981). Due to the lack of wound repair PPD appears, at least in part, to be due to incomplete wound healing (Beeching et al., 1998).

A striking feature of PPD is the accumulation of hydroxycoumarins, such as scopoletin, scopolin, esculetin and esculin, which are products of the phenylpropanoid pathway. Scopolin and esculin are the glycoside of scopoletin and esculetin, respectively. The importance of these compounds is suggested because they cannot be detected in fresh cassava roots but can be found in extremely high concentrations in deteriorated roots. Greater attention is drawn to scopoletin as it peaks within 24 hours after harvesting while others tend to accumulate later (Tanaka et al., 1983). Furthermore, exogenous application of scopoletin (1000 g/dm) to fresh root tissue, but not other hydroxycoumarins accelerates discoloration producing intense symptoms similar to naturally occurring PPD (Wheatley and Schwabe, 1985). Importantly, unlike other hydroxycoumarins, scopoletin accumulation is visually evident due to its ability to fluoresce under UV light, hence making it a useful PPD marker. Whilst the full biosynthetic pathway of scopoletin in cassava is not complete, the major steps have been determined (Bayoumi et al., 2008), also, homologous genes to those involved in *Arabidopsis* scopoletin biosynthesis have been identified in cassava. A project exploiting the pathway is currently in progress to elucidate the role of scopoletin in PPD (S. Liu, *pers. comm.*).

Nevertheless, although wounding has been long recognised as the root cause for PPD, the early events following wounding that may explain the occurrence of PPD was only intensely studied in the recent years. There is accumulating evidence that implicates oxidative stress plays a major role in PPD. Upon wounding, reactive oxygen species form triggering an oxidative burst that leads to the subsequent reactions observed as PPD.

1.5.2.1 Reactive oxygen species

ROS is the unavoidable product of normal metabolism generated mostly in photosynthetic components, mitochondria and peroxisomes. Triplet dioxygen, which is the ground state oxygen, can be converted to more reactive species such as singlet oxygen ($^1O_2$), superoxide (O_2^-), hydrogen peroxide (H_2O_2) and hydroxyl free radicals (•OH).The chemically reactive oxygen known as reactive oxygen species or ROS generally are perceived as harmful to biological systems (Apel and Hirt, 2004).This can occur through either energy or electron transfer.

$^1O_2$ is created in the chloroplast via photo-activation of chlorophyll that transfers its excitation energy to triplet dioxygen (Holt et al., 2005). It is short-lived but capable of transferring this energy to other significant biological molecules including the lipid bilayer in cell membranes and a number of amino acids (Davies, 2004) making it the main source for photo-oxidative damage in plant leaves (Triantaphylidès et al., 2008).
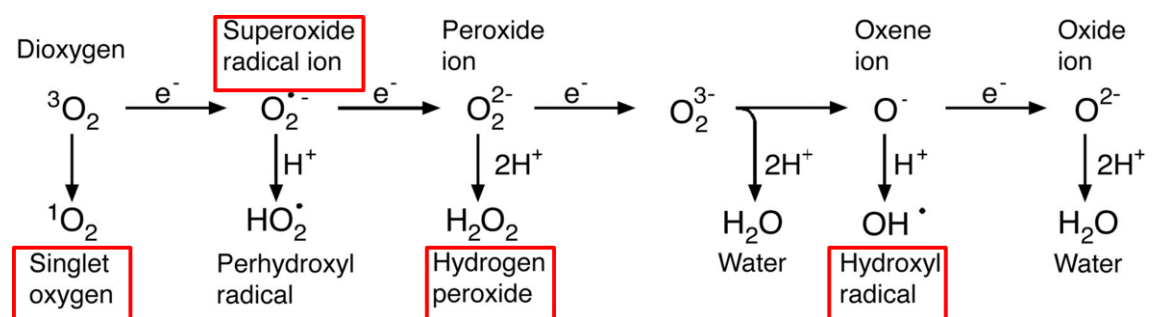
Figure 1.5 Generation of reactive oxygen species (ROS) from dioxygen. Important ROS are highlighted. Figure adapted from Apel and Hirt (2004).

O_2^- is formed as a result of electron transfer rather than energy transfer. In green cells, it forms when triplet oxygen receives leaked electron from photosystem complexes during photosynthesis. Whereas, in most tissues, O_2^- is formed when a small percentage of oxygen molecules entering the mitochondrial respiratory chain are converted to O_2^- by NADPH dehydrogenase in the electron transport chain (ETC) (Navrot et al., 2007). Although it is regarded as precursor of ROS, the deleterious effect of O_2^- is restricted to its production sites as it cannot permeate the cell membrane. Having an unpaired electron, O_2^- is highly prone to pairing to metal-containing enzymes, which eventually destroys them. Also, this promotes protonation of polyunsaturated fatty acid, which then oxidises phospholipids.

O_2^- can be dismutated spontaneously or by superoxide dismutase enzymes to form H_2O_2, which is also destructive to cell components. H_2O_2 is stable with a longer lifespan, and in cells it attacks thiol-containing compounds such as glutathione and protein cysteine residues (Zeida et al., 2012). Unlike O_2^-, it has the ability to diffuse across biological membrane and travel to some distance. Therefore, it is not surprising that the enzymes that detoxify H_2O_2 are multi-compartmentalised (Moller et al., 2007). These enzymes are ascorbate peroxidase and catalase (discussed in Chapter 3).

Through the Fenton reaction H_2O_2 can give rise to a more powerful oxidant, •OH. The effects of •OH are pervasive. It can effectively breakdown mitochondrial proteins, DNA, and lipids leading to cellular damage (Orrenius, 2007). Plant cell wall polysaccharides also are susceptible to •OH as it capable of oxidizing carbohydrates, polyols and sugars (Fry, 1998).

1.5.2.2 Oxidative stress and PPD

ROS is produced in response to physiological stimuli such as growth and development as well as biotic and abiotic stress like pathogen invasion and environmental fluctuations (Apel and Hirt, 2004). O_2^- and H_2O_2 in particular, are important messengers in oxidative signalling of higher plant cells (Foyer and Noctor, 2005). Under normal physiological states, excess ROS is effectively inactivated to form harmless products keeping them at their basal concentration. However, when there is a serious imbalance between ROS production and inactivation, oxidative stress occurs causing the above-mentioned damages (Wojtaszek, 1997).

During PPD, accumulation of O_2^- and H_2O_2 *in vivo* has been observed by staining in a range of cultivars with different susceptibility to PPD (Reilly, 2001). Shortly after harvest, O_2^- was detected with accumulation at 15 minutes after wounding. The accumulation, though rapid, was temporary as O_2^- could no longer be detected after 6-7 hours in some cultivars or 10 hours in others. Intense staining was seen especially in the cell wall junctions of storage parenchyma and cambium than in other parts of the roots. Conversion of O_2^- to H_2O_2 was confirmed as H_2O_2 tended to accumulate later with the highest abundance observed one day post-injury. Given that lipid peroxidation is a characteristic of PPD (Isamah et al., 2003) it is also possible that translocation of H_2O_2 had occurred during this process as staining was strong both in the cortical parenchyma and xylem vessels of the storage parenchyma.

The relationship between ROS and PPD has been suggested in a number studies. Such localisation of H_2O_2, though slightly variable has been observed before. H_2O_2 has also been measured in roots undergoing PPD, showing high point in roots that had been harvested for 24 hours (Buschmann et al., 2000a). Indirect evidence supporting the involvement of H_2O_2 is available including increases of transcript levels of ascorbate peroxidase (APX) and catalase (CAT). Significant upregulation of these enzymes during PPD was confirmed by microarray data prepared from fresh and deteriorating cassava roots (Reilly et al., 2007). However, it is interesting that the superoxide dismutase (SOD) enzyme, which functions to quench O_2^-, was not enhanced at any point during the process; thereby, supporting the hypothesis that the oxidative burst of O_2^- is responsible for causing oxidative stress and initiating PPD (Reilly, 2001). The importance of oxidative stress in causing PPD is further supported as roots with enhanced beta carotene have been shown to exhibit less PPD symptoms, probably due its ability to scavenge ROS (Sanchez et al., 2006). Moreover, recently, simultaneous expression of SOD and CAT gene was proved to delay PPD (Xu et al., 2013b).

1.6   Inhibition of PPD

About 20% of cassava production in Africa is lost to PPD (Nassar and Ortiz, 2010). Therefore, delaying PPD could make a significant contribution to both food security and the livelihoods of resource-poor farmers in that continent.

1.6.1 Conventional methods

Various methods have been practiced to prevent or reduces losses due to PPD. Generally they can be divided into pre-harvest and post-harvest methods.

Due to its perishability, it is common that cassava is only harvested when needed. This in-ground storage method is the most practical pre-harvest method in small-scale production where there is low demand of soil utilisation and rare occurrence of pests and diseases. However, this method may reduce the quality of the roots as starch is lost through metabolism and the roots tend to become fibrous and woody. As PPD usually is more severe in the end close to the peduncle (distal) of the roots, it has been claimed harvesting cassava roots while keeping 2-3 cm stem attached reduces the occurrence of PPD (Diop and Calverley, 1998). Removing green parts of the plant or pruning before harvest is another effective pre-harvest method to prevent PPD. It was

shown in numerous field works that cassava pruned between 20-30 days before harvest minimised the occurrence of PPD for up to 80%. However, counteracting to this is reduction of starch and dry matter content as well as changes in organoleptic properties of the roots (Kato et al., 1991, Data et al., 1984, van Oirschot et al., 2000). While these methods are effective to reduce PPD, it is rare for farmers to invest the care and effort necessary to ensure that the roots are harvested undamaged on such a low value commodity.

The traditional post-harvest methods also lengthen the storage time of the cassava roots and minimise the occurrence of PPD. For example, re-burying harvested roots in soil pit enable the roots to last for up to a few months. Large scale underground storage in trench silos which allow storage hundreds of kg cassava roots at a time is claimed as the most successful (Rees, 2012). Alternatively, as widely practiced in West Africa and India, cassava roots are stored in heaps on the ground and they are kept moist by regular watering. This method of storage takes advantage of curing that successfully delays the onset of deterioration in other root crops by promoting wound healing (Booth, 1976). Limiting oxygen by loam paste coating also is effective to delay PPD by 4-6 days but it is possibly most suitable for small-scale production (Westby, 2002). More modern methods such as freezing, wax-dipping and vacuum-packing are used for roots intended for exports to America and European countries. While these prolong the shelf-life for months or more they are considered too expensive for domestic markets.

1.6.2 Breeding and biotechnology approach

Cassava breeding is relatively new when compared to other food crops. It only begins in the 1970s after the establishment International Centre for Tropical Agriculture (CIAT) and International Institute of Tropical Agriculture (IITA). In general, breeding of cassava is challenging because of its low fertility. Cassava is monoecious with staminate flowers that only open two weeks after openings of pistillate flowers, thus, formation of seeds rarely occurs (Wenham, 1995). In average, only 0.6 viable seed per pollination is produced so obtaining sufficient numbers of seeds for breeding experiments is laborious. While this largely prevents selfing it encourages outcrossing, hence cassava is highly heterozygous. Due to the high heterozygosity, backcrossing are time-consuming and complex making selection of particular elite trait and hybridisation to obtain superior clones become difficult (Ceballos et al., 2004). Generally, cultivars with reduced PPD responses have low dry matter content, which is an undesirable agronomic trait (Salcedo and Siritunga, 2011). Separation of these linked traits may be

possible, but it is likely to be a tedious and lengthy process. Further limits the use of conventional breeding in resolving PPD is lack of genetic variability for PPD tolerance (Ceballos et al., 2004).

In general, the main advantage of genetic engineering or biotechnology over classic plant breeding is that it targets a specific trait without altering others. It is also versatile and the outcome is relatively easier to predict (Ulukan, 2009). The success of exploiting biotechnology relies on modification of the right target genes, either by suppression or overexpression of the genes. Success has been achieved in creating CMD-resistant transgenic cassava using antisense RNA technology (Zhang et al., 2005). Additionally, the knowledge and genes obtained and identified through molecular approaches can facilitate and accelerate breeding strategies through marker assisted selection. For example, gene expression and proteomics analysis can be exploited to obtain reliable molecular markers for PPD (Reilly et al., 2007, Owiti, 2009). With the completion of cassava genome sequencing (Cassava Genome Project, www.phytozome.net/cassava) and the ongoing annotation of the sequences, biotechnology is seen as the most appropriate tool to create PPD-tolerant cassava clones. The genes encoding enzymes and intermediates in biochemical pathways associated with PPD can be manipulated for the purpose of delaying PPD. For example, an RNAi experiment using the homologue of the key gene involved in *Arabidopsis* scopoletin biosynthesis, a member of the 2-oxoglutarate-dependent dioxygenase (2OGD) family, is currently explored. A range of approaches have identified genes that are differentially expressed during PPD, which include those involved in ROS turnover, stress response, metabolism of carbohydrate and protein synthesis (Reilly et al., 2007, Owiti, 2009). These findings are invaluable as not only do they increase our understanding of PPD but can provide target genes whose manipulation may ultimately prevent it.

1.7 Research strategy

The evidence reviewed about implicates oxidative stress as being at the heart of the PPD response in cassava. To investigate this, transformed cassava plants designed to have an enhanced anti-oxidant status through enzymatic and non-enzymatic approaches were created. These plants which contain one of the target genes encoding ROS-scavenging enzyme or the biosynthesis of anti-oxidant molecules are predicted to have enhanced anti-oxidant capacity in the roots and considerable tolerance to PPD because they are driven by a root-specific promoter. The aim of this research was to confirm if PPD is a ROS-mediated process through overexpression of these genes. To achieve this, several objectives were set out.

1. Preliminarily characterise the genotype and the phenotype of the transformed plants in order to select single-insert independent lines for production of storage root suitable for PPD assay.

2. Critically evaluate the existing methods to assay PPD particularly for storage roots grown in the greenhouse and to score the roots based on the PPD symptoms that develop.

 3. Determine the expression pattern of the target genes by patatin promoter by examining the expression pattern of transgenic cassava lines carrying the reporter expression plasmid.

4. Assess PPD and changes of biochemical activities in selected single-insert independent lines.

CHAPTER 2

Materials & Method

2.1   Materials

2.1.1 Plant material

The transgenic cassava lines were made by Bull (2011). They consist of seven transgenic groups. The transgenic lines according to group are as follow:

Pat:SOD;A1, A2, B1- B3, C1,C2, C3, C4, C6, C7, C9, C10, D1, D3 -D10, D12, D13

Pat:APX;A1-A15, B1-B7, C1-C5, D1-D3, E1

Pat:CAT; A1-A10, B1-B10, C1-C5, C7, C9, C10, D1-D13

Pat:GCS; A1-A8, B1-B5, C1-C17

Pat:GAR;A1-A15, B5-B8, B16-B33, C1-C12

Pat:Gus; A1-A20, B1-B6

Pat(-):Gus; A1-A37

Wild type (WT) used in this thesis refers to cassava cultivar TMS60444. Wild type *Arabidopsis* (Col-0) and transgenic *Arabidopsis* StPAT::GusP 7-1 were provided by Page (2009).

2.1.2   Software and programs

Primers were designed using Primer3 online software (http://primer3.ut.ee/). PPD scoring was done using PPD Symptom Score Software developed by the cassava team at Swiss Federal Institute of Technology (ETH, Zurich) (Vanderschuren et al., 2014). Measurement of root lengths from photographs employed ImageJ software (Schneider et al., 2012). Analysis of sequenced DNA fragment was performed using Geneious software (Drummond et al., 2009). Identification *cis*-regulatory motifs were done by submitting promoter sequence to PLACE (http://www.dna.affrc.go.jp/PLACE/) and PlantCARE (http://bioinformatics.psb.ugent.be/webtools/PlantCARE/html/) online database. All statistical analysis was carried out using PASW Statistics18. qPCR data was collected using LightCycler 3.5.3 software.

2.2 Methods - Management of plant materials

2.2.1 Propagation of cassava plants *in vitro*

Stems from parent plantlets were cut using sterile blade and tweezers. Bigger leaves were removed to avoid transpiration and stems were grown on fresh cassava basic media (CBM). The plantlets were kept in a controlled environment chamber at 26–28°C, under relative humidity 40-80% with a 14-hour photoperiod. Propagation was done every six months or when necessary.

2.2.2 Growing cassava plants in greenhouse

One month old cassava plantlets were carefully cleaned with warm, running tap water to remove adhering soil. The plantlets were grown in 9 cm x 9 cm growing pots containing M2 Levington compost and kept in the same growth room used to maintain the *in vitro* plantlets for at least four weeks for acclimatisation. After that, the plants were transferred into a greenhouse with a temperature 26-30°C under relative humidity 40-80% for six months or until required.

2.2.3 Harvesting of cassava

The height of the plants was taken by measuring the length of the stem from the border of the container to the top of the main plant stem. The plants were then removed from compost and the storage roots were cleaned under warm running tap water and dried. The roots were cut from the main stem and weighed immediately.

2.2.4 *Arabidopsis* seeds sterilisation

Arabidopsis seeds were immersed in 30% bleach and 0.1% Triton X-100 for 5 to 10 mins and thoroughly rinsed with sterile water. The seeds were stratified at 4°C for 1 or 2 days.

2.2.5 Seed germination (*in vitro*)

Stratified *Arabidopsis* seed was germinated in Petri dish containing Filter paper wetted with sterile water until 5 days after growth (DAG) under a 14-hour photoperiod at room temperature.

2.3 Methods - DNA manipulations

2.3.1 Cassava leaf genomic DNA extraction

Three leaves from an *in vitro* plantlet were crushed into a 1.5 ml tube containing 2-3 g 1 mm borosilicate glass beads and quickly frozen in liquid nitrogen. The tissue was homogenised to a fine powder using triturator (Silamat ® S5) for 6 seconds and 1 ml extraction buffer was added to the homogenised tissue. To ensure thorough mixing the tube was placed in a shaker at room temperature for 15 mins. The tube was centrifuged in a bench-top centrifuge at 16,000 x g, 4°C for 15 mins. 700 µl of the supernatant was transferred to a fresh 2.0 ml tube. Another 500 µl extraction buffer was added to the previously extracted tissue and centrifuged again at 16,000 x g, 4°C for 10 mins. 300 µl of the supernatant was transferred to the tube containing 700 µl supernatant to make up 1000 µl volume and 5 µl of a 20 mg/ml RNAse A was added to get a final concentration 20 µg/ml. The tube was incubated at 37°C for at least 30 mins to 1 hour. 1 ml phenol (pH 8.0) was added and the mixture was vortexed and centrifuged at 16,000 x g for 5 mins. The resulting upper phase was placed in a new 2 ml tube containing 1 ml phenol:chloroform (1:1) and extracted by vortexing and centrifuge at16,000 x g for 5 mins. The upper phase was removed and placed in a new 2 ml tube containing 1 ml phenol:chloroform:isoamyl (25:24:1) and extracted by vortexing and centrifuge at 16,000 x g for 5 mins. Again, the upper phase was removed and placed in a new 2 ml tube containing 1 ml phenol:chloroform:isoamyl (25:24:1) and extracted by vortexing and centrifuged at 16,000 x g for 5 mins. The upper phase was removed and placed in a new 2 ml tube containing ¼ volume of 10 M ammonium acetate. Two volumes of cold (-20°C) absolute ethanol was added and the tube was inverted several times. The tube was incubated at -20°C for 30 mins to allow precipitation. It was then centrifuged at 16,000 x g 4°C for 25 mins in a bench-op centrifuge. The pellet was dissolved in 750 µl miliQ water and added with 750 µl phenol:chloroform:isoamyl (25:24:1). The solution was mixed by shaking and centrifuge at 16,000 x g for 5 mins. The upper phase was removed and placed in a new 1.5 ml tube containing ¼ volume of 10 M ammonium acetate. Two volumes of cold (-20°C) absolute ethanol was added and the tube was inverted several times. The tube was incubated at room temperature for 5 mins to allow a second precipitation. The mixture was centrifuged at 16,000 x g, 4°C for 15 mins. The pellet was washed with room temperature 70% ethanol by inverting the tubes several times and the tube was centrifuged at 16,000 x g for 10 mins at room temperature. Finally the pellet was dried and dissolved in 50 µl sterile water. The DNA was stored at -20°C.

2.3.2 Quantification of DNA

DNA concentration was determined using a spectrophotometer by taking reading at wavelength of 260 nm. 1 O.D. at 260 nm is equal to 50 ng/ul double-stranded DNA.

2.3.3 Polymerase chain reaction (PCR) for target sequence amplification

A total volume of 20 µl solution mix contains approximately 100 ng DNA template, 1X Thermopol buffer (New England Biolabs), 0.5 µM forward and reverse primers, 200 µM dNTPs and 1U *Taq* polymerase was prepared in a thin-walled PCR tube. Cycling was performed in a Peltier Thermal Cycler PTC-200 by using the following program: 3 mins at 94°C, followed by 34 cycles of 1 min at 94°C, variable min at stated annealing temperature (Table 2.1), and 1 min at 72°C. The program finished with an additional 10 mins extension step at 72°C.

2.3.4   Primers

Primers were designed using Primer3 (Untergasser et al., 2012) and are as listed in Table 2.1. The conditions of PCR are as in Table 2.2.

Table 2.1 Primers used in this thesis

Name	Sequence (5'→3')	Tm (C°)
HygF	CCA CTA TCG GCG AGT ACT TCT ACA CAG C	61.6
HygR	GCC TGA ACT CAC CGC GAC GTC TGT	65.1
Hyg II F	TCT CGA TGA GCT GAT GCT TTG	55.0
Hyg II R	AGT ACT TCT ACA CAG CCA TCG	54.0
DESTSeqF1	CAT CAC TAA TGA CAG TTG CGG TGC	58.5
DESTSeqR1	GCACATACAAATGGACGAACGG	55.0
CATR1	GAA AGC TGG GTC TCA TAT ATT TGG CCT CAC G	61.9
SODR1	AGA AAG CTG GGT CCT ATC CTT GCA AAC CA	63.2
APXR1	AAG CTG GGT GTT ACG CCT CAG CAA ATC C	64.4
GCSR1	GAA AGC TGG GTG TTA GTA CAG CAG CTC TTC	61.0
GARR1	GAA AGC TGG GTC TCA TAA TTC TTC GTC AAC TTC C	61.0
18sFor	ATGATAACTCGACGGATCGC	52.0
18sRev	CTTGGATGTGGTAGCCGT	51.6
Pat-PDESTF	TTGTAGTTAATGCGTATTAGTTTTAGC	50.9
Pat-PDESTR	CAAGCATGGTATATATAGGCACG	51.2
PatSeqF	TGTGGAATTGTGAGCGGATA	51.1
PatSeqR	CAGTCCTTTCCCGTAGTCCA	52.8
GusIntF	TGGGAACCACTGAACACGTA	53.0
GusIntR	CCGAACGGCTCTTCATAGAC	52.5
TransgeneR	GTCACCAATTCACACATCACCAC	54.4
CATintR	CAG CAA ACC AGT TAT CGA TGT TCC	54.6
GusFWD	CAACAACTCGCTGCGTGATGGC	59.5
GusIntR2	CCGAACGGCTCTTCATAGAC	52.5
GCStf	AAC AGG AGT TACG CCT GCG GA	58.1
SODtf	GAC GACA TTC GTC ATG CTG GTG ATC T	59.2
SODtr	GTG AAC AAC GAC TGC CCT TCC TAC	58.0
CATtf1	TCGCAGTATCTGGGTCTCTTACTG	55.5
CATtr	TGGCCTCACGTTGAGACGAGAAG	58.6

Table 2.2 Primer combinations and amplification conditions in PCR

Name	Template	PCR product size (bp)	Extension time (s)	Annealing temperature (C°)
HygF HygR	pDESTs	1000	60	61.0
Hyg II F Hyg II R	pCAMB	400	30	55.0
DESTSeqF1 CATR?	pDEST:CAT	1680	60	60.0
DESTSeqF1 SODR1	pDEST:SOD	661	60	60.0
DESTSeqF1 APXR1	pDEST:APX	952	60	54.0
DESTSeqF1 GCSR1	pDEST:GCS	1761	90	60.0
DESTSeqF1 GARR1	pDEST:GAR	1152	60	60.0
PatSeqF PatSeqR	pDEST:*GusPlus*	1248	60	55.0
DESTSeqF1 GusIntR	pDEST:*GusPlus*	1285	60	55.0
DESTSeqF1 DESTSeqR1	pDEST:*GusPlus*	2485	120	58.0
GusIntF TransgeneR	pDEST:*GusPlus*	1793	90	54.0
PatSeqF PatPDESTR	pDEST:*GusPlus*	1149	60	55.0
DESTSeqF1 TransgeneR	pDEST:*GusPlus*	2087	120	58.0
DESTSeqF1 CATIntR	pDEST:CAT	1141	60	60.0
CATtf1 CATtr	pDEST:CAT/ gDNA	82/179	30	58.0
PatSeqF GusIntR2	pDEST:*GusPlus*(-Pat)	1207	60	53.0
GusFWD TransgeneR	pDEST:*GusPlus*(-Pat)	1530	90	58.0

GCStf TransgeneR	pDEST:GCS	138	30	60.0
SODtf SODtr	pDEST:SOD/ gDNA	135/325	30	60.0

2.3.5 Agarose gel electrophoresis

To estimate the size of PCR product and total RNA, they were run on agarose gels. The concentration of the gel varied between 0.8%-1.5%, depending on the size of nucleic acid sample. Agarose gel was dissolved in 1X TAE buffer and melted in a microwave oven. The gel was allowed to slightly cool before ethidium bromide was added at a final concentration 0.5 µg/ml. It was then poured into a gel cast attached with an appropriate comb to make a gel slab. The solidified gel was covered with 1X TAE buffer which serves as the running buffer. Samples were diluted (if necessary) with MilliQ water and mixed with loading buffer in 1.0 ml tube. Either 1 kb or 100 bp DNA markers were loaded in the first well and this was followed by samples. Electrophoresis was run at a voltage between 85-90 V for 1-2 hours. The gel was visualised under ultraviolet light and the image was documented.

2.3.6 Nucleotide sequencing of DNA

DNA sequencing was performed by Eurofin Genomics (UK).

2.3.7 Southern Hybridisation

2.3.7.1 Preparation of DIG-labelled probe for hybridisation

A total volume of 50 µl solution mix contains 50 ng plasmid pCAMBIA 1305.1, 1X Thermopol buffer (New England Biolabs), 0.5 µM Hyg II F and Hyg II R primers, 1X DIG labelled-dNTPs and 1U *Taq* polymerase was prepared in a thin-walled PCR tube. Cycling was performed in a Peltier Thermal Cycler PTC-200 by using the following program: 3 mins at 94°C, followed by 34 cycles of 1 min at 94°C, 1 min at 55°C and 1 min at 72°C. The program finished with an additional 10 mins extension step at 72°C.The PCR product was purified from the agarose gel with QIAquick Gel Extraction Kit (Qiagen) according to the steps recommended by the manufacturer.

2.3.7.2 Restriction digestion of genomic DNA

The components and concentrations used are as shown in Table 2.3 and digestion was carried out overnight at 37°C.

Table 2.3: Contents of a genomic DNA restriction digestion reaction

Reaction component	Volume (µl)	Final concentration /Amount
DNA	70	~20 µg
Hind III buffer	20	1x
0.1 M spermidine	4	2 mM
Hind III (20,000 U/ml)	4	80 U
Sterile water	101.8	-
RNase (20mg/ml)	0.2	0.02 mg/ml
Total	200	-

2.3.7.3 Precipitation of digested genomic DNA

The digested genomic DNA was precipitated by adding 1/4 volumes of ammonium acetate and 2.5 volumes of cold ethanol at -20°C for 2-3 hours. The mixture was centrifuged at 16,000 g to obtain the pellet. The pellet was allowed to dry and solubilised in 25 µl sterile water.

2.3.7.4 Electrophoresis of digested DNA

Loading dye was added to the DNA at the final concentration of 3X to facilitate visualisation in a long run. Electrophoresis was carried out on 0.7% agarose gel (without ethidium bromide) in a fresh TAE buffer at 80 V for 10 mins. Then the voltage was reduced to 20 V and the electrophoresis was run for 24 hours. A DIG-labelled, DNA molecular weight Marker III, 0.12-21.2 kbp (Roche) was used as DNA marker. 1.5 µl DNA ladder was mixed with 18.5 µl sterile distilled water and 6 µl 5X loading dye.

2.3.7.5 Southern blot preparation

The gel was placed in a clean tray containing sufficient amount of 0.25 N HCl to immerse the gel and shaken for 30 mins. In the same tank, the gel was rinsed with miliQ water and then immersed in Denaturing solution with shaking for 30 mins. In the meantime, the blot apparatus was set up. A thick glass plate was placed on a clean tank half-filled with 20X SSC (running buffer) and 2 sheets of Whatmann 3 mm paper soaked in 20X SSC were placed over the glass plate with both ends of the sheets immersed in the 20X SSC. Any air bubbles were removed by carefully rolling the sheets with a clean glass rod. The gel was placed inverted on the wet paper and a

nylon membrane (N+ Hybond) of the same size as the gel was placed on top. Two pieces of wet Whatmann 3mm paper of the size of the gel was placed above the membrane and each time and air bubbles were removed by gentle rolling. A stack of tissue paper was placed onto the paper and a weigh (~500 g) was added on top to maximize the contact between the membrane and the gel. A piece of cling film was used to wrap around the gel extending to the tray to avoid evaporation. This was allowed to take place overnight.

2.3.7.6 DNA fixation to nylon membrane

The Nylon membrane was placed on a Whatmann paper and the DNA was allowed to permanently link to the membrane by a UV linker.

2.3.7.7 Digoxigenin (DIG) hybridisation

The membrane was placed in a long glass cylinder that had been previously rinsed with distilled water. 10 ml DIG Easy Hyb (Roche) was added and the cylinder was placed in hybridisation chamber set to 43°C for 1 hour for pre-hybridisation. In the mean time 10 ml DIG Easy Hyb was pre-warmed in the chamber. 10 µl (~500ng) hygromycin probe was diluted in 40 µl and heat-denatured at 99°C for 10 mins and added to the pre-warmed hybridisation solution. The cylinder was emptied and the solution replaced with the probe and hybridisation was allowed to take place in the chamber overnight.

2.3.7.8 Washing off unbound DNA

The membrane was taken out and laid in a tray containing W1 and gently shaken for 5 mins at room temperature. This step was repeated. The membrane was moved into a new tray containing 200 ml pre-warmed W2 (70°C) and shaken in a water bath set to temperature 70°C for 15 mins. The membrane was then washed with W3 at the same condition as W2 and with WB at room temperature for 3 mins. The tray was emptied and replaced with B2 and shaken at room temperature for 30 mins.

2.3.7.9 Antibody and CDP star binding

B2 was discarded and replaced with antibody solution (6 µl antibody in 15 ml B2) shaken for 30 mins. The membrane was then washed in WB solution for 15 mins three times, each time in a new tray and fresh WB. Final washing step was carried out in WB for at least 30 mins. The membrane was shaken in 145 ml B3 for 5 mins and the B3 was discarded. The membrane was wetted with enzyme solution (50 µl CDP Star in 5

ml B3) by repetitive pipetting for at least 5 mins. All steps were performed at room temperature.

2.3.7.10 Visualisation

The membrane was placed on Whatmann paper cut to the size of film cassette to remove excess buffer and the membrane was covered with a piece of cling paper. In a dark room, apiece of film (Kodak Biomax Light) was placed onto the membrane and the cassette was incubated at 37°C overnight. The image was developed in an image developer in the darkroom.

2.4   Methods - RNA manipulations

2.4.1   Cassava root RNA extraction

The extraction method was adopted from protocol of pine tree RNA extraction method (Chang et al., 1993). Root sample (without periderm cortex) was grated using a domestic cheese grater and ground into a fine powder in liquid nitrogen in a mortar and pestle. Aliquots of liquid nitrogen were continuously added during grinding to prevent thawing and consequent degradation by RNases in the sample. The powder was kept in 15 ml Falcon tube and stored in -80°C to minimize RNA degradation. Prior to use 2% beta-mercaptoethanol was added to extraction buffer and heated to 50°C. A 0.5 g sample was weighed and put in a 15 ml Falcon tube and 5 ml extraction buffer mixed with beta-mercaptoethanol was quickly added and further heated at 50°C for 10-15 mins. Once in a while the mixture was homogenized by inverting the tube to allow maximum extraction. After 15 mins, 5 ml chilled chloroform: isoamyl alcohol (24:1) was added, mixed and centrifuged at 16,000 x g in a bench-top centrifuge at 4°C for 10 mins. Supernatant from the upper layer was transferred into a new tube, to which was added an equal volume of chloroform: isoamyl alcohol (24:1) and centrifuged again at 16,000 x g at 4°C for 10 mins. The supernatant from the upper layer of this second centrifugation was transferred into new tubes and an equal volume of isopropanol added to it. LiCl solution was then added to 2 M final concentration before the solution was incubated overnight at 4°C. It was then centrifuged at 16,000 x g, 4°C for 30 mins and supernatant was decanted at this stage. The pellet was re-suspended in 1 ml Sterile water and 250 µl 10 M LiCl solution was added, this was incubated on ice for 2-3 hours and centrifuged at 16,000 x g at 4°C to obtain a pellet. The resulted pellet was re-suspended with 250 µl sterile water, 25 µl 3M sodium acetate (pH 5.2) and 1 ml absolute molecular grade ethanol, and allowed to incubate at -20°C for 2 to 3 hours. The mixture was centrifuged again at 16,000 x g at 4°C for 30 mins. The supernatant

was decanted and the final pellet was solubilised with 50 µl sterile water and stored at -80°C for future use.

2.4.2 DNase treatment of RNA

The total RNA was treated with DNase to remove contaminating DNA in the sample using Ambion® TURBO DNA-*free*™ DNase Treatment Kit. The kit consists of 10X TURBO DNase buffer and TURBO DNase (2 U). Samples with more than 200 µg nucleic acid per ml concentration were diluted to 10 µg nucleic acid per 50 µL. 0.1 volume 10X TURBO DNase Buffer and 1 µL TURBO DNase were added to the RNA and mixed gently. This was followed by incubation at 37°C for 30 mins. Finally, 1.5 µl EDTA (0.5 M, pH 8) was added and the solution was heated at 75°C for 10 mins to deactivate the DNase.

2.4.3 RNA quantification

Experion™ RNA StdSens Analysis Kit (Biorad) was used to measure total RNA. This system consists of Experion electrophoresis station, Experion priming station and Experion vortex station, RNA chip and electrophoresis reagents. The protocol used was as recommended by manufacturer.

2.4.4 cDNA synthesis

cDNA was synthesised using SuperScript™III First-Strand Synthesis SuperMix (Invitrogen), oligo(dT) and 1 µg of RNA and as suggested by the manufacturer. cDNA was stored at -20°C until used.

2.4.5 Quantitative real-time PCR (qPCR)

qPCR was performed using LightCycler® System (Roche Diagnostics) based on the SYBR green detection method. A total volume of 25 µl solution mix contains cDNA template, 1X Takara SYBR® Premix ExTaq, 0.2 µM forward and reverse primers and sterile distilled water was prepared in a 0.2 ml tube. The mix was prepared on ice before it was transferred into a capillary tube. The tube was centrifuged at 400 g for 5 s and quickly placed in the LightCycler® machine. Cycling was performed by using the following program: 30 s at 95°C, followed by 39 cycles of 20 s at 94°C, 20 s at annealing temperature, and 20 s at 72°C. This was followed by a melting cycle at 95°C for 15 s and finished by a cooling cycle at 40°C for 2 mins.

2.4.6   Quantification of transcriptional levels using qPCR

The transcriptional level of a transgene was calculated according to the Pfaffl method which measures fold increase in the transgene as a ratio to fold increase in the reference gene (Pfaffl, 2001). The equation is shown below

$$\text{Ratio} = \frac{(AE_{trans})^{\Delta CT\ trans\ (control-treated)}}{(AE_{ref})^{\Delta CT\ ref(control-treated)}}$$

AE = amplification efficiency

trans = transgene

ref = reference gene

CT = threshold value

2.5   Methods- Biochemical assays

2.5.1   Total protein extraction 1

Cassava root tissue was ground into fine powder in liquid nitrogen using a pre-cooled mortar and pestle. 1 ml of 50 mM MES/KOH buffer (pH 6.0), containing 40 mM KCl, 2 mM $CaCl_2$ was added to 0.25 g powder in a 1.5 ml tube and the tube was centrifuged twice at 16,000 x g in a bench-top centrifuge at 4°C for 10 mins. Supernatant/protein extract was stored at -20°C until further use.

2.5.2   Total protein extraction 2

Total protein was extracted from cassava tissue with 50 mM HEPES buffer containing 2 mM metabisulfite. 1 ml of cold extraction buffer was added to 0.1 g frozen plant tissue and vortexed to mix. The slurry was centrifuged at 10,000 g at 4°C for 30 mins and supernatant was collected.

2.5.3   Bradford protein assay

5 µl protein extract was added to 250 µl Bradford Reagent (Sigma-Aldrich) in a microplate well and incubated at room temperature in the dark for 30 mins. It was then read at 595 nm against an assay blank containing buffer and Bradford reagent. The concentration of the protein extract was converted to mg/ml by comparing it to a BSA standard curve.

2.5.4 Ascorbate peroxidase (APX) assay

APX activity was determined according to the method of Murshed et al. (2008) which measured the rate of ascorbate decomposition. The reaction buffer (185 µl/well) consisting of 50 mM potassium phosphate buffer (pH 7.0) and 0.25 mM ascorbic acid was dispensed into all microplate wells. Then 10 µl of protein extract or extraction buffer was placed in each microplate well. The microplate was shaken for 10 s by programming the microplate reader and the absorbance of the reaction was measured at 290 nm for 3 mins. The APX reaction was started by the addition of 5 µl of 200 mM H_2O_2 (5 mM) to all wells using an 8-channel pipette. The microplate was shaken again on the plate reader and activity was determined by measuring the decrease in the reaction rate at 290 nm for 5 mins. Specific activity was calculated using the 2.8 $mM^{-1}\,cm^{-1}$ extinction coefficient. A correction was carried out for the nonspecific oxidation of ascorbate in the sample (first reading) and by H_2O_2 in the absence of the enzyme sample (blank). Total protein in this assay was extracted using Total protein extraction 1 method.

2.5.5 Superoxide dismutase (SOD) assay

Since the assay was intended to specifically measure CuZnSOD activity, 400 µl ice-cold ethanol/chloroform 62.5/37.5 (v/v) was added to 250 µl total protein and vortexed for 30 s. The mixture was centrifuged at 3000 g at 4°C for 5 mins and the upper aqueous layer was collected. CuZnSOD enzyme activity was determined according to the method of Beauchamp & Fridovich (1971) which measured the photoreduction of nitro blue tetrazolium (NBT) at 560 nm. 10 µl protein extract, 164 µl assay buffer (50 mM potassium phosphate buffer pH 7.8, 100 µM EDTA and 13 mM methionine), 10 µl 1.5 mM NBT and 16 µl 0.044 mg/ml riboflavin was mixed in a microplate well. The microplate was placed in a light box fitted with a 15 W fluorescent bulb (Prolite) for 5 mins, then in the dark for 5 mins and the reading was taken. The assay was repeated with pure enzyme with known amounts of SOD to generate a standard curve. Total protein in this assay was extracted using Total protein extraction 2 method.

2.5.6 Catalase assay

Catalase assay was determined according to the method described by Li and Schellhorn (2007) based on the H_2O_2 decomposition at 240 nm (Beers and Sizer, 1952). 20 µl enzyme extract was mixed with 230 µl H_2O_2 in a microplate well and immediately scanned in a microplate reader at 240 nm for 8 mins at 25°C. Total protein in this assay was extracted using Total protein extraction 1 method.

2.5.7 Gus staining assay

The Gus staining assay was performed by incubating plant tissue in Gus buffer at 37℃ for one hour. The plant tissue was rinsed with distilled water before being de-stained in 70% alcohol.

2.5.8 Oxygen Radical Absorbance Capacity (ORAC) assay

20 mg frozen root tissues were extracted in 2 ml 50% acetone in a microfuge tube containing glass beads. The tube was vortexed for 30 s and centrifuged for 3 mins at 4°C. The supernatant was diluted to 100x dilutions in 50 mM potassium phosphate buffer (pH 7). 25 µl of diluted supernatant was added to a microplate well containing 150 µl 0.08 µM fluorescein. The plate was covered and incubated at 37°C for 10 mins before adding 25 µl 2,2′-Azobis (2-methylpropionamidine) dihydrochloride (AAPH) to the well. As AAPH was added, the fluorescence kinetic was immediately read with an excitation wavelength of 485 nm and an emission wavelength of 530 nm for 1 hour at 37°C. A standard curve was generated by replacing the tissue sample with 6-Hydroxy-2,5,7,8-tetramethylchroman-2-carboxylic acid (Trolox) with a concentration range of 2.5 – 20 µM. The oxygen radical absorbance was calculated based on the area under curve (AUC) of the standards and samples against blanks.

2.5.9 Superoxide *in situ* detection

Superoxide production was determined by NBT staining, performed using the method described by Reilly (2001). Root tissue sections of 1 mm thickness were vacuum infiltrated in 0.05% NBT dissolved in 10 ml 10 mM potassium phosphate pH 7.8 buffer for 2 mins before incubating at room temperature for 15 mins under lights. The reaction was stopped with 4 mg/ml chloral hydrate and the root tissue immediately photographed. A control for each root was prepared by vacuum infiltration with buffer only. Leaf samples were treated with the same steps except the chlorophyll was removed with 90% ethanol at the end.

2.5.10 Determination of superoxide concentration

Cassava root tissue that was used for NBT staining was ground with 5 ml 2 M KOH-DMSO using a mortar and pestle. The mixture was centrifuged at 16,000 g for 10 mins at 16 °C and the resultant supernatant was measured at 630 nm against a KOH-DMSO blank. The level of superoxide was determined from a standard curve prepared with known amounts of NBT.

2.5.11 Hydrogen peroxide *in situ* detection

Hydrogen peroxide accumulation in the plant tissue was detected by DAB staining. A thin slice (1 mm) of root tissue was vacuum-infiltrated with1mg/ml DAB solution for 2 mins and incubated at room temperature for 3 hours in the dark. The reaction was stopped with 4 mg/ml chloral hydrate and a photograph was taken immediately.

2.5.12 Determination of hydrogen peroxide concentration

H_2O_2 was determined according to (Velikova et al., 2000) with some modifications. Root tissue (100 mg) was homogenised in 2 ml 0.1% TCA in an ice bath. The homogenate was centrifuged at 12,000 g for 15 mins and the supernatant was collected. 0.5 ml of the supernatant was added to 10 mM potassium phosphate buffer (pH 7.0) and 1 ml potassium iodide. The absorbance at 390 nm was measured in a spectrophotometer. H_2O_2 content in the samples were obtained from a standard curve generated with 20 – 100 µM H_2O_2.

2.6   Reagents and solutions

2.6.1   Cassava Basic Medium (CBM)
One litre CBM consist of

Sucrose	20 g
Murashige and Skoog (including vitamins)	4.4g
$CuSO_4$	0.002 mM
Gelrite	3 g

The culture medium was adjusted to pH 5.8 and autoclaved to sterilize. It was then poured to the height of 1.0-1.5 cm in a 330 ml sterile container and left to cool in the laminar flow hood. CBM was stored at room temperature.

2.6.2   DNA extraction reagents
The DNA extraction buffer contains

Tris-HCl pH 8	0.5 M
EDTA pH 8	0.01 M
SDS	2%
LiCl	0.1 M

Before use, 50 µl of 20 mg/ml Proteinase K was added to a final concentration 10 µg/ml

2.6.3 RNA extraction reagents

The RNA extraction buffer consists of:

CTAB	2% (w/v)
PVP K-30 (soluble)	2% (w/v)
TrisHCl pH 8	100 mM
EDTA	25 mM
NaCl	2M
spermidine (free acid)	0.5 g/l
*β-mercaptoethanol	2% (v/v)

Spatulas, magnetic stirrers and all glassware used in preparation were sterilized. The reagents were dissolved in double-sterilized DEPC-treated water and sterilized once again in an autoclave. A magnetic stirrer was left in the solution because prior to use the buffer must be homogenized.

* Added just before use.

2.6.4 Southern Blotting Reagents

(i)   B1

Maleic acid	100 mM
NaCl	150 mM

Adjusted to pH 7.5. For 1L 11.6 g maleic acid and 8.766 g NaCl were dissolved in sterile distilled water. The pH was adjusted with 10M HCl and the solution was sterilized by autoclave.

(ii)   B2

B2 or blocking buffer was made by adding 1 g blocking reagent (Roche) to 100 ml B1 in two 50 ml Falcon tubes. The tubes were heated to 70°C in a water bath and vortexed several times to facilitate dissolution. It was cooled to room temperature before use.

B3 (equilibrating buffer)

TrisHCl (pH 9.5)	100 mM
NaCl	100 mM
$MgCl_2$	50 mM

The 1 M stock of each solution was prepared separately and autoclaved to sterilize. 50 ml B3 was prepared by mixing 5 ml of 1 M Tris-HCl, 5 ml 1 M NaCl and 2.5 ml 1 M MgCl$_2$ and made up to the final volume with sterile distilled water. Fresh preparation was required and the final pH was checked before use.

(iii)   Wash buffer (WB)

Wash buffer was prepared by adding 3 ml Tween 20 to 1 litre B1. This was stored at room temperature.

(iv)   20X SSC

Sodium citrate   300mM
NaCl   3 M

To prepare 1 litre of this solution 88.23 g of sodium citrate and 175.32 g of NaCl were mixed in sterile distilled water. The pH was adjusted to 7.6 before autoclaving.

(v)   Depurinating solution

1 litre depurinating solution was prepared by adding 25 ml HCl (37%) to 975ml sterile distilled water. The final concentration of this solution is 250 mM HCl. Stored at room temperature.

(vi)   Denaturing solution

NaOH   500 mM
NaCl   1.5 M

It was prepared by mixing 20 g NaOH and 87.66 g NaCl in a final volume of 1 litre sterile distilled water. It was then autoclaved and stored at room temperature.

(vii)   Neutralisation solution

Tris   500 mM
NaCl   1.5 M NaCl
EDTA   1 mM

For 1 litre preparation, 60.57 g Tris, 87.66 g NaCl and 0.3724 g EDTA were dissolved in sterile distilled water and made up to 1 litre.

(viii)   W1 solution

SSC   2X
SDS   0.1%

This solution was prepared by slowly adding 10 ml 10% SDS to 100 ml 20X SSC in a sterile bottle and making up to 1 litre. Shaking must be avoided to prevent bubble formation.

(ix)   W2 solution

SSC   0.2X
SDS   0.1%

This solution was prepared by slowly adding 10 ml 10% SDS to 10 ml 20X SSC in a sterile bottle and making up to 1 litre. Shaking must be avoided to prevent bubbles formation.

(x)   W3 solution

SSC   0.1X
SDS   0.1%

This solution was prepared by slowly adding 10 ml 10% SDS to 5 ml 20X SSC in a sterile bottle and making up to 1 litre. Shaking must be avoided to prevent bubbles formation.

CHAPTER 3

Characterisation of transgenic cassava

3.1   Introduction

3.1.1   Strategy for cassava transformation

It is generally accepted that plant transformation is a difficult task. With exception of *Arabidopsis* and tobacco, transformation of some plant species remains a challenge. Identification of target genes is difficult since the number of full sequences of plant genomes is limited compared to those from other kingdoms. Depending on life cycle of a plant, transformation can take over a year before the product of transformation can be evaluated. The choices of cultivar, cloning strategy, transformation method, selectable marker, as well as gene promoter to drive expression of target genes are key in determining the success of transformation.

Cassava was believed to be recalcitrant to transformation until the mid 1990s. The initial effort towards developing efficient transformation focused on gene transfer at the tissue level (Franche et al., 1991, Luong et al., 1995). The first successful transformation that resulted in fully developed cassava plant was achieved in 1995 (Sarria et al.) and afterwards more transformations of cassavas were attempted. Various modifications were also made in the gene transfer method aiming to improve regeneration of transgenic cassava (Gonzalez et al., 1998, Raemakers et al., 1996, Schopke et al., 1997) and to achieve higher transformation frequencies. The use of selectable marker has also extended from antibiotic and herbicide-resistance (Arango et al., 2010, Gonzalez et al., 1998, Siritunga and Sayre, 2004, Siritunga and Sayre, 2003) to positive selection using mannose (Zhang et al., 2000) and morphological markers (Saelim et al., 2009). Due to the need for the expression of target genes in certain cell types, the use of tissue-specific promoters from other plant system was explored (Arango et al., 2010, Narayanan et al., 2011, Siritunga and Sayre, 2003). Additionally, promoters from cassava itself have also been identified and characterised (Zhang et al., 2003b) but their regulatory functions were relatively weaker than the conventional cauliflower mosaic virus CaMV35S promoter (Arango et al., 2010) making them less favoured in transformation of cassava.

3.1.2 Target genes and promoter used in this study

Previous studies showed oxidative stress is associated with development of PPD symptoms in cassava roots but little is known about the mechanisms. It is thought that wounding sites introduced during harvest expose cassava roots to oxygen and rapidly generate reactive oxygen species (ROS) (Beeching et al., 1998). In an efficient ROS detoxification system, excessive ROS are converted to harmless products to bring down ROS to a safe level but this is not observed in cassava root system.

$$O_2 \longrightarrow O_2^- \xrightarrow{\text{SOD}} H_2O_2 \xrightarrow{\text{CAT}} H_2O + \tfrac{1}{2} O_2$$

$$\xrightarrow{\text{APX}} 2\,H_2O$$

Precursor $\xrightarrow{\text{GAR}}$ AA $\rightleftarrows$ MDHA (MDHAR)

DHA (DHAR)

Cysteine $\xrightarrow{\text{GCS}}$ GSH $\rightleftarrows$ GSSG (GR)
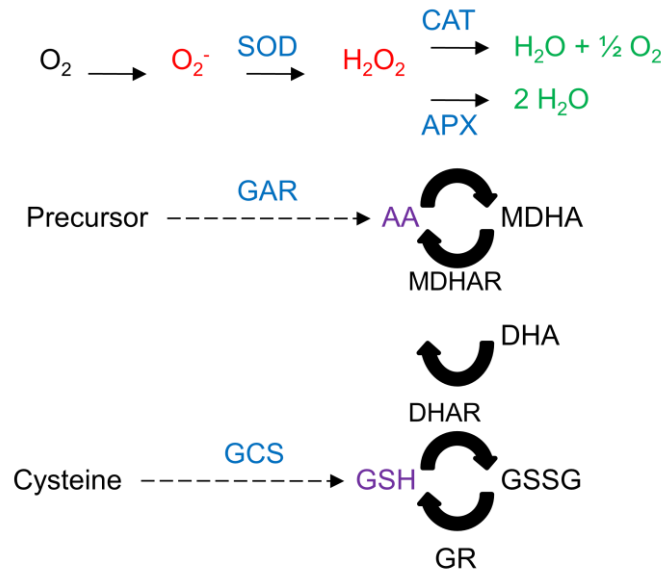
Figure 3.1 The cellular pathways for ROS removal in plants. Superoxide dismutase (SOD) detoxifies superoxide radicals (O_2^-) to generate hydrogen peroxide (H_2O_2) and oxygen. In this form, it is transformed into harmless products by catalase (CAT) and ascorbate peroxidase (APX). Reduction of ascorbate (AA) by APX produces monodehydroascorbate (MDHA) while non-enzymatic cleavage produces dehydroascorbate (DHA). MDHA and DHA are reduced back to AA by monodehydroascorbate reductase (MDHAR) and dehydroascorbate reductase (DHAR), respectively, in which the latter utilises reduced glutathione (GSH) as substrate and simultaneous reduction of glutathione disulfide (GSSG) by glutathione reductase (GR). Galacturonic acid reductase (GAR) and ɣ-glutamyl cysteine synthetase (GCS) are the main enzymes involved in biosynthesis of ascorbate and glutathione, respectively. Highlighted in blue fonts are enzymes involved in this study. Serrated arrow indicates multiple reactions.

In harvested cassava storage roots, ROS detoxification is either delayed or insufficient, causing excessive ROS generation which lead to oxidative stress and eventually irreversible cellular damage (Reilly et al., 2003). As wounding during harvest often is

unavoidable, enhancement of ROS detoxification machinery in developing roots was conceived as a feasible strategy to increase resistance against oxidative stress. To achieve that, five main genes in the common plant cellular pathway of ROS detoxification were selected as the target genes in transformation of cassava TMS60444.

3.1.2.1 Superoxide dismutase

Superoxide dismutase (SOD) is a metalloenzyme (SOD; EC 1.15.1.1) ubiquitous in plant cells. SOD is highly abundant in ROS-generating cellular compartments, thus it is claimed to be the first line of defence against ROS. This enzyme is classified into three groups based on the metal ion co-cofactors required in active sites. MnSOD (co-factor with manganese) is abundant in the mitochondrion where ROS are generated as by-products in the electron transport chain. FeSOD (co-factor with iron) is mostly found in the chloroplast, where it functions to maintain ROS homeostasis in photosystem-II. CuZnSOD (co factor with copper-zinc complex) is known to be the most ubiquitous as it is found in cytosol, chloroplast and peroxisomes (Alscher et al., 2002). Regardless of metal co-factor used, all SODs catalyse the dismutation of superoxide radicals to H_2O_2 and oxygen. All three classes of SOD are present in *A. thaliana* and rice (Schomburg et al., 2013) but to date only two SOD genes have been isolated and characterised from cassava, MecSOD1 (Lee et al., 1999) and MecSOD2 (Shin et al., 2005). Both SOD genes in cassava are CuZn type, cytosolic, highly expressed in cassava stems and lowly expressed in leaves (Lee et al., 1999, Shin et al., 2005).

It appears that SOD confers resistance to abiotic stresses in non-specific ways. For example, overexpression of MnSOD (Gusta et al., 2009) and CuZnSOD (Tang et al., 2006) equally showed resistance to heat stress. On the other hand, expression of pea MnSOD in rice plants showed resistance mainly to drought (Wang et al., 2005) while cedar MnSOD expression in poplar plants showed resistance to salt stress (Wang et al., 2010). However, the magnitude of expression may vary; for example, CuZnSOD1 and CuZnSOD2 in sunflower responded to heat, chilling and wounding stress differently in that the latter was expressed higher (Fernández-Ocaña et al., 2011). Despite its unspecific expression, SOD has been an attractive target for increasing oxidative stress resistance and has shown a degree of success in crops like rice (Prashanth et al., 2008), sugarbeet (Tertivanidis et al., 2004) and canola (Gusta et al., 2009).

In cassava, MecSOD2 is expressed at low level in storage roots compared to MecSOD1 (Lee et al, 1999: Shin et al 2005) but responding to wounding more

substantially than MecSOD1. *In situ* detection of ROS in cassava roots revealed accumulation of superoxide radicals within 15 minutes after wounding; therefore, increasing MecSOD2 expression with an aim to complement MecSOD1 expression is seen as a good strategy for enhanced protection against superoxide. Nonetheless, it is important to keep in mind that the by-products of SOD reactions might also accumulate rapidly as a result of over expression, and that these are also potentially damaging to the cell. This accounts for the increasing attempts to co-express SOD with other antioxidative genes to overcome H_2O_2 toxicity in the cells (Melchiorre et al., 2009, Srinivasan et al., 2009, Tang et al., 2006, Xu et al., 2013a).

3.1.2.2 Catalase

Catalase (CAT; EC 1.11.1.6). is a common enzyme found in both plant and animal tissues. In fact, CAT is one of the first enzymes discovered (Loew, 1900).

CAT exists in three forms – the heme-binding catalase, Mn-catalase and peroxidase catalase. The first form is commonly referred to as typical CAT which requires heme (iron) at its active sites. Although CAT has lower affinities for H_2O_2 than APX, it is known as one of the most efficient enzyme found in cells. The difference in affinities suggests that APX functions to modulate ROS for signalling while CAT functions to remove excess ROS (Noctor and Foyer, 1998). In tobacco plants, application of the CAT inhibitor aminotriazole caused CAT deficiency and this led to severe oxidative stress symptoms despite high APX activity (Gechev et al., 2002). This implies that CAT functions as a sink for H_2O_2 in plants (Willekens et al., 1997).

In cassava, one CAT gene named MecCAT1 has been isolated and characterised so far, but Southern analysis predicted more CAT sequences in the cassava genome (Reilly et al., 2001). Measurement of MecCAT1 transcript accumulation in cassava roots showed stronger CAT expression in the low-PPD cultivar (TMS 30572) than in high-PPD cultivar (MCol 22), suggesting its antioxidative role. In the same microarray data mentioned above, MecCAT1 showed an increase in expression during PPD, being identified as one of the highly upregulated genes in ROS turnover category (Reilly et al., 2007).

3.1.2.3 Ascorbate peroxidase

An alternative scavenging pathway for H_2O_2 is decomposition is by ascorbate peroxidase. Ascorbate peroxidase (APX; EC 1.11.1.11) is a heme-containing peroxidase present in most organisms. H_2O_2 formed as a by-product of SOD reactions is scavenged by APX and its substrate, ascorbate (Asada, 1992). APX has been found in various cellular compartments but its role in ascorbate metabolism is mostly studied in the chloroplasts. Foyer and Halliwell (1976) proposed the redox cycling of ascorbate in the chloroplast called ascorbate-glutathione pathway (later known as Halliwell-Asada pathway) and highlighted APX as the major enzyme in the pathway.
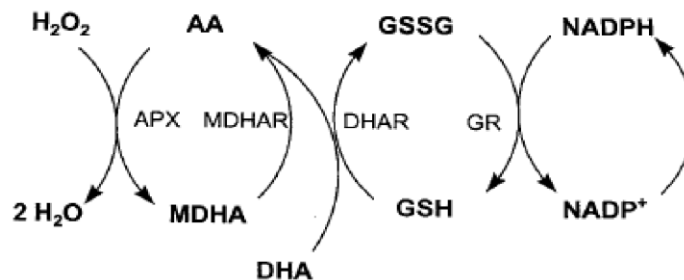
Figure 3.2 Halliwell-Asada pathway as described by May et al. (1998). Reduction of ascorbate (AA) by APX produces monodehydroascorbate (MDHA), while non-enzymatic cleavage produces dehydroascorbate (DHA). MDHA and DHA are reduced back to AA by monodehydroascorbate reductase (MDHAR) and dehydroascorbate reductase (DHAR), respectively, in which the latter utilises glutathione (GSH) as substrate and simultaneously performs NADPH-mediated reduction of glutathione disulfide (GSSG) by glutathione reductase (GR).

To date only one APX gene has been identified in cassava (Reilly et al., 2007) but in the Genbank database there are two accessions of the gene available; MecAPX2 (AY973622) and MecAPX3 (AY973623). However, they appear to be referring to the same sequence and are used interchangeably in many studies. Even so, MecAPX3 is preferred over MecAPX2 in the present study as it is also used in other database including PeroxiBase (Fawal et al., 2013).

Early biochemical studies revealed PPD-related peroxidase activity in cassava storage roots (Tanaka et al., 1983) and its localisation in the epidermis, cortex and xylem tissues (Reilly et al., 2004). Northern blot analysis showed increased of peroxidase mRNA transcript 2-4 days after harvest (Reilly et al., 2004). Consistent with these findings microarray data prepared from deteriorating storage roots showed 1.7- and 1.5-fold increase of MecAPX3 and a secretory peroxidase transcript, respectively, 1

day after harvest (Reilly et al., 2007). While there is no specific evidence indicating that APX could delay post harvest damage in cassava storage roots, overexpression of APX in some plants has led to high resistance to various oxidative-related stresses including salinity and drought (Badawi et al., 2004), heat (Srivastava et al., 2012), pathogen invasion (Sarowar et al., 2005) and high light intensities (Murgia et al., 2004). These findings justify further analyses of APX expression profiles and their roles in cassava in relation to PPD. Besides, overexpression of APX is encouraging as it has higher affinity for H_2O_2 than catalase.

3.1.2.4 Galacturonic acid reductase

H_2O_2 degradation by APX in the Halliwell-Asada pathway involves ascorbate (AA) which serves as a reducing agent. The structure of AA was described in 1933 yet its biosynthetic pathway remains unclear. It has been established that AA in animals and plants is derived from D-glucose, but there are multiple, continuously revised pathways proposed for plants (Figure 3.3).

The L-galactose pathway is considered the predominant pathway in green tissue of higher plants where all the genes involved are already characterised (Oller et al., 2009). In this pathway, AA is synthesised from GDP-D-mannose via GDP-L-galactose, L-galactose, and L-galactono-1,4-lactone (Wheeler et al., 1998). The alternative pathways for AA biosynthesis are the L-gulose and the Salvage pathway. The L-gulose pathway, was proposed based on the evidence that GDP-D-mannose could be converted not only to GDP-L-galactose, but also to GDP-L-gulose, which subsequently converted to L-gulono-1,4-lactone, a structure equivalent to L-galactono-1,4-lactone (Wolucka and Van Montagu, 2003, Wolucka and Van Montagu, 2007). The full set of enzymes converting intermediates in this pathway is largely unknown. The other pathway called the Salvage or "galacturonate" pathway also is poorly studied. Only one enzyme called galacturonic acid reductase (GAR; EC 1.1.1.19) catalysing D-galacturonate to L-galactono-1,4-lactone has been elucidated in this pathway (Linster and Clarke, 2008, Xu et al., 2013c).
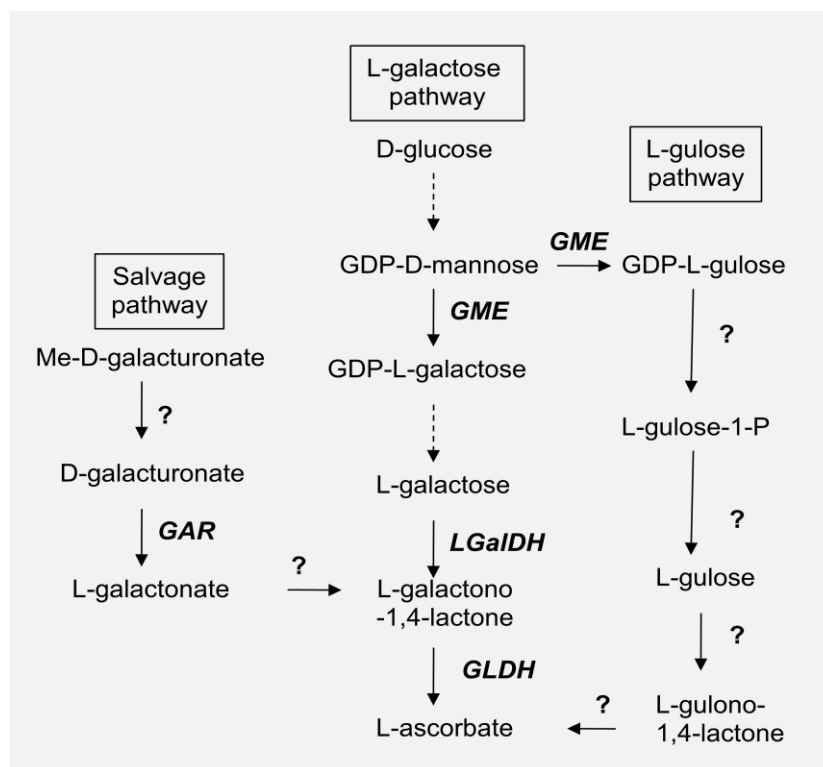
Figure 3.3 Biosynthetic pathways of ascorbate in plant. Serrated arrow indicates multiple reactions, ? indicates unknown enzyme. *GME* = GDP-D-mannose-3',5'-epimerase, *LGalDH* = L-galactose dehydrogenase, *GLDH* = L-galactono-1,4-lactone dehydrogenase, *GAR* = galacturonic acid reductase

It is curious that if the alternative pathways for AA biosynthesis cause its accumulation in other tissues. For example, overexpression of gene encoding GAR (Genbank accession AF039182) under the control of the CaMV35s promoter in strawberry caused increase in the corresponding mRNA transcript that reflected changes of fruit AA content during ripening, suggesting its function in AA biosynthesis. Heterologous expression of the same gene in *A. thaliana* that resulted in 2- to 3-fold increase of AA content supported this interpretation (Agius et al., 2003). An attempt to manipulate AA in cassava using this gene seems promising. A higher AA content was also achieved through the overexpression of this gene in potato tubers. Additionally, the transgenic potatoes showed enhanced tolerance towards various stress conditions compared to the untransformed plants (Hemavathi et al., 2009).

3.1.2.5 ɣ-glutamylcysteine synthetase

Apart from ascorbate, the Haliwell-Asada pathway contains another non-enzymatic component which is glutathione. Reduced glutathione (GSH) and its oxidised form (GSSG) is a major anti-oxidant that primarily functions to protect the photosynthetic apparatus though its ubiquity in non-photosynthetic cells suggests its wide-ranging functions in plant cells including embryo survival (Cairns et al., 2006).
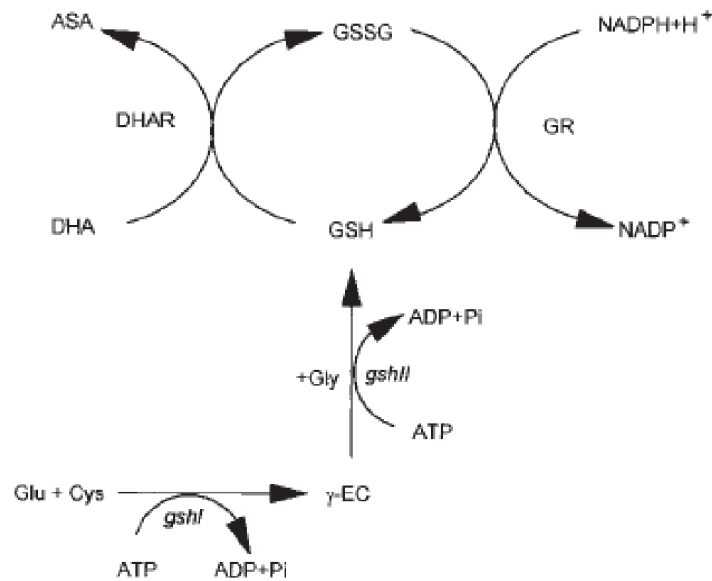
Figure 3.4 Biosynthesis of glutathione (GSH) in *Arabidopsis*. Abbreviations; Glu = L-glutamic acid, Cys = L-cysteine, Gly = glycine, ɣ-EC = ɣ-glutamylcysteine, GR = glutathione reductase, GSSG = glutathione disulphide, ASA = ascorbic acid, DHA = dehydroascorbate, DHAR = dehydroascorbate reductase. Figure adapted from Creissen et al. (1999).

GSH which is a tripeptide consisting of L-cysteine, L-glutamic acid, and glycine is synthesised by two ATP-dependent steps in the chloroplast and cytosol. In the first step, *gshI* or ɣ-glutamylcysteine synthetase (GCS; EC 6.3.2.2) catalyses the formation of ɣ-glutamylcysteine (ɣ-EC) from L-cysteine and L-glutamic acid. In the second step glycine is added to the intermediate product ɣ-EC by *gshII* or glutathione synthetase (GSH-S) (EC 6.3.2.3) (Figure 3.4).

The antioxidative role of GSH is widely accepted but its function is not fully understood. It is proposed that this is associated with the dynamic ratio of GSH to GSSG. In

unstressed plant cells, GSH/GSSG ratio is 9:1 where it is considered in its best redox potential to effectively scavenge ROS. The GSH/GSSG ratio changes in response to various environmental stress including photo-oxidative stress (Melchiorre et al., 2009), heavy metal (Li et al., 2006), high temperature and herbicides (Song et al., 2005). Under the stressed conditions GSH is reduced to glutathione disulfide (GSSG) causing simultaneous reduction of DHA by DHAR to form ascorbate (ASA) in the ascorbate-glutathione pathway. Alternatively GSH is reduced to GSSG by detoxification of H_2O_2 by glutathione peroxidase (GPX), but this occurs at a very low rate compared to that in animals cells due to the predominance of the ascorbate-glutathione cycle in plants (Foyer and Noctor, 2000). GSH is replenished by glutathione reductase (GR).

GSH biosynthesis is primarily controlled by GCS activity and cysteine availability (Noctor et al., 2002), although increasing evidence shows possible regulation by several factors. A GCS1 (*gshl*) knockout in *Arabidopsis* resulted in GSH deficiency (Cairns et al., 2006), and co-expression of GCS1 and GCS2 in maize caused a 4-fold increase of GSH content (Gómez et al., 2004). Unsurprisingly, wheat protoplasts over-expressing GR showed an increased in GSH and in the GSH/GSSG ratio when subjected to light stress (Melchiorre et al., 2009). In the same work, GSH content decreased as result of H_2O_2 build up. In contrast to this finding, GSH level was increased by H_2O_2 in CAT-deficient plants and accompanying this was upregulation of genes for enzymes involved in the formation cysteine and other amino acids (Queval et al., 2009). The conflicting findings about the regulation of GSH suggest its complex interactions with other components of the ROS scavenging machinery as well as the influence of environmental factors, which requires further experimental effort in the future. However, the curiosity to elucidate GSH modulation is not the objective of this research, but rather to explore the role of GSH in the PPD of cassava using the key enzyme GCS. Since GCS has not been characterised in cassava, *Arabidopsis* GCS (*gshl*) was selected as the target gene.

3.1.2.6 Patatin promoter
The choice of promoter is as equally important as is the choice of the target genes. Since the aim of the target genes expression was to improve anti-oxidant status of cassava storage root the ability of the promoter to drive high expression in the target tissue is crucial. Meanwhile, the responsiveness to PPD–related stresses would be an added advantage.

A number of root-specific promoters have been identified in cassava and a few meet the criteria for our promoter. p15 isolated from cassava root cDNAs was shown to have related functions to cytochrome P450 proteins and found to be highly expressed in the starch-rich parenchyma cells from roots and xylem vessels of vascular tissues from leaves (Zhang et al., 2003b). Curiously, expression of uidA gene using this promoter in a carrot root system showed the lowest level of Gus when compared to other promoters including the constitutive promoter CaMV35s (Arango et al., 2010). Other tissue-specific promoters are p54 and its homologue Mec1 coding for glutamic acid-rich proteins (Pt2L4), also shown to highly expressed in root tissue systems of cassava and *Arabidopsis* (de Souza et al., 2009, de Souza et al., 2006, Zhang et al., 2003b). Fairly recently, a light- and sucrose-inducible promoter containing the cassava granule-bound starch synthase (GBSS) was isolated and showed a remarkable increase of gene marker activities in the storage roots compared to other tissues (Koehorst-van Putten et al., 2012). These promoters are interesting and have potential; however, when this work was started they were insufficiently characterised to be considered as strong candidates. In order to achieve optimal expression of the target genes and to allow straightforward assessment of their performance an established tuber-specific promoter patatin was chosen.

Patatin is a storage protein found in potato (*Solanum tuberosum*) that unusually possesses lipid acyl hydrolase (LAH) activities. This enzyme functions to catalyse the cleavage of fatty acids from membrane lipids (Andrews et al., 1988, Macrae et al., 1998) suggesting a dual function against pathogens in potato tubers. Patatin sequences are retrievable from many online databases and the related information has been documented. The organ specificity is confirmed where up to 20 times more activity was reported in potato tubers compared to the roots and leaf, stem and roots (Rocha-Sosa et al., 1989, Naumkina et al., 2007). In cyanogen-reduced transgenic cassava patatin has driven 2-20 fold increase of hydroxynitrilelyase (HNL) mRNA transcript relative to untransformed plants and 5-6 fold increase relative to those driven by the CaMV35s promoter (Narayanan et al., 2011). Heterologous patatin-driven Gus and anti-oxidant gene expression in non-storage roots like those of *Arabidopsis* has been achieved and reported, including with the expression cassette used in this study (Page, 2009). The utilisation of patatin is also intriguing since it has been found to be resistant to ROS *in vitro* (Liu et al., 2003).

3.1.3 Construction of expression plasmids and generation of transformants

This section will briefly introduce the expression plasmids, their creation, as well as development of transgenics that were produced previously by Page (2009) and formed the basis of much of the work in this thesis.
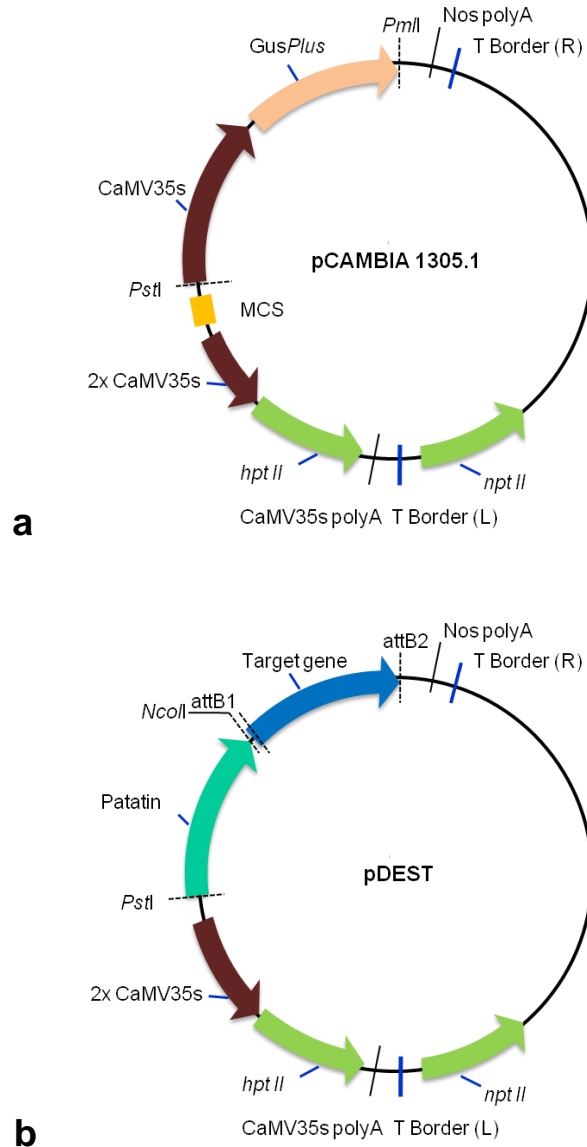
Figure 3.5 (a) A simplified map of unmodified pCAMBIA 1305.1 showing T Borders (blue thick lines), *GusPlus r*eporter gene, CaMV35S promoter, multiple cloning site (MCS), hygromycin resistance gene (*hptII*) and neomycin phosphotransferase (*nptII).* The positions of restriction enzymes *Pst*I and *Pml*I used for removal of CaMV35S. *GusPlus are* indicated **(b)** The removed fragment was replaced by a patatin:target gene fragment to generate a modified expression plasmid (pDEST). The positions of *Pst*I and *Nco*I used to remove Patatin sequence are shown (b). Figure reproduced from Page (2009).

Following identification and isolation of the potential target genes, a Gateway-compatible plasmid was created from pCAMBIA 1305.1 cloning vector. Digestion of the plasmid with restriction enzyme *Pst*I and *Pml*I excised CaMV35S promoter and *GusPlus* sequence from the vector allowing incorporation of the Patatin promoter (Page, 2009). Addition of Gateway cassette with partial att sites upstream Patatin sequence converted it to be Gateway compatible enabling attB-containing target sequences to be inserted (Figure 3.5).

Table 3.1 Target sequences used in expression plasmids. Target sequences are coding region of genes encoding the five enzymes that are involved in the main cellular pathways for ROS removal in plants.

Expression plasmid	Target gene	Source of organism	Genbank accession	cDNA length (bp)
pDEST:SOD	MecSOD2	*M.esculenta*	AY642137	459
pDEST:APX	MecAPX3	*M.esculenta*	AY973623	753
pDEST:CAT	MecCAT1	*M.esculenta*	AF170272	1479
pDEST:GCS	*gshI*	*A.thaliana*	AF419576	1569
pDEST:GAR	FaGAR	*F.ananassa*	AF039182	960
pDEST:*GusPlus*	*GusPlus*	*Saccharomyces*	AF354045	2078
pDEST:*GusPlus* (-Pat)	*GusPlus*	*Saccharomyces*	AF354045	2078

The final version of expression plasmid containing target gene (Table 3.1) was independently introduced into cassava cultivar TMS60444 via *Agrobacterium*-mediated transformation of friable embryogenic callus (FEC). In order to evaluate the expression pattern and performance of the Patatin promoter, two Gus reporter plasmids were crafted and transformed in cassava. pDEST:*GusPlus* was constructed by simple replacement of target sequence with *GusPlus* sequence whereas pDEST:*GusPlus* (-Pat) was created by digestion of pDEST:*GusPlus* with restriction enzymes *Pst*I and *Nco*I to remove Patatin (Figure 3.5). Cassava transformation was carried out by Bull (2011).

3.1.4 Management of samples

Transformations of TMS60444 with the seven constructs described above produced 284 *in vitro* plantlets (Bull, 2011). Each of which was a putative independent transgenic line carrying separate target genes; these were labelled as Pat:target gene (for example Pat:SOD). All lines were indexed by Pat:target gene, transformation group and plantlet number. Transformation group either represents separate transformation event or FEC used. For example Pat:SOD C2 is the second plantlet generated from the third transformation event with pDEST:SOD.

Table 3.2 Transgenic plants used in this research. Number of surviving plants was recorded at the beginning of research being conducted

Transgenic	Expression plasmid	No of groups	No of plantlets regenerated	No of surviving plantlet	% of surviving plantlet
Pat:SOD	pDEST:MecSOD2	4	32	24	75
Pat:APX	pDEST:MecAPX2	5	31	31	100
Pat:CAT	pDEST:MecCAT1	4	56	41	73
Pat:GCS	pDEST:AtGCS	3	30	30	100
Pat:GAR	pDEST:FaGAR	3	72	49	68
Pat:Gus	pDEST:*GusPlus*	2	26	26	100
Pat (-): Gus	pDEST:*GusPlus* (-Pat)	1	37	37	100

All the regenerated lines showed normal phenotypic characteristics upon early sub-culturing. However, repeated sub-culturing occasionally led to loss of plantlets due to contamination, which is an ever-present risk in tissue culture maintenance. This explains how one putative line which had been selected could not be subjected to further analysis because of the loss of parent line.

3.2   Research aim

This chapter is concerned with the preliminary characterisation of the previously transformed cassava plants. The genetic content of the plants will be assessed for successful T-DNA integration with an aim to identify single-insert independent lines. These lines will be grown to mature cassava plants to produce storage roots and to enable full characterisation of their phenotypes. The detailed effects of the various gene-constructs will be fully explored in subsequent chapters.

3.3 Results

3.3.1 Stable integration of the gene construct in the cassava genome

Prior to going on to detailed analyses of the putative transgenic lines it was essential to confirm their transgenic nature and identify independent single-insert lines. Therefore, the transgenic cassava plants were subjected to molecular assays to verify transformation using genomic DNA extracted from cassava leaf tissue. The transgenics are as listed in Section 2.1.1 but for simplification only selected transgenic lines are presented.
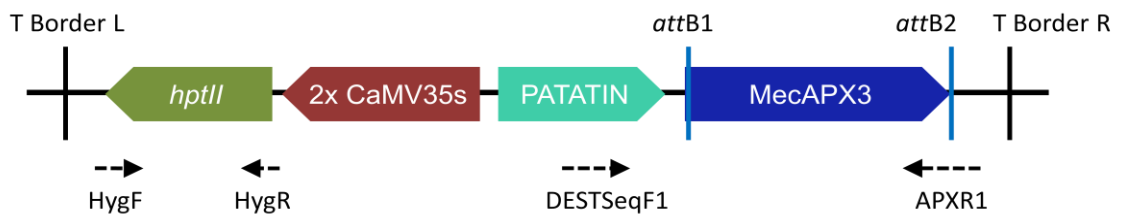
Figure 3.6 Composition of T-DNA region of pDEST:APX. *hptII* encodes gene for hygromycin resistance. The positions of primers for amplification of *hptII* and transgene MecAPX3 are indicated.

The plants were checked for presence of foreign genes in the genome to distinguish transformed plants from the non-transformed and then to confirm the integration of the correct Pat:target gene fragment. This involved a two-step screening through amplification of genomic DNA by PCR. The first screening was amplification of the *hptII* and the second screening was amplification of the respective target gene. Since both constitute the T-DNA region of the expression plasmid, they should only be detected in transformed plants. Unlike GCS- and GAR-transformants which contain exogenous target gene, SOD-, CAT- and APX-transformants contain targets gene that were derived from cassava itself. Therefore, with these transformants it is crucial to discriminate from endogenous genes to avoid false positive amplification. For that reason, the sequence flanking the 180 bp downstream patatin promoter region was used for creation of the forward primer DESTSeqF1, whereas nucleotides flanking target gene's stop codon and attB2 were designed as the reverse primer. The locations of these primers in Pat:APX are shown in Figure 3.6. This strategy was established as a rapid screening method for all transgenic lines. The results of PCR genotyping with *hptII* and individual target gene (now termed as transgene) are shown below. Identification of Pat:Gus and Pat(-):Gus will be described in Chapter 5.

Transgenic lines which amplified both the *hptII* and the correct transgene were referred to as 'positive transformants' to indicate successful uptake of Pat:target gene fragment. PCR analysis of Pat:SOD using *hptII*- and transgene-specific primers resulted in amplification of 1 kb and 0.7 kb fragments respectively. All 24 of Pat:SOD lines amplified *hptII* gene while only 23 amplified MecSOD2, this corresponds to 96% positive transfomants (Figure 3.7).
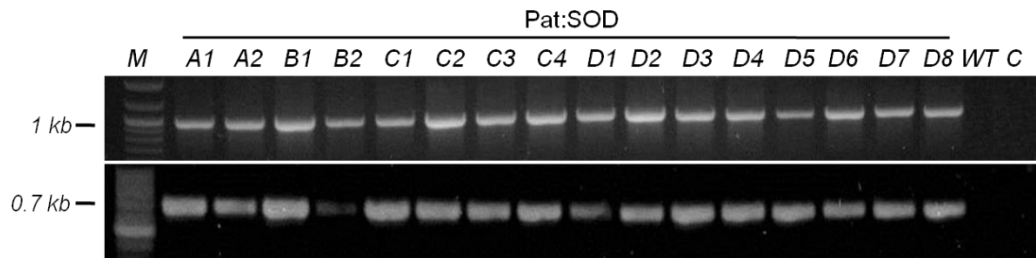
Figure 3.7 Amplification of *hptII* gene (upper panel) with HygF and HygR and MecSOD2 (lower panel) with DESTSeqF1 and SODR1 primers. Genomic DNA extracted from cassava leaf tissue of Pat:SOD A1-D8. DNA marker (M) size, wild type TMS60444 (WT) and no template control (C) shown.

In Pat:APX, 29 out of 31 putative transgenics amplified *hptII,* 27 amplified transgene MecAPX2. Since only 26 plants amplified both genes, this reduced the percentage of positive transfomants to 84% (Figure 3.8).
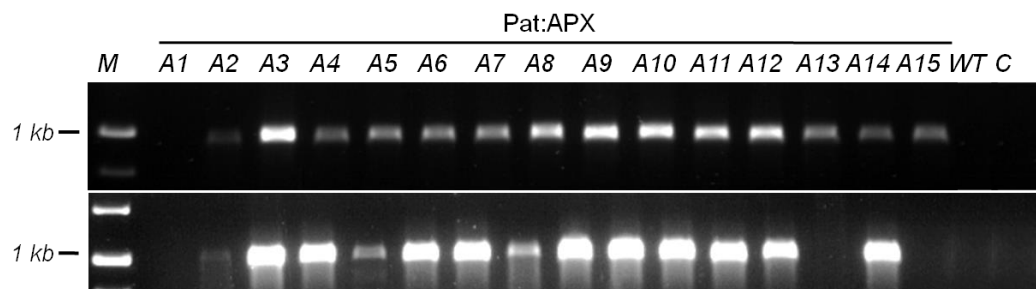
Figure 3.8 Amplification of *hptII* gene (upper panel) with HygF and HygR and MecAPX3 (lower panel) with DESTSeqF1 and APXR1 from genomic DNA extracted from cassava leaf tissue of Pat:APX A1-A15. DNA marker (M) size, wild type TMS60444 (WT) and no template control (C) shown.
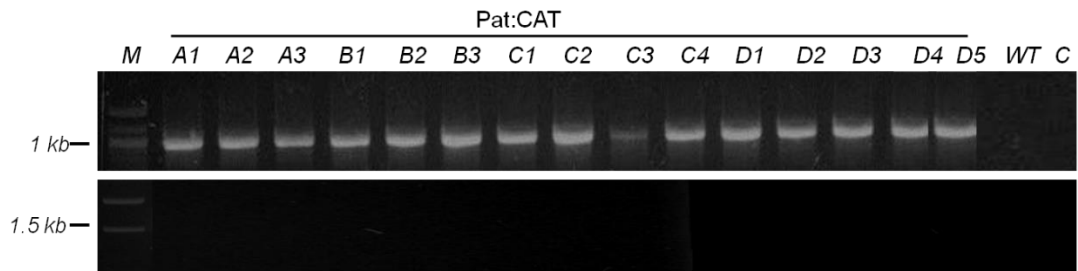
Figure 3.9 Amplification of *hptII* gene with HygF and HygR from genomic DNA extracted from cassava leaf tissue of Pat:CAT A1-D5. Amplification with DESTSeqR1 and CATR1 did not produce amplicons. DNA marker (M) size, wild type TMS60444 (WT) and no template control (C) shown.

Transformation of Pat:CAT was obviously not successful. Although nearly all putative CAT trangenic lines amplified *hptII* but disappointingly none amplified the 1400 bp MecCAT1 transgene (Figure 3.9). Later in this thesis I return to these transgenics in order to identify what may have occurred.
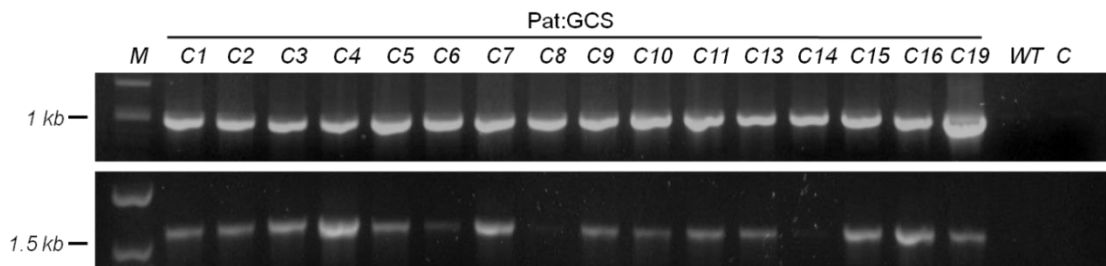
Figure 3.10 Amplification of *hptII* gene (upper panel) with HygF and HygR and *gshI* (lower panel) DESTSeqF1 and GCSR1 from genomic DNA extracted from cassava leaf tissue of Pat:GCS C1-C16. DNA marker (M) size, wild type TMS60444 (WT) and no template control (C) shown.

All Pat:GCS putative transgenic lines analysed amplified *hptII* gene but 3 lack the 1749 bp GCS transgene PCR product reducing the percentage of positive transformants to 87% (two shown in Figure 3.10). Pat:GAR had the highest number of faulty expression cassettes as 10 putative transgenic lines failed to amplify the GAR transgene despite amplifying the *hptII* gene. This brought down the percentage of positive transformants to only 75% (three shown in Figure 3.11).
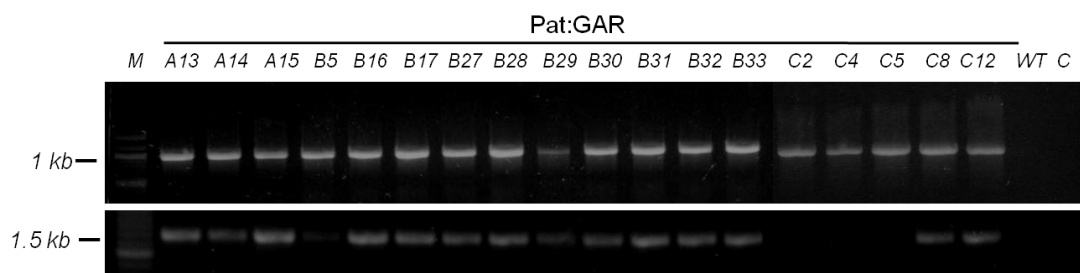
Figure 3.11 Amplification of *hptII* gene (upper panel) with HygF and HygR and FaGAR (lower panel) DESTSeqF1 and GARR1 from genomic DNA extracted from cassava leaf tissue of Pat:GAR A13-C12. DNA marker (M) size, wild type TMS60444 (WT) and no template control (C) shown.

The result of PCR genotyping is summarised in Table 3.3. It appears that Pat:SOD had the highest percentage of positive transformants despite having the least number of surviving lines. In contrast, Pat:GAR which had the highest number of surviving lines had the lowest percentage of positive transformants (excluding the unexpected Pat:CAT lines). Due to the work involved it was decided to reduce the number of the Pat:GAR lines to be analysed closer to the other transgenics.

Table 3.3 Analysis of transgenic lines with PCR. Positive transformants are lines amplified both the *hptII* and the correct transgene.

Transgenic	Total no of lines	*hptII* present	Transgene present	No of positive transformants	Positive transformants (%)
Pat:SOD	24	24	23	23	96
Pat:APX	31	27	29	26	84
Pat:CAT	41	40	0	0	0
Pat:GCS	30	30	26	26	87
Pat:GAR	49	47	39	37	75

In order to get a manageable number of transformants, only lines positive for both the *hptII* and the respective transgene were used for further screening. Next, the transgenics were analysed by Southern blot to determine copy number and to identify independent transgenic lines. Only 15 or 16 lines per transgene were subjected to Southern blot analysis. Genomic DNA extracted from cassava leaf tissue, digested with *HindIII* and hybridised with a DIG-labelled probe. For convenience, all Southern hybridisation reactions were performed with a *hptII*-annealing probe prepared as described in Section 2.3.7. Although this kind of probe may possibly reduce specificity through hybridising to the selectable marker rather than to the transgene of interest, it

is preferred over a transgene probe to eliminate the possibility of hybridising to a gene family. The probe and restriction enzyme were chosen to give only a single, but of variable size, band per insert event; thus the number of hybridising bands reflects the number of inserts per genome, while band size indicates different insertion sites. Therefore, lines with single bands of different size indicate different independent single-insert lines; one of each was selected for further analysis.
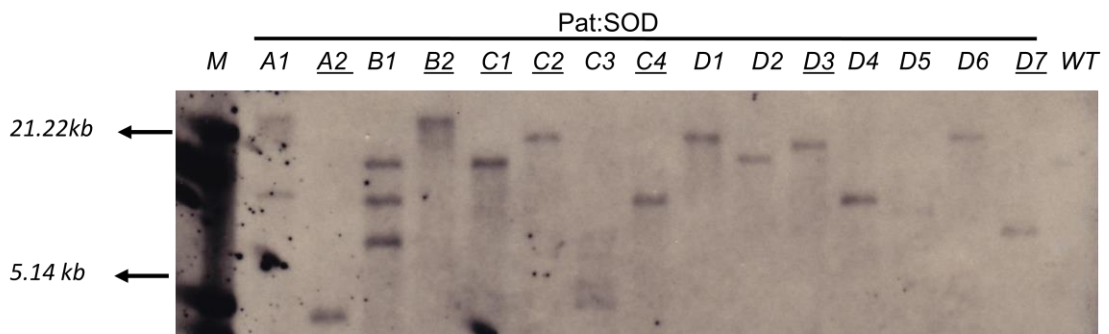
Figure 3.12 Southern hybridisation of *HindIII*-digested cassava genomic DNA of Pat:SOD transgenics with hygromycin probe. Underlined are independent single-insert transgenic lines. DNA (M) marker is shown.

11 out of 16 Pat:SODs examined had a single insertion but only 7 were identified as single-insert independent lines. This represents the majority (69%) of the transformation events. The rest of the lines include a three-insert lines and several poorly hybridising lines (Figure 3.12).
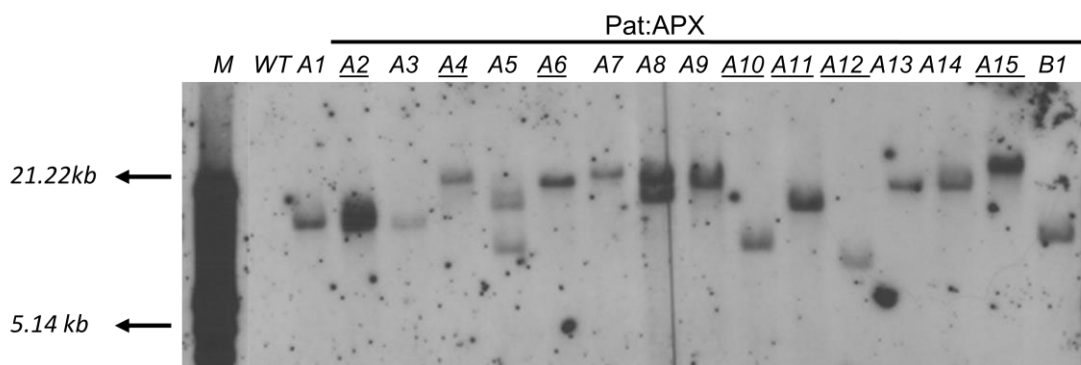
Figure 3.13 Southern hybridisation of *HindIII*-digested cassava genomic DNA of Pat:APX transgenics with hygromycin probe. Underlined are independent single-insert transgenic lines. DNA marker (M) is shown.

Pat:APX had the highest percentage of single insertions as 14 out of 16 or 88% had one insert in their genome. From this, half of them were identified as independent lines (Figure 3.13). The other two lines had two inserts each in the plant genome.
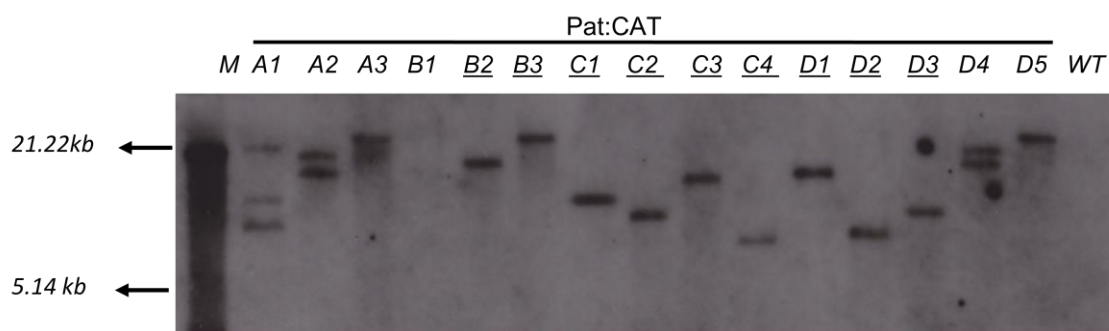
Figure 3.14 Southern hybridisation of *Hind III*-digested cassava genomic DNA of Pat:CAT transgenics with hygromycin probe. Underlined are independent single-insert transgenic lines. DNA marker (M) is shown.

On the other hand, Pat:CAT had the lowest percentage of single inserts among the transgenic analysed in which only 10 out 15 or 67% of the lines were identified as single-inserts. Three of the lines or 20% of the transgenic had 2 inserts while the remaining one line had 3 inserts. Approximately 9 independent lines were identified from this (Figure 3.14). Of course it is important to remember, that in the case of the Pat:CAT lines, the PCR results shown earlier in this chapter suggest that the CAT gene, or at least one of the primer sites is defective or absent. The number of single-insert independent lines is summarised in Table 3.4.

Table 3.4 Plasmid insertion frequency in transgenic cassava. Percentage of single insertion is shown as single insertion often is desired in transformation.

Transgenic	Line tested	Single insertions	Two insertions	Three insertions	% Single insertions	Independent lines
Pat:SOD	16	11	2	1	69	7
Pat:APX	16	14	2	0	88	7
Pat:CAT	15	10	3	1	67	9

Pat:GCS and Pat:GAR transgenics copy number had been checked and reported previously, using similar methods (Bull, 2011); hence the lists of independent lines instead of hybridisation pictures are presented here. Approximately 10 independent lines were identified from Pat:GCS and 9 from Pat:GAR. Pat:GCS independent lines consist of Pat:GCS C2, C5, C6, C10, C11, C12, C13, C16, C19 and Pat:GCS B4. Pat:GAR independent lines include Pat:GAR A13, A15, B16, B27, B29, B30, B33, C8

and C12. Characterisation of transgenic cassava has identified a total of 42 independent transgenic cassava lines. All lines were grown in the greenhouse according to method in Section 2.2.2.

3.3.2 Characterisation of mature transgenic cassava plants

3.3.2.1 Mature transgenic plants exhibited phenotypes of WT plants

Wild type *in vitro* plantlets grown on MS medium pH 5.8 have green leaf foliage, pale green stem and petiole. New green tissue cuttings required approximately one week to develop fully formed shoots and roots and the growing plantlets could be maintained in the same culture medium for a maximum of six months. Contamination with fungi was always a risk but avoided at any cost. Essentially all transgenic plantlets provided at the beginning of this research exhibited normal or wild type-like phenotype.
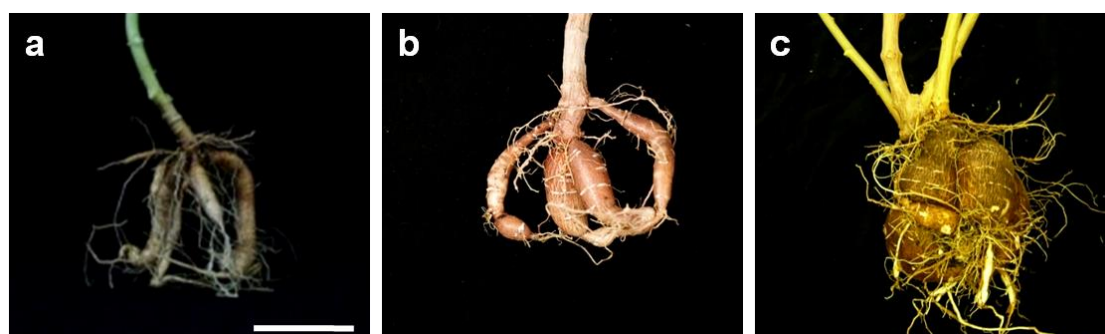
Figure 3.15 Size comparisons of storage roots at different growth period. (a) Storage roots harvested at 4, (b) 6 months and (c) 12 months after planting.

Due to time constraints and logistic issues, transgenics were grown at different times of the year. Modification of post-harvest experiments required different number of replicates per line but all plants were grown in the same way using a standard procedure. Generally one month old *in vitro* plantlets were removed from the sterile environment, transferred onto soil medium in 9 x 9 cm containers, kept in the growth room for 4 weeks and finally transferred to a horticulture setting in the greenhouse. All plants were harvested at approximately 6 months and this appeared to be the optimal age for the size of the greenhouse and the pots in which they were grown. At 3 or 4 months cassava plants produced storage roots too small to be manipulated for PPD assay while at 12 months the roots were too bulky and often woody. The growth duration had allowed plants to grow to just about one metre tall or less ensuring equal provision of light. Furthermore, restricting plant development in small containers

beneficially promoted storage root formation to the size suitable for use in laboratory (Figure 3.15).

Figure 3.16 Example of greenhouse cassava plants at various growth period. Abbreviation: mo = months old.

After 6 months the majority of plants became fully developed and produced storage roots of average length 10 cm. Observation of the physical characteristics of a mature transgenic plant and its roots revealed similar features to a WT including the form and the volume of leaf foliage, the colour of leaves and the petioles as well as the form of the storage roots (Figure 3.16). All measurements were recorded at time of harvest; for example, plant height was measured immediately before being removed from soil and fresh storage roots were weighed when the stems were detached from the shoots to avoid loss of moisture. Harvesting could be the most labour-intensive activity, as it often involved a lot of plants and occasionally many post-harvest treatments. Depending on the design of experiment the number of plants varied, but importantly all post-harvest treatments were precisely timed to ensure correct interpretation of results.

3.3.2.2 Transgenic cassava plants exhibited variable growth

The growth parameters of the transgenics and WT cassava were taken during harvest. The height of the plant was measured from the base to the top of the main plant stem while the roots were weighed after cutting them from stems. The height reflects plant size while storage root weight indicates yield which is an important agronomic trait of cassava.

Pat:SOD transgenics were grown three times and they were all harvested at similar period after planting. Table 3.5 shows the growth data of the first planting of Pat:SOD transgenic plants. Nearly all plants were significantly taller than the WT, except for B2. Measurement of fresh storage root weight showed that Pat:SOD, in general, produced significantly greater yield than the WT except C1 and D7.

Table 3.5 Mean height of cassava plants and storage root mean weight of the first planting of Pat:SOD. Asterisk (*) denotes significant differences at the 95% level using the Student's t-test. na= not applicable.

Plant lines	Height (cm)	Height (SD)	t-test height	Weight (g)	Weight (SD)	t-test weight
Pat:SOD A2	61.7	2.4	0.01*	45.4	1.6	0.01*
Pat:SOD B2	56.2	7.0	0.08	42.7	4.2	0.01*
Pat:SOD C1	55.7	1.9	0.01*	33.9	2.9	0.27
Pat:SOD C2	58.2	0.5	0.01*	49.6	4.3	0.00*
Pat:SOD C4	63.7	4.1	0.01*	42.1	4.2	0.04*
Pat:SOD D3	62.7	7.6	0.01*	42.5	1.4	0.01*
Pat:SOD D7	66.2	3.1	0.00*	33.9	6.8	0.39
WT	43.0	4.3	na	29.6	3.7	na

However, data collected from the second planting suggests that the differences in size and yield exhibited by Pat:SOD transgenics was not consistent. Pat:SOD transgenic plants appeared to grow more variably in the second planting and not significantly different from the WT (Table 3.6). In terms of yield, no significant difference was found between the transgenics and the WT except in one line (D7).

Table 3.6 Mean height of cassava plants and storage root mean weight of the second planting of Pat:SOD. Asterisk (*) denotes significant differences at the 95% level using the Student's t-test. na= not applicable.

Plant lines	Height (cm)	Height (SD)	t-test height	Weight (g)	Weight (SD)	t-test weight
Pat:SOD A2	76.3	17.1	0.40	63.5	11.6	0.56
Pat:SOD B2	75.1	10.4	0.11	63.7	19.6	0.59
Pat:SOD C1	69.9	6.7	0.77	49.8	7.0	0.06
Pat:SOD C2	66.0	6.6	0.75	63.0	8.4	0.36
Pat:SOD C4	75.7	8.5	0.24	55.3	4.9	0.19
Pat:SOD D3	73.8	8.0	0.40	61.7	7.8	0.62
Pat:SOD D7	77.1	9.2	0.20	40.9	8.7	0.01*
WT	69.7	12.2	na	59.7	10.0	na

The third planting confirmed the inconsistency in Pat:SOD growth (Table 3.7). Transgenic cassava plants showed no significant difference in height as they grew comparably with the WT. The plants also showed no significant differences in yield except in C1 which produced significantly low-weight storage roots.

Table 3.7 Mean height of cassava plants and storage root mean weight of the third planting of Pat:SOD. Asterisk (*) denotes significant differences at the 95% level using the Student's t-test. na= not applicable.

Plant lines	Height (cm)	Height (SD)	t-test height	Weight (g)	Weight (SD)	t-test weight
Pat:SOD B2	98.7	10.8	0.85	46.7	4.5	0.44
Pat:SOD C1	84.3	5.5	0.24	18.9	10.0	0.04*
Pat:SOD C4	102.3	13.7	0.10	74.0	20.4	0.64
Pat:SOD D7	103.7	13.6	0.63	47.1	8.6	0.29
WT	96.3	12.7	na	61.7	23.2	na

To explain the inconsistencies, data from all plantings were compared. Since the third planting involved only four transgenic lines, the other lines were excluded from the analysis. Table 3.8 shows that taller plants were produced in the subsequent planting than in the first. There was no significant difference shown by the transgenics in these plantings because all plants grew at similar rate in these plantings. The significant

difference shown by the transgenics in the first planting appeared to be caused by unusually shorter WT plants.

Table 3.8 Mean height of Pat:SOD plants as compared to WT plants from three independent plantings and harvests. Plants significantly taller than the WT are marked by asterisk.

Line	1st planting	2nd planting	3rd planting
Pat:SOD B2	56.3 ± 7.0	75.1 ± 10.4	98.7 ± 10.8
Pat:SOD C1	61.8 ± 2.4*	76.3 ± 17.1	84.3 ± 5.5
Pat:SOD C4	63.8 ± 4.1*	75.7 ± 8.5	102.3 ± 13.7
Pat:SOD D7	66.3± 3.1*	77.1± 9.2	103.7 ± 13.6
WT	43.0 ± 4.3	69.7 ± 12.2	96.3 ± 12.7

Table 3.9 Mean weight of Pat:SOD roots as compared to WT roots from three independent plantings and harvests. Plants produced significantly lower/higher storage root weights are marked by asterisk.

Line	1st planting	2nd planting	3rd planting
Pat:SOD B2	42.7 ± 4.2*	63.7 ± 19.6	46.7 ± 4.5
Pat:SOD C1	45.4 ± 1.6*	63.5 ± 11.6	18.9 ± 10.0*
Pat:SOD C4	63.8 ± 4.2*	55.3 ± 4.9	74.0 ± 20.4
Pat:SOD D7	33.9 ± 6.8	40.9 ± 8.7*	47.1 ± 8.6
WT	29.6 ± 3.7	59.7 ± 10.0	61.7 ± 23.2

Also most of the transgenics appeared to have significantly greater yield because, in the first planting the WT produced extremely low yield. Similarly, in the subsequent plantings, some of the transgenics had significantly lower yield than the WT because they produced unusually lower weight of storage roots (Table 3.9).

Pat:CAT, Pat:GAR, Pat:GCS and Pat:Gus transgenic plants were highly variable in terms of heights and storage roots weights they produced. (See Appendix Table 9.1, 9.2, 9.3 and 9.4 for the growth data of Pat:CAT, Pat:GAR, Pat:GCS and Pat:Gus transgenic plants respectively). Nevertheless, the growth data for Pat:APX could not be analysed because the WT plants in this transgenic group were lost to contamination while the growth data for Pat(-):Gus was insufficient for statistical analysis so it was dismissed.

The growth of all transgenic cassavas in this study is summarised, data from all transgenics including those from Pat:APX and Pat:Gus are gathered (Table 3.10). Overall, there was high variation in the height of the plants and the weight of roots they produced. Correlation test between plant height and yield found no association between these two parameters (R^2= 0.011). The tallest group of plants grown was the Pat:SOD from the third planting with an overall height nearly 100 cm while the shortest group was Pat:SOD from the first planting with average height approximately 60 cm. In terms of yield, the highest was produced by the Pat:Gus while the lowest was produced by the Pat:SOD in the first planting.

Table 3.10 Summary of the overall growth measurement of cassava plants including WT and transgenics harvested at different time of year.

Transgenics	n	Mean height (cm)	Mean weight (g)	Root: shoot	Plant/Harvest time
Pat:SOD (1)	4	61.1 ± 8.5	40.5 ± 6.4	1: 1.5	Sep 2010/Feb 2011
Pat:SOD (2)	9	73.8 ± 4.6	58.0 ± 8.0	1: 1.3	Aug 2011/Jan 2012
Pat:SOD (3)	3	97.1 ± 7.7	49.7 ± 20.6	1: 1.9	Nov 2012/Apr 2013
Pat:CAT	9	69.7 ± 4.4	49.0 ± 11.9	1: 1.4	Aug 2011/Jan 2012
Pat:APX	9	80.2 ± 5.3	43.1 ± 4.5	1: 1.9	Oct 2011/Mar 2012
Pat:GAR	3	85.8 ± 7.2	90.5 ± 17.7	1: 1	July 2011/Dec 2012
Pat:GCS	12	63.1 ± 5.4	60.7 ± 10.2	1: 1	Mar 2012/Aug 2012
Pat:Gus	3	70.0 ± 3.7	98.2 ± 14.4	1: 0.7	Apr 2011/Sep 2011

The variation showed here was investigated by assessing the root:shoot ratio (which also serves as a plant health indicator) and the season which the plants were harvested. It was found that the ratio was the highest in Pat:Gus which was harvested in the end of summer. The ratio was smaller (1:1) in Pat:GCS which was harvested in the mid summer and also in Pat:GAR which was harvested during the coldest winter season. The ratio was even smaller in Pat:CAT, (1:1.4) as well as in the first (1:1.5) and the second planting of Pat:SOD (1:1.3) and these three groups were harvested in the beginning of the year or during winter. The ratio was the lowest (1:1.9) in the third batch of Pat:SOD and Pat:APX which also were harvested around the same time of year. The data gathered suggest that the ratio was not influenced by season or hours of daylight the plants were exposed to. The second batch of Pat: SOD, Pat:CAT and

Pat:GAR plants were equally exposed to decreasing daylight over their growth period as they were planted in summer and harvested in winter had distinct root:shoot ratio. Similarly, Pat: GCS and Pat:Gus plants which escaped the cold season and were exposed to longer daylight over their growth period also had different root:shoot ratio.

3.4   Discussion

The success of transgenic identification relies on two major factors; 1) the use of a suitable gene to discriminate the WT lines; 2) the use of a reliable probe to confirm T-DNA integration in the genome. Transformation often generates many transgenics lines transformed with the same construct as uptake of external genetic material is rare and difficult especially in higher organisms. To increase the chance of obtaining lines that acquire the construct it is necessary to create, screen and verify a huge number of transgenic lines. In this study, verification was done by amplification of *hptII* gene and transgene which proved to be relatively efficient and rapid as many samples can be analysed at one time. Importantly the use of more than one gene (*hptII* and transgene) has discriminated between the WT and many untransformed and suspicious lines such as the Pat:CAT lines. The use of the *hptII* probe in Southern blots to differentiate between complex and simple transformation events was also successful, leading to the identification of several single-inserts independent lines including from Pat:CAT transformations, though whether these contain the catalase gene remains to be seen. The percentage of independent single-insert lines in this work was high (60-90%) where only 30-40% is expected in most cassava research (Ihemere et al., 2006, Zhang et al., 2003b). It is worth mentioning that the work presented here was not completed in linear fashion but rather done concurrently. This explains why Pat:CAT lines were subjected to Southern blot and subsequently grown to mature plants despite ongoing investigation on the MecCAT1 constructs.

The main purpose of growing the selected transgenics to fully-developed plants was to obtain storage roots so the role of target genes in reference to PPD can be assessed. Phenotype observations showed that all transgenic lines maintained the normal features of a healthy cassava plant. Maintaining the features of untransformed plants is particularly important in analysis like the PPD assay that can be difficult if the transgenics produced abnormal storage roots. Morphology determination was done by comparing the height of the plants and the weight of storage roots they produced to the WT. Pat:GCS and Pat:SOD, respectively, had 4 and 6 lines that were significantly taller than the WT suggesting transformation with these genes may modify the size of the

plants. However, this was not observed in the subsequent harvests, as none of the Pat:SOD lines showed a significant height difference from the WT. Likewise, the role of SOD gene in storage root formation was unclear as some of the lines showed a significant increase of yield in one harvest but showed non-significant increase in the following harvest. This phenomenon partly resulted from inconsistencies in the WT growth itself. The WT plant height varied from 40 to over 80 cm while the roots weighed from 30 to 100 g. Essentially, there were many factors determining the growth of plants in the greenhouse. Although it was designed to maintain a certain temperature, humidity and light provision, these could vary with the outside environment (J. Watling, *pers. comm.*). Being known as a cold-sensitive tropical plant growing cassava in non-tropical environment might also affect its growth (An et al., 2012). However, precise control of the growth conditions was not possible. In a condition that allows large scale planting, plants could be randomly selected but this was not possible in this work.

The change in plant height is not a great concern because it is not an agronomic trait for cassava but the root weight is. Therefore, the decrease in yield observed in Pat:GCS must be investigated with more replicates and several rounds of plantings. The discrepancies demonstrated in the growth and the yield of cassava transgenic lines; however, were unlikely to influence PPD-related experiments. What was observed was natural variation in plant height and root weight that was not affected by the presence of any of the transgenes under investigation. In conclusion, the aim to select single-insert independent lines for production of storage root suitable for PPD assay was successfully achieved.

CHAPTER 4

Assessment of PPD

4.1   Introduction

Primarily, PPD consists of biochemical and physiological changes in the cassava storage root, some of which are manifested as visual symptoms, that can render them unacceptable as food or as input to processing (Beeching, 2001). According to the FAO, delaying PPD up to two weeks would significantly improve the value of cassava, particularly its potential as an export commodity (Wenham, 1995). In view of this, extensive studies have been conducted to understand the biochemical activities and pathways involved in PPD. To evaluate the result of the studies measuring of PPD symptoms is often necessary, which is usually based on a visual scoring system.

The main PPD symptom is vascular streaking, but typically it is accompanied by browning of parenchymatic tissue (Hirose et al., 1983). The streaks or occlusions which tend to initiate at the root periderm are formed from pigment accumulation in the xylem vessels, which then spread to the adjacent parenchymatic xylem. Browning of parenchymatic tissue, which is initiated as a bluish pigmentation occurs when the pigments finally spread to parenchyma cells. In general, vascular occlusion is a response to environmental stress or pathogen infection. In a living plant tissue, the occlusions block transport of water causing increased respiration and wilting. Vascular occlusion is well-studied in grapevine (Sun et al., 2008) and cut flowers (da Silva Vieira et al., 2013), and in these plants its occurrence mostly is associated with tylose formation. In the cassava storage root, tylose formation is related to PPD but it was found in the pigmented and non-pigmented xylem vessels. Microscopy and cytochemical tests confirmed that the streaks contain lipids, carbohydrate and phenolic compounds (Rickard et al., 1979). Interestingly, although *Penicillium, Aspergillus, Fusarium,Cladosporium, Bacillus and Xanthomonas* species have been routinely isolated from fresh cassava root surfaces, vascular streaking is not pathological in nature due to the failure to isolate microorganisms from the occlusions (Noon and Booth, 1977, Averre, 1967). However, physiological deterioration is always followed by microbial deterioration in which various fungi like *Aspergillus flavus, Botryodiplodia theobromae, Fusarium solani, Trichoderma harizianum* and saprophytic bacteria are

involved (Booth, 1976). This normally occurs from 5 days of harvest onwards and the typical signs include softening of the root and an unpleasant smell. Microbial deterioration, especially initially, is not easily distinguished from physiological deterioration as existing vascular streaking may mask its presence. To avoid this, the evaluation of PPD symptoms often is done prior to 5 days after harvest.

CIAT has proposed a standard procedure for assaying cassava roots for PPD and a standard method to score the symptoms the roots develop. According to the CIAT method, mature cassava roots of commercial size are cut at both ends to approximately 15 cm length. The distal end of the root is covered with PVC film to maintain moisture content and to promote initiation of deterioration from the proximal end. These roots are stored at ambient temperature and away from sunlight and pests for 3 days or more. To estimate PPD, the roots are cut transversely to make seven root sections of approximately 2 cm thickness. To determine the roots susceptibility to PPD each root section is scored from 0 to 10 based on the percentage of discoloration as shown in a reference picture (Figure 4.1). The final score of an individual root is the highest score among the root sections. This assay and scoring method is published in Wheatley et al.(1985).

Figure 4.1 CIAT PPD scoring reference picture consisting cassava root sections showing a range of PPD symptoms. These root sections were obtained from highly susceptible cultivar that was stored at 21-28°C and 70-80% relative humidity for 3 days. Picture is courtesy of CIAT.

The CIAT PPD assay is commonly practiced but the scoring method and the reference picture tend to vary with research group preference. Figure 4.2 shows the reference used by the Philippine Root Crop and Research Training Centre (PRCRTC) to score their roots where the degree of discolorations were divided into 5 scale according to percentage (Hirose et al., 1983). With this reference picture, the roots were scored from 1 to 5. Note that the symptomless roots were given score 1 while in the CIAT

method it is assigned as 0. For PPD estimation, 11 sections of 1 cm thick were used as oppose to 7 sections of 2 cm thick in the CIAT method. Misinterpretation of PPD symptoms are likely to arise from this when an equivalent root sample is compared, for example score of 1.5 for a root sample is equivalent to 15% deterioration if one is using the CIAT reference picture but this score indicates no PPD symptoms with the PRCRTC reference picture. Modifications are also made in the calculation the final score of a root sample, for example, Morante et al. (2010) who followed the CIAT method use the average score of the root section rather than the highest score among the root section as the final score, despite working at CIAT. At another extreme, Booth (1976) scored deteriorated roots on a scale of 0 to 4 without a reference picture. Scores were assigned as based on individual judgement; 0 = no deterioration, 1 = slight deterioration, 2 = up to half of root deteriorated, 3 = half to three quarters of root deteriorated, 4= three quarters to complete root deterioration. From these scores the percentage or the index of deterioration was established.
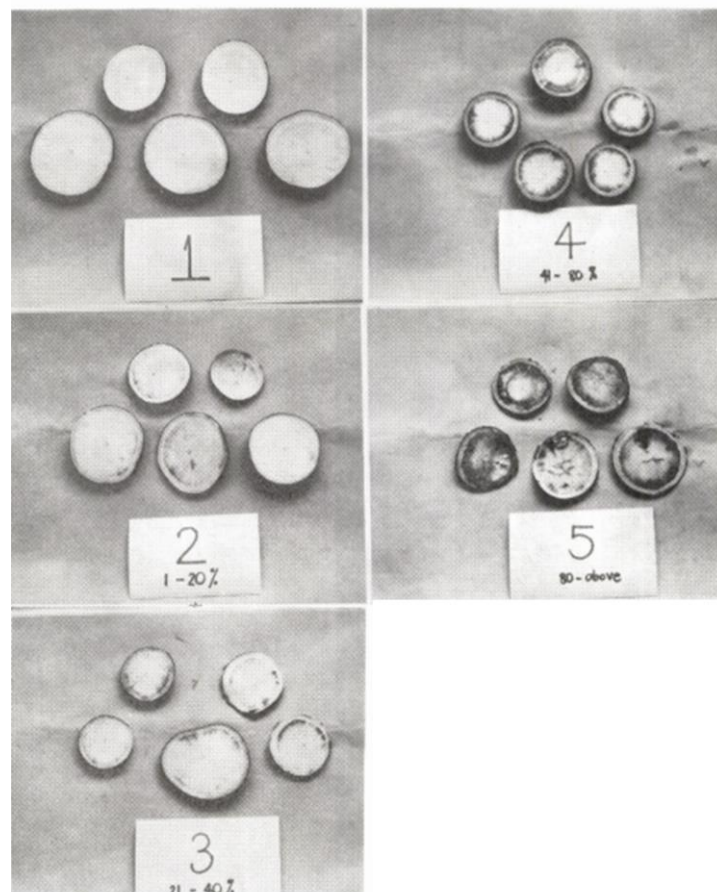
Figure 4.2 PPD symptoms reference picture used in PRCRTC to estimate PPD. The roots were given score based on the percentage of deterioration and classified into 5 categories. Score 1 is designated for fresh and symptomless root section whereas

score 5 is for deteriorated root section that includes both the physiological and microbial deterioration symptoms. No details were given on the PPD assay used on the roots to produce the scores (Hirose et al., 1983).

During PPD, a range of secondary metabolites accumulate, including the hydroxycoumarins, scopoletin, scopolin, esculetin and esculin; it is the oxidation of some of these that leads to the blue-black vascular streaking symptoms (Wheatley and Schwabe, 1985). These compounds are suitable as an alternative visual assessment mainly because they fluoresce under ultra-violet (UV) light. Amongst these compounds scopoletin fluoresces most intensely. Scopoletin and the other hydroxycoumarins derive from general phenylpropanoid metabolism, the key entry enzyme to which is phenylalanine ammonia-lyase (PAL) (Vogt, 2010), which increases in activity during the early response of PPD (Tanaka et al., 1983). In freshly harvested cassava roots scopoletin is barely detectable but its abundance increased rapidly after one day of harvest. It is unclear to what extent the increase of scopoletin abundance during PPD is due to its *de novo* synthesis or to the de-glycosylation of its glycone, scopolin.

Quantification of hydrocoumarins in storage period over 6 days at 2-day intervals revealed high differences between varieties. However, it can be generalised that scopoletin concentration peaked at day 2 and gradually decreased by day 4 and 6 in highly susceptible cultivars while in less susceptible cultivars it peaked at day 6 (Buschmann et al., 2000b). On the other hand, scopolin, esculetin and esculin concentrations fluctuated with storage time but generally were found in lower concentrations than scopoletin making them less reliable as potential markers of PPD (Buschmann et al., 2000b). Scopoletin also lends itself as a preferred biochemical marker over other alternatives because its distribution across along the root length is more homogenous. Measurement of fluorescence from the proximal to distal end from 25 different cultivars showed high consistency of scopoletin than the PPD symptoms (Salcedo et al., 2010).

4.2   Research aim

Development of PPD assays and scoring methods has been centred in countries where cassava is cultivated and materials for PPD assessment are plentiful. However, in the past 15 years an increasing number of PPD research teams are based in countries where field cassava cultivation is not suitable. As an alternative, cassava is grown under greenhouse conditions on a smaller scale. Under such conditions space is at a premium, which leads to lower numbers of plants being grown, the use of small pots to encourage early rooting, and limiting the growth period of the plants to a few months. As a result the storage roots tend to be small and often distorted by the cramped space in which they are grown; thereby rendering them rather different from field grown roots. This makes the implementation of the above-mentioned PPD assessment method a challenge. The need to develop a reliable PPD scoring method or modify the existing method is urgent, especially as the generation of reliable data that can be shared or compared between institutions is desirable. Therefore, the aim of this chapter is to find a reliable method to assay PPD particularly for storage roots grown in the greenhouse and to score the roots based on the PPD symptoms that develop. The PPD symptoms will be assessed by an image processing software and a subjective rating method where appropriate. The criteria to be evaluated include the length of the assay, the intensity of the PPD symptoms, microbial infection risks as well as dehydration state. The role of hydrocoumarins as a PPD marker will also be examined in the later sections.

4.3   Results

In all PPD assays, storage roots produced from 6 months old cassava plants grown in a greenhouse were used (Section 2.2.2).

4.3.1   PPD Assay 1: Intact cassava storage roots deteriorate with high variations in PPD symptoms

Six Pat:SOD lines and the WT roots were examined at 0, 1 and 3 days after harvest (DAH). For each line, 9 average size storage roots from 9 plant replicates were harvested. As shown in Figure 4.3, the plants produced various sizes and forms of roots. Therefore selecting roots with a standard parameter for PPD assessment could not be applied rigorously. Instead, selection was made by human judgement.

Figure 4.3 The forms and sizes of storage roots commonly produced by plants grown in a greenhouse including in this assay. The plants either produced (a) a massive and straight storage root (b) or two roots of different sizes (c) or smaller roots of identical lengths. Long storage roots tend to be distorted because of growth restriction in a small container as seen in b. Bar represents 2 cm.

The roots were assayed according to the CIAT assay method with some modifications. The roots were removed from the stem by cutting off peduncle but were not cut in the distal ends. Instead, to ensure deterioration would only initiate in the proximal ends unharmed roots were used. Except for the 0 DAH root samples, all roots were placed on an open Petri dish lined with a dry filter paper and stored in a growth room at 25-27°C until analysed. At each time point, the roots were sliced into approximately 1 cm cross sections and photographed under white light. The 0 DAH root sections were photographed immediately after harvest. All roots were scored by visual rating using a reference picture (Figure 4.4). Each root section was assigned a score in percentage which reflects the percentage of discoloration or PPD symptoms. The sum of the scores was divided by the number of the root sections to obtain the mean PPD score of the root.
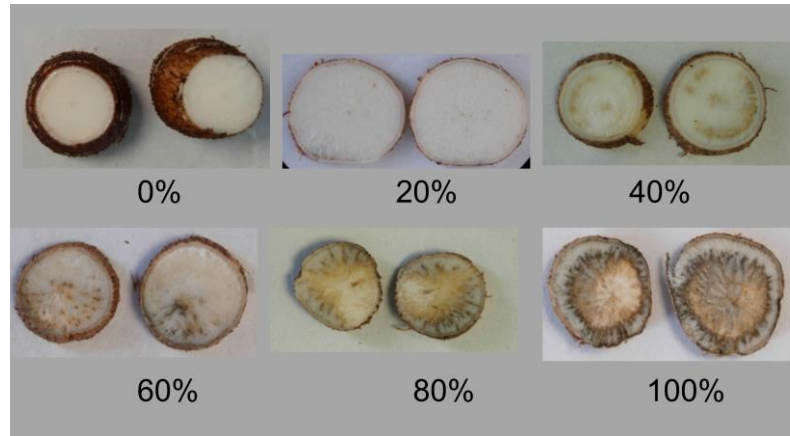
Figure 4.4 Reference picture used in the present study. The degree of root discoloration or PPD symptoms on parenchymatic tissue are indicated in percentage. The picture was prepared from root sections stored in a growth room at 25-27°C.

Figure 4.5 shows the photographs of the roots and Table 4.1 shows the scores assigned to the individual root samples. As expected, none of the roots showed visible PPD symptoms at 0 DAH and so were given a 0% score. The PPD symptoms were also not visible in the majority of the roots at 1 DAH but only became obvious in some of the roots at 3 DAH. Intense PPD symptoms were observed in Pat:SOD A2, B2, C1 and D7 causing dramatic increase in PPD scores.
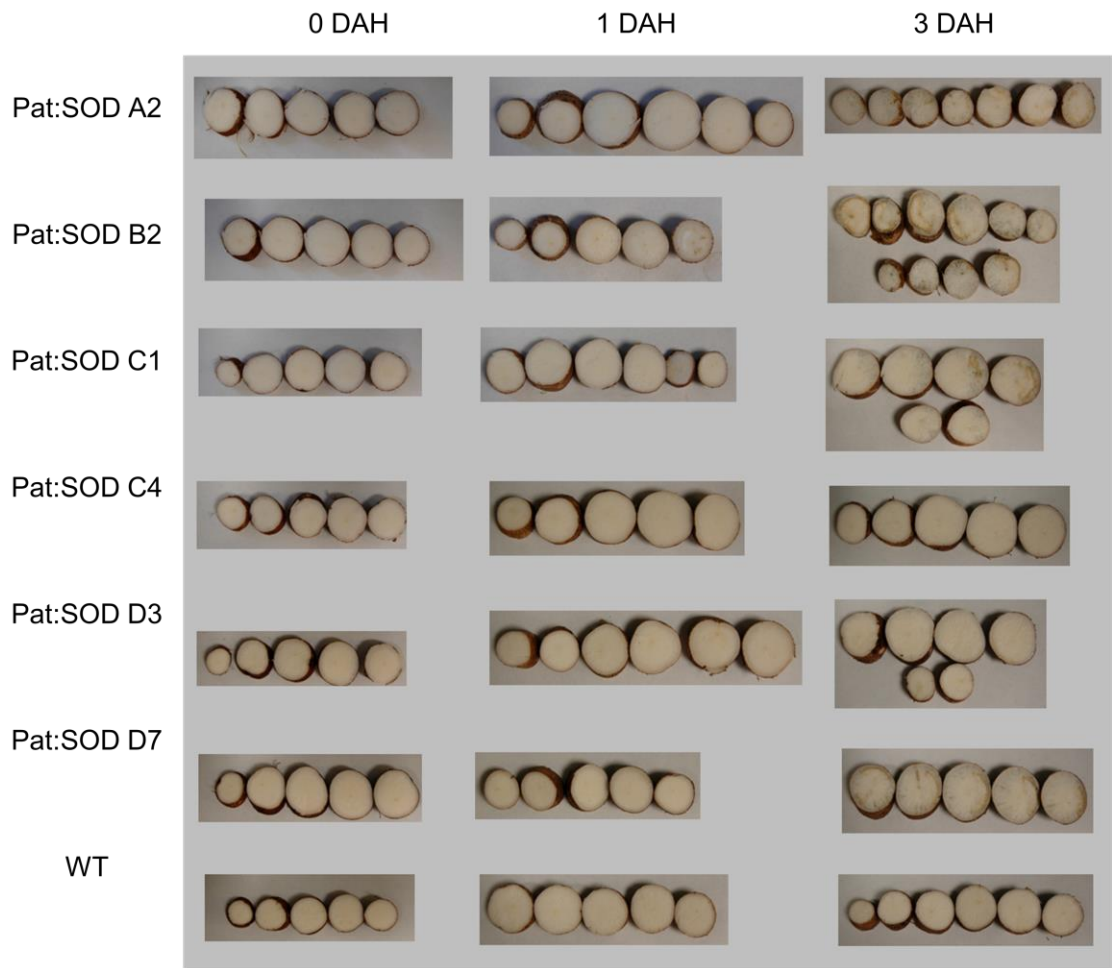
Figure 4.5 Representatives of Pat:SOD roots following harvest. The root sections were laid from the proximal (injured site) to the distal ends (from right to left). The sections were approximately 1 cm thick and the numbers of sections varied with the length of the roots.

Table 4.1 Pat:SOD group root samples PPD scores scored by visual assessment. The roots were assayed with PPD Assay 1 which was the modified CIAT assay method. The number of root sections generated from the individual root samples and their score are shown. These scores were obtained by comparing PPD symptoms in reference pictures (Figure 4.4) to PPD score showed by the roots. At 0 and 1 DAH most of the roots seemed fresh; PPD symptoms did not appear until 3 DAH. SD value indicates the variation between root sections.

Cassava lines		No of root sections	0 DAH	No of root sections	1 DAH	No of root sections	3 DAH
Pat:SOD A2	P1	5	0.0	6	0.8 ± 2.0	7	25.7 ± 14.0
	P2	6	0.0	6	0.0	-	-
	P3	5	0.0	7	0.0	-	-
Pat:SOD B2	P1	5	0.0	8	5.0 ± 0	10	46.0 ± 15.1
	P2	5	0.0	8	0.0	8	42.5 ± 16.7
	P3	5	0.0	5	1.0 ± 2.2	-	-
Pat:SOD C1	P1	6	0.0	6	0.0	6	41.7 ± 14.7
	P2	4	0.0	6	0.0	5	32.0 ± 8.4
	P3	5	0.0	5	0.0	-	-
Pat:SOD C4	P1	5	0.0	5	0.0	5	0.0
	P2	5	0.0	5	0.0	10	0.0
	P3	4	0.0	5	0.0	8	0.6 ± 1.8
Pat:SOD D3	P1	5	0.0	6	0.0	9	2.2 ± 2.6
	P2	5	0.0	6	0.0	8	0.0
	P3	5	0.0	7	0.0	6	0.0
Pat:SOD D7	P1	7	0.0	5	0.0	5	42.0 ± 4.5
	P2	5	0.0	4	0.0	4	35.0 ± 5.8
	P3	5	0.0	4	0.0	7	34.3 ± 11.3
WT	P1	6	0.0	5	0.0	6	0.0
	P2	5	0.0	5	0.0	3	5.0 ± 5.0
	P3	5	0.0	5	0.0	5	1.0 ± 2.2

Although some of the root samples showed deterioration symptoms at 1 DAH it was clear from the photographs and the PPD scores that PPD symptoms only appear after 3 days of harvest. The change at 3 DAH was statistically significant as tested (p=0.05). However, the PPD scores of the roots at this time point were lower than expected and this mainly arose from high variations in the PPD score of root sections as shown by high SD in Table 4.1. For example, some of the root sections of Pat:SOD B2 showed up to 60% PPD symptoms but the individual root score was reduced to 42 to 47% as the other sections showed low or no PPD symptoms. Variations between root sections were higher in the low scored roots such as Pat:SOD C4 P3 and Pat:SOD D3 P1 as well as the WT P2 and WT P3 but this plausibly was caused by random deterioration of the roots. By following the Morante et al. (2010) approach, the scores in Table 4.1 were averaged to get mean scores of individual lines (Table 4.2) where the SD value were

smaller at 3 DAH than those observed in Table 4.1 suggesting low variations between plant replicates. However this might only be true in high-scored lines (Pat:SOD A2, B2, C1 and D7) rather than the low-scored lines which were thought had develop arbitrary PPD symptoms. Nonetheless this is questionable as among the high-scored lines only Pat:SOD D7 had sufficient number of replicates.

Table 4.2 Mean PPD scores of all Pat:SOD lines and the WT assayed with PPD Assay 1 in percentage. SD value indicates variations between plant lines.

Cassava lines	0 DAH	1 DAH	3 DAH
Pat:SOD A2	0.0	0.3 ± 0.5	25.7
Pat:SOD B2	0.0	2.0 ± 2.6	44.3 ± 2.5
Pat:SOD C1	0.0	0.0	36.8 ± 6.8
Pat:SOD C4	0.0	0.0	0.2 ± 0.4
Pat:SOD D3	0.0	0.0	0.7 ± 1.3
Pat:SOD D7	0.0	0.0	37.1 ± 4.3
WT	0.0	0.0	2.0 ± 2.6

Visual examination of the PPD symptoms revealed two types of discolorations that were commonly observed in deteriorated cassava roots. The first type was vascular streaking, which is indicated by a blue-black precipitate and the second type was a brown staining. In this assay the deteriorated roots showed either one or both types of discolorations as depicted in Figure 4.6. It was expected that development of deterioration symptoms would be highest in the proximal end and lowest in the distal end as the former was exposed while the latter was sealed, but this was not observed. The pattern of discoloration extending from the injury sites or proximal ends varied between roots. There were roots showing brown staining in the proximal ends and vascular streaking in the distal ends while others showed the opposite. Additionally, the symptoms were also found to be scattered on the root surfaces and not evenly distributed on the periphery of the roots as illustrated in the CIAT and PRCRTC reference picture. The irregularities in symptoms development observed in this PPD assay was the rationale of choosing Morante's approach rather than Wheatley's approach that take the highest score as the final individual root score.

Figure 4.6 The variations in the development of PPD symptoms in cassava roots examined at 3 DAH. Both roots were injured at proximal ends during harvest and stored at 25-27°C room. (a) Some of the roots developed brown staining at the proximal ends and blue-black discoloration towards the distal ends. (b) However some of them showed the opposite where blue-black discoloration developed at the proximal ends and brown staining was prominent at the distal ends.

The scores at 0 DAH or during harvest are crucial for accurate comparison of PPD symptoms of the subsequent PPD times. They serve as background scores to accurately calculate the actual PPD symptoms of the later PPD times. With the assumption that all the 0 DAH roots were non-deteriorated; they were given the score of 0% although there could be minor differences between them that were not visible to the human eye. To investigate this, the root samples were subjected to computer-based scoring using image processing software created by a research team at ETH-Zurich called PPD Symptom Score Software. This software specifically converts images to greyscales and use the grey value of a selected area as the intensity of root discoloration. Each root section was measured and the average score of a whole root was obtained by dividing the sum score by the number of root sections. The actual PPD score for each line at each PPD times was calculated as the percentage of PPD symptoms in relative to scores at 0 DAH. The examples of roots that were converted to greyscale are shown in Figure 4.7.
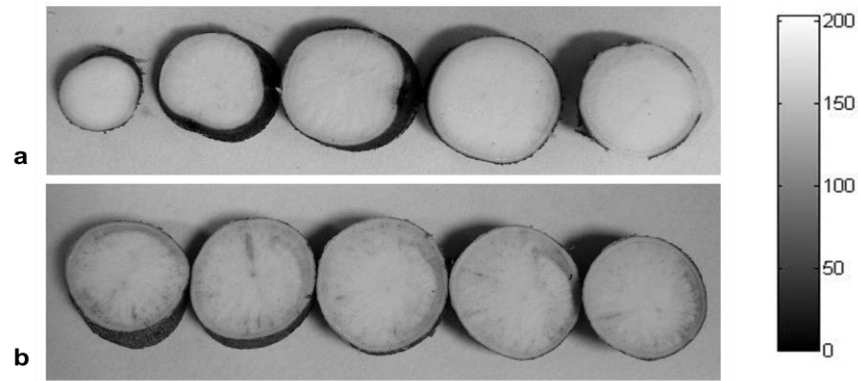
Figure 4.7 Computer-scoring of root sections of Pat:SOD D7 at (a) 0 DAH and (b) 3 DAH. Scores were given based on the Colourbar scale shown on right side of the picture. The 0 DAH root sections were scored between 106 and 164 and the whole root was given an average score of 25.4%. The 7 DAH root sections were scored between 91 and 157 and the whole was given an average score of 34.4%.

Since the photographs were taken under automatic mode, the greyness scores were normalised against the filter paper on which the roots were photographed. Scoring of 0 DAH by this method could be used to determine a base line reference for scoring at later time points. At all PPD times, there were minor variations detected (indicated by SD values) but they were generally small. In the visual rating method, the variation or SD values were high in the 3 DAH root but the values were severely much reduced in the computer scoring. This is mainly because computer scoring reduces human bias as the vascular streaking and browning symptoms were treated as a single parameter in which only the intensities of the symptoms were computed.

Table 4.3 Greyness scores of all Pat:SOD group root samples at all PPD time points generated by computer scoring method. These scores were obtained by converting the photographs to greyscale and measuring the greyness intensities on the surface of the roots. The representation of these scores shows the accuracy of computer scoring method due to its ability to detect minor differences.

Cassava lines		0 DAH	1 DAH	3 DAH
Pat:SOD A2	P1	20.6 ± 5.1	16.0 ± 7.5	24.1 ± 3.9
	P2	20.9 ± 3.0	15.8 ± 2.6	-
	P3	16.4 ± 4.2	19.2 ± 3.6	-
Pat:SOD B2	P1	18.3 ± 2.9	18.7 ± 2.5	30.2 ± 4.4
	P2	16.2 ± 4.7	15.3 ± 3.6	24.5 ± 2.5
	P3	15.3 ± 2.9	16.1 ± 2.1	-
Pat:SOD C1	P1	18.6 ± 7.2	15.5 ± 2.8	18.7 ± 5.2
	P2	10.4 ± 0.6	16.7 ± 2.7	25.7 ± 3.1
	P3	14.6 ± 1.5	13.4 ± 3.1	-
Pat:SOD C4	P1	14.6 ± 2.7	14.3 ± 1.8	16.3 ± 4.4
	P2	15.8 ± 3.3	17.4 ± 1.7	15.4 ± 2.7
	P3	13.1 ± 2.2	15.5 ± 3.6	14.0 ± 2.2
Pat:SOD D3	P1	18.7 ± 2.8	14.8 ± 3.5	19.9 ± 5.9
	P2	17.8 ± 2.1	14.1 ± 3.9	16.8 ± 1.8
	P3	16.2± 2.0	17.9 ± 4.8	14.7 ± 1.4
Pat:SOD D7	P1	19.1 ± 4.3	18.3 ± 3.7	26.4 ± 3.9
	P2	17.4 ± 1.7	18.6 ± 2.8	24.2 ± 1.7
	P3	18.8 ± 3.6	20.3 ± 2.6	26.3 ± 2.2
WT	P1	19.1 ± 3.6	14.8 ± 3.8	18.2 ± 2.2
	P2	17.6 ± 4.0	14.5 ± 3.2	17.3 ± 1.8
	P3	14.9 ± 3.4	16.8± 1.7	24.3 ± 1.5

They mean greyness scores of individual lines were obtained from 3 plant replicates (Table 4.4). For calculation of PPD scores, the mean greyness score at the later PPD times were normalised against the mean greyness score 0 DAH by using equation below. To get PPD score at 3 DAH, the equation used is

PPD score = ((Mean Greyness Score 3 DAH – Mean Greyness Score at 0 DAH)/ Mean Greyness Score at 3 DAH)) x 100%

Table 4.4 Mean greyness scores of all Pat:SOD group root samples at all PPD time points generated by computer scoring method Student t-test was performed at p =0.05, two-tailed level of significance to test the hypothesis that the PPD scores after storage were higher than PPD scores at harvest. na = not applicable. SD value indicates variations between plant lines.

Cassava lines	0 DAH	1 DAH	3 DAH
Pat:SOD A2	19.3 ± 2.6	17.0 ± 1.9	24.1
Pat:SOD B2	16.6 ± 1.5	16.7 ± 1.8	27.3 ± 4.0
Pat:SOD C1	14.5 ± 4.1	15.2 ± 1.7	22.2 ± 4.9
Pat:SOD C4	14.5 ± 1.4	15.7 ± 1.5	15.3 ± 1.2
Pat:SOD D3	17.5 ± 1.3	15.6 ± 2.0	17.1 ± 2.6
Pat:SOD D7	18.4 ± 0.9	19.0 ± 1.1	25.7 ± 1.2
WT	17.2 ± 2.1	15.4 ± 1.3	17.0 ± 1.3
Max	19.3	19.0	27.3
Min	14.5	15.2	15.3
Mean	16.9 ± 1.8	16.4 ± 1.4	21.3 ± 4.8
t-test (p value)	na	0.58	0.02

Table 4.5 PPD scores of Pat:SOD root samples at 3 DAH determined by visual scoring (Vis.) and computer scoring (Comp.). In the visual scoring, the PPD symptoms represent the PPD scores, while in computer based scoring PPD scores were calculated by normalising greyness scores of roots at harvest.

Cassava lines	PPD Score (Vis.)	PPD score (Comp.)
Pat:SOD A2	25.7	24.9
Pat:SOD B2	44.3	64.9
Pat:SOD C1	36.8	52.9
Pat:SOD C4	0.2	5.3
Pat:SOD D3	0.7	-2.3
Pat:SOD D7	37.1	39.2
WT	2.0	-0.9

The change of greyness score at 1 DAH was only statistically significant at 3 DAH (p <0.05) thus PPD scores at this time point were calculated and compared with the visual rating scores. It is shown that the computer scoring method produced PPD scores approximately similar to those obtained from visual rating method. The root replicates with minimal or no PPD symptoms were scored low both with visual rating and the computer scoring method and vice versa. However, two lines (Pat:SOD B2 and Pat:SOD C1) showed higher scores using the computer scoring than the visual rating method and these scores matched the symptoms. It was difficult to claim if one of the

scoring methods could effectively score PPD with high certainties and this mainly due to small sample size. However, storing cassava roots as a whole for 3 days for PPD assessment as practiced by CIAT was proved ineffective with our root samples. Under this condition, PPD symptom developed too slowly that it appeared randomly across the root length. This has led to alternative PPD assay methods that aim to speed up the process.

4.3.2 PPD Assay 2: Using root sections to measure the development of PPD symptoms

The PPD response starts when harvesting injuries expose root tissue to oxygen and an oxidative burst is initiated that spreads through the root due to inadequate wound healing. The slow rate of deterioration observed in the entire greenhouse-grown roots evaluated in the preceding sections may be due to the exposure of a small surface area to air which then slowed down the development of PPD. Thus to increase the surface area, the roots were set to deteriorate in the form of root sections.

Five Pat:GCS lines and a WT line were used in this method and each line was analysed in triplicate. For this assay a pair of root sections of approximately 2 cm thickness was prepared from a storage root of each plant replicate. Since this method does not require evaluation of the whole sample, storage roots of a diameter 1.5–2.0 cm were selected. The root sections were placed in an open Petri dish lined with a dry filter paper and were stored in the same conditions (25-27°C) as the intact roots in PPD Assay 1. The pictures of the same root sample were taken at 0, 1 and 4 DAH to observe the change in PPD symptoms. As the surface are of the root dried out under these conditions a thin layer of the root sections surface was cut prior to photographing. Computer scoring was used to determine PPD scores in this assay to avoid scoring bias. Similar to PPD Assay 1, the greyness scores were normalised against the filter paper used to support the roots during photographing. Accordingly, PPD scores were calculated using the same approach.

Figure 4.8 shows PPD symptoms in cassava root sections over the storage times and Table 4.6 shows the greyness scores of all root replicates. It is clear that deterioration occurred rapidly in this assay as PPD symptoms were visible even in 1 DAH root samples which then intensified at 4 DAH. Nevertheless, 60% of the roots at 4 DAH were severely dehydrated and the rest showed the common PPD symptoms but were slightly dried out.
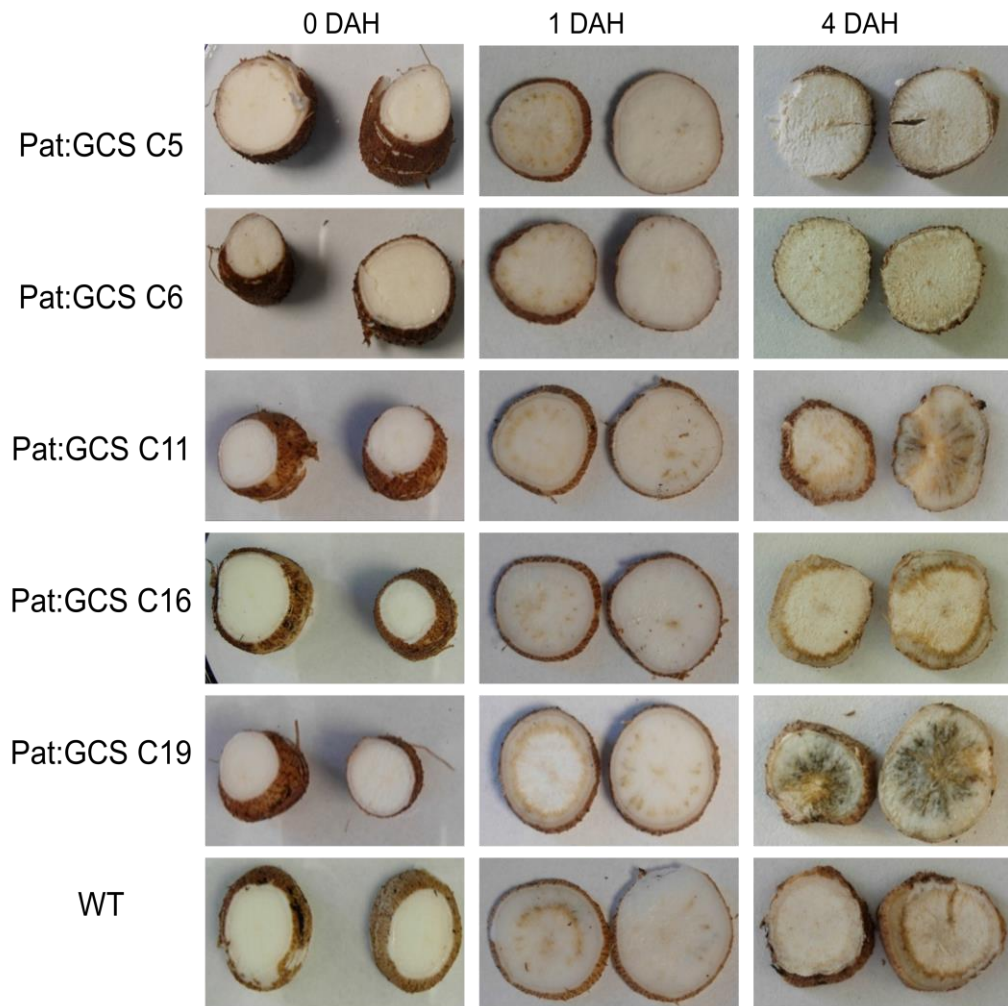
Figure 4.8 Pat:GCS lines and the WT root sections photographed following storage in a warm room at 25-27°C. Photographs were taken by removing dried out layers at each PPD times. Pictures are representative from three biological replicates.

A small number of the roots showed microbial infection symptoms. This was indicated by soft and spongy texture in the centre while the dehydrated roots turned to dry and hardened structure. Surface dehydration had severely affected the calculation of PPD score because it masked the true greyness scores. It also caused a high variation of the greyness score when only one of the root sections was dehydrated, as indicated by high SD value (Table 4.6) which then led to high variations between root replicates.

Table 4.6 Greyness scores of all Pat:GCS group root samples at all PPD time points generated by computer scoring method. ¥ indicates both root sections were severely dehydrated, ꝺ indicates one of the root section was dehydrated, * indicates only one of the root section pair was available due to damage, na indicates root sample not available due to inadequate size for PPD assay.

Cassava lines		0 DAH	1 DAH	4 DAH
Pat:GCS C5	P1	18.0 ± 3.8	21.1 ± 6.2	24.8 ± 1.9$^{¥}$
	P2	18.5 ± 2.3	21.5 ± 5.4	32.9 ±5.6$^{¥}$
	P3	16.2 ± 0.1	29.1 ± 4.0	19.7 ± 3.3$^{¥}$
Pat:GCS C6	P1	19.6 ± 4.4	17.7 ± 2.9	26.1$^{¥}$ *
	P2	20.3 ± 1.6	21.9 ±1.9	30.4 ± 0.43$^{¥}$
	P3	19.4 ± 0.5	23.2 ± 0.6	27.3 ±2.28$^{¥}$
Pat:GCS C11	P1	15.0 ± 1.6	18.9 ± 0.3	64.8 ± 26.5
	P2	21.7 ± 0.1	20.8 ± 2.1	38.3 ± 11.3
	P3	na	na	na
Pat:GCS C16	P1	15.1 ± 1.5	20.8 ±0.4	38.7 ± 8.28^{ꝺ}
	P2	15.2 ± 2.5	19.3 ± 2.1	51.1 ± 1.59
	P3	9.6 ± 2.5	13.3 ± 1.5	53.5 ± 9.28^{ꝺ}
Pat:GCS C19	P1	11.9 ± 2.2	22.3 ± 3.0	62.2 ± 2.0
	P2	17.8 ± 4.5	24.1 ±6.1	60.6 ± 4.0
	P3	18.0 ± 0.7	22.3 ± 2.1	71.8 ± 5.9
WT	P1	11.4 ± 0.1	21.5 ± 10.4	36.5 ± 18.2^{ꝺ}
	P2	18.6 ± 1.6	23.4 ± 6.6	26.7 ± 3.2$^{¥}$
	P3	18.8 ± 2.7	20.7 ± 1.3	68.4 ± 3.9

The same PPD assay was applied to Pat:SOD roots except the roots were photographed at 3 DAH instead of 4 DAH (Figure 4.9). Compared to the Pat:GCS roots, the Pat:SOD root samples became dehydrated much earlier in which some of the roots turned white and chalky at 1 DAH. At 3 DAH most of the roots were completely hardened due to loss of water although some developed PPD symptoms at certain extent. PPD scores for the roots were not scored. Removal of dried out layers prior photographing caused introduction of new wound response, made the root sections became thinner and eventually causing the roots sections more prone to dehydration.
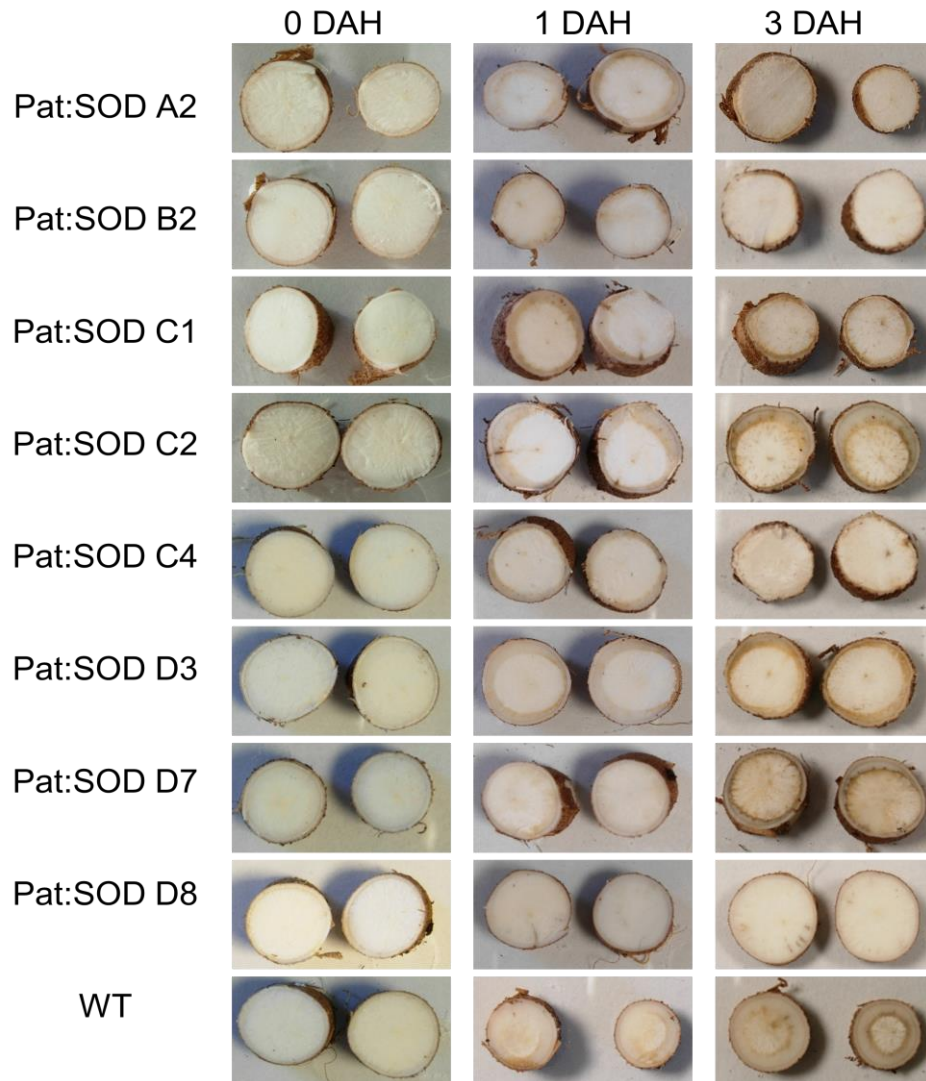
Figure 4.9 Pat:SOD lines and the WT root sections photographed following storage in a warm room at 25-27°C. Photographs were taken by removing dried out layers at each PPD times. Pictures are representative from three biological replicates.

Ultimately, the high frequencies of dehydration in the 3 and 4 DAH roots prevented an accurate calculation of PPD scores. This was evident when the majority of the roots at this time-point were scored more than 100% and up to 300% which did not match their actual PPD symptoms (data not shown). Although this method was proved to speed up PPD, dehydration issue clearly was its main weakness. The occurrence of microbial deterioration was another reason to dismiss this method.

4.3.3 PPD Assay 3: Overcoming the dehydration and microbial deterioration problem

The main advantage of using root sections in PPD Assay 2 was formation of clearly visible PPD symptoms which manifested on the surface of the roots. Cutting cassava roots into sections caused greater exposure of the surface area to the air compared to using it as a whole as it accelerated deterioration through oxidative damage. However, apart from becoming more receptive to oxidative damage, high surface area promotes moisture loss which eventually causes dehydration. At each time point the roots were wounded to remove the dried out surface and this was thought to exacerbate dehydration problem. To overcome this, some changes were made to PPD Assay 2. Instead of using the same root sections for analyses at separate PPD times, a pair of root sections was assigned to a single time-point. Selection of root samples followed the criterion mentioned in PPD Assay 2 (1.5-2 cm diameter). To minimise surface dehydration the root sections were placed in a covered Petri dish. A dry filter paper was used to support the base of Petri dish to avoid excessive transpiration. To reduce the probability of microbial infection the Petri dishes were kept in an incubator at 27°C instead of the common warm room.

Photographs were taken at 0, 1, 3 and 4 DAH. The 3 DAH time-points was introduced to track changes in PPD symptoms more carefully and to obtain PPD symptoms optimum for scoring. All photographs were taken using PENTAX K20D camera under the following settings; relative aperture f/2.8, exposure time 1/45 seconds, ISO 400. At each PPD time, the root sections were photographed and the pictures were used to find their greyness scores with a computer scoring method. For each PPD time-point the roots were analysed in triplicates, this required a total of 72 root sections pair in which 5 Pat:GCS lines and the WT line involved.
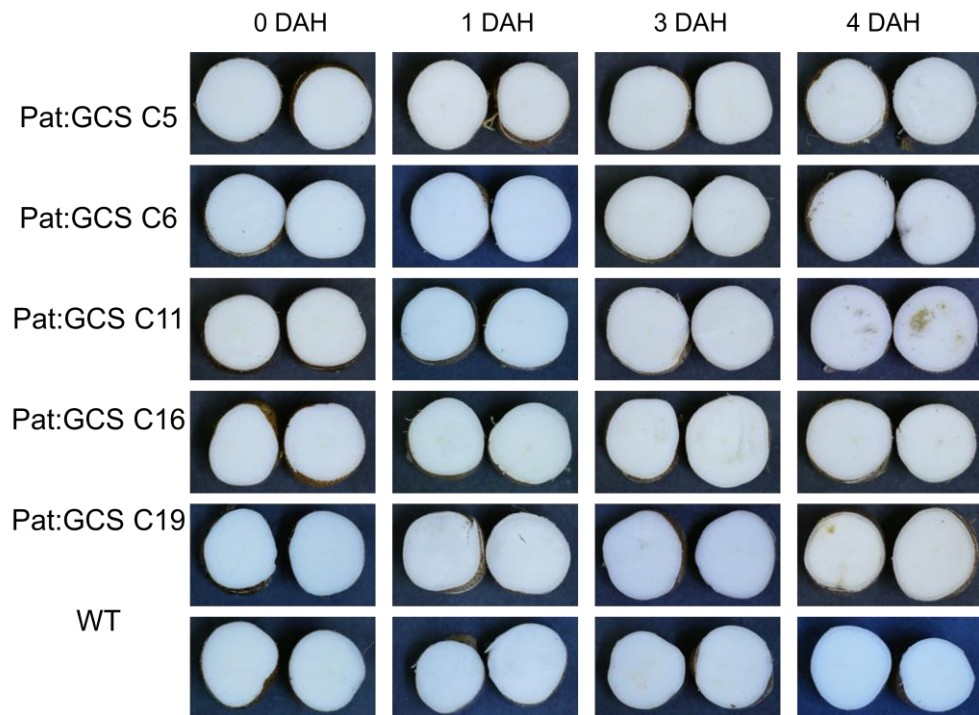
Figure 4.10 Pat:GCS lines and the WT root sections after harvest. Each root section was derived from a single cassava plant. The roots were incubated in a 27°C incubator. Pictures are representative of three biological replicates.

Compilation of root sections taken over the storage period revealed an unexpected result (Figure 4.10). None of the samples showed any PPD symptoms until at 4 DAH and this have made calculation of PPD scores unfeasible. Relatively the root sections at this time course appeared moist compared to those observed in PPD Assay 1 and 2 and only a small percentage of them appeared slightly discoloured. Although this assay method effectively resolved dehydration problem by reducing water loss from the root sections it inadvertently delayed the development of PPD symptoms. Failure to induce PPD symptoms in the recommended storage period was identified as the main disadvantage of this method.

4.3.4 PPD Assay 4: Controlled moisture loss and multiple wounding of root sections are essentials to a successful PPD assay

The rationale for assigning an individual pair for a PPD time in PPD Assay 3 was to allow the roots to deteriorate without excessive dehydration and to avoid multiple wounding, which proved to be the case. However, this also slowed down PPD considerably, so that it was very difficult to examine the development of PPD symptoms even at 4 DAH. Covering the Petri dish also found to delay PPD as it prevented water loss. At this point, wounds and sufficient water loss during storage were recognised as important aspects in deterioration. This eventually led to revision of PPD Assay 2 which had shown encouraging outcomes.

Selection of root samples followed the criterion described in PPD Assay 2 and 3 (1.5 - 2 cm diameter). Two root sections were prepared from each plant replicate and placed on a Petri dish lined with a dry filter paper. The Petri dishes were kept covered to prevent microbial contamination and stored in a 27°C incubator instead of the warm room. Humidity was provided by distributing approximately 100 ml distilled water in two Petri dishes which were left uncovered. All roots were analysed in triplicate, where 15 pairs of root sections were prepared from Pat:SODs and the WT root. The surface of the root sections were photographed at 0 DAH after harvest and the same root samples were photographed again at 1, 2, 3 and 4 DAH. Prior to photographing a thin layer of dried out surface was removed. All photographs were taken using PENTAX K20D camera under uniform lighting and with the following settings; relative aperture f/5.6, exposure time 1/200 seconds, ISO 400. The photographs were then used for estimation of greyness score using the computer scoring method (Figure 4.11). Since all samples were taken under fixed camera settings, normalisation against the photographs background was not required. PPD scores at each time points were calculated by normalising the greyness scores obtained at harvest.
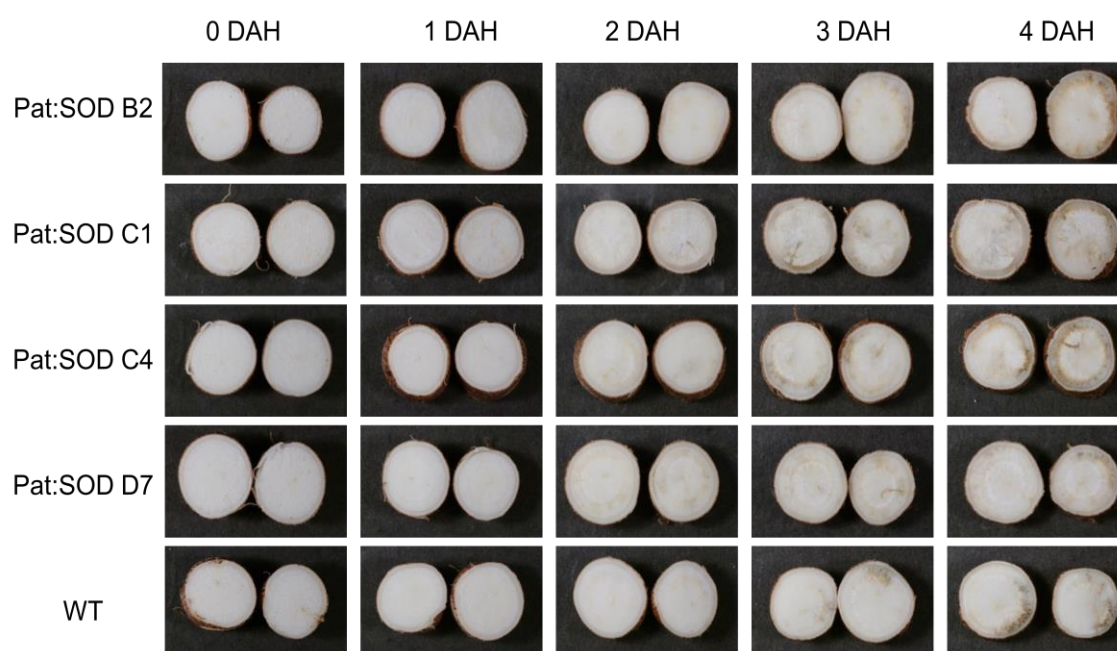
Figure 4.11 Pat:SOD lines and the WT root sections photographed at harvest,1,2,3 and 4 DAH. The roots were assayed with PPD Assay 4. Pictures are representative of three biological replicates.

Table 4.7 Greyness scores of Pat:SOD root samples measured by PPD Symptom Score software following harvest. SD values indicate PPD symptoms variation between two root sections. na indicates root sample not available due to inadequate size for PPD assay.

Cassava lines		0 DAH	1 DAH	2 DAH	3 DAH	4 DAH
Pat:SOD B2	P1	17.5 ± 0.7	22.6 ± 0.4	22.6 ± 1.5	31.7 ± 3.1	34.9 ± 0.9
	P2	18.2 ± 0.1	24.6 ± 1.7	26.9 ± 1.5	34.4 ± 0.7	34.9 ± 3.1
	P3	na	na	na	na	na
Pat:SOD C1	P1	18.0 ± 1.2	21.1 ± 0.1	20.8 ± 0.4	28.1 ± 1.5	37.1 ± 3.2
	P2	17.2 ± 0.2	20.7 ± 0.1	23.2 ± 0.9	26.2 ± 1.8	32.3 ± 2.8
	P3	18.0 ± 1.3	19.9 ± 0.5	25.9 ± 2.2	26.3 ± 1.2	25.5 ± 1.2
Pat:SOD C4	P1	18.1 ± 0.8	19.7 ± 0.8	23.8 ± 2.7	34.7±6.6	33.5±3.3
	P2	17.0 ± 1.3	15.8 ± 0.4	19.3 ± 0.8	25.7 ±0.6	36.4±0.3
	P3	18.3 ± 0.9	23.8 ± 0.1	26.8 ± 1.2	28.9 ±1.0	38.3±3.7
Pat:SOD D7	P1	18.2± 1.1	18.5±0.1	18.4 ±1.2	21.7±2.6	24.3±3.0
	P2	17.1±1.1	19.7±0.1	21.8±1.8	28.1±1.8	34.4±2.5
	P3	17.5±0.1	18.0±0.9	26.8±0.1	28.4± 0.9	32.7± 0.4
WT	P1	19.8 ±1.2	18.0±0.2	24.4± 0.0	30.1±1.7	33.3±3.6
	P2	19.4 ±1.1	26.7±2.8	25.2±1.3	28.1±5.2	38.8±3.8
	P3	19.2 ±0.8	18.3±0.8	19.8±2.2	25.1±1.3	43.5±1.5
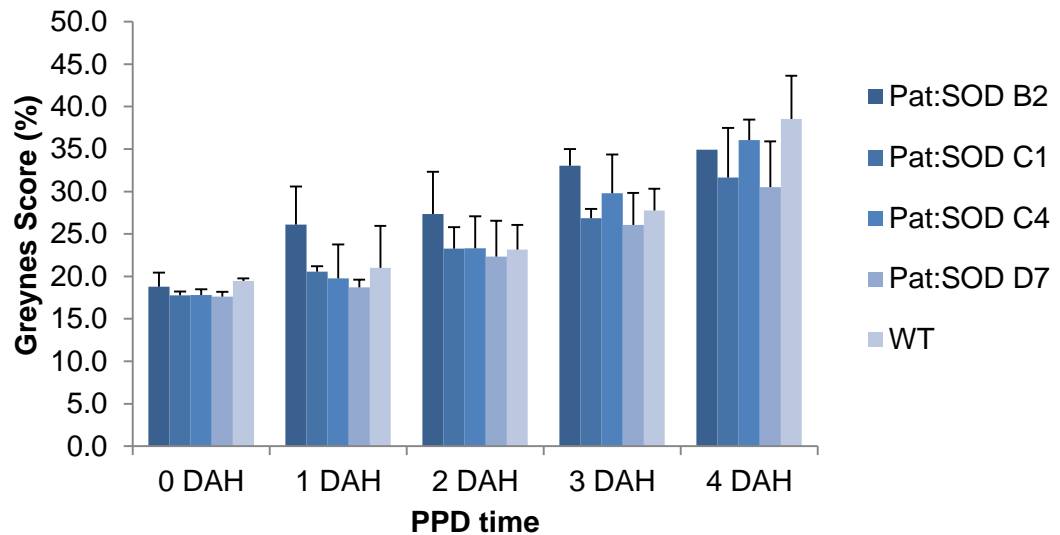
Figure 4.12 Mean greyness scores of Pat:SOD root sections over storage times. SD represents biological replicate variations, n=3.

The greyness score of individual root sections pair is presented in Table 4.7. These values were used to calculate mean greyness score and to see the change of PPD symptoms by plotting the scores over storage time. Figure 4.12 clearly shows a steady increase of PPD symptoms over storage period with highly visible symptoms observed at 3 and 4 DAH. Interestingly, the changes in PPD symptoms from 0 DAH were significant at all PPD times (t-test, $p < 0.05$) except for at 2 DAH.

The PPD symptoms developed in this PPD assay were the usual types, the root sections either showed brown staining or blue-black discoloration or both symptoms. Importantly, none of the root sections showed either microbial deterioration or excessive dehydration until at 4 DAH. Supplying water in the incubator chamber had resolved dehydration problem by maintaining high humidity during the course of deterioration. The absence of dehydrated samples had enabled measurement of greyness scores even at late storage times, to be done with greater accuracy. Additionally, in this assay the root sections deteriorated more homogenously compared to those observed in PPD Assay 2, as indicated by lower SD values (Table 4.7). Despite this, variations between root replicates were still high in both the transgenic lines and the WT line as can be seen from 2 DAH onwards.

This PPD assay also was applied to the Pat:GAR transgenic group with more root samples. A total of 24 pairs of root sections were prepared from 24 transgenics and the WT. These root samples were assayed in the same conditions as Pat:SOD roots. The root samples were also treated and photographed similarly except that photographing at 2 DAH was omitted. Photographing was also done with the camera settings and the photographs were used for computation of greyness scores which then were used for calculation of PPD scores. Again, normalisation was not required because all photographs were taken under fixed camera settings.
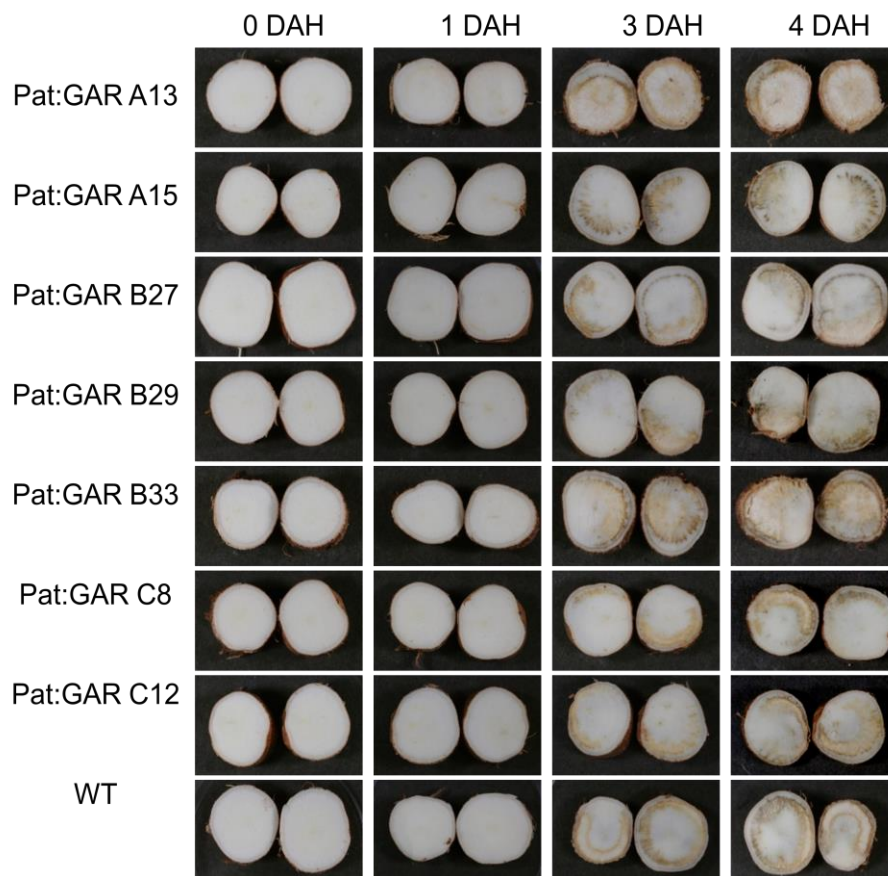

Figure 4.13 Pat:GAR lines and the WT line root sections photographed at harvest,1,3 and 4 DAH. The roots were assayed with PPD Assay 4. Pictures are representative of three biological replicates.

All roots deteriorated as anticipated as none were found severely dehydrated or attacked by microbes. Figure 4.13 shows root samples photographed over PPD times from which greyness scores were computed. PPD symptoms were clearly visible at 3 DAH and became more intense at 4 DAH with brown staining being noticeably more prominent than the vascular streaking.

In PPD Assay 2, it was assumed that high SD values would be obtained when one of the root sections of a root sample was dehydrated as this caused unequal rate of deterioration. This was supported by data gathered from Pat:SOD group samples using PPD Assay 4 where none the root samples were dehydrated and variations between root sections were remarkably reduced. However, this assumption might not be true as high variation was still be observed in Pat:GAR especially at 4 DAH even though none of the samples dehydrated (Table 4.8)

Table 4.8 Greyness scores of Pat:GAR root sample replicates measured by ETH software following harvest. SD values indicate PPD symptoms variation between two root sections.

Cassava lines		0 DAH	1 DAH	3 DAH	4 DAH
Pat:GAR	P1	18.1 ± 3.5	18.0 ± 8.5	21.5 ± 12.8	30.3 ± 14.2
A13	P2	15.0 ± 4.4	16.0 ± 2.9	41.7 ± 4.3	52.5 ± 5.9
	P3	14.6 ± 2.9	19.3 ± 4.7	48.8 ± 0.4	43.4 ± 2.7
Pat:GAR	P1	15.7 ± 9.4	21.2 ± 2.4	36.3 ± 7.5	32.5 ± 14.3
A15	P2	17.7 ± 6.3	19.8 ± 2.7	45.2 ± 9.7	44.4 ±1.6
	P3	16.8 ± 2.3	16.8 ± 8.8	32.7 ± 2.6	30.7 ± 18.3
Pat:GAR	P1	14.7 ± 4.6	16.4 ± 4.9	36.8 ± 0.2	42.3 ± 0.2
B27	P2	15.4 ± 5.9	17.7 ± 3.1	37.9 ± 2.9	37.9 ± 6.9
	P3	15.0 ± 8.3	17.4 ±5.1	36.5 ± 8.7	17.2 ± 12.4
Pat:GAR	P1	15.1 ± 4.7	20.7 ± 10.6	34.3 ± 6.9	34.3 ± 14.2
B29	P2	14.4 ± 4.7	17.2 ± 3.6	31.2 ± 7.8	32.5 ± 1.0
	P3	18.5 ± 11.3	16.9 ± 7.0	34.0 ±4.4	43.8 ± 0.7
Pat:GAR	P1	17.4 ± 8.8	20.5 ±8.7	45.6 ±5.8	35.2 ±11.6
B33	P2	19.6 ± 3.3	22.7 ±4.2	43.8 ±1.1	53.3 ±19.1
	P3	15.7 ± 6.3	16.6 ±3.9	37.4 ±4.9	30.0 ±8.3
Pat:GAR C8	P1	16.0 ±0.5	17.9 ±2.6	33.7 ±4.5	33.5 ±2.4
	P2	17.5 ±3.4	17.5 ±5.9	24.6 ±1.7	20.6 ±11.8
	P3	15.6 ±4.0	20.5 ±2.8	33.2 ±6.6	27.2 ±18.7
Pat:GAR	P1	14.8 ±5.9	17.2 ±5.1	30.6 ±0.9	32.2 ±0.1
C12	P2	18.4 ±2.3	21.2 ±7.5	49.4 ±11.4	38.0 ±7.3
	P3	16.6 ±3.3	18.1 ±3.0	30.6 ±12.0	21.6 ±15.4
WT	P1	17.9 ±4.0	20.8 ±2.7	29.5 ±4.9	29.7 ±9.6
	P2	16.4 ±6.6	18.5 ±10.2	33.8 ±2.0	30.1 ±16.6
	P3	12.4 ±7.1	15.2 ±6.0	37.0 ±3.4	44.8 ±5.1

The mean greyness scores were calculated from the plant/root sample replicates and were plotted against PPD times (Figure 4.14). It clearly shows a sharp increase of PPD symptoms occurred at 3 DAH and 4 DAH. The change in PPD symptoms from 0 to 1 DAH was small but significant (t-test, $p < 0.05$). On the other hand, as can be inferred from the root sections pictures, the changes in PPD symptoms at 3 and 4 DAH were considerable, but were only statistically significant at 3 DAH. This is because, at 4 DAH not only high variations were observed within the same root samples but also between the root sample replicates.
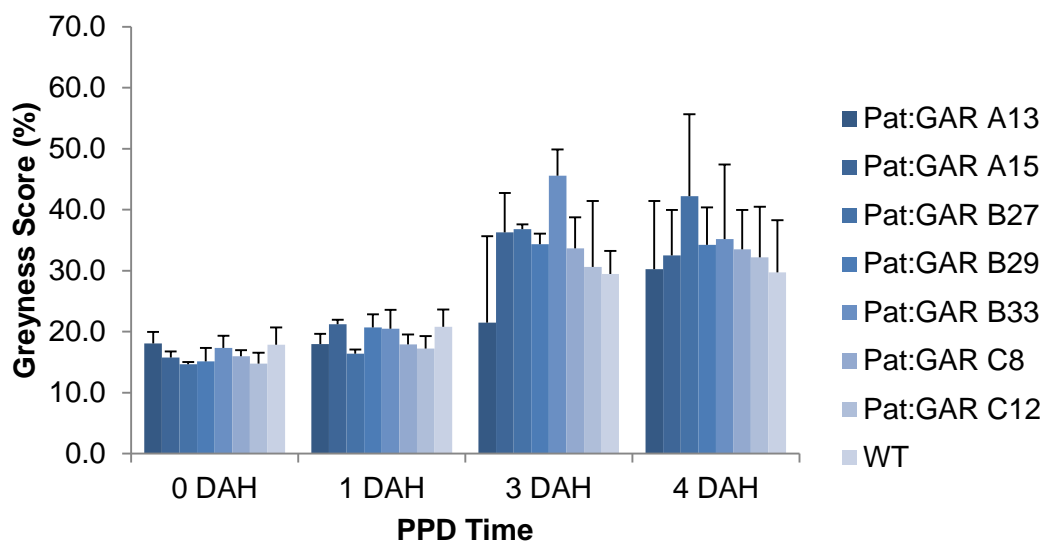
Figure 4.14 Mean greyness scores of Pat:GAR root samples over storage times using computer scoring. SD represents biological replicate variations, n=3.

4.3.5 Extensive variations of PPD symptoms between root samples and reproducibility of the computer scoring method

High variations in PPD symptoms are undesirable but were consistently observed in all PPD assays trials except in PPD Assay 3. In PPD Assay 1, this was probably caused by the slow PPD response that meant that at 3 DAH the symptom development was still ongoing in some roots. On the other hand, in PPD Assay 2 high PPD symptoms variation was attributed to dehydrated root sections and to a too rapid PPD response. While these problems were effectively tackled in PPD Assay 4, variation in PPD symptoms was only reduced in one transgenic group but persisted in another.

It is not surprising if PPD symptoms in transgenic plant lines originated from the same transgenic group to vary but this is unexpected in the WT line. The WT is not genetically modified and served as a control line. In all PPD assays, 3 WT roots were used and pooled here are the WT root samples at 'late' PPD times where the PPD symptoms were evident.

Figure 4.15 clearly shows variation of PPD symptoms in PPD Assay 1 and PPD Assay 2 respectively. In PPD Assay 1 only Root 2 was severely deteriorated after 3 days storage while others appeared undeteriorated despite being harvested at the same time and assayed in a similar way. Similarly, in PPD Assay 2 only Root 3 showed PPD symptoms as the other two were severely dried out. However, making a valid comparison was difficult in both cases as the assays themselves were defective in many aspects as previously discussed.
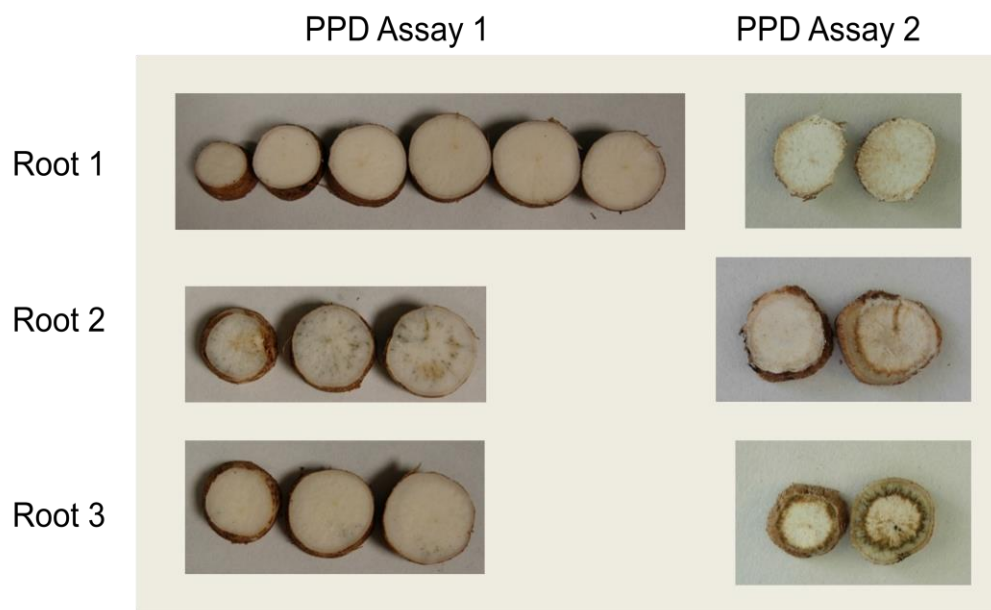
Figure 4.15 Three WT root replicates at 3 DAH assayed with PPD Assay 1 and root replicates at 4 DAH assayed with PPD Assay 2. In both assays the roots were stored at 25-27°C except that PPD Assay 1 involved incubating the whole storage roots while PPD Assay 2 utilised root sections. Each root was obtained from a single cassava plant.

Although PPD Assay 4 was not a significant improvement over the methods tested, it is justified to claim it as the best PPD assay attempted in this study. It succeeded in controlling two responses that interfered with measuring PPD symptoms, through reducing dehydration and preventing root decay caused by bacteria. Two transgenic groups were assayed with this method, the Pat:SOD and the Pat:GAR. Roots 1-3 served as control in Pat:SOD group while roots 4-6 served as control in Pat:GAR group (Figure 4.16). The pictures of the roots at 3 and 4 DAH were presented here since only at these times PPD symptoms were clearly visible. At either PPD times no commonalities in PPD symptoms were detected among these roots, the intensities as well as the type of symptoms developed were variable. Variation in PPD symptoms was not only found between sample replicates but also apparent in root sections derived from a single a root. This is not unusual as it is equally observed in other transgenic groups and PPD assays.
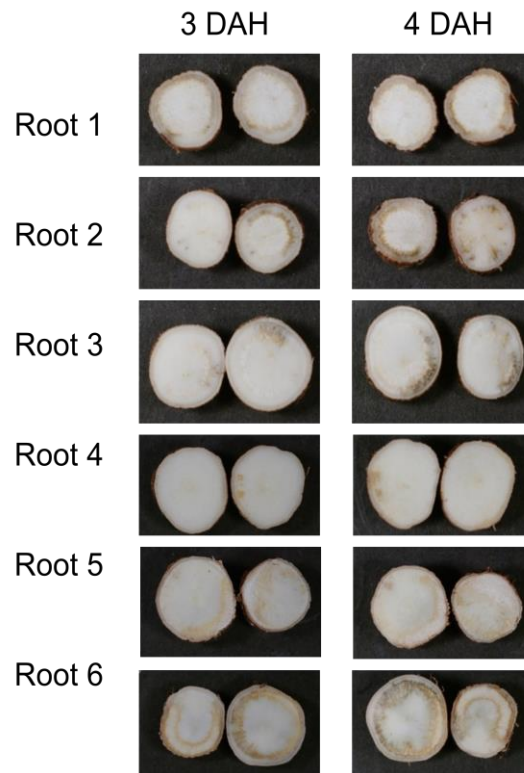
Figure 4.16 WT root samples assayed with PPD Assay 4 at 3 and 4 DAH. Root 1-3 was the control samples in Pat:SOD group, Root 4-6 were the control samples in Pat:GAR group. All roots were obtained from different plants and captured with fixed camera settings.

In the present study, all the PPD assays were evaluated based on analysis by computer scoring. The reliability of the computer scoring method was tested by 'compare and contrast' of the PPD score calculated and the visual rating score. Regression analysis of all root sample pictures involved in PPD assay 4 proved that approximately 80% of the computer-generated score matched the visual scores. Pearson test confirms that these two scores are significantly correlated (r (74) = 0.88, p < 0.05). The remaining 20% mismatch scores is owing to variable type of PPD symptoms developed by the entire root samples which has made visual scoring that completely based on subjective decision become difficult. However, this is only true in root samples at 3 and 4 DAH as the earlier PPD time root sections tend to be scored 0 by visual rating method. To demonstrate this, Figure 4.16 which consists of root sections of highly variable symptoms were used to compare the computer-generated scores and the visual scores.

	3 DAH	Comp.	Visual	4 DAH	Comp.	Visual
Root 1		34.4	30.0		40.7	30.0
Root 2		30.9	30.0		50.0	50.0
Root 3		23.5	20.0		55.9	45.0
Root 4		4.6	0		15.5	5.0
Root 5		22.8	20.0		27.9	20.0
Root 6		66.5	60.0		72.3	70.0

Figure 4.17 Comparison between PPD scores of root sections from Figure 4.15. (Comp.) refers to PPD scores calculated from the greyness scores generated by the ETH software and (Visual) refers to PPD scores assigned based on Reference picture (Figure 4.4).

Figure 4.17 shows that the majority of the root samples had comparable scores. Essentially, the nature of these methods caused the computer-scoring method to generate slightly higher PPD score than the visual rating method. In the computer

scoring method, the software is incapable of differentiating vascular streaking and tissue browning thus scores them equally. On the other hand, in the visual method brown staining often is underestimated because this type of symptoms is not found in the reference picture. Therefore, the visual method is more appropriate for a study that aims to look for a general deterioration. For a study that requires rigorous evaluation of PPD and its symptoms, the computer scoring is highly recommended. Nevertheless, the aim to standardise the scoring method between labs could only be achieved with the computer scoring especially if the roots developed inconsistent and highly varied PPD symptoms.

4.3.6 Fluorescence and scopoletin accumulation as markers in PPD assessment

Scopoletin can be visualised without any pre-treatment of the roots. It fluoresces under UV light, thus provision of a UV lamp is sufficient to see its production. The use of scopoletin-induced fluorescence as a PPD marker was tested in a preliminary experiment where root sections from the WT lines were monitored over a 7-day time course for fluoresce and by PPD Assay 4. This showed that there was no or minimal fluorescence in the root samples at 0 DAH but the fluorescence intensified a day after. At 3 and 5 DAH the fluorescence level were slightly different between the two sets of roots. However, it is interesting to note that at 5 DAH Root 2 sections that were microbially decayed stopped fluorescing under UV light while Root 1 that underwent the expected physiological deterioration continued to mildly fluoresce until at 7 DAH (Figure 4.18).
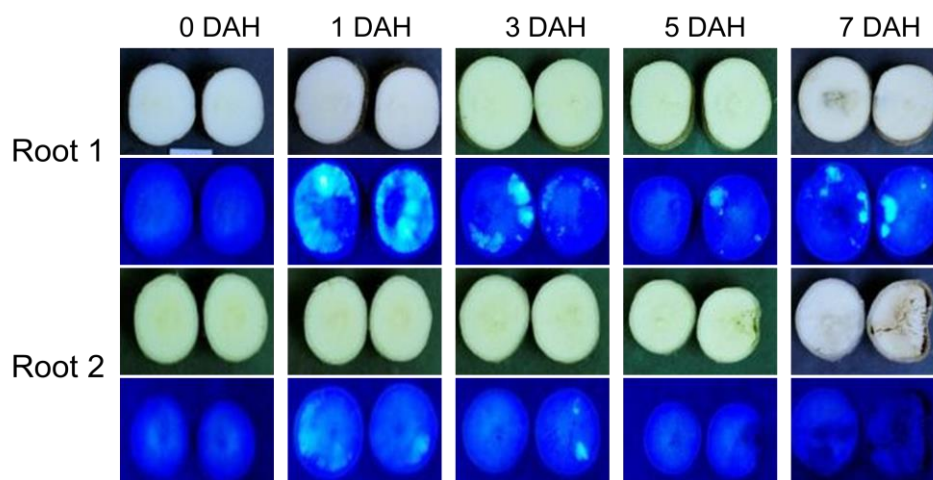
Figure 4.18 Two root samples were tested for the relationship between PPD and scopoletin–induced fluorescence. Root 1 had undergone normal PPD response until at 7 DAH and was showing scopoletin production while Root 2 was attacked by microbes at 5 DAH stopped producing scopoletin. Both roots were the WT roots and assayed with PPD Assay 4.

4.3.7 Fluorescence accumulation and its association with PPD symptoms

To investigate the potential of scopoletin, three different transgenic groups were used. Their root sections were photographed under UV light (in addition to the white light) in order to detect the accumulation of scopoletin-induced fluorescence and relate it to visible PPD symptoms. They were the Pat:SOD group, the Pat:GAR and the Pat:GCS

group. All UV photographs were taken in a dark room using PENTAX K20D camera with the following settings; relative aperture f/2.8, exposure time 0.7 seconds, ISO 400. The photographs were then used to estimate fluorescence accumulation over storage time by visually rating the percentage of fluorescence produced on the surface of the root sections. In this case, a visual rating method was applied because fluorescence could not be accurately computed with the same software used to measure PPD symptoms as converting UV captured pictures to greyscale pictures caused saturation of score. Besides, the software was also unable to differentiate between fluorescence and PPD symptoms which lead to a combined measure. To find the association between fluorescence score and PPD score, the correlation of these scores were computed with either Pearson Correlation at $p = 0.05$, two-tailed level of significance or the Spearman rank correlation test also at $p = 0.05$, two-tailed level of significance.

The Pat:SOD roots were assayed with PPD Assay 4, in which pairs of root sections were observed over a time-course by removing successive layers of dried out root surface. Figure 4.19 shows the representative of Pat:SOD root samples photographed under UV light at various PPD times.
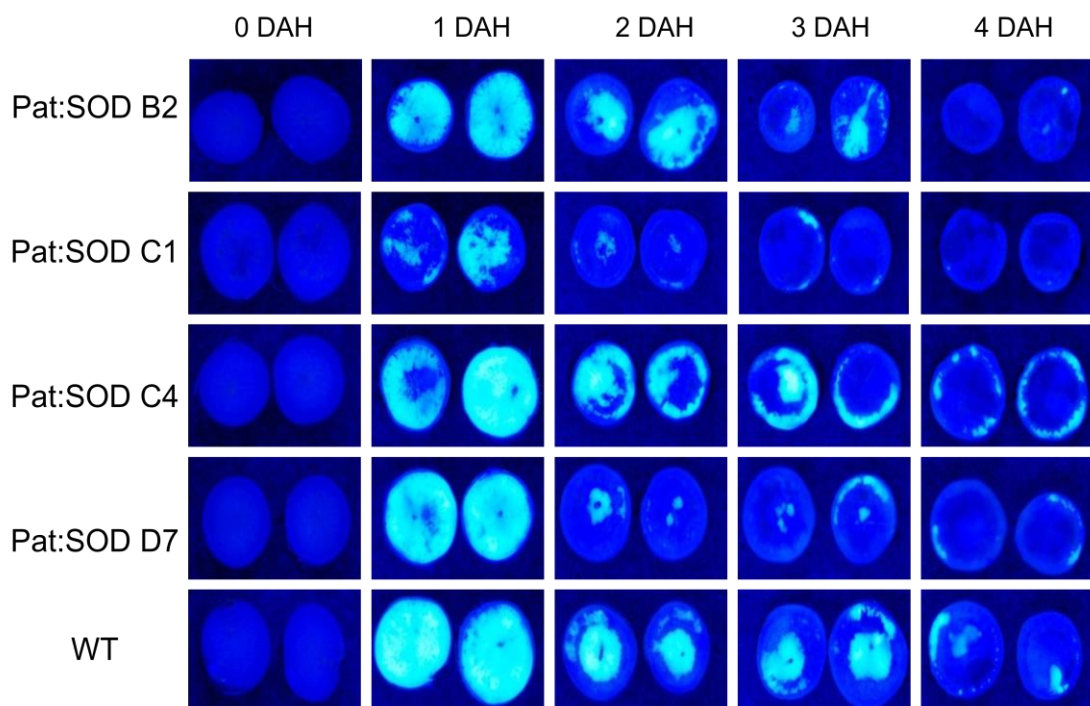
Figure 4.19 The Pat:SOD lines and the WT root sections photographed under UV lights following. The roots were assayed with PPD Assay 4. Photographs are the same root samples taken under white light above (Figure 4.11).

Figure 4.20 shows Pat:GAR root samples that were assayed in parallel to the Pat:SOD roots were also viewed and photographed under UV light to observe fluorescence production.
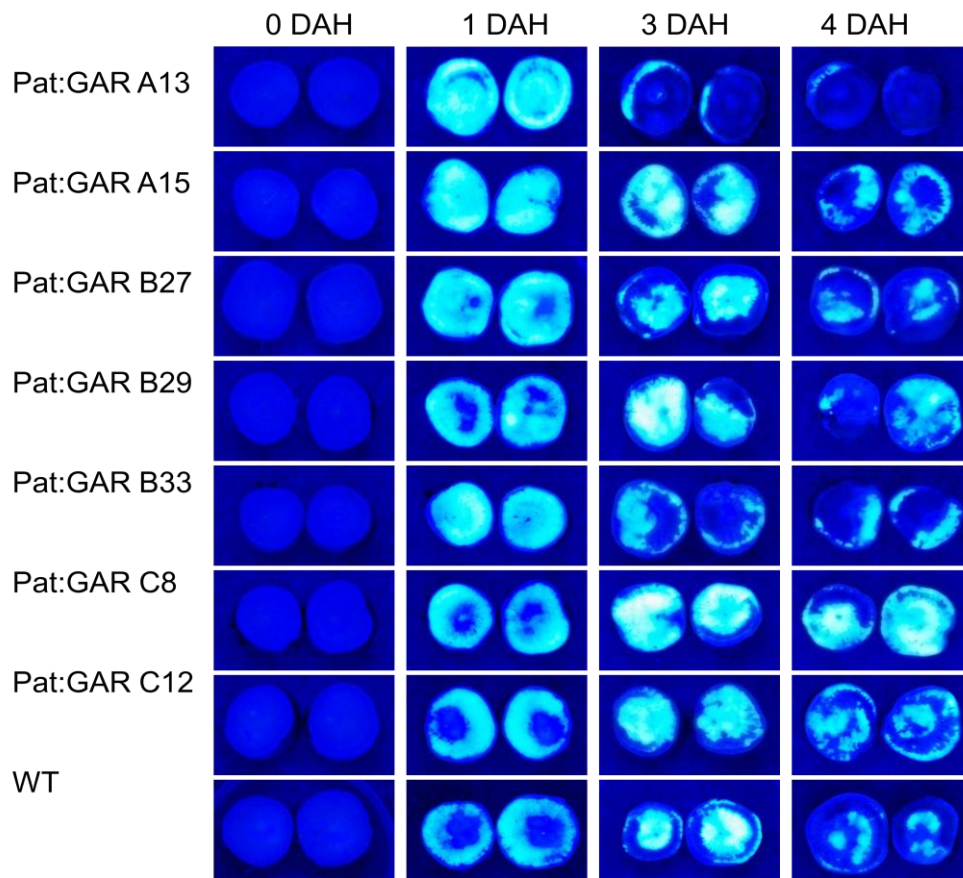
Figure 4.20 The Pat:GAR lines and the WT root sections photographed under UV lights. The roots were also assayed with PPD Assay 4. Photographs are the same root samples taken under white light (Figure 4.13).

The Pat:GCS roots were assayed with PPD Assay 3 in which individual root sections were assigned to each PPD times in order to avoid multiple wounding and excessive dehydration. They were also viewed and photographed under UV light as shown in Figure 4.20.
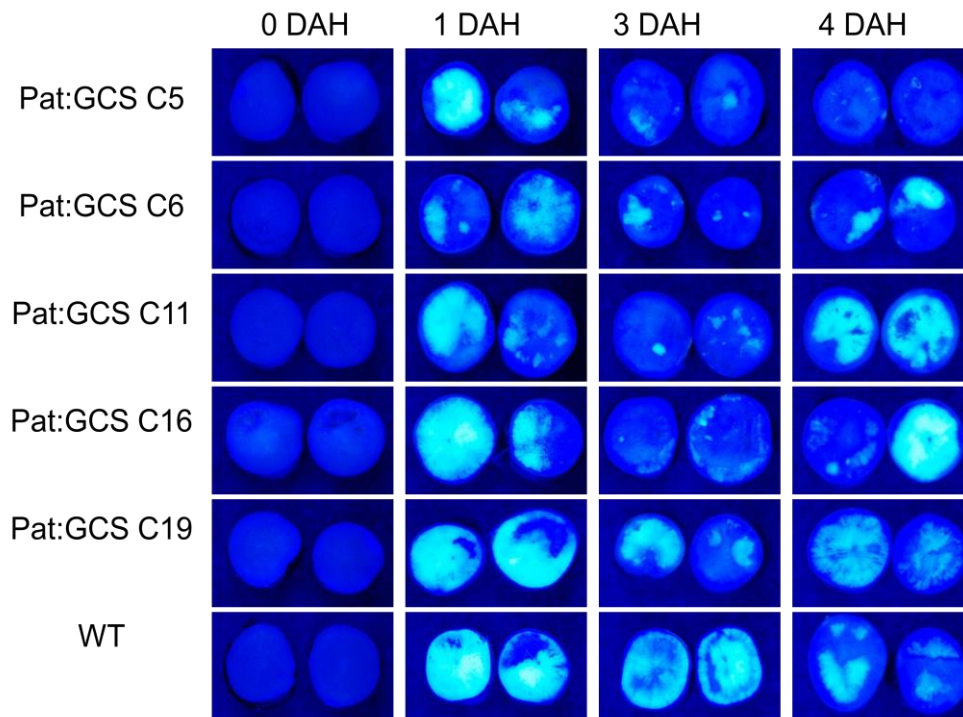
Figure 4.21 The Pat:GCS lines and the WT root sections photographed under UV lights following. The roots were assayed with PPD Assay 3. Photographs are the same root samples taken under white light (Figure 4.10).

Figure 4.19, 4.20 and 4.21 are the representatives of root samples of all lines in the respective transgenic groups. The fluorescence scores from these root samples were pooled and the mean fluorescence scores were calculated and plotted against PPD times along with PPD scores to see how they change over storage time (Figure 4.22).

According to Figure 4.22, neither PPD symptoms nor fluorescence were detected at 0 DAH. After 24 hours, both the PPD symptoms and fluorescence started to significantly ($p < 0.05$) accumulate except that fluorescence accumulated more rapidly than the PPD symptoms. At 3 DAH most PPD symptoms became more visible, causing significant ($p < 0.05$) increase in PPD scores, but on the contrary the fluorescence level decreased significantly ($p < 0.05$). At 4 DAH the scores showed an opposite trend as the PPD symptoms became more visible but the roots fluoresced significantly less than at 3 DAH. However, the increase in PPD scores from 3 to 4 DAH was not significant ($p = 0.23$).
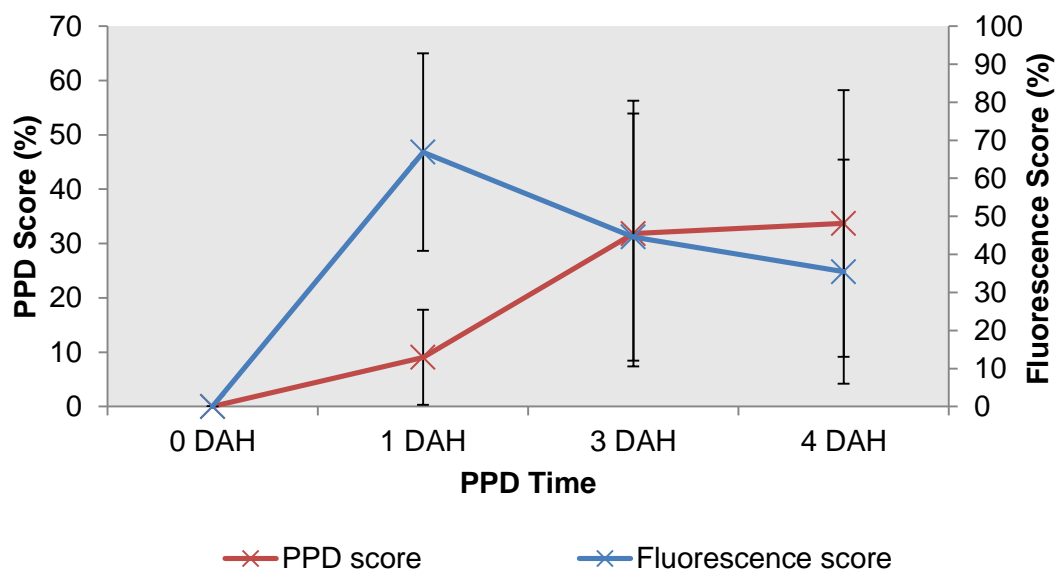
Figure 4.22 Changes in PPD symptoms (PPD scores) and fluorescence (Fluorescence score) over storage time. The mean scores at each time point were derived from root samples in Pat:SOD, Pat:GAR and Pat:GCS transgenic group.

The relationship between fluorescence score and PPD score was examined at all PPD times. This is depicted in Figure 4.23. In general, a non-linear correlation was exhibited at all storage times, so the Spearman test was chosen over the Pearson test. Overall analysis of fluorescence and PPD scores also revealed a poor relationship ($R^2 = 0.018$) and little correlation between the two scores (r (216) = -0.32, $p < 0.05$). It is obvious that the correlation between the two scores was significant at 0 DAH as the roots did not either develop PPD symptoms or fluorescence shortly after harvest. Also, there was significant relationship between the two. However, as predicted from Figure 4.22, the relationship between two scores was found to be weak at 1 DAH ($R^2 = 0.004$) and the Spearman test confirms that there was no correlation between scores (r (54) = 0.07, $p > 0.05$) as visibly apparent. There was a very weak positive relationship between the fluorescence produced by the roots and the PPD symptoms they developed at 3 DAH ($R^2 = 0.070$). But, despite the poor relationship of the scores they were significantly correlated (r (54) = 0.27, $p < 0.05$), showing consistency of fluorescence and PPD symptoms at this storage time. At 4 DAH, the opposite trend of the two scores suggest a poor relationship between them and this was confirmed ($R^2 = 0.099$). Also, the correlation at this storage time was significantly negative (r (54) = -0.32, $p < 0.05$) as tested.
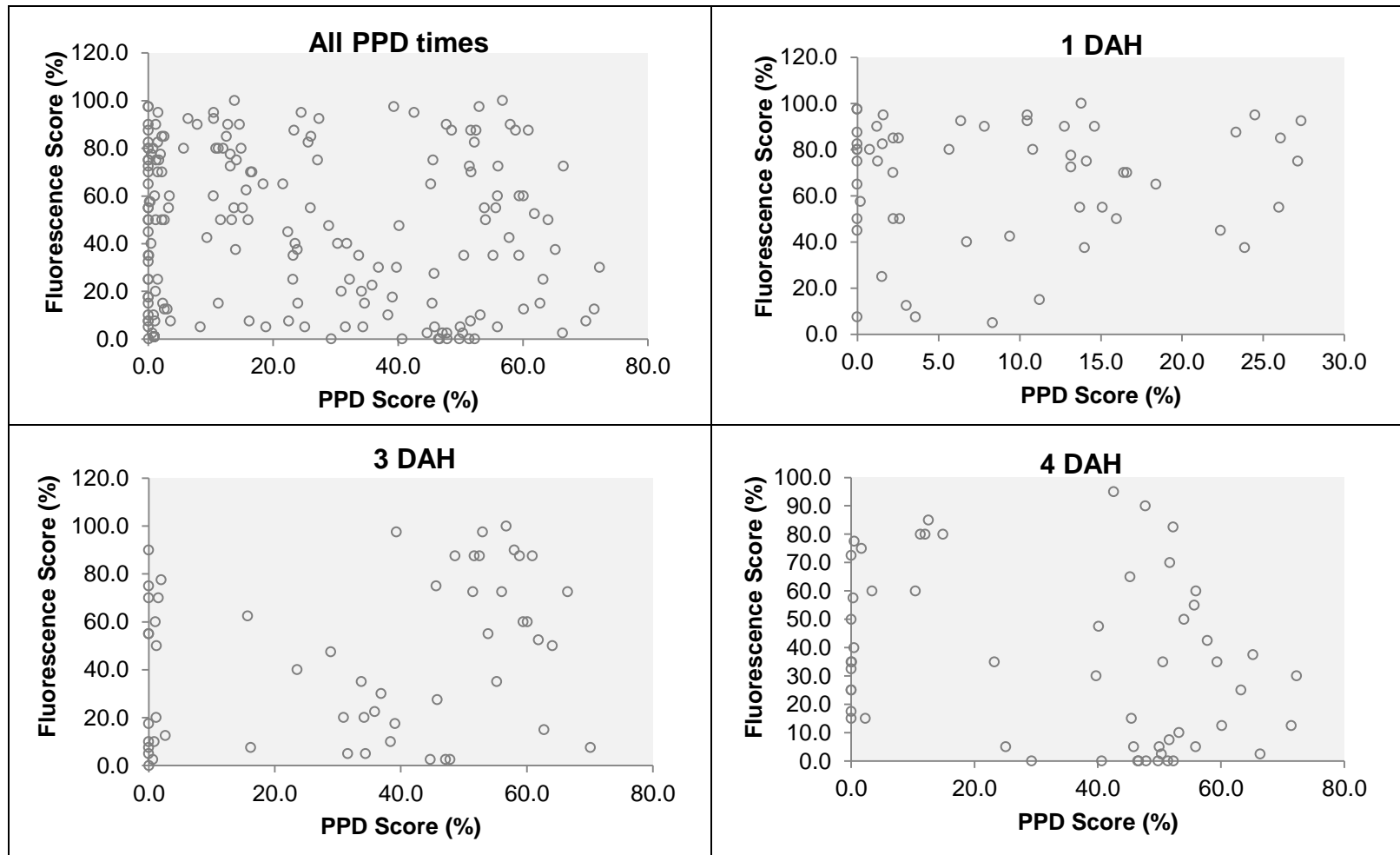
Figure 4.23 Association between PPD scores and fluorescence score at all PPD times and individual PPD times. PPD scores were determined using ETH software and the fluorescence scores were estimated by visual rating. These data were pooled from materials in Pat:SOD, Pat:GAR and Pat:SOD.

In general, the above findings demonstrate an indirect association between the fluorescence produced by the roots and the PPD symptoms they developed. An alternative interpretation of this is the possible role of coumarin-induced fluorescence (mainly by scopoletin) as an early signal of PPD. On the other hand, the PPD symptoms which tend to appear later on might be accurately considered as a late PPD signal. To investigate this possibility, the association between fluorescence scores at 1 DAH and PPD symptoms at 4 DAH were assessed. These data were chosen because fluorescence was emitted the highest at 1 DAH and the PPD symptoms were the most visible at 4 DAH.
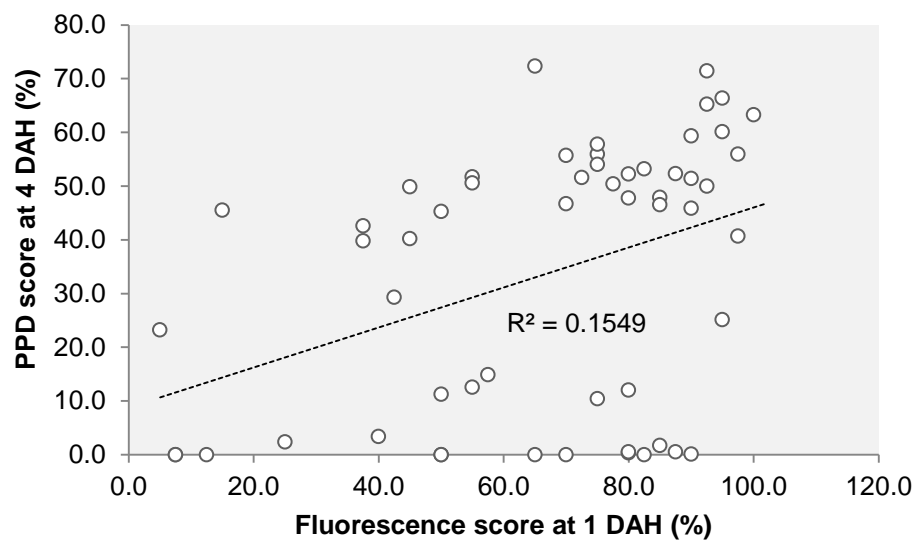
Figure 4.24 Association between fluorescence score at 1 DAH and PPD symptoms at 4 DAH. Data analysed from Pat:SOD, Pat:GAR and Pat:GCS group.

Figure 4.24 shows a medium positive relationship (R^2 = 0.154) between fluorescence produced in the early harvest time and PPD symptoms exhibited by the storage roots later on. However, the two scores were significantly correlated (r (54) = -0.39, p < 0.05) supporting scopoletin-induced fluorescence as a candidate marker. An important point worth noting is PPD symptoms were not visible in most of Pat:GCS roots at 4 DAH and this may considerably weaken the statistical analysis. However, unless this is examined with a larger sample size, the claim that fluorescence level as an early marker of PPD is poorly justified.

4.4   Discussion

PPD Assay 1 or the 'whole root' method is based on the most commonly used assay in the cassava research community working with field-grown material. It offers a great advantage because it simulates the natural occurrence of deterioration in cassava (Morante et al., 2010). Unfortunately, employing this assay with our root samples caused PPD to take place too slowly, so that at 3 DAH the PPD symptoms had not fully established. This is probably due to the exposure of a small cut root surface to the atmospheric oxygen delaying the onset of PPD. Essentially, this contrasts with CIAT's practice that 3 days following harvest is sufficient for the roots to develop PPD symptoms ideal for scoring. However, it is perhaps not surprising because in contrast to the greenhouse-grown roots CIAT uses roots grown in the field.

In this study, the reproducibility of the 'whole root' method was challenged by several factors. They are size, form, and age of the roots used. Traditionally, the roots used for PPD assays are those harvested from field-grown plants and have an average size of 30 to 40 cm. In this study, restricted greenhouse space limits the size of plants as well as the roots produced to 1/4. Simple size downscaling did not work perfectly as the roots physical shape was altered. As compared to the field-grown roots which tend to grow horizontally, the roots in this study were mostly distorted and their size varied as a result of growing in a small container. For example, one plant may grow a single bulky storage root where others grow several roots of smaller sizes. Variations in the forms have made selections of roots difficult as it affected the lengthwise measurement of the roots and the way they were cut into sections for photography. In many cases, starting the experiment with equal root lengths would not necessarily give equal numbers of root sections. Additionally, the roots produced in the greenhouse were grown for a limited period and were harvested at a younger age than the roots grown in the field. Plant age determines dry matter and water content of the roots, so that that mature roots are found to have high dry matter due to formations of woody substance (Ro and Douglas, 2004). High dry matter content is a desirable trait in cassava industry and has been reported to positively correlate with PPD (Sanchez et al., 2006, Benesi et al., 2010). Although this was not measured, the roots used in this study probably had low dry matter because they were harvested at early growing period and because being grown in small pots, they were watered frequently to prevent drying out, which would lead a delayed development of PPD. More homogenous PPD symptoms would be expected if the roots were to be stored longer but this might not be a practical solution as this increased the risk of microbial contamination. At ETH, several attempts to assay greenhouse storage roots with the CIAT method were similarly found to be

unsuccessful, which led to some modifications being made. These include extending the length of storage time but microbial deterioration took place 4 days after harvest. Also, cutting the storage roots into two and storing them in a greenhouse under high humidity condition caused them not to develop PPD as most of the root suberised (I. Zainuddin, *pers. comm.*).

To overcome the above-mentioned problems roots were cut into sections. Assessing PPD using root sections has been practiced in many laboratories that grow their cassava plants in greenhouse (Bull, 2011, Owiti, 2009, Page, 2009). It is more flexible because only a part of the roots are required. Root sections had successfully speeded up the development of PPD symptoms, but it also increased the risk of surface dehydration (PPD Assay 2) as a result of large surface area being exposed to the air. Surface dehydration had been recognised in the past and one of the solutions proposed to minimise it was using moist filter paper to support root sections and covering the Petri dish during storage time (Owiti, 2009). This strategy prevented dehydration effectively but the roots turned soggy and showed symptoms of microbial degradation at late PPD time points and in addition to developing PPD symptoms, which made it difficult to measure PPD in these roots (S. Bull and Owiti, *pers. comm.*). Bull (2011) also investigated the effect of moist filter paper using the same method and found that it caused the roots to undergo mixed PPD and microbial deterioration rather than just the former. In a separate experiment, Page (2009) found this method had increased the occurrence of microbial deterioration. These observations were the reason for not considering this specific PPD assay in this study. Instead, separate root samples were used in an attempt to minimise dehydration (PPD Assay 3). It was interesting that this assay revealed two important aspects in accelerating PPD that is minimal dehydration and wounding. Loss of water through evaporation is expected but severe dehydration could possibly affect the biochemical activities involved in the formation PPD symptoms, such as vascular streaking therefore must be avoided. On the other hand, wounding has been long recognised as important aspect to initiate the PPD response by triggering general wound responses including increasing root respiration (Marriott et al., 1978, Marriott et al., 1979) so including it in a PPD assay leads to a more rapid PPD response.

The evaluation of these factors finally led to a more reliable PPD assay, PPD Assay 4. In this assay, both factors were considered; severe dehydration was prevented and the roots were repeatedly wounded. Consequently PPD symptoms and PPD scores increased with storage times, approximately in parallel with those observed in field-grown material using the traditional CIAT method. Furthermore, microbial deterioration

was also prevented. The reproducibility of this assay method was confirmed, as the Pat:SOD and Pat:GAR root sample group yield similar results but ideally it would be best to extend this analysis with a larger sample.

Curiously, none of the assay methods reduce the large variations measured in PPD symptoms. It was suggested that growing plants in a greenhouse for PPD evaluation would reduce inter-season and environmental effects as found in field-grown, roots but this proved not to be the case (Rodriguez, 2001).Variations were commonly found not only between roots produced from the same lines but also among root sections derived from the same plants. The main problem produced by this high variation in PPD symptoms was the level of noise in the data that reduced the quality of assessment. Only by using much larger sample sizes, not readily feasible when growing plants in the green house, would the detection of minor differences in PPD response between different cassava lines be feasible. This high variation occurred in all the plants assayed, transgenics as well as the WT roots, which would make measuring subtle effects of the transgenes on PPD challenging.

The assessments on PPD assays were all made based on calculation of PPD scores using the computer-based scoring. Since the commercial image analysis software like ImageJ, Pixcavator have become available, subjective visual PPD scoring is getting less popular among the PPD research community (Xu et al., 2013b, Salcedo et al., 2010). Although it was time-consuming compared to visually scoring the roots, it was found to be more objective and reliable. It eliminated scoring bias which could result from the two common PPD symptoms, vascular streaking and root discoloration (browning). In the most recent study, the use of image-based analysis using the PPD Symptom Score Software was proved effective in measuring the effects of glutathione peroxidase (GPX) gene overexpression. The transgenic roots showed less PPD symptoms than the control roots (Vanderschuren et al., 2014). In that particular study, they found that the analysis is only applicable to early stages of PPD (0-48 hours), as values from later time points caused saturation of PPD score. Such problem was not encountered in the present study probably because our PPD assay utilised root sections instead of thin slices which took longer to deteriorate. Computer scoring is seen as a major advance towards the improvement of PPD scoring. By employing a standard computer program and a PPD assay, cross comparison of experiments conducted in a separate laboratories become valid. However, it is essential that a standard approach to lighting and photographing the samples is used too.

The association between fluorescence measurements and the PPD scores generated from normal light photographs of the roots was also explored in the present study. To the best of our knowledge, this is the first report on the fluorescence profiles of greenhouse roots. In general, all freshly harvested root samples lacked fluorescent but after 24 hours they fluoresced to a high level (Hirose et al., 1983). However, this amount was not maintained, but slowly decreased with storage time and finally disappeared. This profile substantiates the results of many reports that measured the biochemical concentration of scopoletin and found that this fluorescing compounds peaked after 24 hours and gradually decrease with storage time (Rodriguez, 2001, Buschmann et al., 2000b, Wheatley and Schwabe, 1985). However, this might only be true in cassava with high susceptibility to PPD, as in the same work Rodriguez (2001) found that hydroxycoumarins concentration only increased dramatically after 5-7 days of harvest in the low susceptibility cassava. Besides, Buschmann (2000b) also found that hydroxycoumarins concentrations vary with cassava cultivar but were not necessarily associated with their susceptibilities towards PPD.

The occurrence of intense fluorescence at 1 DAH was not accompanied by intense PPD symptoms. Fluorescence level declined when visible PPD symptoms developed. Reduction of fluorescence is probably associated with oxidation of scopoletin to unknown compounds that form coloured deposits visible as vascular streaking; this was corroborated by high peroxidase activities and increased peroxidase gene expression in the roots during the later storage period (Tanaka et al., 1983, Buschmann et al., 2000b, Reilly, 2001). However, the suggestion that root samples with high fluorescence tend to produce more PPD symptoms was weakly supported by the results in this chapter. Some of the root samples were found to continuously fluoresce by 4 DAH. It is possible that during the time course, scopolin (the glycosylated form of scopoletin) is deglycosylated back to scopoletin, hence producing fluorescence. Unless this is further investigated with larger samples using a reliable objective scoring method, the use of fluorescence or scopoletin as an alternative marker for PPD does not appear to be very useful, mainly because it does not parallel with most of the PPD symptom accumulation observed. Also, its use as an advance marker for PPD needs to be proved with extensive testing due to weak relationship between fluorescence scores and PPD symptoms.

Overall, this chapter summarises the challenges in evaluating PPD using greenhouse-grown roots and the measures taken to overcome them. As opposed to field-grown materials, the available material used in this study was limited in number, which meant that an assortment of transgenics plants had to be used in addition to wild type in

developing a reliable PPD assay. Additionally, inadequate and varying sample sizes were not ideal and reduced the quality and accuracy of analyses. Consequently, the results presented here, while useful, must be considered as preliminary and as a result are not definitive. However, based on the data presented in this chapter, PPD Assay 4 is the best method to evaluate PPD for storage roots produced in the greenhouse and computer scoring method was shown to be a reliable tool to measure it. The usefulness of scopoletin as an alternative marker for PPD remains unconvincing and subjected to improvement. It is worth stressing that the investigation conducted here was a chronological effort in obtaining meaningful data for assessment of PPD. The awareness of the difficulty in assessing PPD emerged as more samples were harvested. Eventually, a failure of one assay method led to another. This chapter probably summarises the frustrations of many other researchers particularly those working with the greenhouse-grown materials.

CHAPTER 5

Expression analyses of Patatin

5.1   Introduction

In transformation studies, it is a common to construct an expression plasmid carrying a reporter gene. The plasmid is usually introduced in the same way as the plasmid carrying the target gene. The reporter gene-construct is an excellent means to predict the probable expression profiles of target genes as well as to characterise the promoter driving the target genes. Additionally, it can serve as a useful confirmation of transformation. In the present study, the reporter lines carrying reporter gene *GusPlus* was utilised to study the expression profile of the patatin promoter in transgenic cassava.

Patatin is a soluble storage protein found in potato tubers (*Solanum tuberosum*). It constitutes about 40% of the total soluble protein in potato tubers. Patatin genes from different potato cultivars and clones have been sequenced and found to be nearly identical, particularly in the coding region (Mignery et al., 1984). However, the genes tend to vary in the non-coding region; hence this is used as a basis for patatin classification. The promoter region comparison shows that Class I does not possess a 22-bp insertion found in Class II. Apart from this insertion, nucleotides 87 bp upstream transcription site share high similarity in both classes (Mignery et al., 1988).

In general, patatin is more abundantly expressed in the root than in other plant tissues, but class I is exclusively expressed in tubers while class II can be found in both roots and tubers. Expression of patatin in leaves can be induced by the addition of sucrose, a condition that is thought to promote starch accumulation in tubers (Wenzler et al., 1989), but this is only observed in Class I patatins (Koster-Topfer et al., 1989). The sucrose inducibility characteristic is attributed to a conserved sequence motif known as the sucrose regulatory element (SURE), which is located towards the proximal end of the patatin promoter near the TATA box (Liu et al., 1990). This motif is often found together with a sequence motif related to tuber-specificity and this forms a 100 bp of highly conserved sequence called A+B repeats (Grierson et al., 1994). Fusion of three copies of the A+B repeats and a truncated CaMV35s promoter to a beta-glucuronidase gene (Gus) gene resulted in high Gus activity in potato tubers, whereas deletion of these repeats from a minimal wild type class I patatin promoter reduced Gus activity

(Grierson et al., 1994). The nuclear binding protein factors for both motifs have been proposed (Kim et al., 1994), and the one binding to B repeats was later identified as Storekeeper (Zourelidou et al., 2002). Patatin is developmentally regulated as its transcriptional activity is first detected during the transition from stolon to tuber, and maximum levels are detected in mature tubers (Stupar et al., 2006, Bachem et al., 2000).

Unlike other storage proteins, patatin exhibits non-specific lipid acyl hydrolase activities, which indicates an additional physiological role during pathogen invasion (Andrews et al., 1988). The dual function of patatin is unique and has been elucidated through its ability to hydrolyse various lipids (Strickland et al., 1995) as well as in its protein structure where an active site resembling that of human phospholipase has been found (Rydel et al., 2003, Hirschberg et al., 2001).

5.2   Research Aim

In the present study, two reporter lines called Pat:Gus and Pat(-):Gus lines were created as described in Chapter 3. The Pat:Gus line contains pDEST:*GusPlus* in which *GusPlus* gene is fused to Patatin and was designed to study Patatin promoter behaviour in cassava. Its pattern of expression would be compared to the 'promoterless-Gus' lines which lack the Patatin promoter, the Pat(-):Gus. The expression plasmid for the Pat(-):Gus is pDEST:*GusPlus*(-Pat). Both expression plasmids had been transformed in *Arabidopsis* previously and were reported not to cause any morphological changes (Page, 2009). The genetic map of both cassettes is represented in the schematic diagram below.
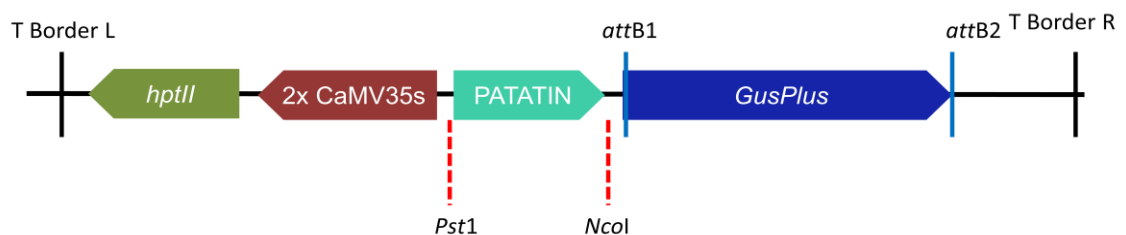
Figure 5.1 The genetic map of pDEST*:GusPlus* expression plasmid modified from pCAMBIA 1305.1 in which CaMV35s was replaced by Patatin by performing a restriction digest with *Pst*I and *Nco*I and fused to attB-tagged *GusPlus.* pDEST*:GusPlus*(-Pat) is a promoterless expression plasmid in which Patatin was removed from pDEST*:GusPlus* by performing a restriction digest with the same restriction enzymes.

5.3 Results

5.3.1 Verification of transgenic plants

Transformation of cassava with pDEST:*GusPlus* and pDEST:*GusPlus*(-Pat) had generated 26 Pat:Gus and 37 Pat(-):Gus putative cassava lines respectively. However, only 18 Pat:Gus and 34 Pat(-):Gus surviving lines were analysed. As with other putative transgenics, the transgenic nature of the plants was initially checked for amplification of *hptII* gene with HygF and HygR primers. To discriminate between the two reporter lines, the Patatin sequence was amplified instead of the *GusPlus* gene. The primers used were Pat-pDESTF and Pat-pDESTR which were designed to amplify *GusPlus*-driven Patatin. pDEST:*GusPlus* and pDEST:*GusPlus* (-Pat) plasmid was used as positive control for Pat:Gus and Pat(-):Gus respectively.
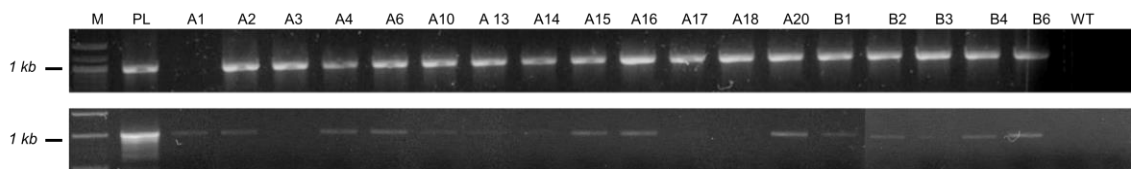
Figure 5.2 Amplification of the *hptII* gene from the Pat:Gus lines DNA (upper panel) and the Patatin promoter (lower panel). M = DNA marker, PL = pDEST:*GusPlus* plasmid, WT = Wild type line, C = negative control. The expected size of the PCR product for both PCRs is 1kb.
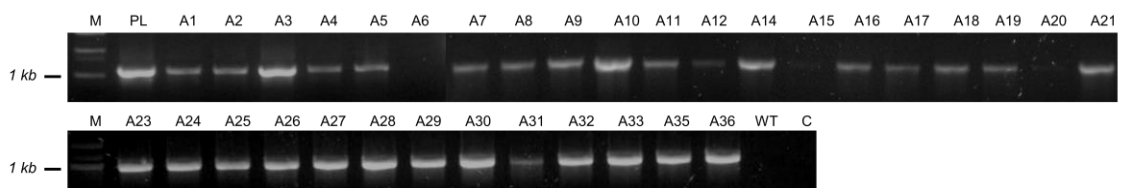
Figure 5.3 Amplification of the *hptII* gene from Pat(-):Gus lines DNA. M = DNA marker, PL = pDEST:*GusPlus*(-Pat) plasmid, WT = Wild type line, C = negative control. The expected size of the PCR product is 1 kb.
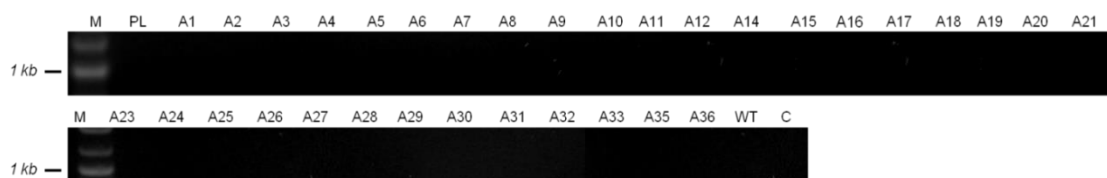
Figure 5.4 Amplification of the Patatin promoter from Pat(-):Gus lines DNA. M = DNA marker, PL = pDEST:*GusPlus*(-Pat) plasmid, WT = Wild type line, C = negative control. The expected size of the PCR product is 1 kb.

Table 5.1 Analysis of transgenic cassava by PCR. Positive transformants in Pat:Gus are those lines amplified by both the *hptII* and Patatin, while positive transformants with Pat(-):Gus are those amplified *hptII* alone.

Transgenic	Total no of lines	*hptII* present	Patatin present	No of positive transformants	Positive transformants (%)
Pat:Gus	18	17	15	14	78
Pat(-):Gus	34	31	0	31	91

In nearly all the Pat:Gus lines both fragments were amplified, except for one in which the *hptII* gene was not amplified, and three in which the Patatin sequence did not amplify (Figure 5.2). Also, only 3 out of 34 Pat(-):Gus lines did not amplify *hptII* gene but none amplified Patatin (Figure 5.3 and 5.4) as expected. This accounts for high percentage of positive transformants in both types of reporter line (Table 5.1).

5.3.2 Screening of transgenic cassava reporter lines by Gus histochemical staining

5.3.2.1 Sucrose treatment and *GusPlus* expression in cassava leaves

The Gus staining method used was as described in Section 2.5.7. All the 18 surviving putative Pat:Gus lines and 34 putative Pat(-):Gus were assayed for Gus activities. Initially, the *in vitro* plantlets were used to select the Gus-positive lines by staining leaf samples of one-month old plantlets. To test sucrose inducibility characteristic of Patatin, the samples were vacuum-infiltrated with 20% sucrose and stained for Gus activities afterwards.
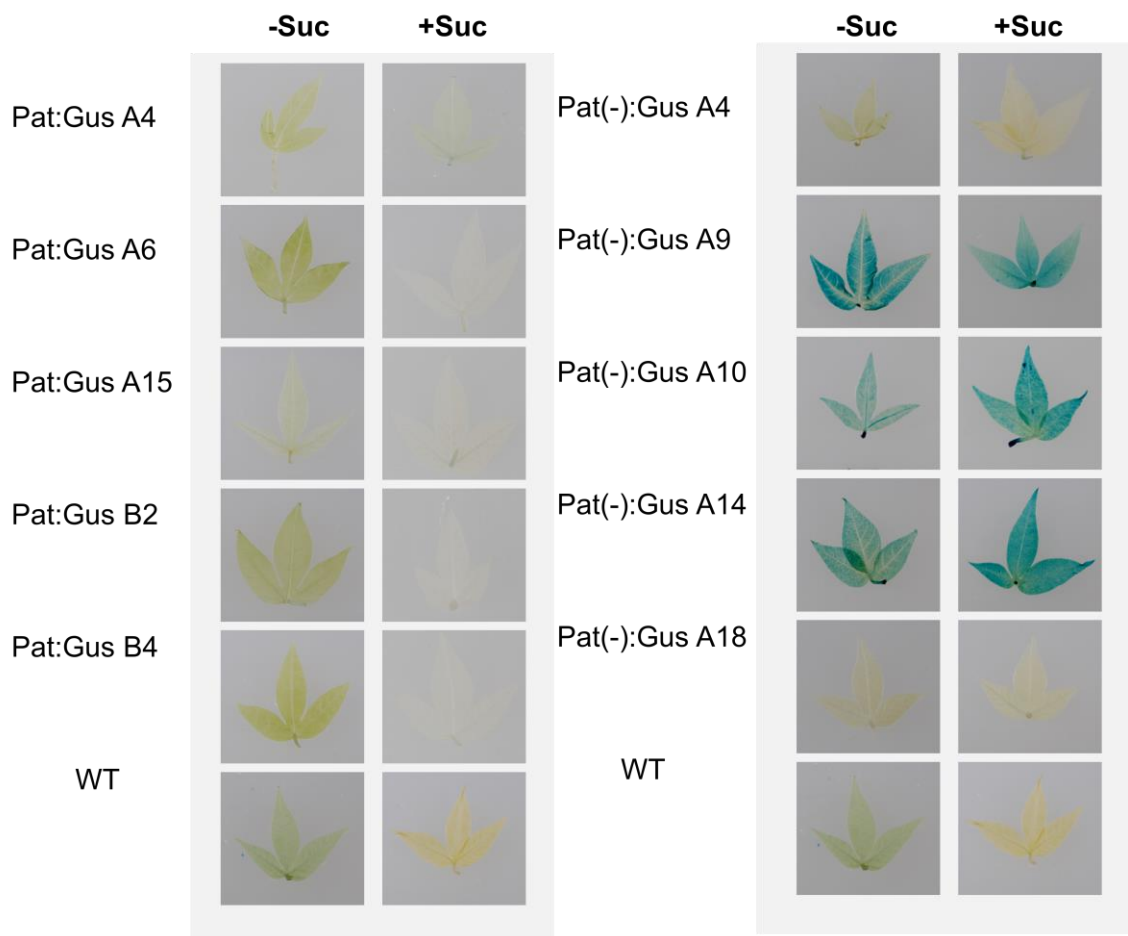
Figure 5.5 Gus staining of selected Pat:Gus and Pat(-):Gus leaf samples. The lines used are those confirmed as positive transformants (Section 5.3.1). Left panel shows Pat:Gus samples with and without sucrose treatment. Right panel shows Pat(-):Gus samples with and without sucrose treatment. –Suc = untreated, +Suc = sucrose-infiltrated.

Gus assays conducted with the cassava Pat:Gus leaves found no samples with Gus activities as none of them were stained including those treated with sucrose. In contrast, the Pat(-):Gus samples showed *GusPlus* activities in the leaf tissue of three of the five lines tested both with and without the sucrose treatment (Figure 5.5). These data imply that these lines will need closer examination. Moreover, leaf staining might not be an efficient method to select the positive Pat:Gus samples as *GusPlus* gene were not readily expressed in leaf or sufficiently induced by sucrose. However, expression in leaf following wounding has been demonstrated previously (Page, 2009). Therefore, wounding was used as an alternative method to screen the positive Pat:Gus samples.

5.3.2.2 Wounding treatment and *GusPlus* expression in cassava leaves

For wounding treatment, leaf samples were pricked with a sterile needle several times before being quickly incubated in Gus buffer. Figure 5.6 shows that no Pat:Gus leaves respond to wounding as indicated by unstained leaf tissues. On the other hand, the Pat(-):Gus lines shown to express Gus activity in Figure 5.5 were intensely stained not only at the pricked site but throughout the whole leaf tissue, while the ones lacking expression when unwounded remained unstained. However, because of the heavy staining in these samples, it was not clear if the wound increased *GusPlus* expression in the injured area compared to the unwounded leaves.
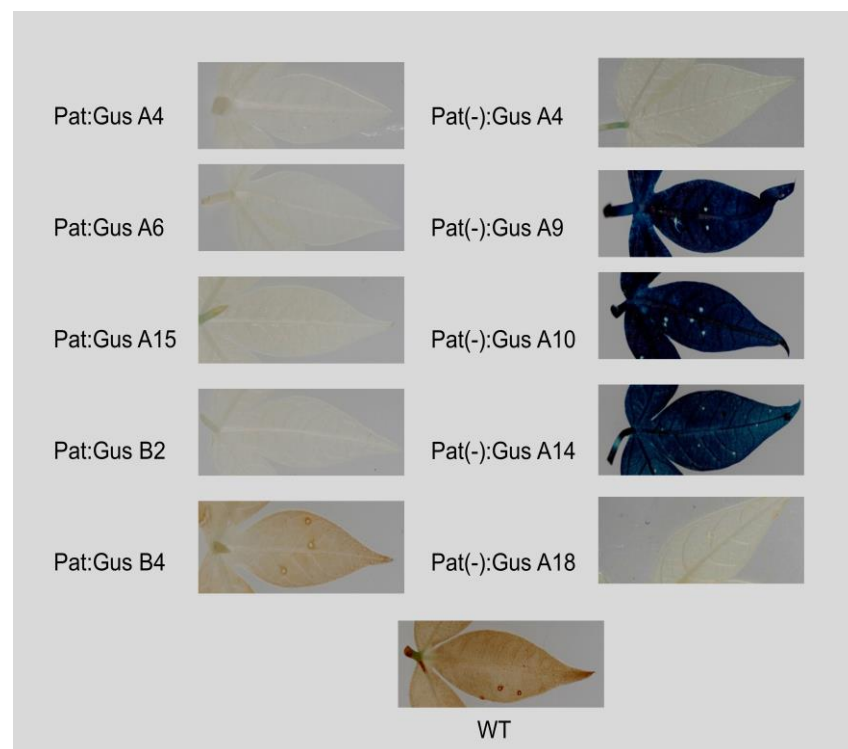
Figure 5.6 Leaf samples from one-month old *in vitro* plantlets that were pricked with a needle and checked for Gus activities. The injured sites were not visible due to negative response with Gus buffer, while intense staining in three Pat(-):Gus lines prevented determining whether there was a response to wounding over and above that observed in the unwounded leaves for these lines. Colour differences showed by WT and Pat:Gus B4 were caused by incomplete de-staining.

Negative results obtained from Gus staining of Pat:Gus leaves either untreated or treated with sucrose as well as when wounded led to assumption that expression might not be targeted to leaf but other tissues. To investigate this, the whole plantlets were assayed for Gus activities.

5.3.2.3 Localisation of *GusPlus* expression in *in vitro* cassava plantlets

To determine the localisation of Gus expression and to screen for positive Pat:Gus samples, one-month old *in vitro* plantlets were incubated in Gus buffer. Using the whole plantlets, the effect of sucrose induction was explored by supplying sucrose in the growth medium.
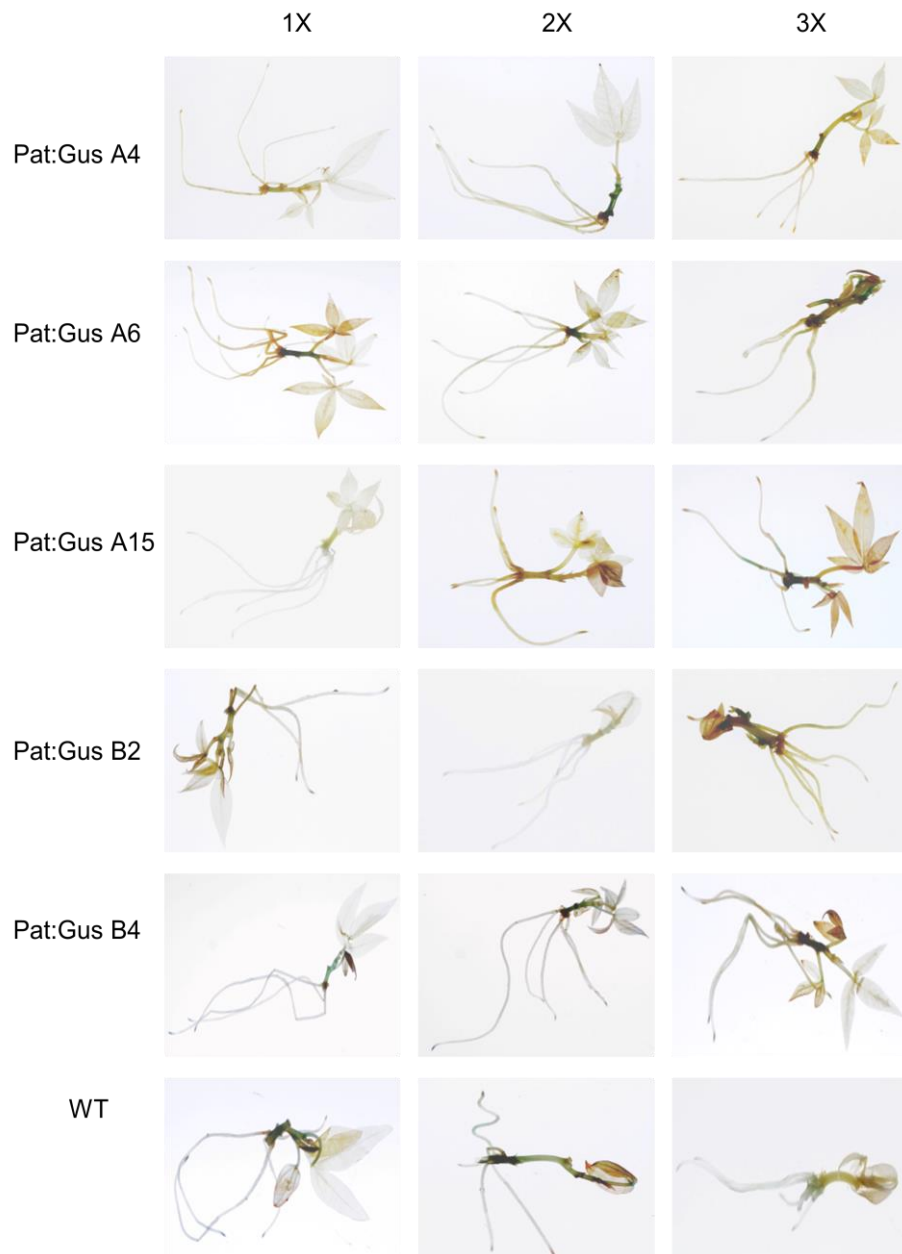
Figure 5.7 Staining of Pat:Gus plantlets grown on Cassava Basic Medium (CBM) of variable sucrose concentrations. The plantlets were incubated in Gus staining buffer for one hour at 37°C and de-stained with alcohol afterwards to remove chlorophyll.

Cassava plantlets normally are propagated on Cassava Basic Medium (CBM) containing 2% sucrose. For the sucrose treatment, the cassava plantlets were

propagated on CBM containing 2X and 3X sucrose concentrations. The plantlets were grown for one month before being checked for Gus activities. Surprisingly, Gus activities were not detected in any part of the Pat:Gus plantlets, including their roots, whether or not they had been supplied with additional sucrose. The anticipated inductive effect of sucrose on the Patatin promoter failed to be observed as Gus staining failed to detect *GusPlus* expression in any tissues (Figure 5.7). On the other hand, except for the four lines not expressing *GusPlus* as mentioned earlier, staining of the Pat(-):Gus plantlets propagated on CBM containing 1X sucrose consistently revealed high *GusPlus* expression in the whole plantlet, in the same lines as previously (Figure 5.8). However, sucrose induction was not tested in Pat(-):Gus lines. Also, no-sucrose experiment could be conducted due to failure of the growth medium to induce root formation in the absence of the basal level of sucrose in the medium.

| Pat(-):Gus A4 | Pat(-):Gus A9 | Pat(-):Gus A10 | Pat(-):Gus A14 | Pat(-):Gus A18 |
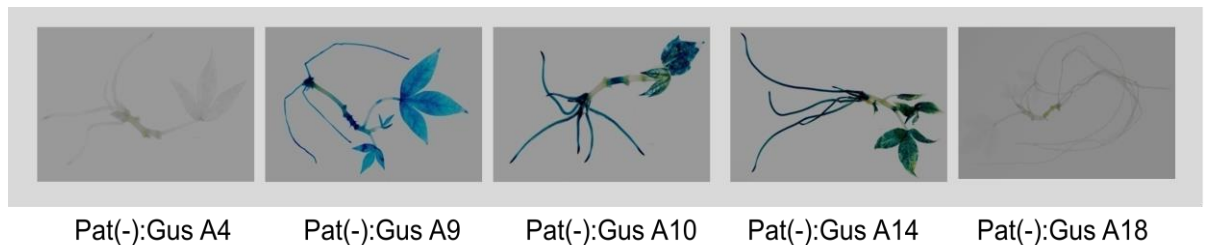
Figure 5.8 Staining of one-month old Pat(-):Gus cassava plantlets grown on Cassava Basic Medium (CBM) with 1X sucrose concentration. The plantlets were incubated in Gus staining buffer for one hour and de-stained with alcohol afterwards to remove chlorophyll.

The main objective of staining the whole plantlets was to locate Gus expression in the cassava tissue. However, it was not achieved in this experiment and this possibly related to the natural expression of patatin which is in tubers or more broadly in storage roots. Moreover, other patatins have been shown to have higher expression in mature tubers including cassava (Abhary et al., 2011, Narayanan et al., 2011).Therefore, to test this, the Pat:Gus along with the Pat(-):Gus plants were grown to produce storage roots to be used for Gus staining.

5.3.2.4 *GusPlus* expression in deteriorating cassava roots

Gus activity was checked in mature cassava roots using three lines each of the Pat:Gus and Pat(-):Gus transgenic plants. The roots were harvested from 6 months old cassava plants, cut into thin sections and let to deteriorate at room temperature to induce PPD. By doing this, the expression pattern of Patatin following cassava roots harvesting could be simultaneously assessed. The root sections were checked for Gus

activities before being photographed. Figure 5.9 (A) showed staining of the representative root sections at 0, 1, 4 and 6 hours after harvest and Figure 5.9 (B) showed staining at 16, 24, 48 and 72 hours after harvest.
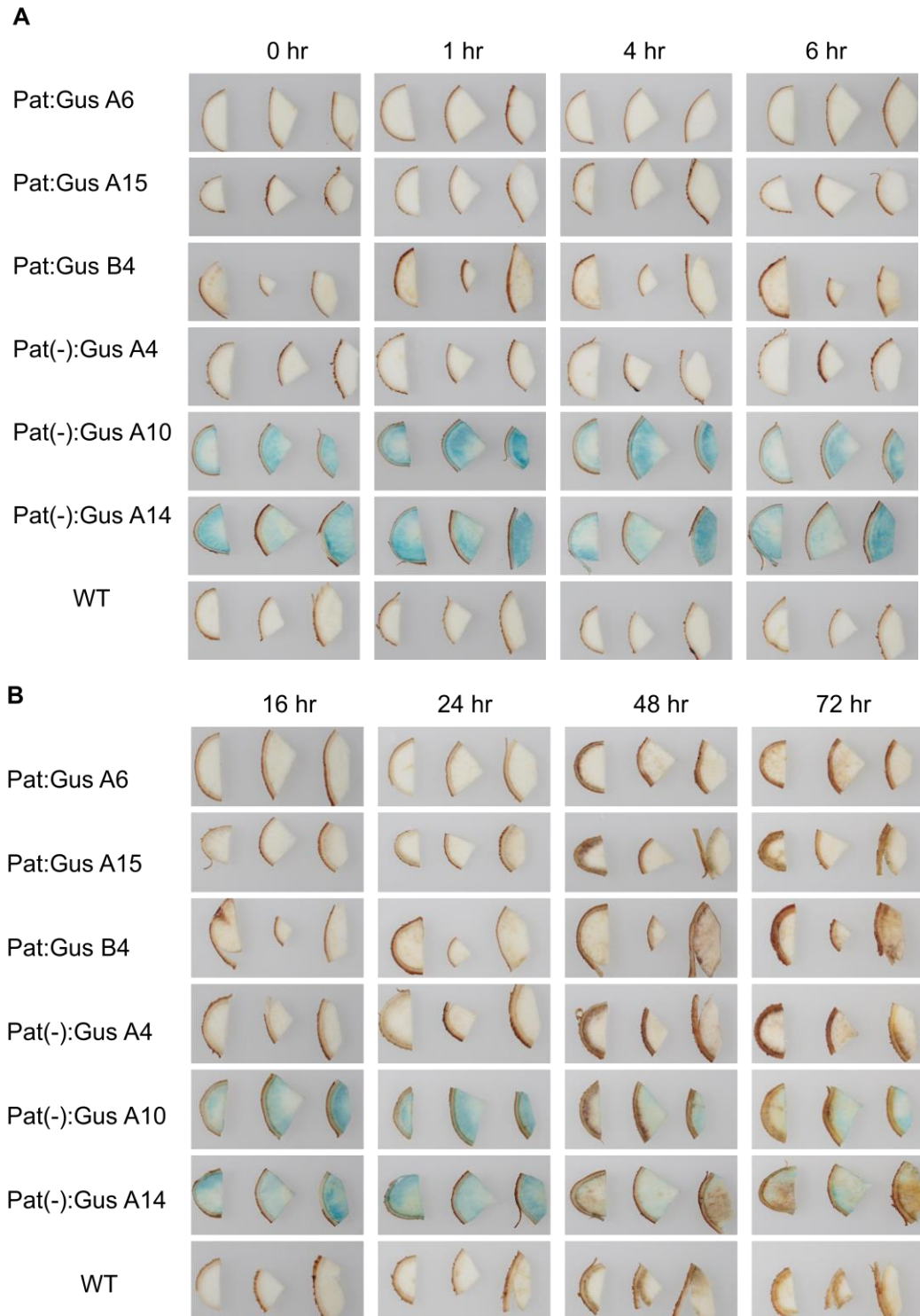
Figure 5.9 Gus-staining of selected storage roots harvested from 6 months old cassava plants. The roots were cut into thin sections and stained at the indicated time points.

Overall, the root samples showed no PPD symptoms until 48 hours after harvest. Similar to the data presented above, in Pat:Gus, Gus activity was not observed in either the freshly harvested or in the deteriorating root samples. On the other hand, Pat(-):Gus A10 and Pat(-):Gus A14 which showed clear Gus activities in the *in vitro* samples consistently showed similar result in the mature storage roots. These samples maintained strong blue staining from harvesting until 6 hours after that but it gradually decreased as PPD symptoms became visible at 48 hours after harvest. The intensities of the staining were weaker in the storage roots than in *in vitro* samples, perhaps due to the high starch content.

The results from the analyses of the Pat:Gus transgenic plants were unexpected as all the possible aspects regarding the behaviour of the Patatin promoter had been tested. The Gus staining was performed on various plant materials including the *in vitro* leaves, the whole plantlets as well as the storage roots. Then, the plant materials were subjected to wounding and sucrose treatment which was the conditions thought to induce *GusPlus* expression. Also, Gus activities were examined in deteriorating storage roots to see if expression was delayed. However, frustratingly, none of these were successful to produce Gus activities.

5.3.3 Re-confirmation of Pat:Gus plants transgenic nature

Failure to see Gus activities in the Pat:Gus plants suggested the need to confirm the fine detail of the transformed DNA in order to determine whether any mutation, rearrangement or error had occurred that might affect either the activity of the Patatin promoter or of the *GusPlus* enzyme. This required sequencing of key components of the construct. To achieve this, the key components were amplified by PCR from genomic DNA extracted from leaf tissue of Pat:Gus plantlets. The primer pairs used are shown below.
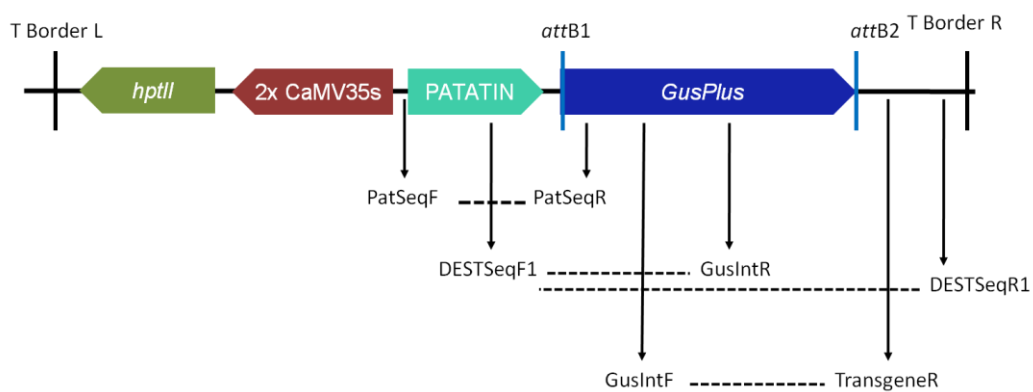
Figure 5.10 Primers PatSeqF/PatSeqR were designed to amplify and sequence Patatin. DESTSeqF1/DESTSeqR1 is a primer pair used to check the presence of the Patatin-driven *GusPlus* gene. Since the *GusPlus* gene is approximately 2 kb, two internal primers were created in order to get high quality reads. They were GusintF and GusintR which were paired with TransgeneR and DESTSeqF1 respectively.

The PCR method used is described in Section 2.3.3. pDEST:*GusPlus* plasmid was used as positive control. Amongst the primer pairs described above, only PatSeqF/PatSeqR amplified the correct PCR product size (Figure 5.11). DESTSeqF1/DESTSeqR1, which had been used as a primer pair to amplify other Patatin-driven transgenes in other transgenic plants failed to produce any PCR product from Pat:Gus DNA. On the other hand, GusintF/TransgeneR and DESTSeqF1/GusintR primers pairs produced multiple unspecific bands. Amplifications of five selected lines with the primers are shown below.
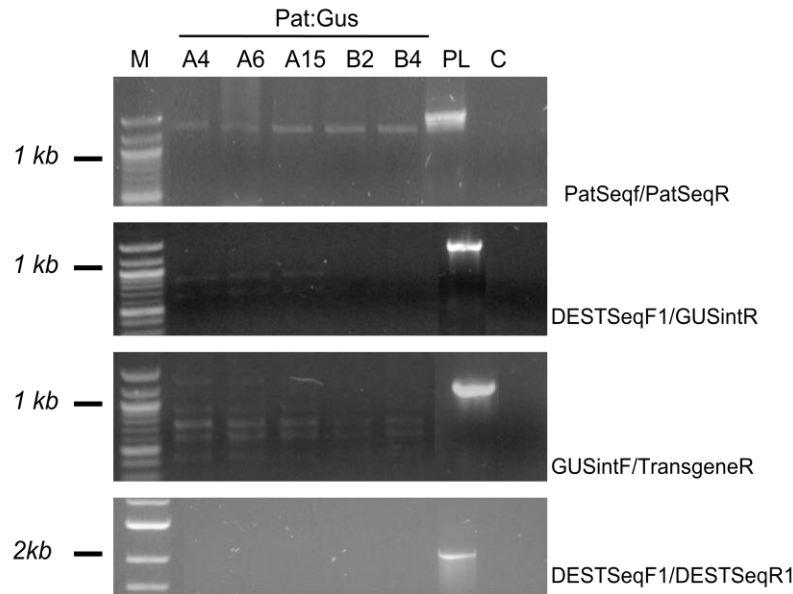
Figure 5.11 Amplification of selected Pat:Gus DNA with various primer pairs. PL = pDEST:*GusPlus* plasmid as template or positive control, C = water as template or negative control. The predicted PCR product size for amplification with PatSeqF/PatSeqR was ~1.3 kb and this was obtained in PL but slightly smaller products were obtained from Pat:Gus samples. DESTSeqF1/GUSintR which targets the 5' end of Patatin promoter and internal sequence of *GusPlus* gene amplified the predicted ~1.3 kb product in PL but multiple PCR products in Pat:Gus sample. The same was observed in the amplification with GUSintR/TransgeneR, which targets an internal *GusPlus* sequence plus a region between attB2 and right T-border, as only PL produced the expected ~1.1 kb product. DESTSeqF1/DESTSeqR1, which was designed to amplify Patatin-driven *GusPlus*, did not generate any PCR products in the Pat:Gus samples but did amplify the predicted 2 kb fragment in PL. The Pat:Gus samples shown are the same lines as those shown in Gus staining data, above.

The PCR products amplified by the PatSeqF/PatSeqR primers were sent for sequencing and the resulted DNA sequences were aligned with pDEST:*GusPlus* full sequence. Surprisingly, it was found that only the fragment amplified from plasmid DNA was Patatin while those amplified from Pat:Gus DNA was not. Instead, BLAST search suggested the fragment was a part of the constitutive promoter CaMV35s. To investigate if Pat:Gus was inadvertently confused with the Pat(-):Gus, the sequenced fragments were aligned with Pat(-):Gus sequence but no consensus was found from this alignment. The attB1 sequence which constitutes a part of Gateway cloning was not found within the fragment. This ultimately led to assumption that an unmodified plasmid was transformed in the Pat:Gus transgenic plants. To confirm this, the sequenced fragment was aligned with unmodified pCAMBIA 1305.1 sequence.
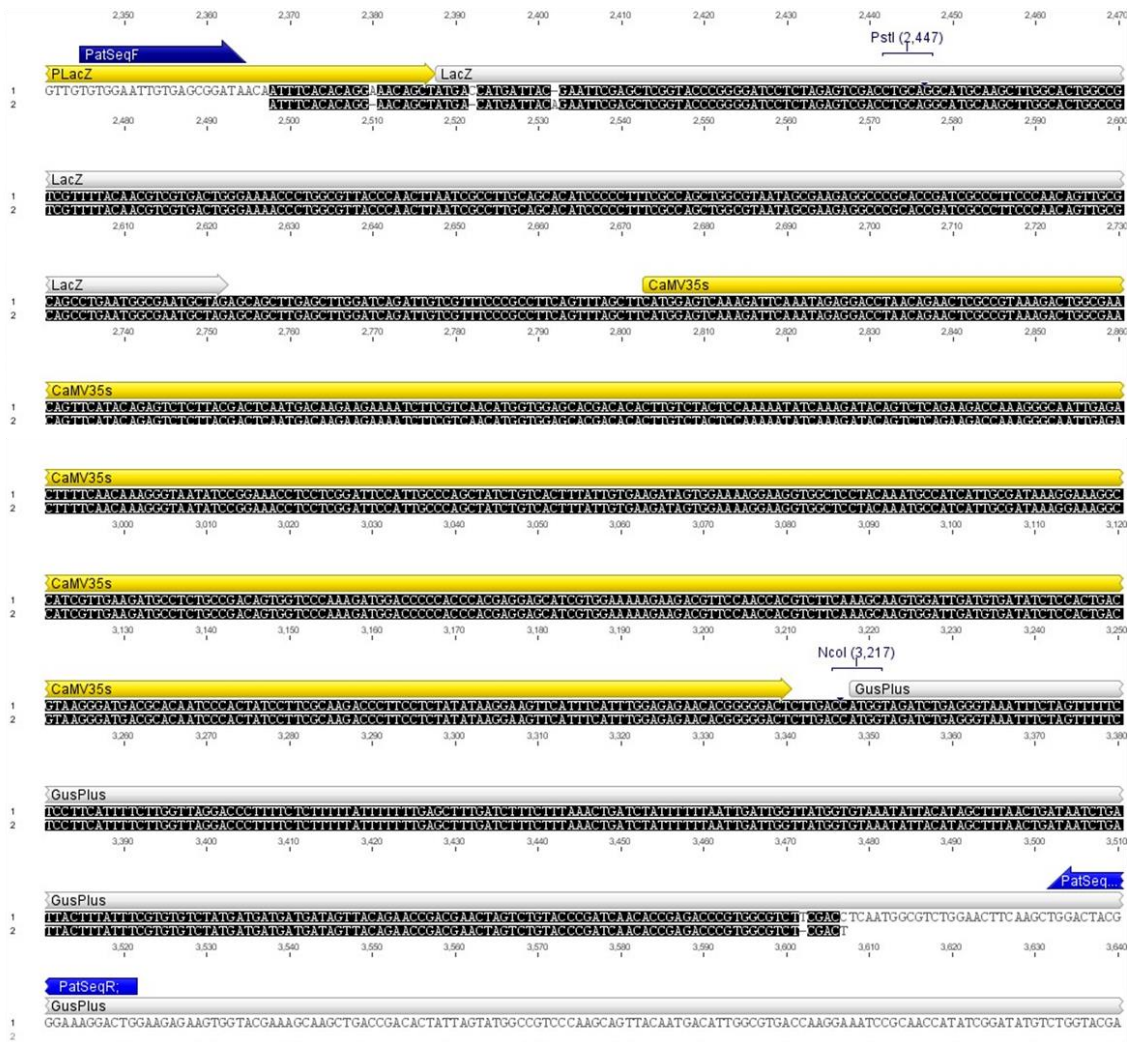
Figure 5.12 Sequence alignment of (1) pCAMBIA 1305.1 and (2) PCR product amplified from Pat:Gus by PatSeqF/PatSeqR primers. The positions of the primers and the restriction enzymes (*Pst*I and *Nco*I) used to remove the CAMV35s promoter are shown.

The alignment is shown Figure 5.12 where PatSeqF primer flanks the LacZ gene promoter (pLacZ) in PCAMBIA 1305.1 and PatSeqR flanks approximately 250th nucleotide of the G*usPlus* gene. While this initially suggested that Pat:Gus was transformed with an unmodified pCAMBIA 1305.1, confusingly, no Gus expression was observed in Pat:Gus plants (Section 5.3.2). It appears that some modification might have occurred to the *GusPlus* gene preventing its expression and this is supported by the failure of GusintF/TransgeneR and DESTSeqF1/GusintR to amplify the remaining *GusPlus* DNA sequence (Figure 5.11). From the data gathered, it was confirmed that Pat:Gus plants were transformed with a truncated pCAMBIA 1305.1.

5.3.4 Verification of other transgenic plants by DNA sequencing

5.3.4.1 Verification of putative Pat:CAT lines

The error in transformation of the supposedly Pat:Gus lines was frustratingly unfortunate, and it emphasises the need for a more rigorous checking though sequencing of all steps in the production of gene constructs and the generation of the transgenic lines. In the present study, amplification of *hptII* and transgene was used as a rapid screening method for the identification of transgenic lines. Using this method, transgenic plants were successfully discriminated from the untransformed plants, except those putatively transformed with the pDEST:CAT expression cassette (Section 3.3.1). In these plants, only *hptII* was amplified but the transgene MecCAT1 remained undetected by PCR. This has raised an important question whether the correct expression cassette had been transformed.

Several combinations of primers targeting various T-DNA regions in pDEST:CAT were used to investigate this (Figure 5.13). pDEST:MecCAT1 plasmid was used as a positive control.
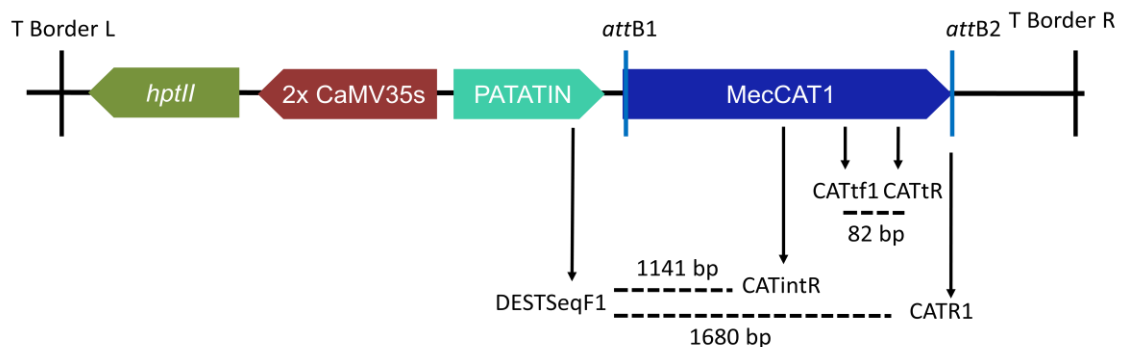
Figure 5.13 The primers used to amplify MeCAT1 sequence in pDEST:MecCAT1 expression plasmid. The expected size of each PCR product is indicated.

Genomic DNA from Pat:CAT leaf tissue was used as a template and PCR was conducted using method described in Section 2.3.3. Since the same expression plasmid had been transformed in *Arabidopsis* plant, it was also sequenced. The transgenic *Arabidopsis* lines used were At 2.3, At 3.8, At 9.2 (Page, 2009).

PCR reaction with DESTSeqF1/CATR1 primers which flank a part of Patatin sequence and the 3' end of MecCAT1 spanning the attB2 Gateway tags did not amplify any PCR product from Pat:CAT DNA and the WT. However, the *Arabidopsis* line and the plasmid control amplified PCR products of the correct size (Figure 5.14).
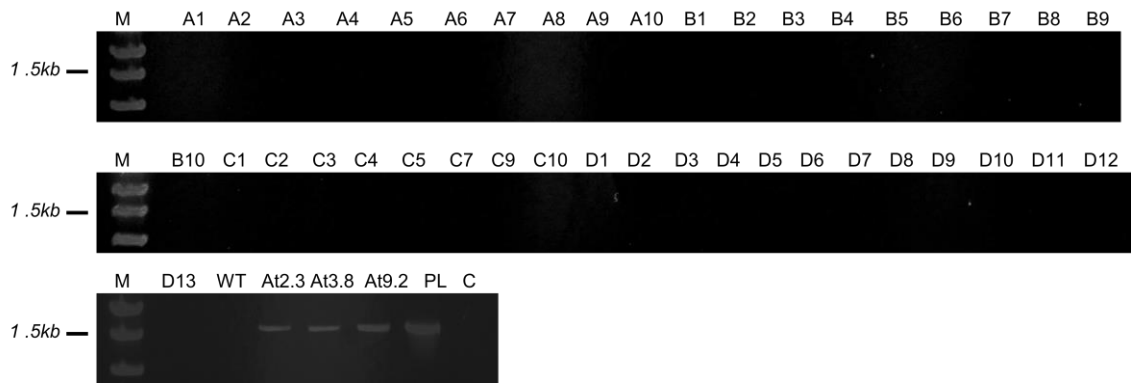
Figure 5.14 PCR with DESTSeqF1/CATR1 primers amplified Patatin-driven MecCAT1 in *Arabidopsis* DNAs (At 2.3, At 3.8, At 9.2) and a plasmid positive control. None of the putative Pat:CAT transgenic cassava DNA gave an amplified PCR product (A1-D13). The size of expected PCR product is approximately 1.7 kb. M is DNA marker, WT is wild type, PL is plasmid, C is negative control or sterile water template.

Similarly, amplification with DESTSeqF1/CATintR also did not amplify any PCR product from the genomic DNA of Pat:CAT but amplified the correct PCR product size from the transgenic *Arabidopsis* genomic DNA and the plasmid (Figure 5.15).
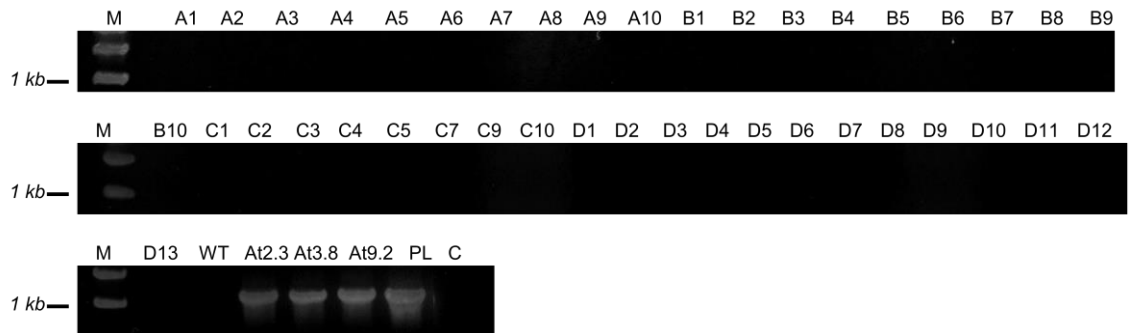
Figure 5.15 PCR with DESTSeqF1/CATintR primers amplified Patatin-driven MecCAT1 in *Arabidopsis* DNAs (At 2.3, At 3.8, At 9.2) and a plasmid positive control. None of the putative Pat:CAT DNA (A1-D13) amplified a PCR product from putative cassava transgenic lines (A1-D13). The size of expected PCR product is approximately 1.1 kb. M= DNA marker, WT = wild type, PL = plasmid, C = negative control or sterile water template.

Next, a primer pair was designed to differentiate genomic DNA and cDNA of MecCAT1. In theory, genomic DNA should produce a longer PCR product as it spans an intron, while the cDNA should produce a shorter one (Figure 5.16). Therefore, if an intact

MecCAT1 cDNA was present in the genome of putative transgenic cassava, two PCR products of different sizes should be produced.
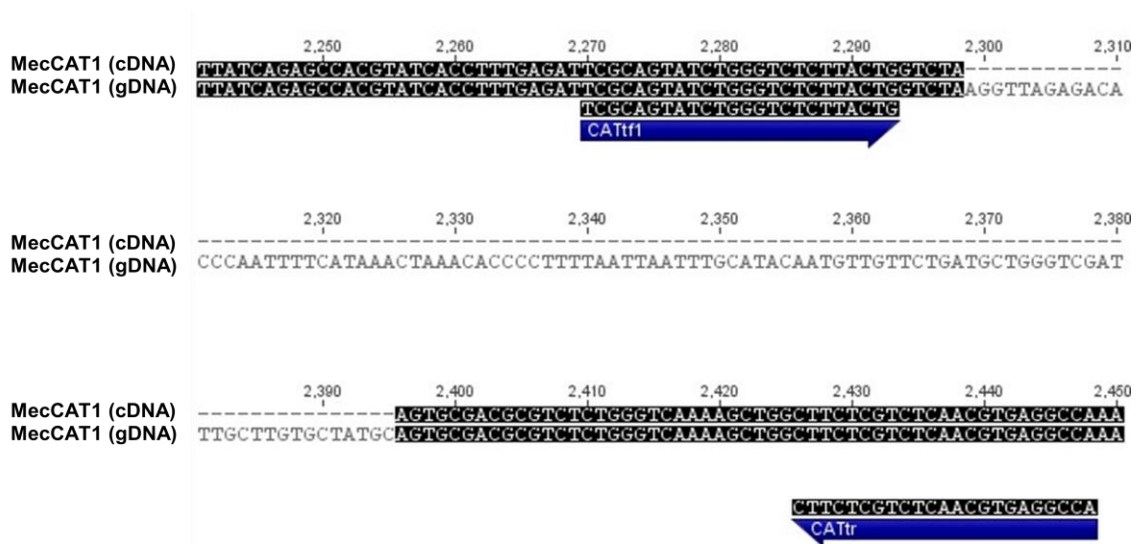
Figure 5.16 Primers designed to amplify MecCAT1. Primers designed span the intron (serrated line), so will produce a 179 bp PCR product if only MecCAT1 from genomic DNA was present. If the cDNA copy of MeCAT1 is present in the transformed gene construct, another PCR product of 82 bp would also show. This effectively verifies if cassava plants were correctly transformed with expression plasmid carrying MecCAT1 of pDEST:CAT.

However, these tests showed that only the genomic sequence of MecCAT1 amplified by the putative Pat:CAT lines. The *Arabidopsis* putative transgenics which lack MecCAT1 genomic fragment amplified the MecCAT1 cDNA (Figure 5.17). The *hptII* gene had been amplified in the putative Pat:CAT lines (Section 3.3.1) confirming the integration of the expression cassette. However, the key components of the cassette could not be verified as a range of primers combination failed to generate PCR products. The results gathered so far suggest numerous possibilities including the DNA sequence used to design those primers may have altered. However, to correctly resolve this sequencing was carried out.
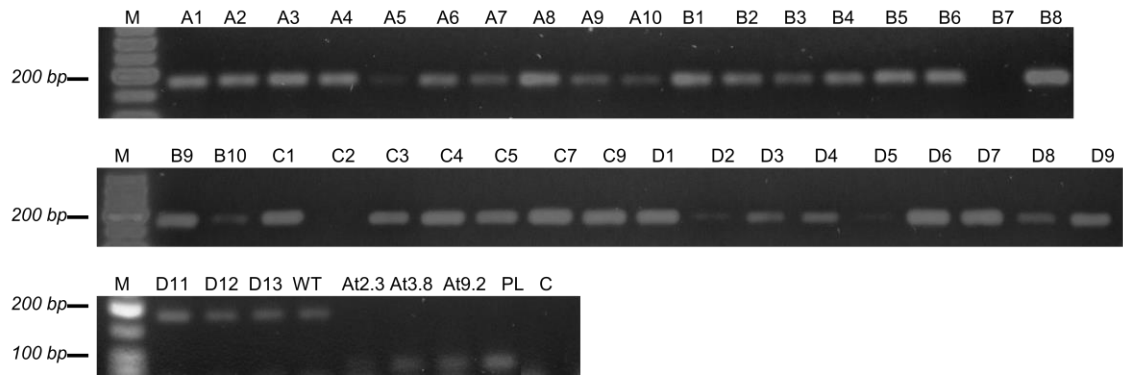
Figure 5.17 PCR with CATtf1-CATtr primers for amplification of MecCAT1. The expected size of genomic and cDNA sequence (transgene) of MecCAT1 is 179 bp and 82 bp respectively. Nearly all putative Pat:CAT lines (A1-D13) and the WT amplified the genomic fragment but none amplified the transgene fragment. On the other hand, *Arabidopsis* transgenics amplified the cDNA MecCAT1 fragment. M is DNA marker, WT is wild type, PL is pDEST:CAT plasmid, C is negative control or sterile water template.

For sequencing of Pat:CAT key components, two primer pairs were created. They were PatSeqF/PatPDESTR to amplify the Patatin sequence and DESTSeqF1/TransgeneR to amplify Patatin-driven MecCAT1 (Figure 5.18).
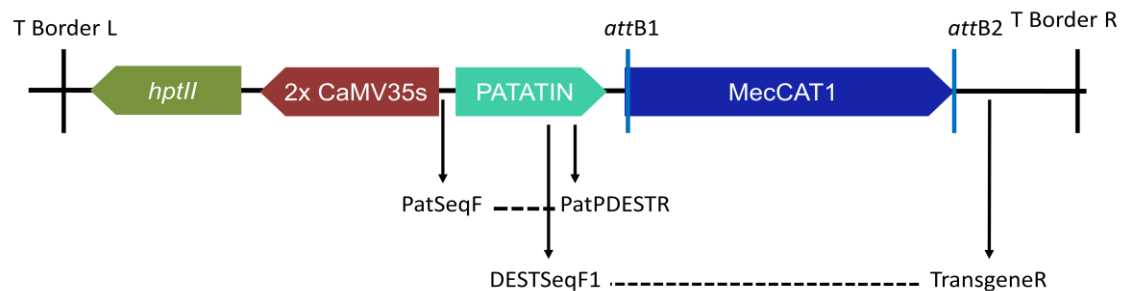
Figure 5.18 Diagrammatic presentation of primer pairs created for sequencing Patatin-driven MecCAT1. PatSeqF/PatPDESTR was created to amplify Patatin. DESTSeqF1 and TransgeneR should amplify MecCAT1 fused to Patatin. The expected size for Patatin amplification was 1366 bp while the expected size for MeCAT1 was 1704 bp.
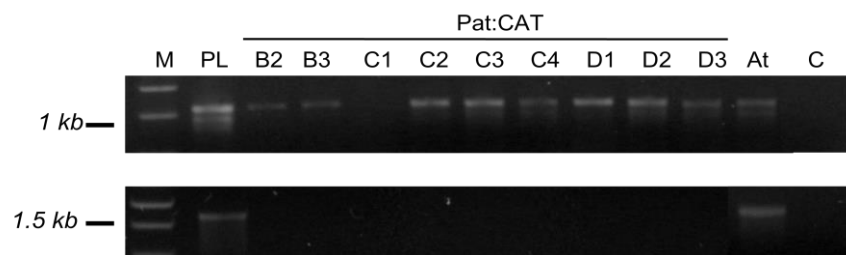
Figure 5.19: Amplification of Pat:CAT DNA with PatSeqF/PatPDESTR which targets Patatin (upper panel) and DESTSeqF1/TransgeneR which targets the Patatin-driven MecCAT1 (lower panel). Cassava transgenic lines are indicated alphanumerically, At denotes the *Arabidopsis* transformed with the same expression cassette (At 3.8). M = DNA marker, PL = positive control (plasmid), C = negative control (water).

Nine Pat:CAT lines and one *Arabidopsis* Pat:CAT (At 3.8) were used for amplification with these primers. PatSeqF/PatPDESTR amplified Patatin successfully in all the tested lines except in one line. Three of the PCR products (C2, C3, D1) and the At 3.8 were sent for sequencing (Figure 5.19). As expected, the DNA sequence was from Patatin and it corresponded to that sequenced from the expression plasmid pDEST:CAT. However, MecCAT1 fragment using primer pair DESTSeqF1/TransgeneR only amplified in At 3.8 (Figure 5.19). No PCR product was obtained from the cassava Pat:CAT. Sequence analysis of the Patatin region amplified by PatSeqF/PatSeqR showed that DESTSeqF1 primer binding region was present in the sequence (Figure 5.20) indicating failure to recover MecCAT1 through primer pairing CATR1 (Figure 5.14) and CATintR (Figure 5.15) in the putative cassava Pat:CAT may be due to alterations to MecCAT1 and other DNA regions from it. On the other hand, sequencing of At 3.8 revealed the expected DNA fragment which is the MecCAT1 (See Appendix, Figure 9.1 for full sequence Pat:MecCAT1 fragment in At 3.8).
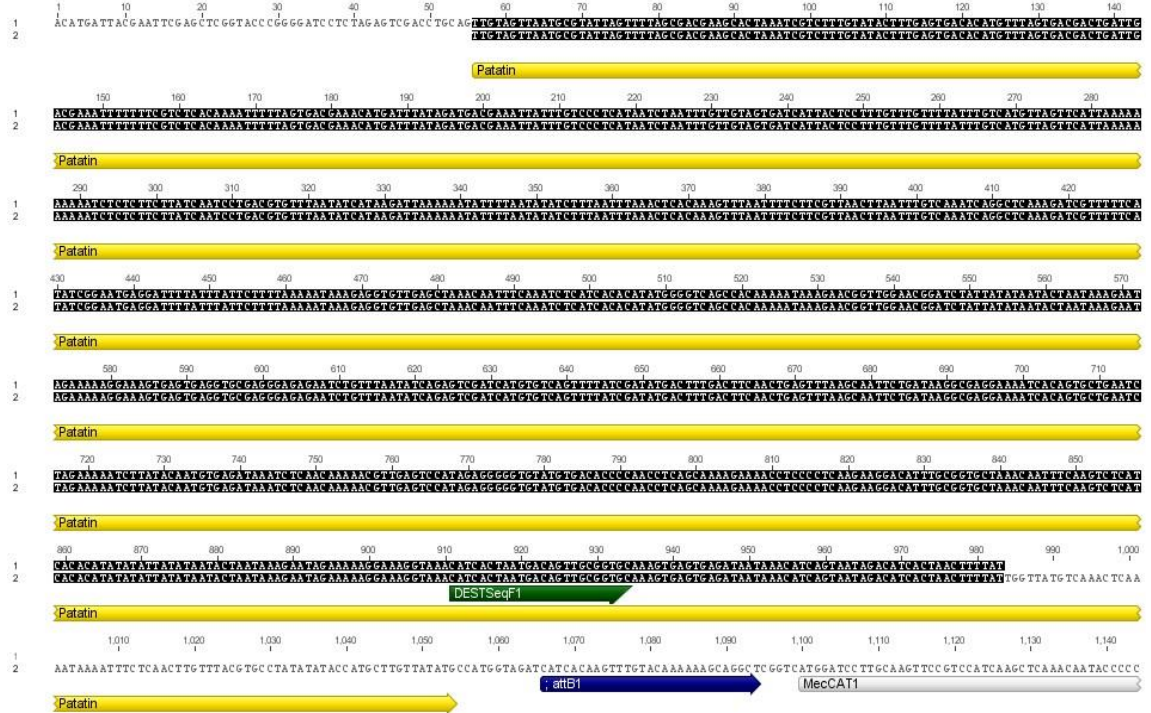
Figure 5.20 The DESTSeqF1 primer sequence was found within the sequenced Patatin fragment amplified by PatSeqF/PatPDESTR. DESTSeqF1 is the forward primer designed to amplify the target gene fragment, MecCAT1 in this case. 1 = sequenced fragment of Pat:CAT C3, 2 =.partial sequence of pDEST:CAT DNA. attB1 located upstream of the target gene MecCAT1, which is part of the Gateway cloning is also indicated.

The Pat:CAT DNA was also amplified with DESTSeqF1 in combination with other transgene reverse primers designed from the other transgenes, to find out if it was mistakenly transformed with an expression plasmid other than pDEST:CAT, but nothing was amplified suggesting that this was not the case (data not shown).This was not unanticipated as the combination of DESTSeqF1 and TransgeneR primers should have produced a product with any of the transgene cassettes, though of different sizes, as the forward primer is located in the Patatin promoter while the reverse primer is located beyond the inserted cDNA, in other words the primer pair are outside the attB1 and attB2 sites used for Gateway cloning. These data imply that the gene cassette used to produce the putative Pat:CAT lines in cassava has at some stage undergone significant changes from the original construct and from that which is found in the transgenic *Arabidopsis* containing the Pat:CAT cassette. This finding, although not expected has further highlighted the need to sequence the constructs of other putative transgenic lines.

5.3.4.2 Verification of other putative transgenic lines

Similar primer pairs as were used to investigate Pat:CAT were used to sequence other Patatin-driven transgenes. They were PatSeqF/PatPDESTR and DESTSeqF1/TransgeneR to amplify the Patatin sequence and individual transgene respectively (Figure 5.21). In all the transgenics, PatSeqF/PatPDESTR should amplify approximately 1.3 kb PCR product, while the DESTSeqF1/TransgeneR product should vary with transgene size. Internal forward and reverse primers were also designed for transgene sequences greater than 1 kb length. For each transgenic group, at least three cassava lines, which had been confirmed to amplify the *hptII* gene, were checked. PDESTs containing the different individual expression cassettes served as positive controls. In addition, the Patatin-driven transgenes were also amplified from *Arabidopsis* transformed with the same expression cassette.
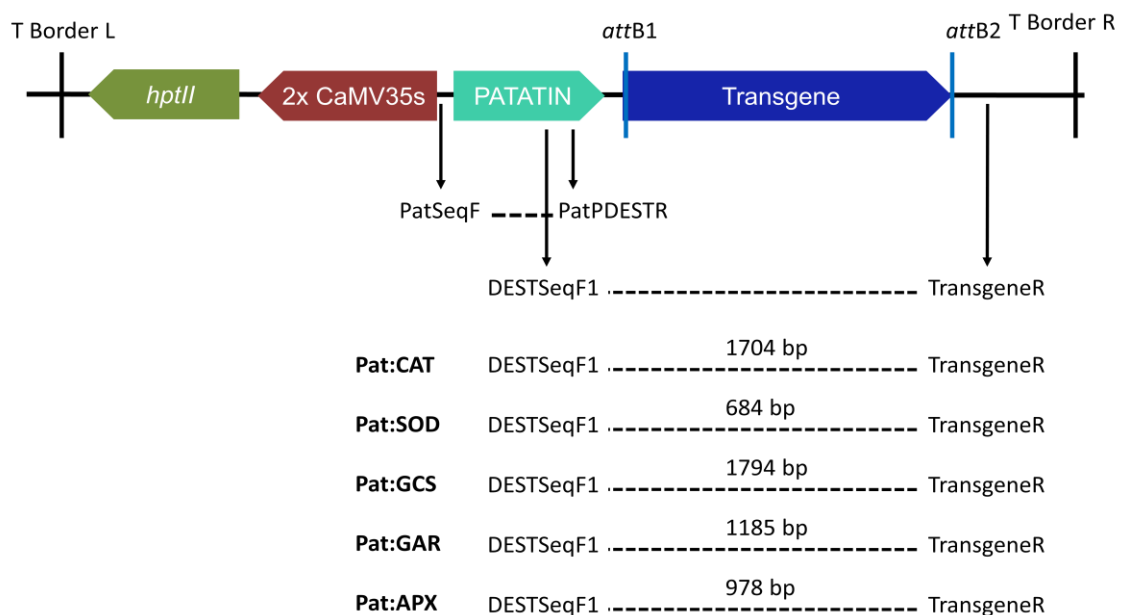
Figure 5.21 Diagrammatic presentation of the sequencing strategy used to check expression cassettes transformed into cassava plants. PatSeqF/PatPDESTR targets Patatin and DESTSeqF1/TransgeneR targets Patatin-driven transgene. The expected size for Patatin amplification was 1366 bp while the expected sizes for transgene vary with the size of transgenes as indicated.
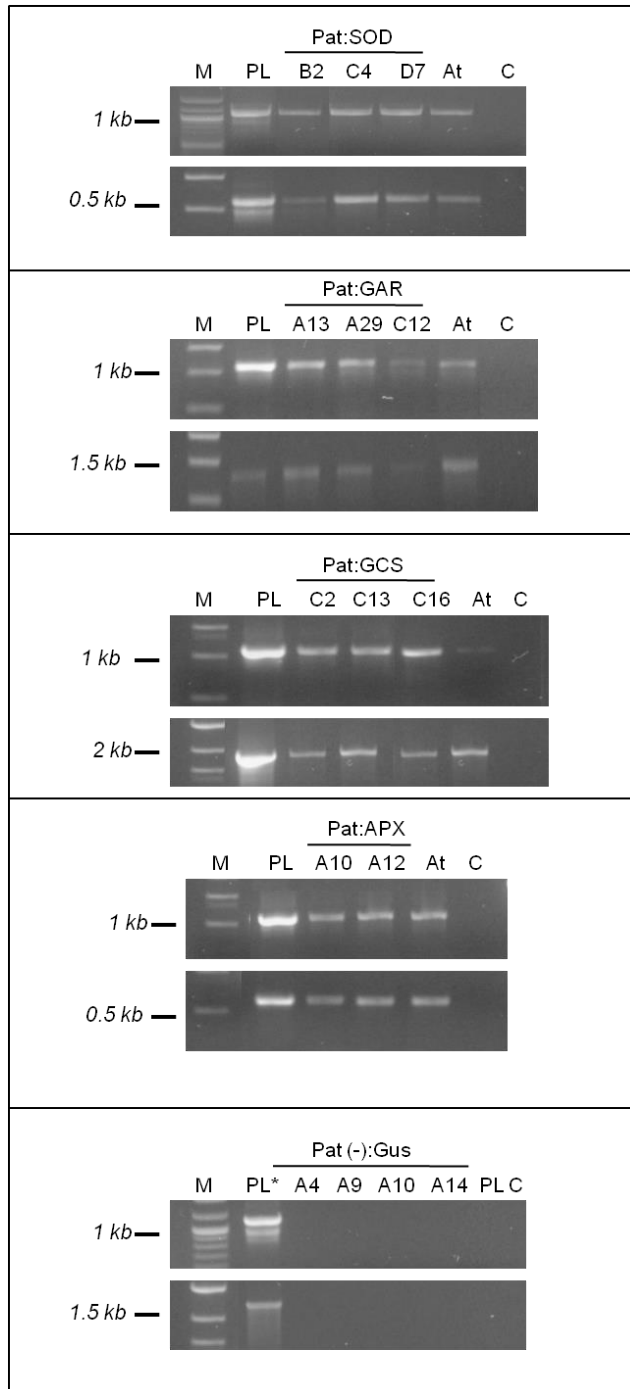
Figure 5.22 Amplification with PatSeqF/PatPDESTR which targets Patatin (upper panel) and DESTSeqF1/TransgeneR which targets the Patatin-driven transgene (lower panel). Cassava transgenic lines are indicated alphanumerically, At denotes the *Arabidopsis* transformed with the same expression cassette. M= DNA marker, PL = positive control (plasmid), C = negative control (water). Note: PL* in Pat(-):Gus is PDEST:*GusPlus* plasmid.

In Pat:SOD, the expected size of transgene amplification was 684 bp and the correct size of Patatin and MecSOD1 were amplified from all DNA samples. Sequence assembly showed these PCR products were MecSOD1 cDNA sequence coupled to Patatin. The expected size of the second fragment in Pat:GAR, Pat:GCS and Pat:APX were 1185 bp, 1794 bp and 978 bp respectively. From Figure 5.22, it can be seen that all PCR products were of expected sizes in all DNA samples including in *Arabidopsis*. Also, these PCR products correspond to the fragment in the respective plasmids. Importantly, sequencing result showed all transgenes were intact with initiation and stop codon (see Appendix Figure 9.2, 9.3, 9.4, 9.5 for the full sequence of Pat:transgene in Pat:SOD, Pat:GAR, Pat:GCS and Pat:APX respectively).

Pat(-):Gus was included in the analysis although the fragments required for sequencing could not be obtained using the same combination of primers (PatPDESTR and DESTSeqF1 target the Patatin sequence). Nevertheless, PCR with these primers confirmed that Patatin and Patatin-driven *GusPlus* sequences not present in Pat(-):Gus constructs as no PCR products were amplified. For sequencing of the Pat(-):Gus, two different set of primers were created. Due to deletion of Patatin promoter (~ 1 kb), PatSeqF was paired with GUSintR instead of PatSeqR (used in Pat:Gus verification) to generate a longer product. GusFWD/TransgeneR was used for amplification of the remaining *GusPlus* gene sequence (Figure 5.23). Genomic DNA extracted from lines showing Gus activities (Section 5.3.2.3) were used as templates.
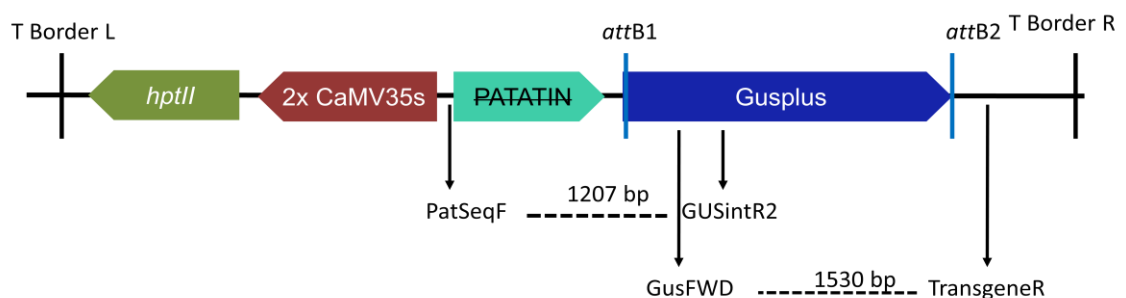
Figure 5.23 Diagrammatic presentation of Pat(-):Gus expression cassette pDEST:*GusPlus* (-Pat) and the primers used to verify the putative Pat(-):Gus cassava plants. The expected sizes of PCR products (without Patatin) are indicated.

PCR with the primers produced the correct PCR product sizes (Figure 5.24). Sequencing revealed that PatSeqF/GUSintR amplified the first half of the *GusPlus* gene including the attB1 sequence while GusFWD/TransgeneR amplified the remaining of the sequence (See Appendix, Figure 9.6). This confirmed that the correct expression plasmid was transformed into Pat(-):Gus plants.
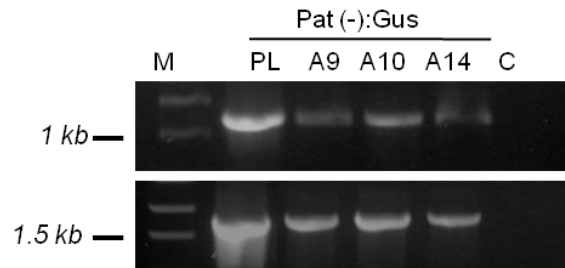
Figure 5.24 Amplification with PatSeqF/GUSintR2 and DESTSeqF1/TransgeneR and GusFWD/TransgeneR (lower panel). Cassava transgenic lines are indicated alphanumerically, M= DNA marker, PL = positive control (pDEST:*GusPlus* (-Pat) plasmid), C = negative control (water).

Overall, sequencing of the Patatin promoter and the individual transgene found that all the transgenic cassavas were transformed with the correct expression plasmid except the Pat:Gus and Pat:CAT. Pat:Gus was transformed with a truncated pCAMBIA 1305.1 while the Pat:CAT contains Patatin fused to an unknown or altered DNA fragment. Nevertheless, it was confirmed that the genomes of the other transgenic to possess the Patatin and the individual target gene.

5.3.5   Analysis of Patatin promoter from *Arabidopsis* Pat:Gus

5.3.5.1 Prediction of putative regulatory elements

Absence of transgenic cassava plants transformed with a reporter gene construct has not permitted the study of Patatin behaviour and its expression profile. However, the Patatin from the corresponding construct in *Arabidopsis* has been sequenced (See Appendix Figure 9.7) and subsequently analysed.

For prediction of regulatory elements or transcriptional motifs, the promoter sequence was searched against PLACE (Higo et al., 1999) and PlantCARE database (Rombauts et al., 1999) and this identified a number of critical transcriptional elements. Only matches with 90% or above identity are presented in Figure 5.25. The classification of the motifs according to function is presented in Table 5.2.

Both search tools identified a CAAT box and TATA box near the proximal end of the promoter. At least four different motifs related to root specificity were found in the 999 bp promoter. The root nodule elements called OSE1 and OSE2 were found at bp 360 and 240, respectively (Vieweg et al., 2004). The rest of the root-specific related motifs include RAV1AAT (Kagaya et al., 1999) and TAPOX1 (Elmayan and Tepfer, 1995), which are implicated in directing expression in roots, were also found scattered along the sequence. However, despite generally being abundant in root-related motifs, this promoter was found to lack auxin-responsive motifs. No sequence consensus to the motifs like the canonical AuxRE (TGTCTC) (Goda et al., 2004) and NtBBF1 (ACTTA) (Baumann et al., 1999) were found. Nevertheless, a total of five sucrose responsive elements consisting of SURE1, SURE2 and SURECORE were found indicating its sucrose inducible activities. Additionally, the A+B repeat consensus, which also contains 10 base pairs motif within the B-box that involve in the binding of Storekeeper, was also found (Zourelidou et al., 2002).
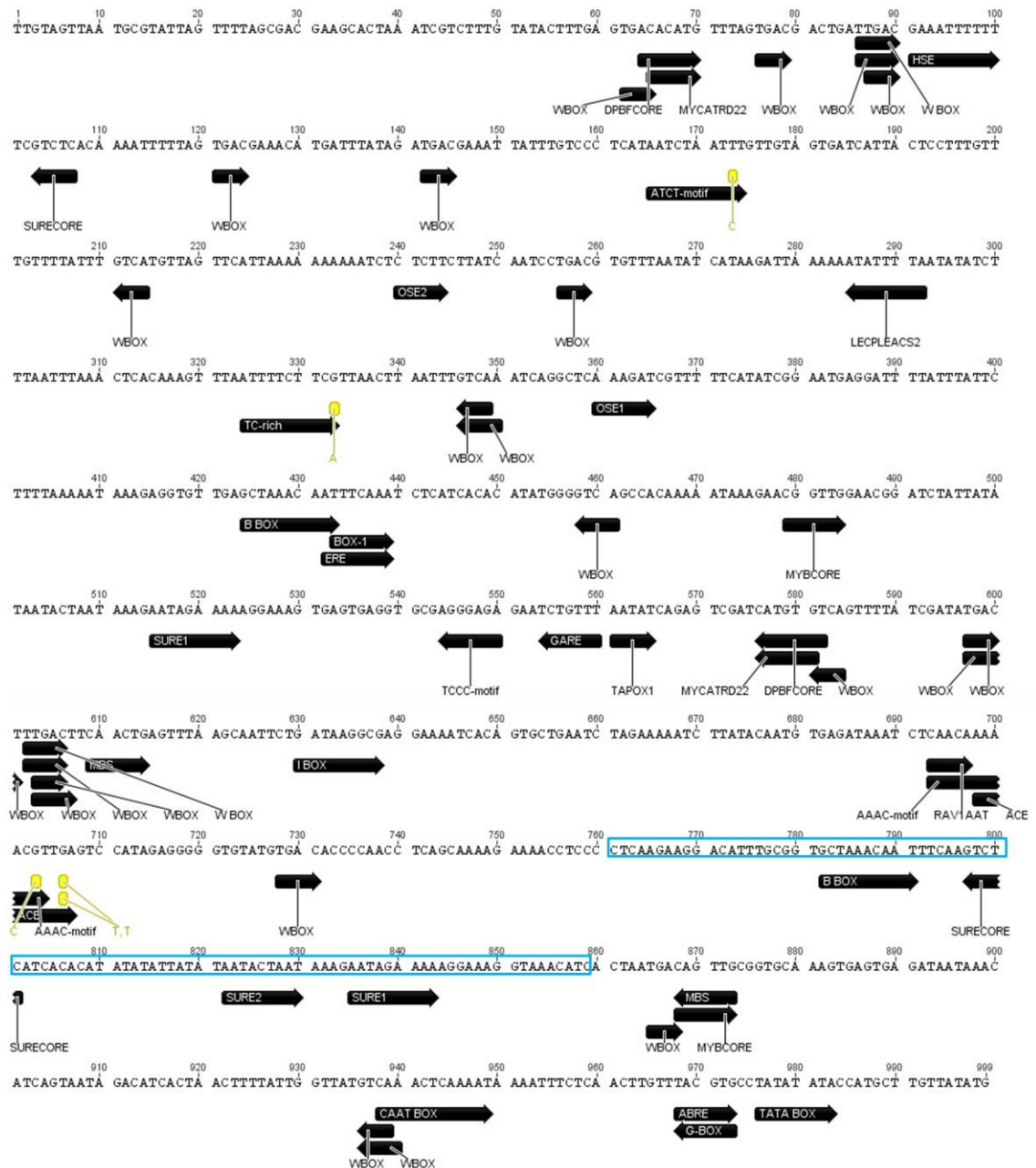
Figure 5.25 The key regulatory elements of the Patatin promoter predicted with PLACE and PlantCARE database. The arrow facing the right direction indicates motifs found in the positive strand while the arrow facing the left direction indicates motifs found in the negative strand. The A+B repeat is highlighted in blue box. Nucleotides in the yellow fonts indicate mismatch.

Table 5.2   Analysis of the Patatin promoter sequence with PlantCARE and PLACE database predicted numerous common cis-elements. Only motifs with 90% or more identity are described.

Function	Consensus sequence	Position	Identity (%)	Strand
Tuber-specificity				
OSE1	AAAGAT	360-365	100	+
OSE2	CTCTT	240-244	100	+
RAV1AAT	CAACA	693-697	100	+
TAPOX1	AATAT	360-365	100	+
Sucrose-inducibility				
SURE1	AATAGAAAA	515-523,835-843	100	+, +
SURE2	AATACTAAT	822-830	100	+
SURECORE	GAGAC	103-107,797-801	100	-, -
Hormone				
ERE	ATTTCAAA	432-439	100	+
GARE	AAACAGA	554-560	100	-
DPBFCORE	ACACATG	64-70, 576-582	100	+,-
MYCATRDD2	CACATG	65-70, 576-581	100	+,-
LECPLEACS	ATATTTTA	285-292	100	-
Flavonoid				
MYBCORE	CNGTTG	479-484,868-873,	100	+,+
MBS	CAACTG	609-614,868-873	100	+,-
Light-response				
AAAC-motif	CAACAAAAACGT	693-704	92	+
ACE	AAAACGTTGA	697-707	91	+
ATCT motif	AATCTAATTT	165-174	90	+
BOX-1	TTTCAAA	433-439	100	+
G-BOX	CACGTA	968-973	100	-
I-BOX	GATAAGGCG	630-638	100	+
TCCC-motif	TCTCCCT	544-550	100	-
Stress				
ABRE	TACGTG	968-973	100	+
TC-rich	ATTTTCTTCG	324-333	91	+
Wound				
WBOXATNPR1	TTGAC	86-90,602-606	100	+,+
WBOXHVISO1	TGACT	597-601,603-607	100	+,+

Interestingly, more than 20 wound-related motifs were identified. This so-called WBOX motif includes the well-studied WBOXATNPR1 that is specifically recognised by salicylic acid-induced WRKY binding proteins. To extend the search for wound-related motifs, a number of *cis*-elements implicated in wound response of wound inducible genes were gathered from the literature and searched for manually.

Table 5.3 The putative wound-inducible motifs searched in Patatin sequence.

Putative motifs	Sequence	Reference
Z-element	GCACATACGT	An et al. (1990)
WUN	ATGAAATTT	Pastuglia et al. (1997)
AG-motif	AGATCCAA	Sugimoto et al. (2003)
GCC-box	AGCCGCC	Fujimoto et al. (2000)

They included the nopaline synthase promoter that contains a Z-element, which is equally induced by wounding and auxin. Others were the Myb2 gene in tobacco which contains the AG-motif, STH-2 gene from potato which contains the WUN motif, and the poxA gene from rice containing the GCC-box (Table 5.3). However, searching for these motifs in the Patatin promoter only identified sequences with very low similarity.

The search tools also predicted motifs indirectly associated with wound responses. In plants, common responses following wounding area rapid oxidative burst and the production of hydrogen peroxide. These are accompanied by the upregulation of the phenylpropanoid pathway, inactivation of photosynthetic components, and the accumulation of ethylene. In the second phase, the plant initiates its defence system by producing secondary metabolites before returning to its normal physiology. There were two motifs related to the biosynthesis of ethylene found in the Patatin promoter, namely an ethylene responsive element (ERE) and LECPLEACS (Matarasso et al., 2005). These motifs are significant, especially as ethylene accumulation is a typical aspect of PPD. Equally significant is the MYB binding domain, a transcription factor related to flavonoid synthesis (Bedon et al., 2010, Tamagnone et al., 1998, Park et al., 2008), which is also associated with PPD.

Additionally, motifs associated with stress and plant defence are scattered throughout the sequence. These include an abscisic acid response element (ABRE), a TC-rich repeat, and two other *cis*-elements related to abscisic acid responsiveness, DPBFCORE and MYCATRD22, which were also shown to be involved in oxidative stress responses (Jiang and Zhang, 2001). Moreover, the Patatin promoter contains seven different light-responsive elements and six highly conserved heat shock elements (HSE).

5.3.5.2 Classification of the Patatin promoter

The Patatin promoter used here was obtained from a research group working with cassava in the Shanghai Institute for Biological Sciences, which also used it to drive the expression of their genes of interest. However, it has not been characterised as a class I or a class II. Expression in tubers by a class I patatin is extremely high compared to that of the Class II as it constitutes 98% of the total Patatin mRNA (Wenzler et al., 1989). Therefore, classification of patatin is crucial to predict the expression profile of the target genes used in this study.

Class II is differentiated from a class I by the presence of 22-bp insertion in the untranslated region close to the initiating methionine (ATG). In the class II, the 22-bp is highly identical and located at the same position (Mignery et al., 1988). Except for the insertion, the Patatin promoter of both classes is highly homologous especially towards the 3' end of the promoter so sequence alignment at this end should effectively discriminate patatin promoters. Therefore, to determine the class of our Patatin, it was aligned with a number of class I and class II patatin sequences available in the Genbank database (Figure 5.26).

```
                -160        -150        -140        -130        -120        -110
        B33     AACATCACTA  ACTTTTATTG  GTTATGTCAA  ACTCAAAgTA  AAATTTCTCA  ACTTGTTTAC
        PS20    AACATCACTA  ACTTTTATTG  GTTATGTCAA  ACTCAAAgTA  AAATTTCTCA  ACTTGTTTAC
        PS3     AACATCACTA  ACTTTTATTG  GTTATGTCAA  ACTCAAAATA  AAATTTCTCA  ACTTGTTTAC
        PAT21   AACATCACTA  ACTTTTATTG  GTTATGTCAA  ACTCAAAATA  AAATTTCTCA  ACTTGTTTAC
        PS18    CTCAT-AC-A  AC-TTATTG   GTTATGTCAA  ACTCAAAATA  AAATTTCTtA  ACTTGTTTAC
        PS22    TTCAT-AC-A  ACTTTTATTG  GTTATGTCAA  ACTCAAAATA  AAATTTCTCA  ACcTGTTTAC
        PS26    CTCAT-AC-A  ACcTTTATTG  GTTATGTCAA  ACTCAAAATA  AAATTTCTCA  ACTTGTTTAC
        Pat     GACATCACTA  ACTTTTATTG  GTTATGTCAA  ACTCAAAATA  AAATTTCTCA  ACTTGTTTAC

                -100        -90         -80         -70         -60         -50
        B33     GTGCCTATAT  ATACCATGCT  TGTTATATGC  TCAAAGCACC  ---AACAAAA  TTTAAAAACA
        PS20    GTGCCTATAT  ATACCATGCT  TGTTATATGC  TCAAAGCACC  ---AACAAAA  TTTAAAAACA
        PS3     GTGCCTATAT  ATACCATGCT  TGTTATATGC  TCAAAGCACC  ---AACAAAA  TTTAAAAACA
        PAT21   GTGCCTATAT  ATACCATGCT  TGTTATATGC  TCAAAGCACC  ---AACAAAA  TTTAAAAACA
        PS18    -TGaCTATAT  ATGccatgct  -GTTATATGt  TCAAAGCACC  C--AAaAAAA  ATTAAAAACA
        PS22    GTGCCTATAT  ATACCATGCT  TGTTATATGC  TCAAAGCACC  ---AAaAAAA  TTTAAAAACA
        PS26    GTGaCTATAT  ATACCATGCT  TGTTATATGt  TCAAAGCACC  CAAAAAAAAA  aTcAAAAACA
        Pat     GGTCCTATAT  ATACCATGCT  TGTTATATG-  ----------  ----------  ----------

                -40         -30         -20         -10         +1
        B33     CTTTGAA--   ----------  ----------  CATTTGCAAA  ATG
        PS20    CTTTGAA--   ----------  ----------  CATTTGCAAA  ATG
        PS3     CTTTGAA--   ----------  ----------  CATTTGCAAA  ATG
        PAT21   aTTTGAA--   ----------  ----------  CATTTGCAAA  ATG
        PS18    CaTTGAGAT   ATTAGTTTTT  ATTAATTATA  -ATcTGCAAA  ATG
        PS22    CTTTGAGAT   ATTAGTTTcT  ATTAATTATA  -ATcTGCAAA  ATG
        PS26    CTTTGAGAT   ATTAGTTTTT  ATTTATTATA  -ATcTGCAAA  ATG
        Pat     ---------   ----------  ----------  ----------
```

Figure 5.26 Sequence alignment of class I (B33, PS20, PS3 and PAT21) and class II patatins (PS18, PS22, PS26) with the Patatin used in this study. B33 was obtained from Rocha-Sosa et al. (1989), PAT21 from Bevan et al. (1986) while PS20, PS3, PS18, PS22 and PS26 were from Mignery et al. (1988). The CAAT and TATA boxes are indicated in a light grey and a blue shading respectively. The 22-bp insertion is highlighted in orange font. The initiating Met is indicated by +1.

From the sequence alignment, the 22-bp insertion was identified in all the class II patatins, where it was found at the bp position -32 to -11. The class I patatins did not possess this insertion. However, the alignment shows that the Patatin used in this study is missing 40 to 60 nucleotides at the 3' end, which include the region containing the definitive insertion/deletion. Since the missing nucleotides include the region used to differentiate between classes, it cannot be confirmed that our Patatin belongs to either class I or class II. Nevertheless, the Class II patatins used in this analysis also lack nucleotides at -152 and -155, which are present in the Class 1 patatin and our patatin promoter, thus suggesting that our patatin promoter may in fact be derived from a Class I. Despite not being able to classify the Patatin with absolute certainty, the CAAT and TATA boxes are present, so the Patatin was expected to function effectively. Certainly, its regulation *in planta* would help to elucidate this.

5.3.6 The Patatin promoter activity *in planta*

The Pat:Gus expression cassette was previously transformed into *Arabidopsis* by Page (2009). This had generated 5 homozygous potential Pat:Gus lines called StPAT::GusP 2-8, 7-1, 10-6, 13-4 and 16-5. In the next sections, StPAT::GusP 7-1 was used to examine overall expression of *GusPlus* in the whole plant, root specificity, wounding and sucrose inducibility. For simplicity, it is denoted as AtPat:Gus in this thesis. *Arabidopsis* B33:Gus (abbreviated AtB33:Gus) was also tested for comparative analysis and Col-0 served as WT control. B33 is a class I promoter that was used in analysis of the Patatin promoter in the previous section and the AtB33:*Gus* has been to confirmed root-specific The promoterless version of the expression cassette (Pat(-):Gus) in *Arabidopsis* was not available, so it could not be analysed. Unless otherwise stated, the *Arabidopsis* samples used were mainly seedlings that had been germinated in water for five days (5 DAG) at 25-27°C, under a 14-hour photo period. The Gus assay was conducted based on the method described in Section 2.5.7.

5.3.6.1 AtPat:Gus demonstrated root specificity and wound inducibility

The *GusPlus* expression by the Patatin promoter under non-stressed condition was examined by staining the 5 DAG seedlings for Gus activities. In this assay the root-specificity of the Patatin promoter was shown by a clear expression of the *GusPlus* gene in roots with no expression detected in hypocotyls or leaves.
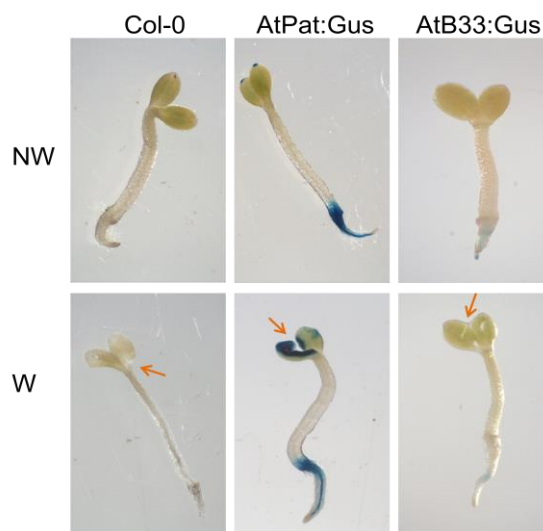
Figure 5.27   Root specificity of AtPat:Gus and AtB33:Gus is demonstrated in non-wounded (NW) samples. The wounded samples (W) showed wound inducible characteristic in AtPat:Gus by showing heavy staining at the pierced site (indicated by arrow). The experiment was performed on 5 days after germination (DAG) seedlings.

Close examination revealed occasional staining in hydathodes. B33, being root-specific also demonstrated Gus expression in roots but it was not as strong as that observed in the AtPat:Gus. The differences between the Patatin and B33 suggests that the higher root-specific expression could be achieved using the patatin utilised in this study (Figure 5.27).

Depending on the handling of the samples, staining was occasionally observed on the leaf tissues of At:PatGus. However, this was not observed in B33. As no additional treatments applied including addition of sucrose, the mechanical damage introduced during handling was thought to induce this. This characteristic is unique and must be confirmed. To do this, the leaf was pierced with a sterile needle prior to staining with Gus buffer. As shown in Figure 5.26, the wound inducibility characteristic is confirmed as the leaf developed Gus activity specifically at the wounded site. In contrast, the B33 was found lacking this characteristic as the pierced B33 leaf remained unstained.

5.3.6.2 Wound response by Patatin is rapid

Wound inducibility is an important aspect in PPD especially with respect to the oxidative damage that causing it. Since an oxidative burst can occur shortly after wounding and afterwards cascades causing irreversible oxidative damage (Reilly, 2001), it became crucial to determine the speed of the wound response in the promoter used. To assess this, AtPat:Gus leaves were wounded and then stained over a time-course of wounding. Leaves were carefully pricked with tweezers and stained with Gus buffer before rinsing with sterile distilled water to stop the reaction. The 0 min leaf sample was rinsed immediately after incubation while other samples were rinsed after the designated time points.
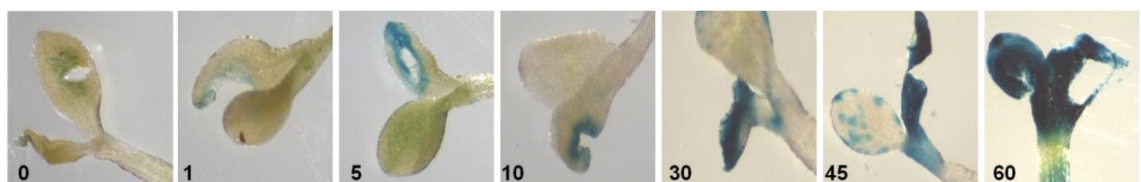
Figure 5.28 *GusPlus* expression in response to wounding in Pat:Gus as shown by the intensity of Gus staining. Numbers represent time after wounding in minutes.

Figure 5.28 shows the progress of Gus staining over 60 minutes. The wounding response appears to be extremely rapid as Gus-staining is detectable after one minute of wounding. It is clearly shown that *GusPlus* expression increased with time as

heavier staining was shown in leaves that had been wounded for a longer period of time.

5.3.6.3 *GusPlus* expression in Pat:Gus leaf was achieved with sucrose

Sucrose inducibility is a distinctive feature of class I Patatin, so it was tested by incubation in different sugar solutions. 5 DAG seedlings that had been germinated in water were incubated in sucrose, glucose and fructose (0, 10, 100 mM) at room temperature for 24 hours before being stained for Gus activities.
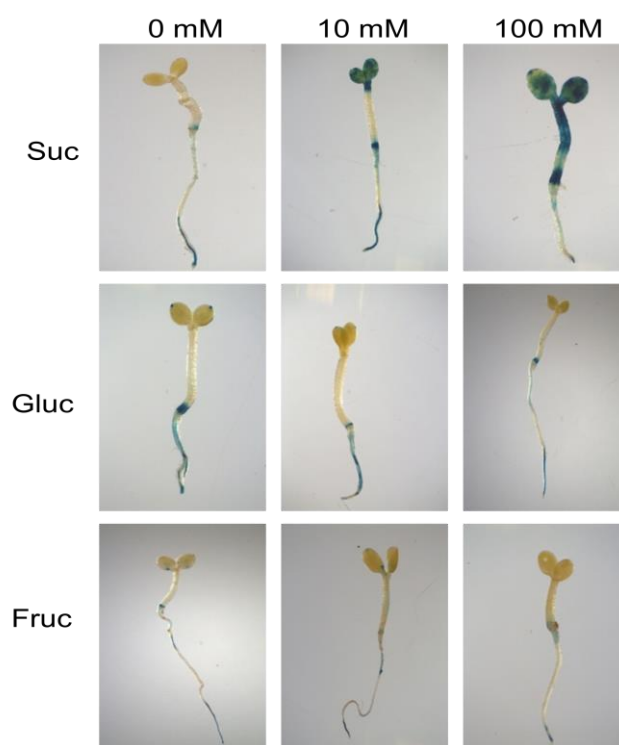
Figure 5.29 Staining of AtPat:Gus in various concentration of sugar solutions.The seedlings were stained following 24 hours of incubation. Suc = sucrose, Gluc = glucose, Fruc = fructose.

The role of the sugar solutions in enhancing Gus activities is assessed visually. Basically, incubation in water (0 mM sugar solution) reflected the normal Gus activities in AtPat:Gus which demonstrated Gus activities exclusively in roots. Figure 5.29 shows that induction of expression is apparent in the AtPat:Gus plantlets that had been supplied with sucrose. In 10 mM sucrose the expression extended to the leaf tissue, while increasing the concentration by 10 times caused expression in the whole plant. On the other hand, glucose and fructose were found less effectively to induce Gus

expression in tissues other than root as adding these sugar to the same concentration of that sucrose did not change the pattern of Gus activities in the AtPat:Gus.
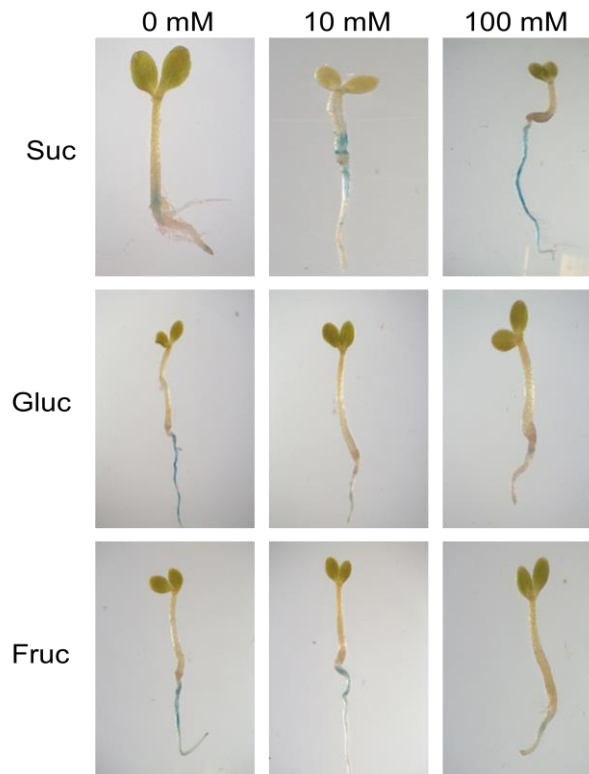
Figure 5.30 Staining of AtB33:Gus in various concentration of sugar solutions.The seedlings were stained following 24 hours of incubation. Suc = sucrose, Gluc = glucose, Fruc = fructose.

The response towards exogenous supply of sugars was also examined in the B33 promoter. AtB33:Gus was subjected to the same treatment and assessment as AtPat:Gus. In AtB33:Gus, it was found that sucrose confers its inductive effect to the B33 promoter in a relatively different manner than the Patatin. Increasing sucrose solution effectively enhanced Gus expression in the root, but no expression in leaves or other tissues was observed. Such response was not expected as B33 is a class I promoter but one possible explanation for this might be the highest concentration tested here was not sufficient to induce expression in leaf and to cause observable activities. However, whether adding more sucrose would induce expression in the leaf was not investigated. Interestingly, glucose and fructose seems to suppress the B33 promoter as less Gus expression was observed in AtB33:Gus plants supplied with these sugar solutions. As shown in Figure 5.30, glucose is more effective than fructose

as only 10 mM glucose is required to inhibit Gus expression while 100 mM fructose is required to exert the same effect.

5.3.6.4 The effects of hormone regulators

Tuber formation is largely regulated by phytohormones such as auxins, cytokinins and gibberellins (Aksenova et al., 2012). Therefore, it is of interest to examine the effects of these phytohormones on Patatin promoter expression. Since *Arabidopsisis* a non-tuberous species this could only be studied in the roots through supplying the chemicals during the plant's active growing phase. To do this, 5 DAG seedlings were incubated in 0.1, 1 and 10 µM phytohormone solutions at room temperature for 24 hours. 2,4-Dichloropenoxyacetic acid (2,4-D) and Indole-3-acetic acid (IAA) represented auxins, while 6-benzylaminopurine (BAP) and Gibberellic acid (GA_3) represented cytokinins and miscellaneous phytohormones respectively. Seedlings that were incubated in water (0 Mm) served as a positive control.
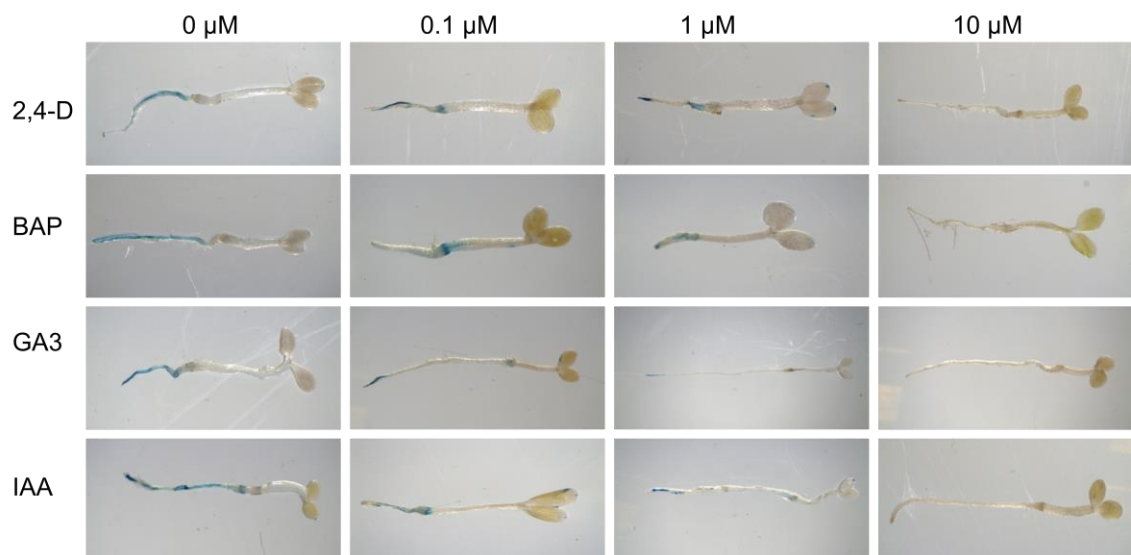
Figure 5.31 Phytohormone treatments of 5 DAG AtPat:Gus seedlings with phytohormone solutions of various concentrations. Incubation in water (0 Mm) represents untreated samples. 2,4-D = 2,4-Dichloropenoxyacetic acid, BAP = 6-benzylaminopurine (BAP), GA3 = Gibberellic acid (GA_3), IAA = Indole-3-acetic acid.

Figure 5.31 shows that AtPat:Gus was not affected by any phytohormones at 0.1 and 1 µm concentrations but at 10 µm the phytohormones effectively inhibited Gus expression as shown by absence of Gus staining. In contrast, AtB33:Gus was shown more sensitive to phytohormones than the At:PatGus. Apart from GA_3, all types of phytohormone inhibited Gus expression at 0.1 µM and higher concentration (Figure 5.32).

	0 µM	0.1 µM	1 µM	10 µM
2,4-D				
BAP				
GA3				
IAA				
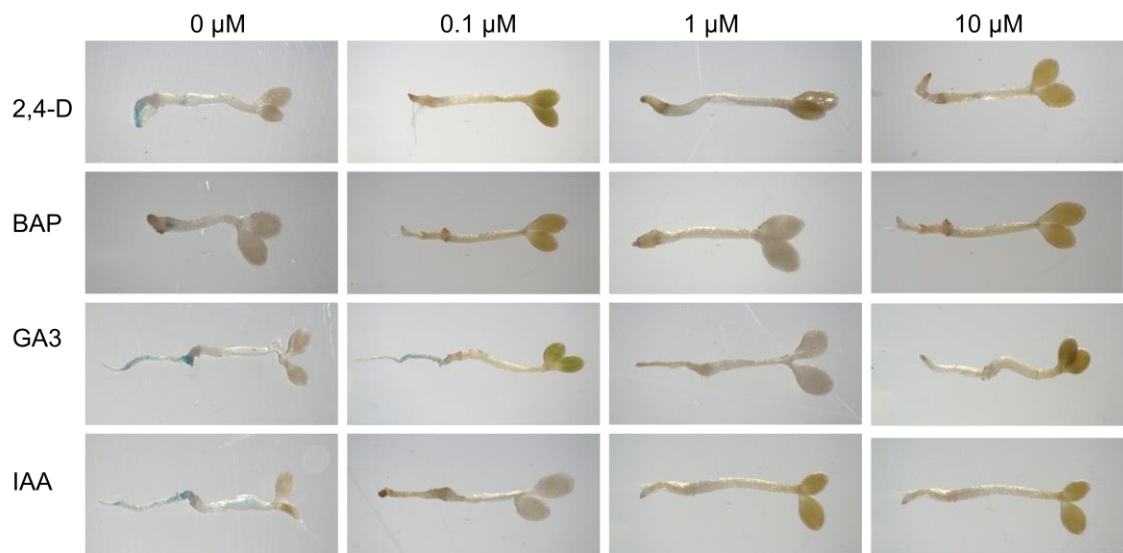
Figure 5.32 Phytohormone treatments of 5 DAG AtB33:Gus seedlings with phytohormone solutions of variable concentrations. Incubation in water (0 Mm) represents untreated samples. 2,4-D = 2,4-Dichloropenoxyacetic acid, BAP = 6-benzylaminopurine (BAP), GA3 = Gibberellic acid (GA$_3$), IAA = Indole-3-acetic acid.

This finding suggests a strong regulation by the phytohormones in the B33 promoter which substantiates the previous findings that patatin, in general is highly regulated by developmental change (Stupar et al., 2006). A possibly weaker regulation by the phytohormones is proposed in our Patatin.

5.3.6.5 Patatin regulation towards general stressors

Plants are consistently exposed to various stresses of abiotic and biotic origin. However, regarding to PPD, abiotic stress is of more concern than the biotic stress. To visualise Patatin regulation towards the general abiotic stresses, the seedlings were subjected to various treatments. To examine the effects of darkness, the *Arabidopsis* seeds were germinated for the same period and at the same temperature as the normally germinated seedlings, but with no exposure to light. For cold stress, the 5 DAG seedlings were incubated in 4°C for 24 hours. Jasmonic acid (JA) and its derivative methyl jasmonate is an essential component of the systemic wound signal. Therefore, its effect was examined by incubating 5 DAG seedlings in 10 µM methyl jasmonate for 24 hours. AtPat:Gus seedlings that were germinated under normal light conditions served as a positive control and Col-0 served as a negative control. The results of these treatments are summarised in Figure 5.33.
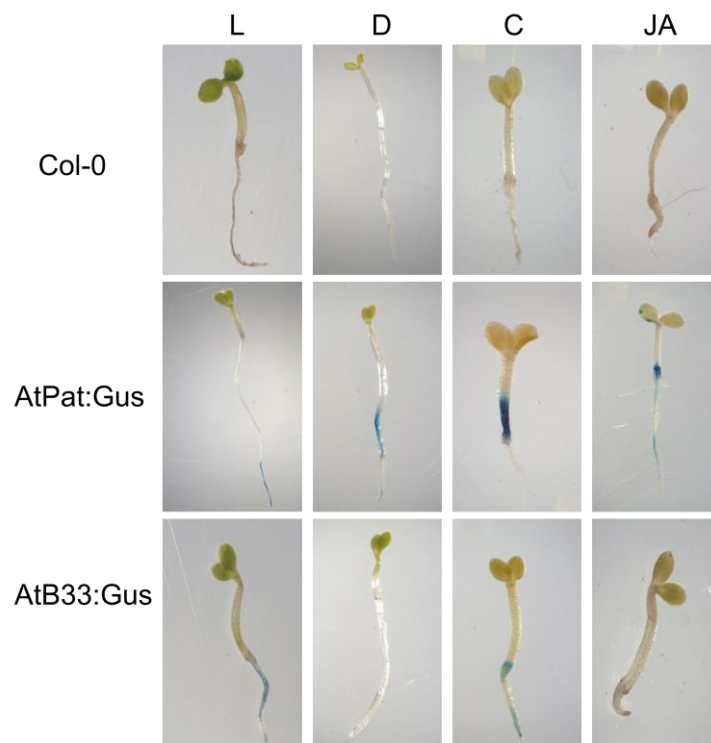
Figure 5.33 Gus activities of *Arabidopsis* seedlings in response to various stresses such as darkness, cold and accumulation of jasmonic acid (10 µM). All seedlings were Gus-stained following the treatments. L = light, D = dark stress, C = cold stress, JA = jasmonic acid.

It was found that the dark treatment had no effect on the AtPat:Gus samples as the root tissue consistently develop Gus activities. This observation suggests that light responsiveness probably is not an established characteristic of Patatin. On the other hand, B33 was severely affected by the absence of light in which it prevented Gus expression in all tissues of the seedlings. The JA treatment also produced contrasting results between the Patatin and the B33 promoter. JA at 10 µM had effectively prevented Gus expression in AtB33:Gus but it caused no change of expression in AtPat:Gus. Nevertheless, both promoters were shown not to be affected by low temperature as a similar expression pattern was observed in cold-stressed and non-stressed condition.

5.3.6.6 Patatin expression is expected in fully-grown plants

Figure 5.34 An AtPat:Gus plantlet plant at 14 DAG showing Gus activities in the same fashion as the seedlings. Here, leaves are stained due to presence of sucrose in the growth medium.

It is now evident that the Patatin used in this study is regulated by many factors and in a slightly different way to the B33. However it is crucial to determine the stability of the promoter. Staining of AtPat:Gus that had germinated for two weeks showed the plants maintained the same expression pattern as the seedlings (Figure 5.34). Gus staining was consistently observed in the primary and hairy roots. Here, sucrose inducibility of Patatin was demonstrated as the *Arabidopsis* leaves showed Gus activities without any treatment. This may be because *Arabidopsis* was grown in MS salt containing sucrose which is the standard i*n vitro* growth conditions. Besides, growth was retarded when grown on MS salts without sucrose, so obtaining healthy plantlet *Arabidopsis* grown under this condition could not be achieved.

5.4 Discussion

Since an identical Patatin promoter was used in all expression plasmids created, it was crucial to examine the regulatory pattern of Patatin by monitoring *GusPlus* expression. In the present study, Patatin regulation in cassava could not be examined as the cassava reporter lines did not exist. Sequencing of the key components of the supposedly Pat:Gus expression cassette confirmed that the constructed expression plasmid pDEST:*GusPlus* was not transformed into cassava. Instead, it was transformed with pCAMBIA 1305.1 with a truncated *GusPlus* sequence. Therefore, the *Arabidopsis* that had been transformed with the same expression plasmid that contained the full patatin promoter and *GusPlus* gene (Page, 2009), was analysed and the outcome was expected to be comparable.

Patatin is closely associated with tuber formation in its native species, potato. Its expression was detected during the stolon initiation stage and gradually increased with the formation of mature tubers (Bachem et al., 1996, Stupar et al., 2006, Xu et al., 2011). Being a tuberless species, Patatin demonstrated its tissue-specificity in *Arabidopsis* by showing Gus activities exclusively in roots. Therefore, its expression seemed not to be limited to storage organs as it was shown to be transcriptionally active in tobacco roots (Page, 2009). This root-specificity is the main indicator of Patatin function. Importantly, it parallels with our goal, which is to enhance the antioxidative capacity in order to modulate oxidative damage in cassava roots containing genes fused to Patatin. Root or tuber specificity is an established characteristic of Patatin and has been previously observed in heterologous expression in *Arabidopsis* using B33, a class I patatin. Quantification of Gus activity showed that B33:Gus caused increase of activity in roots by up to 18 and 85 times than in hypocotyls and cotyledon respectively (Naumkina et al., 2007). In cassava itself, patatin has been widely used as a promoter due to this characteristic. For example, overexpression of hydroxynitrilelyase (HNL) caused increases of the mRNA level by 20-fold and protein level by 3-fold, thereby reducing cyanogen content in cassava roots (Narayanan et al., 2011). Patatin also was used to accumulate zeolin, a storage protein, in cassava aimed at increasing the nutritional protein of cassava roots, in which the transgenic was found to have a four times higher protein level than the non-transgenic (Abhary et al., 2011).

Apart from being specific to root tissue, our Patatin was found to be highly responsive to wounding. The wound inducibility characteristic of our Patatin was discovered by Page (2009) and confirmed in the present study. It is novel since it has never been reported in any classes of patatin, including B33, despite the abundance in W-box motifs in the promoter regions (Prestridge, 1991). Moreover, patatin is not known as a defence-related protein involved in wound healing but rather in defence against pathogenic attack (Tonón et al., 2001). With respect to PPD, utilising Patatin is an excellent strategy because evidence suggests that PPD is the consequence of an incomplete wound response and wound-induced oxidative stress (Beeching et al., 1994, Beeching et al., 1998). Wounded cassava storage root tissue rapidly accumulates reactive oxygen species (ROS) that disrupt the redox balance in the cells, while the anti-oxidant enzymes and compounds to neutralise them either accumulate to inadequate levels or too late. This leads to an oxidative burst and finally the formation of vascular streaking (Reilly et al., 2003). For example, superoxide dismutase (SOD) which is a frontline enzyme in ROS detoxification is only actively transcribed between 12 to 24 hours after harvesting or wounding (Owiti, 2009, Shin et al., 2005) and catalase, which neutralises the toxic by-products of SOD, is up-regulated a few days after that (Reilly et al., 2003). The wound inducibility characteristic by Patatin can presumably be attributed to the numerous wound-response elements found in the sequence, the W-boxes in particular. The W-box is a generic name for wound-response *cis*-acting elements of (T)(T)TGAC(C/T) sequence elements found in many plant defence-related genes which require WRKY binding factors to promote transcriptional activities. While there is limited information available regarding the activation of the wound response of PPD-related genes, the discovery of a WRKY binding factor gene homolog through cDNA-AFLP pinpoints the potential of the Patatin promoter in cassava (Kemp et al., 2005).

Another prominent characteristic of Patatin is the induction of expression in non-storage tissue, especially in leaves, by sucrose. The strong inducibility demonstrated by sucrose explains why histochemical analysis in the present study utilised water-germinated seedlings instead of fully-grown plantlets which would require sucrose during growth. Sucrose catabolism involves either sucrose synthase or invertase, in which the latter predominates when oxygen is plentiful (Geigenberger, 2003). Although cassava itself does not produce a true tuber and its storage root is relatively low in sucrose, an increase in invertase activity has been detected following harvesting, indicating the accumulation of sucrose during PPD (Tanaka et al., 1984). Additionally, there is also evidence that at least 5% sucrose is required for initiation of cassava

storage roots from fibrous roots *in vitro* (Medina et al., 2007).The sucrose regulation by our Patatin is also specific as glucose and fructose at the same concentration could not induce expression in leaves. The specific induction by sucrose was previously examined and proved not to be due to changes in osmotic pressure as replacing sucrose with mannitol did not induce Gus expression (Martin et al., 1997). Nevertheless, although sucrose is recognised as an important metabolite in patatin induction, it was found not to directly modulate patatin, but requires supplementary modulators like glutamine and is also induced in the presence of light (Peña-Cortés et al., 1992). It is worth mentioning that the sucrose-inducible characteristic is not only unique to Patatin, as it is also involved in mediating the expression of the storage protein, Sporamin, in sweet potato (Hattori et al., 1991).

In the present study, the light-dependent expression as observed by Peña-Cortés et al., (1992) was confirmed in B33, but not in our Patatin as this appeared not to be affected by the absence of light. However, the expression of both promoters was greatly inhibited by high concentration of phytohormones, although our Patatin was not affected by low concentration of phytohormones. Suppression of patatin expression by GA_3 has been reported (Xu et al., 1998, Rodríguez-Falcón et al., 2006), but that by auxins and cytokininsis unclear as these are necessary components for tuber formation (Gukasyan et al., 2005, Romanov, 2009). Nonetheless, the data using phytohormones presented here are qualitative, so the precise active concentrations remain to be established. Combined treatments of physical and chemical stress would also further illuminate the regulatory function of our Patatin.

Patatin classification has been attempted in order to discriminate between and to characterise the numerous copies of Patatin found in potato tubers. Since the coding region and the immunological responses of the protein are similar, classification based on the promoter sequence has been used. For example, class I, being exclusively expressed in tubers has been shown to cause thousands fold more mRNA production in tubers. So, overexpression of transgenes in tubers is best achieved using this promoter rather than a promoter from a class II patatin (Wenzler et al., 1989). Because of some unexpected expression data from patatin-gene fusions, including patatin-*GusPlus*, in cassava, a detailed analysis of the nature of the patatin promoter found in some of the transgenic cassava and *Arabidopsis* was carried out. The amplified fragment was sequenced and this revealed that the Patatin used in our experiments to be slightly shorter than those of other characterised patatin promoters. Analysis of this sequence showed that nucleotides the proximal end which carries a common determinant used in patatin classification was missing. However, despite the missing

nucleotides it retained critical features of a Class I patatin. For example it contains A+B repeats that are responsible for the sucrose-inducible characteristic. Moreover, sucrose activation pattern showed our Patatin to have a classic response found exclusively in class I patatins. It is unclear from the literature whether the "missing" sequence containing defining 22 bp plays a functional role in the expression profiles of these two classes of patatin.

The characterisation of Patatin was intended to be studied by observing *GusPlus* expression in experiments that included cassava plants transformed with promoterless expression plasmid called pDEST:*GusPlus* (-Pat) as a control. In this promoterless control, the Patatin promoter had been excised leaving *GusPlus* positioned adjacent 2X CaMV35s in the reverse orientation that drove the selectable marker *hptII*. Unexpectedly, without a patatin promoter, Gus activity was observed indicating *GusPlus* expression. Having confirmed, though sequencing, that these transgenic plants possessed the correct construct, *GusPlus* minus the Patatin promoter, it was concluded that this unexpected result is probably due to the constitutive CaMV35s being able to drive *GusPlus* expression in the whole plant despite being in reverse direction. Interestingly, Gus staining of these transgenic cassava materials showed particularly intense staining.

In conclusion, although the Patatin promoter expression profile could not be examined in cassava plants, the findings gathered from transgenic *Arabidopsis* have provided important indication of functions. It is worth highlighting that the root-specific and wound-induced features demonstrated by this promoter are important qualities as they should facilitate the accomplishment of the main objectives of this study.

CHAPTER 6

Effects of anti-oxidant genes to PPD

6.1 Introduction

Reactive oxygen species (ROS) have been implicated as a causal agent in PPD. Accumulation of ROS following wounding of the storage roots has been observed. Like in other plants, cassava is equipped with ROS detoxification systems but they are inadequate in the harvested storage roots, leading to inefficient ROS scavenging (Beeching et al., 1999). Prolonged accumulation of ROS eventually causes oxidative stress, cell damage and tissue discolouration. The existing knowledge about the native expression of the target genes used in this study, including their response towards general abiotic stressors, is reviewed here.

Superoxide radical anion (O_2^-) is normally produced from leakage in the electron transport chain (ETC) but also can be artificially produced by treatment with a redox-cycling herbicide, such as methyl viologen (MV). In the plant cells, O_2^- is dismutated to H_2O_2 either spontaneously or enzymatically by superoxide-dismutase (SOD) (Bowler et al., 1994). In cassava storage roots O_2^- can be detected within 15 minutes of tissue wounding. The importance of SOD and its classification have been discussed in Section 3.1.2.1. At least seven SOD isozymes were identified in cultured cassava cells, (You, 1996) but to date, only two SOD genes have been isolated and characterised. They are MecSOD1 and MecSOD2. Both genes are cytosolic, CuZn- type and are present as single copies in the cassava genome. However, MecSOD1 has been more studied than MecSOD2, with high expression detected in stems and storage roots, and low expression detected in non-storage roots and leaves. MecSOD2 expression in stems, leaves and storage roots resembles those of MecSOD1, but its expression in non-storage roots has not been investigated (Shin et al., 2005). Interestingly, MecSOD1 is also upregulated by sucrose, although it has not been determined whether this is a result of changes in osmotic pressure or metabolic activities (Lee et al., 1999). Nevertheless, both are also highly upregulated by wounding treatments, though the MecSOD1 expression data were obtained using storage roots of unknown cultivars (Owiti, 2009). In terms of response to ROS treatments, increased expression was more rapidly achieved in MecSOD2 than MecSOD1, with increased expression at 6 hours and 30 hours, respectively. The high sensitivity demonstrated by MecSOD2 is a useful criterion for studying the role of SOD in PPD. The SOD expression pattern in

storage roots has been determined in a separate experiment by monitoring transcript abundance of a putative SOD gene that is highly identical to MecSOD1 at the amino acid level. In four cultivars with different PPD susceptibilities examined, the expression level was constant, but low, from day 1 to day 5 of harvest (Reilly, 2001).

Peroxidase (POX) activity has been associated with the PPD symptoms developed in deteriorated cassava roots. For example, the blue-black discoloration has been shown to be a result of oxidation of polyphenols such as catechin, which present in higher concentration in deteriorated cassava roots, by POX (Tanaka et al., 1983). This is supported by the observation that the treatment with horseradish peroxidase increased formation of coloured deposits in cassava roots (Marriott et al., 1980) and the gradual increase of total POX activities in stored cassava roots over the course of deterioration (Tanaka et al., 1983). Several types of POXs, including those that oxidise scopoletin, which is the main compound associated with PPD symptoms, have been identified (Reilly, 2001, Gómez-Vásquez et al., 2004). Moreover, microarray analysis of deteriorating vs fresh cassava roots showed upregulation of a secretory POX (MecPX3) after 12 hours of harvesting. In addition to those POX that oxidise phenolic compounds, ascorbate peroxidase (APX), which is involved in the ascorbate-mediated detoxification of the by-product of O_2^- dismutation to H_2O_2, plays a role in ROS detoxification in cassava roots post-harvest. The general mechanism of APX activity is discussed in Section 3.1.2.3. Nucleotide BLAST searches using *Arabidopsis* APX sequences predicted seven orthologous sequences in cassava (Bull, 2011), but so far only one APX has been isolated from the cassava genome, MecAPX3 (Reilly et al., 2007), which was used in this study. Therefore, while the general expression profiles of POXs have been determined in cassava roots, that of MecAPX3 has been specifically studied and shown to have transient expression between 6-12 hours after harvesting (Owiti, 2009, Reilly, 2001). However, its response towards abiotic stimuli has not been determined.

The non-enzymatic components for modulating ROS include glutathione (GSH/GSSG) and ascorbate (AA), which are involved in the ascorbate-glutathione cycle for ROS detoxification. In *Arabidopsis*, ɣ-glutamylcysteine synthetase (GCS) is proposed to be the key enzyme for GSH (reduced glutathione) formation, which is a powerful compound against oxidative stress (Szalai et al., 2009). The pathways for the biosynthesis of GSH and its antioxidative properties have already been discussed in Section 3.1.2.5. Microarray experiments using deteriorating cassava roots revealed upregulation of glutathione S-transferase (GST), which is an enzyme involved in catalysing the detoxification of metabolites resulting from cell damage, but there was

no report on expression of genes involved in glutathione biosynthesis, including GCS (Reilly et al., 2007). Hence, the gene encoding this enzyme has yet to be isolated and its expression profile to be determined in cassava.

Similarly, the gene encoding galacturonic acid reductase (GAR) has not been isolated in cassava, so data on its expression profile is currently not available. GAR is the enzyme identified in the galacturonate pathway in AA biosynthesis whose overexpression has been shown to increase AA levels substantially in strawberry fruit and *Arabidopsis* (Agius et al., 2003) .The other pathway for AA biosynthesis is described in Section 3.1.2.4 and the GAR gene used in this study is listed in Table 3.1. The cassava root is relatively low in AA, though examination of 30 cassava genotypes found some indication that AA content might increase resistance to PPD (Chavez et al., 2000).

6.2   Research aim

This chapter aims to assess PPD symptoms and changes of biochemical activities in cassava roots from plants transformed with the above mentioned anti-oxidant genes. Assessments involve the putative single-insert lines which have been confirmed carrying correct expression cassettes as identified in Chapter 3 and Chapter 5.

6.3 Results – MecSOD2

Seven single-insert independent lines had been identified from the pDEST:MecSOD2-transformed cassava. From this, selected lines were grown in the greenhouse for six months to produce storage roots (Section 2.2.2). Assessments of yield and phenotypes from three Pat:SOD plantings did not find conclusive differences between the transgenics and the WT plants due to extensive variations (Section 3.3.2.2). Further, four of the total numbers of the single-insert lines were used for expression analysis, enzyme activity, ROS detection and PPD assessment.

6.3.1 Cassava harbouring the pDEST:MecSOD2 cassette over-express the transgene in root tissue

6.3.1.1 RNA isolation method produced RNA of good quality

Total RNA isolation from cassava roots is complicated by high starch and polyphenols in which commercial kits failed to yield good quality RNA.
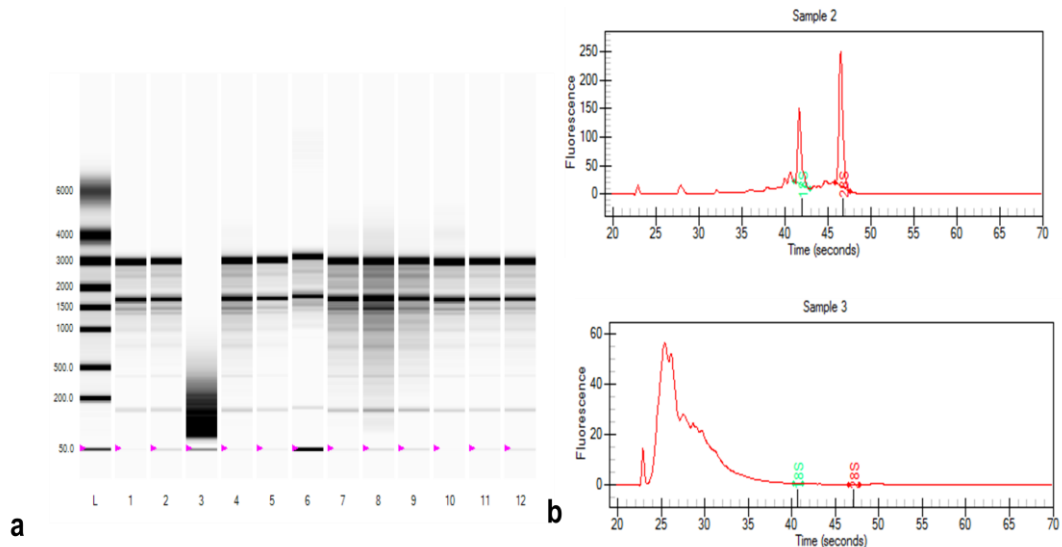
Figure 6.1 The data obtained from Experion™ Automated Electrophoresis System (a) A simulated agarose gel of RNA showing that two bands corresponding to 18s and 28s rRNA were obtained in all samples except in Sample 3.(b) Chromatograms of good (Sample 2) and poor (Sample 3) quality RNA. 18s and 28s peaks are clear in Sample 2 but these are not shown in Sample 3.

Therefore, it was extracted according to a conventional method used for isolation of RNA from recalcitrant pine needle (Chang et al., 1993). RNA was quantified using Experion™ Automated Electrophoresis System which simultaneously checked the integrity of the RNA (Section 2.4.3). Simulated gel showed the typical 18s and 28s RNA indicating clean RNA preparations (Figure 6.1). Unless a high quality of RNA was obtained from a sample, re-extraction was performed.

6.3.1.2 Validation of target gene and reference gene primers for qPCR

qPCR was performed according to the Pfaffl method which measures fold-increase in the transgene as a ratio to fold-increase in the reference gene (Pfaffl, 2001). While the gene encoding a housekeeping gene 18s was selected as a reference gene based on recommendations in the literature (Bas et al., 2004), as the target gene requires rigorous validation. Since cassava possess an endogenous MecSOD2 gene it was decided that it would be more biologically relevant to design primers that would measure the transcript levels derived from both genes, endogenous and transgene, rather than primers that could differentiate between them (Figure 6.2). Therefore, the primers called SODtf and SODtr were designed based on the MecSOD2 coding region. A similarity search of the primers against the cassava genome database in Phytozome and the T-DNA region found no other target sequence than MecSOD2. To detect contaminating genomic DNA the primers were designed to span an intron to discriminate amplification from genomic DNA and cDNA by size. Amplification from pure cDNA would generate a smaller sized PCR product (135 bp), if contaminating genomic DNA was present in the cDNA preparation another PCR product of greater size (325 bp) would appear on the electrophoresis gel.
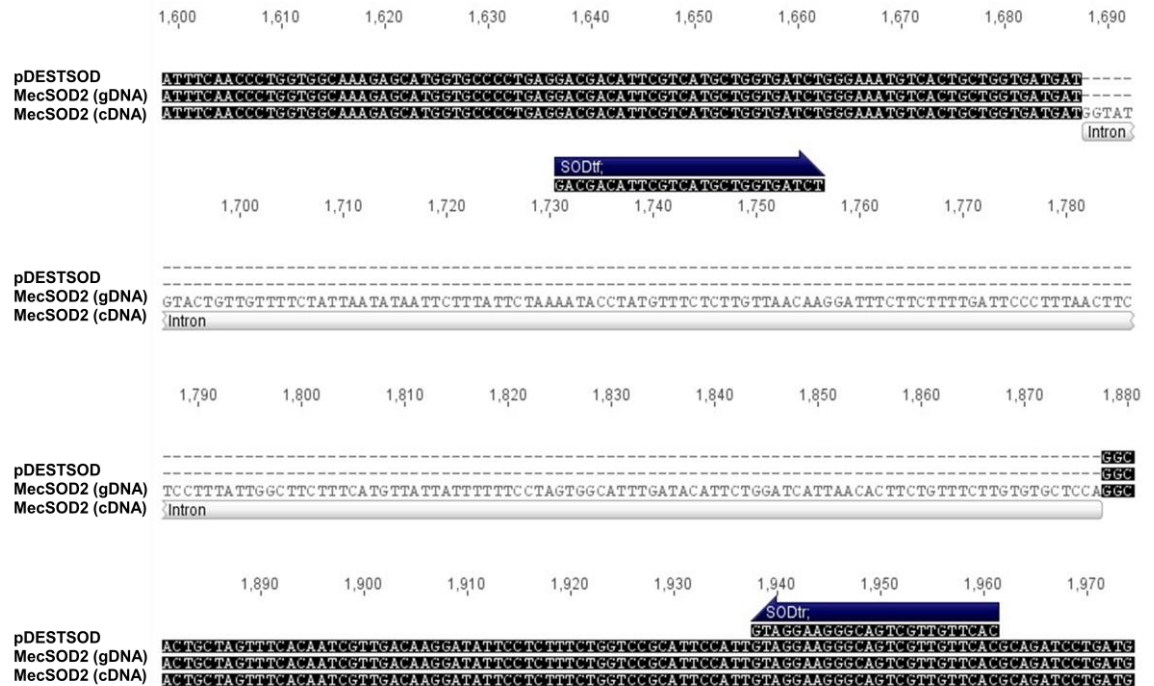
Figure 6.2 Nucleotide alignment of the expression plasmid (pDEST:SOD), genomic DNA sequence of MecSOD2 (gDNA, phytozome: cassava 4.1_018289) and the coding sequence of MecSOD2 (cDNA). Intron, forward primer (SODtf) and reverse primer (SODtr) are indicated.
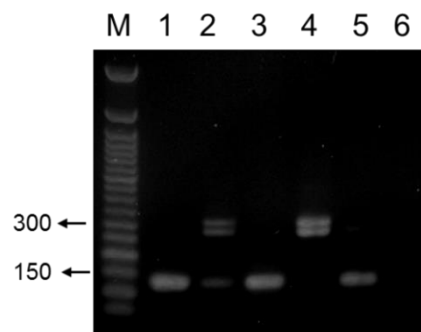
Figure 6.3 PCR of various DNA templates using primers SODtf and SODtr with *Taq* polymerase. Amplification from plasmid and cDNA template generated a single PCR product of 135 bp. Amplification from a transgenic genomic DNA template generated the 135 bp PCR products and two additional PCR products. M = DNA marker, 1 = positive control (pDEST:MecSOD2 plasmid), 2 = transgenic genomic DNA, 3 = transgenic cDNA, 4 = WT DNA, 5 = WT cDNA, 6 = negative control (water).

The primers specificities were validated by conventional PCR using *Taq* Polymerase. PCR with cDNA templates generated a single PCR product of the correct size but PCR with transgenic genomic DNA generated three PCR products instead of two (Figure

6.3). The smaller PCR product was the transgene MecSOD2 fragment while the other two were believed to be the genomic fragments of MecSOD2 because similar PCR products were obtained from the WT genomic DNA. Alignment of SODtf and SODtr primers with MecSOD2 homolog (phytozome: cassava 4.1_018294) found putative non-specific binding of the primers with expected PCR product of approximately 300 bp (Figure 6.4). Thus, this explains the presence of additional PCR product in genomic DNA template. The PCR products amplified from WT cDNA and transgenic cDNA were sent for sequencing and they were confirmed a MecSOD2 coding sequence fragment (data not shown).

Figure 6.4 Primer alignment of SODtf and SODtr to MecSOD2 homolog (Phytozome: cassava4.1_018294) in cassava genome. This unspecific binding has caused an additional PCR products of 300 bp to be amplified from cassava genomic DNA.

Amplification with *Taq* polymerase confirmed the primers specificities but this requires further validation in the actual qPCR reaction. To do this, a melting curve analysis was performed.

6.3.1.3 Melting curve analysis

The specificities of both the target and reference gene primers in qPCR reaction were determined by melting curve analysis. This is an indispensable step in qPCR utilising SYBR green. Amplification of cDNA templates derived from the WT and Pat:SOD with SODtf/SODtr primers generated a single fluorescence signal peak confirming measurement of only transgene and absence of unwanted products such as primer

dimers. Similar results were obtained for the reference gene 18s, where a single fluorescence peak was obtained (Figure 6.5). Difference in melting temperature is attributed to the properties of the PCR products.
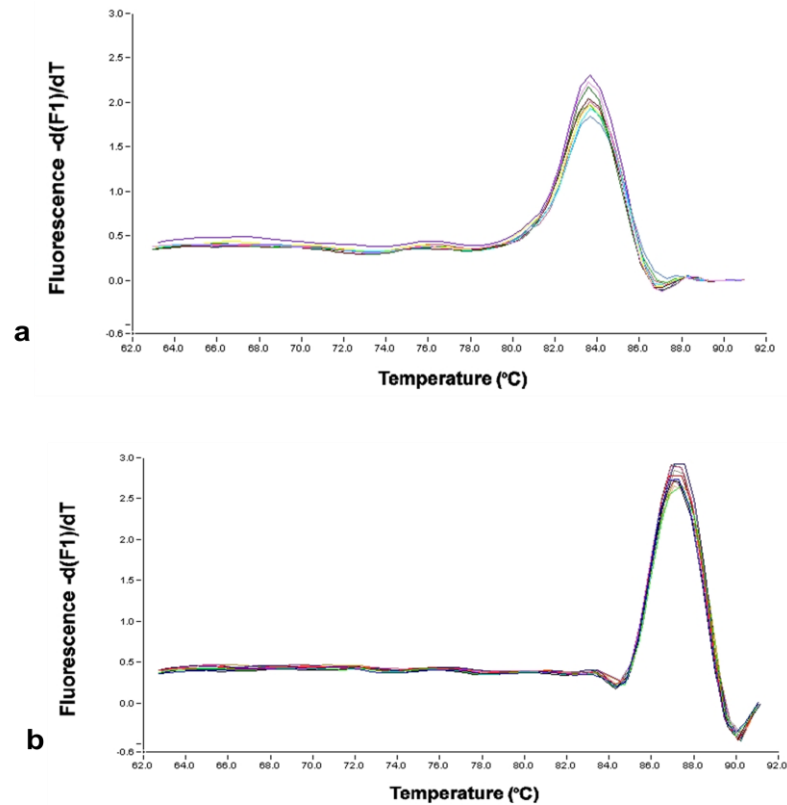
Figure 6.5 Melting curve analysis (a) transgene MecSOD2 and (b) reference gene amplification. Presence of a single fluorescence peak confirms specificity of the primers in qPCR reaction.

6.3.1.4 Determination of amplification efficiencies of target and reference gene

Another indispensable step in the Pfaffl method is determination of amplification efficiencies (AE) of the target and reference genes using standard curve analysis. The standard curve is constructed by plotting CT values and the amount of cDNA template used. AE would be used in quantification of the target gene transcript (Section 2.4.6). Five cDNA dilutions derived from WT roots harvested at 0, 1 and 3 DAH were prepared and amplified with the proposed qPCR primers using SYBR green. AE was determined from the slope of the standard curve (Figure 6.6). A similar approach was applied to the reference gene (Figure 6.7).

155
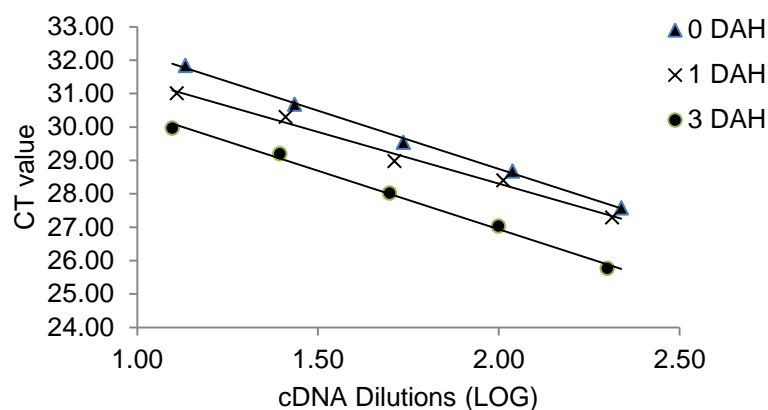
Figure 6.6 Standard curve analysis of qPCR amplification. Dilutions of WT-derived cDNA amplified with SODtf and SODtr primers. 0 DAH; y= -3.493x + 35.73 (R^2 = 0.997), 1 DAH; y = -3.099x + 34.50 (R^2 = 0.988), 3 DAH; y= -3.501x + 33.94 (R^2 = 0.994).
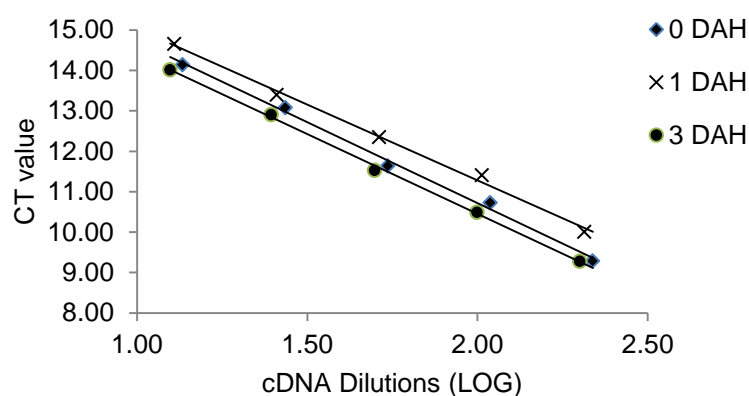
Figure 6.7 Standard curve analysis of qPCR amplification. Dilutions of WT-derived cDNA amplified with 18s For and 18s Rev. 0 DAH; y= -4.085x + 18.90 (R^2 = 0.993), 1 DAH; y = -3.748x + 18.78 (R^2 = 0.996), 3 DAH; y= -3.953x + 18.36 (R^2 = 0.998).

In all the materials, excellent correlation coefficients were found between the amount of templates and CT values as suggested by the high R^2 values (R^2 > 0.980), but AEs varied between materials and genes. According to Table 6.1, target genes had high AEs as more than 90% were achieved with the designed primers. Reference gene AEs were generally lower than those of targets genes in which only 76-85% were achieved.

Table 6.1 Amplification efficiencies of target gene (MecSOD2) and reference gene (18S) as determined from the slope.

Materials	Reference gene		Target gene	
	Slope	AE(%)	Slope	AE(%)
0 DAH	-4.085	76	-3.493	93
1 DAH	-3.748	85	-3.099	110
3 DAH	-3.953	79	-3.501	92

6.3.1.5 Transcriptional levels of MecSOD2 and CuZnSOD activity in Pat:SOD roots over a PPD time-course.

MecSOD2 transcriptional levels were determined using cDNA derived from fresh cassava roots as a template. This was quantified as fold differences normalised to transcriptional levels in the WT. The changes in transcriptional level over harvesting times were determined by normalising qPCR reactions to the transcriptional level in WT roots at 0 DAH setting the fold of expression to 1.0. For measurement of CuZnSOD activities, total protein was extracted from the root samples and quantified according to the methods in Section 2.5.2 and 2.5.3, respectively. The SOD activities were determined and based on a standard curve constructed from photoreduction of nitrobluetetrazolium (NBT) at A560 (Figure 6.8) (Section 2.5.5)
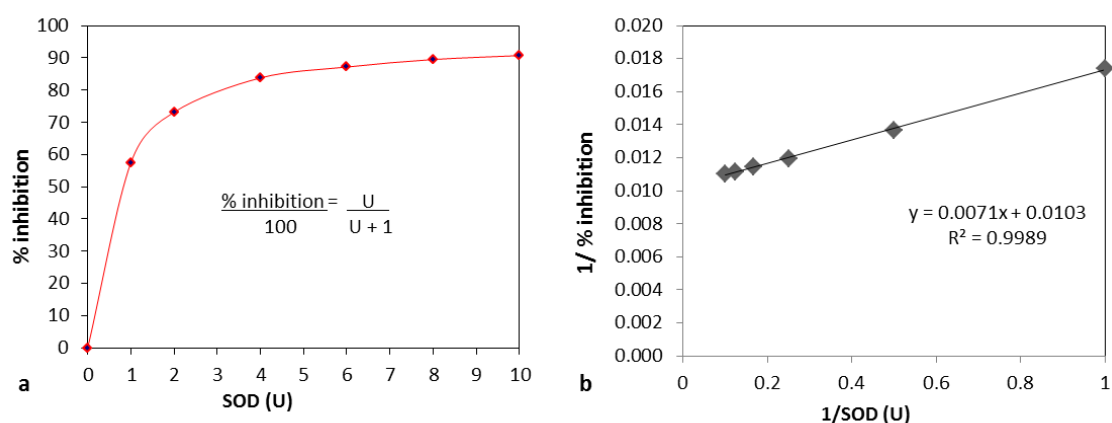
Figure 6.8 Typical SOD standard curve showing percentage inhibition as a function of amount of SOD added (a) and a linear double-reciprocal standard curve (b). R^2 is shown.
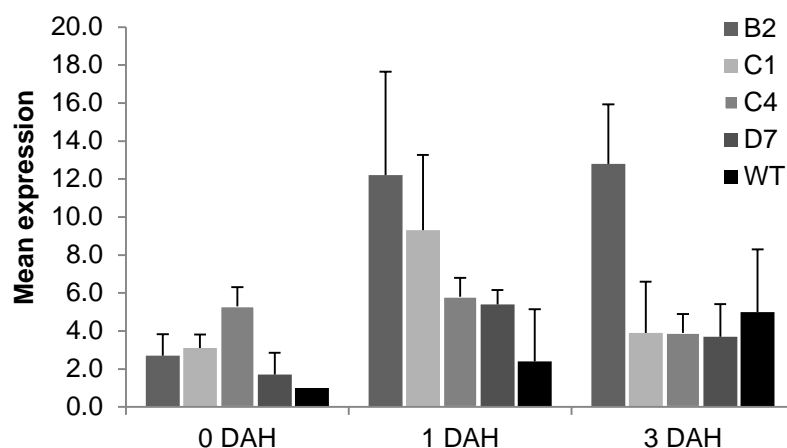
Figure 6.9 Mean relative expression of MecSOD2 in Pat:SOD transgenic roots compared to the WT roots following harvest. n = 3, SD shown.

Figure 6.9 shows the transgenic cassava roots have higher MecSOD2 transcriptional level than the WT indicating transgene expression in transgenic cassava. Between 1.7- to 5.3- fold increase was achieved in the fresh transgenic cassava with significantly higher expression shown in C1 (t-test: WT vs. C1, p=0.003) and C4 (t-test: WT vs. C4, p=0.005). High variations of transcriptional level were observed in both the transgenics and the WT roots in the roots undergoing deterioration but it was possible to differentiate a general trend in the transcriptional profile of MeCSOD2 and the WT. After 24 hours of harvest, the transcriptional level increased in both the transgenics and the WT but this was much greater and significant in the transgenics. B2 root samples showed the highest average increase with up to 12-fold compared to the WT which only showed an insignificant average increase of 4.4. Interestingly, the high transcriptional level of B2 remained at the same level until 3 DAH while the rest of the root samples changed variably but non-significantly. Overall, it can be concluded that the transgenics tended to have a significant transient increase of transcription at 24 hours after harvest compared to the harvest point, while the WT had a slight, though not statistically significant increase.
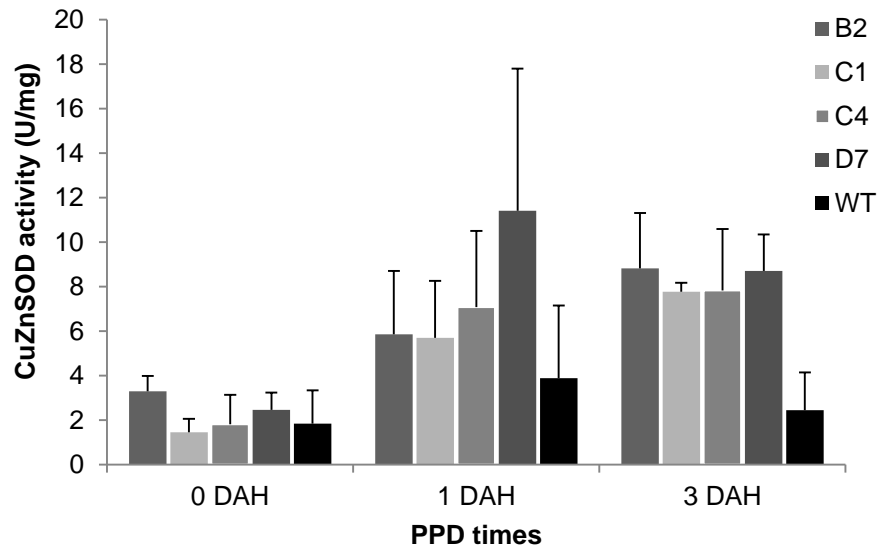
Figure 6.10 Mean CuZnSOD activities in Pat:SOD transgenic roots compared to the WT roots following harvest. n = 3, SD shown.

The measurement of CuZnSOD activities also produced highly variable data, as seen by the large standard errors (Figure 6.10). In the fresh cassava roots, the CuZnSOD activities were low in both the transgenics and the WT and there was no significant difference between the activities in the transgenics and the WT at this time point. As may be inferred from the graph, at 1 DAH, activities increased in all lines but this was not statistically significant. Also not significant were the difference between the activities in the WT at this time point. Only after 3 days of harvest, the CuZnSOD activities were found increased significantly (t-test, 3 DAH vs 0 DAH, $p < 0.05$) in the transgenics. Additionally, (except in C4) their activities were significantly higher than that of the WT at this time point. In contrast, the activities of the WT roots did not change significantly at 3 DAH although it appears to have decreased slightly.

From this, it can be summarised that CuZnSOD activities were constant throughout PPD times in the WT roots but it increased at 3 DAH in the transgenics. Clearly, the increase was not parallel with the enhanced expression of MecSOD2 that occurred at 1 DAH. The difference could be due to differential turnover rates for the mRNA and the enzyme. Nevertheless, the trend in the CuZnSOD activities was not expected as it was predicted that the patatin-driven transgene would lead to an increased CuZnSOD expression during root development rather than after harvest, unless the wound-induced expression of patatin is also playing a role.

6.3.2 Does the increase in SOD activities cause changes in H_2O_2-detoxifying enzymes?

In a normal plant ROS scavenging network, an enhanced SOD activity would lead to the production of H_2O_2, which would require the activity of CAT and APX enzyme to complete the ROS detoxification. To investigate if the same events have occurred in transgenic cassava roots, the activities of these enzymes were measured. The CAT enzyme activities were measured by monitoring the rate of H_2O_2 decomposition at A240 (Section 2.5.6) while APX activities were determined by taking the rate of AA oxidation to dehydroascorbate (DHA) at A290 (Section 2.5.4).
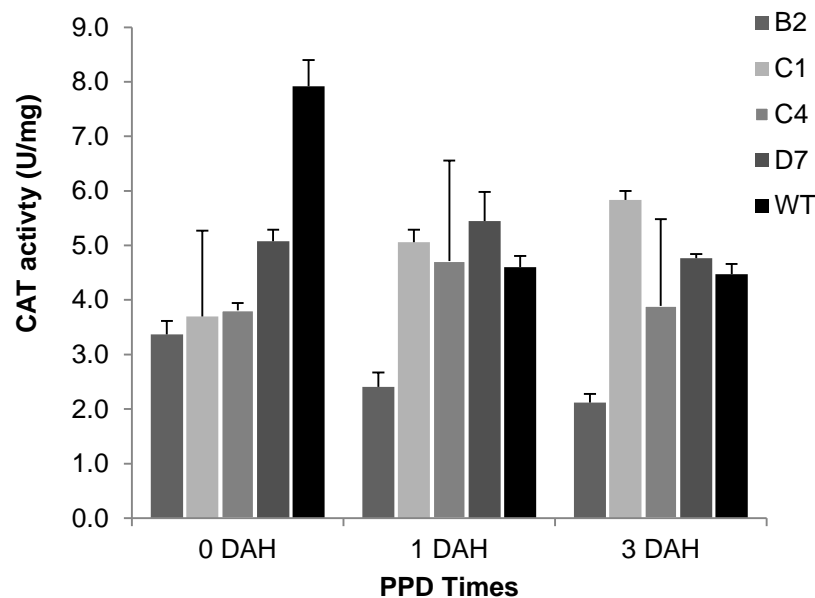
Figure 6.11 Mean CAT activities in Pat:SOD roots measured at 0, 1 and 3 DAH. n=3, SD shown. n = 3, SD shown

The CAT and APX activities are shown in Figure 6.11 and 6.12, respectively. According to Figure 6.11, there was no clear changes in CAT enzyme activities in the Pat:SOD transgenic roots during the course of deterioration. Although it may appear to increase or decrease in some lines, this was not statistically significant. The CAT activities can be concluded as being at the same level from the point of harvest until 3 DAH. However, it should be noted that at 0 DAH, the CAT enzyme activities of the Pat:SOD roots were significantly lower than the WT.
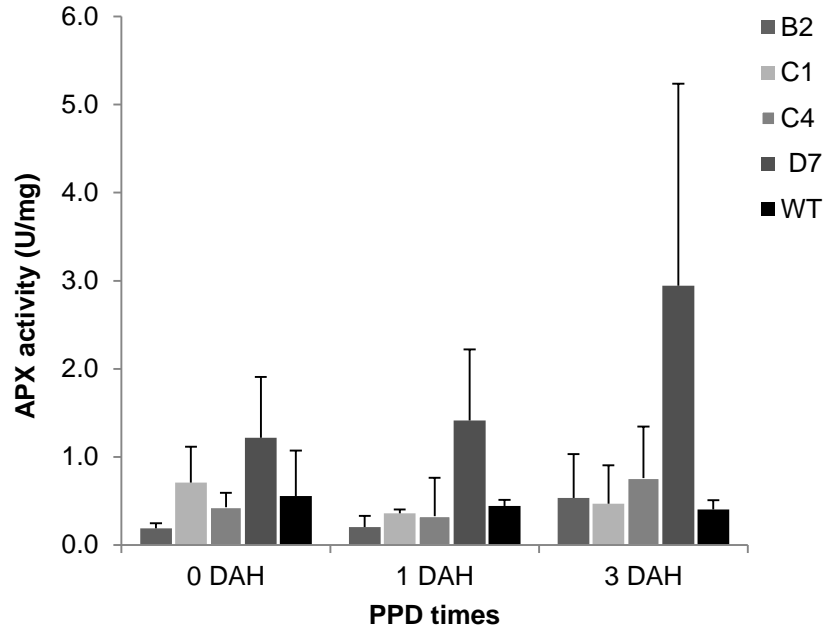
Figure 6.12 Mean APX activities in Pat:SOD roots measured at 0, 1 and 3 DAH. n =3, SD shown.

It can be seen in Figure 6.12 that the APX enzyme activities were changing erratically in all lines, except in D7. D7 showed a steady increase and exceptionally high activities at all time-points, but this was largely caused by variation between biological replicates. Moreover, statistically, the activities in this line were not significantly different from the WT. Similarly, the APX enzyme activities in all lines including the WT were not statistically significant. Therefore, it can be summarised that the APX enzyme activities, in both transgenics and the WT did not change over the course of PPD.

In conclusion, measurement of CAT and APX enzyme activities showed that these were not affected by changes in MecSOD2 expression, which might have been expected were the anti-oxidant system acting as an integrated network. The significant increase of SOD activities at 3 DAH failed to increase the activities of these enzymes accordingly. Consequently, this caused inefficient detoxification of H_2O_2 which then led to oxidative stress due its accumulation in the storage roots.

6.3.3 Does the enzyme activities affect ROS production pattern?

Superoxide was quantified according to the method in Section 2.5.10 and based on the standard curve in Figure 6.13.

$$y = 0.1114x + 0.0565$$
$$R^2 = 0.9949$$
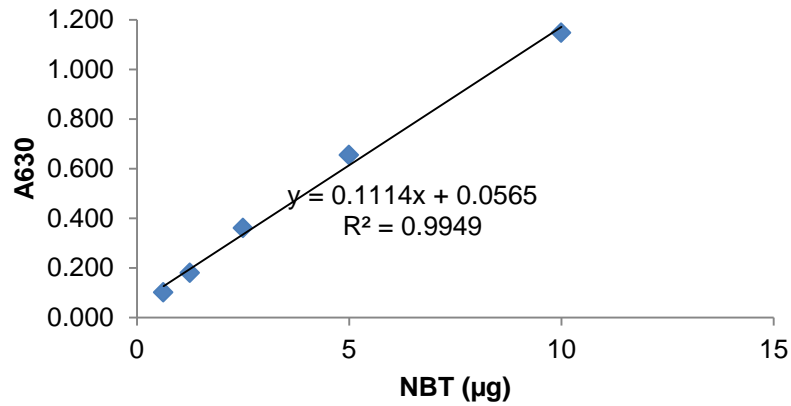
Figure 6.13 Standard curve constructed from known amount of NBT for quantification of O_2^- in cassava root tissue.

Figure 6.14 shows the level of O_2^- in all lines during the PPD times. While high variation is detected there is no significant change of O_2^- over the time-course. Certainly, there was no clear differences of O_2^- level between the Pat:SOD roots and the WT. With highly variable data measured at all time-points it was not possible to differentiate the trend of O_2^- accumulation in the transgenics and the WT.
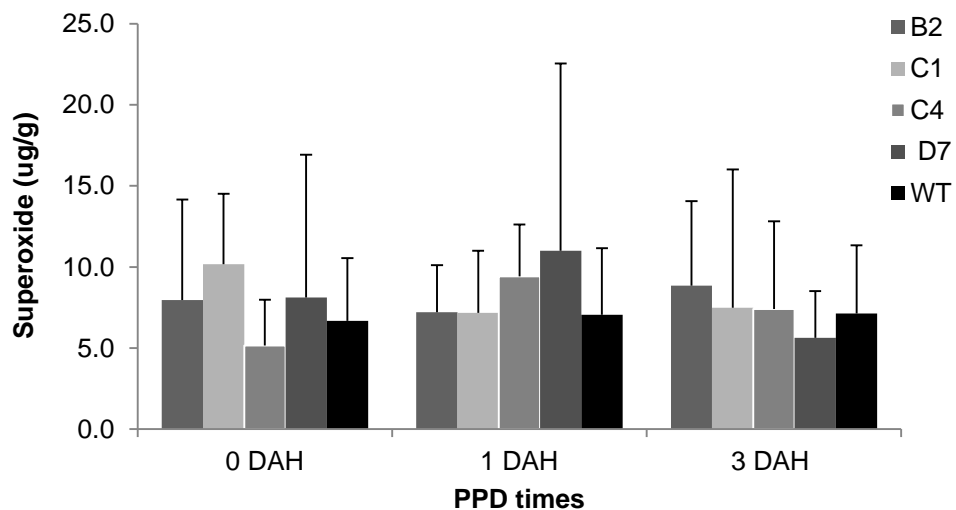
Figure 6.14 O_2^- levels in Pat:SOD roots undergoing PPD. B2 - D7 indicate Pat:SOD transgenics . n = 3, SD shown.

H_2O_2 was quantified according to Section 2.5.12. A standard curve constructed using known amounts of H_2O_2 was used to determine H_2O_2 in the root samples (Figure 6.15).
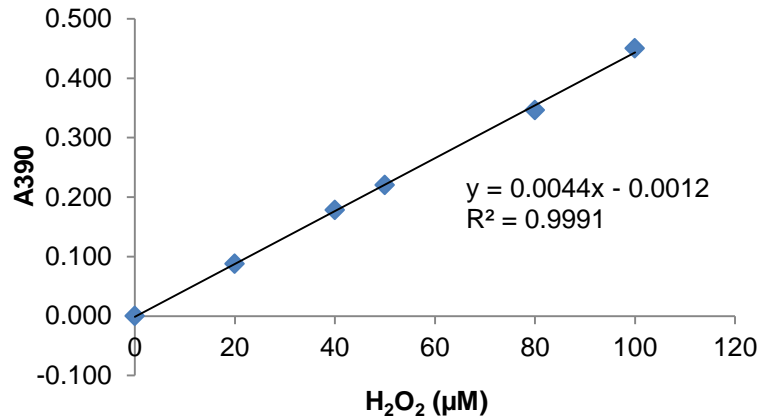
Figure 6.15 Standard curve constructed from H_2O_2 of known concentrations for determination of H_2O_2 in cassava root tissue.
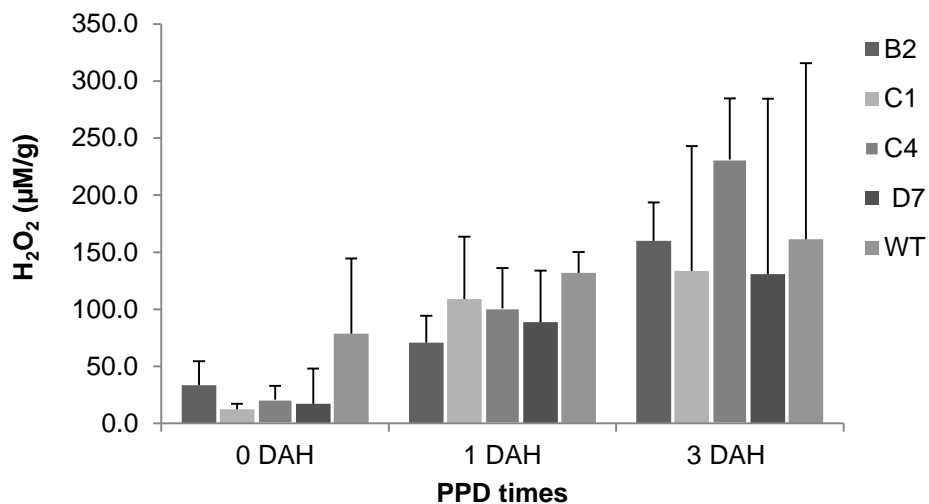
Figure 6.16 H_2O_2 in Pat:SOD roots undergoing PPD. B2 - D7 indicate Pat:SOD transgenics . n = 3, SD shown.

Production of H_2O_2 over PPD time course is shown in Figure 6.16. It suggests that there was general increase of H_2O_2 production in all roots but due to highly variable data this could not be statistically confirmed. Also, it could not statistically be confirmed whether there were any differences in H_2O_2 production between the transgenics and the WT.

To elucidate the pattern of O_2^- and H_2O_2 production in Pat:SOD transgenic roots, a preliminary ROS staining experiment was carried out. The root samples were subjected to NBT and DAB staining to detect O_2^- and H_2O_2 respectively (Section 2.5.9 and 2.5.11). Briefly, for the NBT staining root samples were vacuum-infiltrated with NBT and incubated for 15 minutes. For the DAB staining, root samples were vacuum-infiltrated with DAB and incubated for 3 hours. The results are shown below.
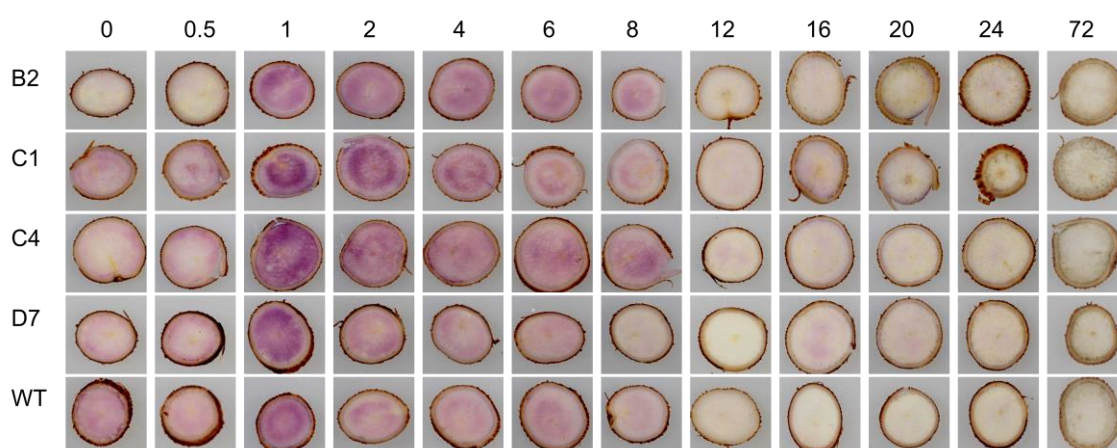
Figure 6.17 *In situ* detection of O_2^- by NBT staining. Formation of purple insoluble product called formazan corresponds to O_2^- liberation. Number indicates time (hour) after wounding/harvest. B2-D7 indicate Pat:SOD transgenics.

O_2^- detection was carried out on a limited number of samples. Because of this, it could not be confirmed if there were clear-cut differences in terms of O_2^- production pattern between the transgenics and the WT. However, this experiment allows a general observation to be drawn. For example, O_2^- was found to be produced within 0 to 15 minutes after wounding, primarily in the storage parenchyma, substantiating the occurrence of a wound-induced oxidative burst by Reilly (2001). After one hour, O_2^- peaked transiently before it decreased to a lower level at 12 hours after wounding. By 24 and 72 hours after wounding, superoxide could no longer be detected in any of the root samples. This result indicates superoxide abundance tended to change within 0 to 12 hours after harvest, so it is sensible to measure it within this time frame. It also explains why this change was not captured in the previous quantitative determination.
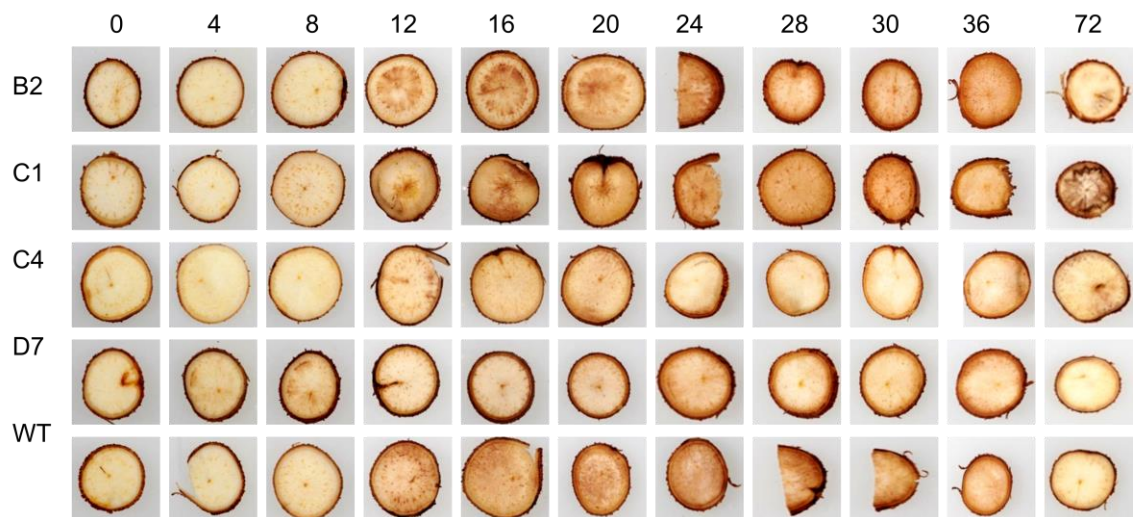
Figure 6.18 *In situ* detection of H_2O_2 by DAB staining. Formation of brown precipitates corresponds to O_2^- liberation. Number indicates time (hour) after wounding/harvest. B2-D7 indicate Pat:SOD transgenics.

Similar to O_2^- detection, H_2O_2 detection was carried out on limited number of samples (Figure 6.18). Therefore, the aim of this experiment was rather to see the general trend in H_2O_2 production than to find the differences in H_2O_2 accumulation between the transgenics and the WT. It is evident that accumulation of H_2O_2 occurred intensely after 12 hours after harvest in the majority of the root samples including the WT particularly in storage parenchyma. H_2O_2 accumulation was noticeable in the first few hours after harvest as found by Reilly (2001) but it is difficult to be categorical about this because of the very mild staining. Generally, H_2O_2 remained in high concentration until 72 hours, although in some roots it may be that some decrease in concentration had taken place. Overall, the data presented, although not conclusive, supports the view that there was increasing H_2O_2 production in cassava roots as measured previously.

6.3.4   Do the Pat:SOD transgenic plants confer tolerance to oxidative stress?

The tolerance to oxidative stress at the plant level was assessed by propagating Pat:SOD plantlets on Cassava Basic Medium (CBM) plate containing H_2O_2. All single-insert independent lines were used for this experiment. After two weeks, photographs of the plates were taken and the average root lengths of three replicates were measured using ImageJ.
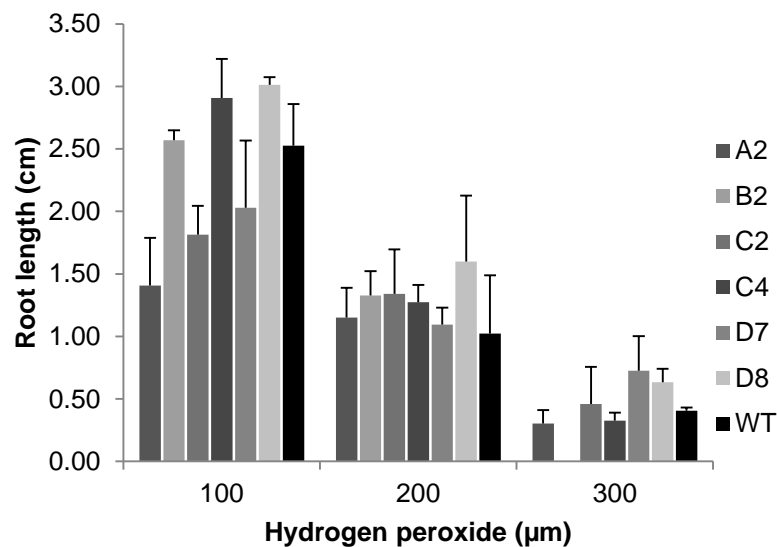
Figure 6.19 Mean root lengths of plantlets grown on various concentration of H_2O_2. A2 – D8 indicate Pat:SOD transgenics. n = 3, SD shown.

In all plant lines, reduction in root length was clear with increasing H_2O_2 concentration (Figure 6.19). In CBM supplied with 100 µm H_2O_2, variable tolerance was exhibited by the transgenics with the transgenic line A2 and B2 growing significantly shorter roots. When the concentration of H_2O_2 was increased to 200 µm, there was a significant reduction of root lengths (t-test, 100 µm vs 200 µm, $p < 0.05$) shown by all lines indicating lack of tolerance to H_2O_2. However, this was not shown by A2 and C2, which may suggest some gain of tolerance in these lines. When the concentration of H_2O_2 was increased to 200 µm, the root lengths was again reduced significantly (t-test, 200 µm vs 300 µm, $p < 0.05$) in all lines except in the WT and D7. Although this may suggest some tolerance, it is unlikely that the tolerance was conferred by the transgene because the WT also responded to the increasing H_2O_2 in the same way. Based on these data, it could be concluded that over-expression of MecSOD2 almost certainly did not confer tolerance to oxidative stress generated by H_2O_2.

6.3.5 Does overexpression of MecSOD2 alter the PPD response?

The Pat:SOD transgenic plants were planted three times, but all were harvested and assayed differently for the PPD assessment. The first batch was assayed with PPD Assay 1, which has been criticised for not producing uniform PPD symptoms suitable for scoring, while the second batch was assayed with PPD Assay 2, which caused the roots to be severely dehydrated. Despite of the weaknesses of the assays, examination of the roots could provide some insights as to whether MecSOD2 affects PPD.
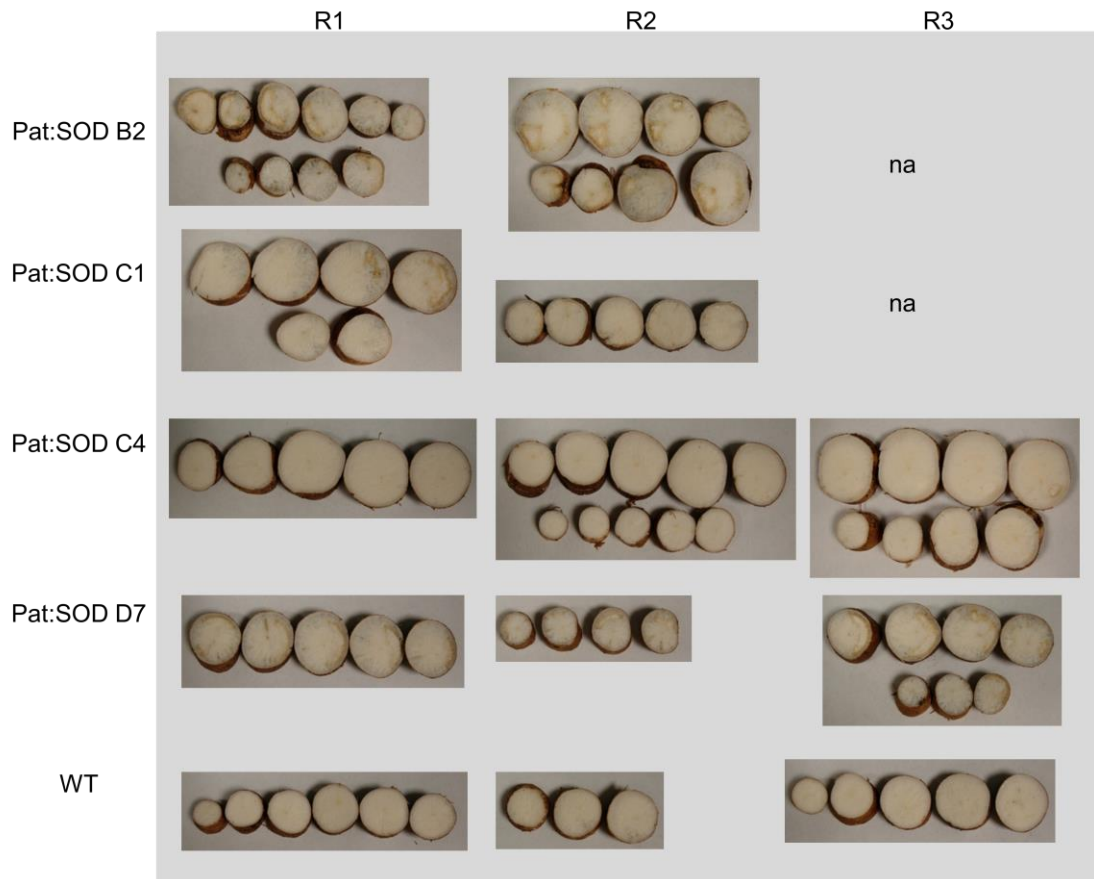
Figure 6.20 Pat:SOD root samples assessed for PPD using PPD Assay 1. In this assay, the roots were left to deteriorate intact at 25-27°C. Prior to photographing the roots were cut to 2cm thickness to reveal PPD symptoms. na = not available

In PPD Assay 1, cassava roots were let to deteriorate intact. Figure 6.20 shows the root samples at 3 DAH. It is apparent that the transgenics, except C4, had developed visible PPD symptoms at this time-point while the WT had not. The most affected line was B2, followed by D7 and C1.
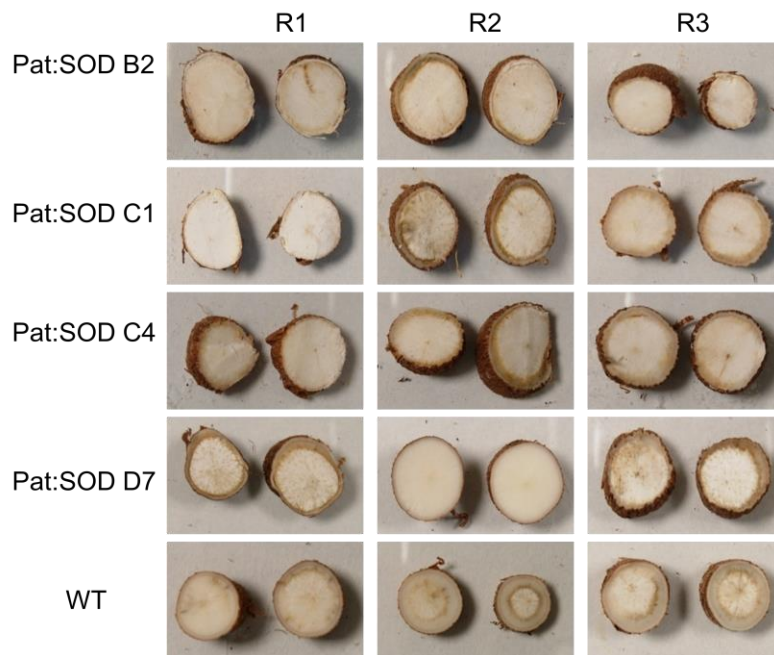
Figure 6.21 Pat:SOD root samples assessed for PPD using PPD Assay 2 at 3 DAH. In this assay the, two root sections of 2 cm thickness were incubated at 25-27°C.

The second batch of Pat:SOD roots was assayed with PPD Assay 2 in which the roots were cut into 2 cm sections. In this assay, generally most of the roots turn dry and chalky (Figure 6.21). Even so, it should be noticed that the WT samples appeared more deteriorated in this assay compared to those in Assay 1 and this might be due to the nature of the Assay 2 that accelerates PPD. Meanwhile, B2 root sample which showed apparent PPD symptoms in PPD Assay 1 now did not seemed deteriorated.

Only in the third planting were the roots assayed with PPD Assay 4, which was the most reliable method so far. Therefore, data from this were used to evaluate PPD in Pat:SOD transgenics. Deterioration was most prominent at 4 DAH, thus greyness scores at this time point were calculated and normalised to greyness scores at 0 DAH to get PPD scores of the root samples. Basically, high PPD scores indicate highly visible deterioration symptoms and vice versa. The root pictures are shown in Figure 6.22 and the PPD scores are as in Table 6.2.
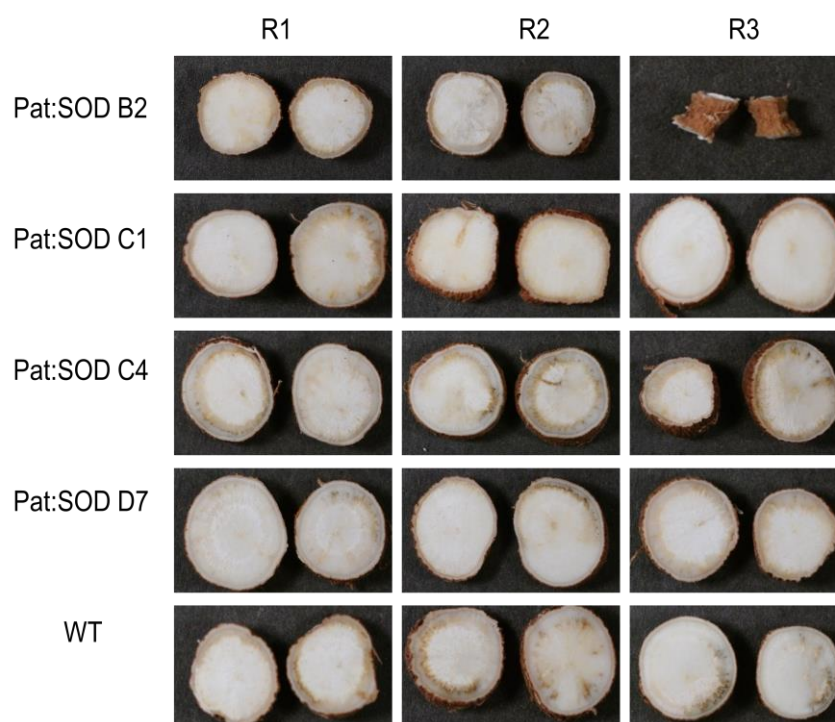
Figure 6.22 PPD Assay 4 of Pat:SOD roots harvested from six months plants. The roots were photographed at fixed camera settings and scored for PPD using PPD Symptom Score software. Pat:C1 R3 was not assessed for PPD because due to small size.

Table 6.2 Individual and mean PPD scores of deteriorated cassava root samples four days after harvest (4 DAH). The scores were obtained by taking percentage difference of greyness score of root samples at 4 DAH and the greyness scores during harvest (0 DAH).

Plant line	Mean score ± SD (max,min)	t-test
Pat:SOD B2	42.5 ± 11.6 (51.4 / 29.3)	p = 0.47
Pat:SOD C1	48.9 ± 1.4 (49.8/47.9)	p = 1.00
Pat:SOD C4	50.4 ± 4.0 (53.2. / 45.9)	p = 0.77
Pat:SOD D7	40.7 ± 13.6 (50.4/ 25.1)	p = 0.30
WT	48.9 ± 7.7 (55.9 / 40.7)	-

A general observation was that some of the root samples deteriorated at different rates compared to those observed with the two other assay methods, but this may be due to the unreliable and unsatisfactory nature of those methods. For example, B2 and D7 assayed with PPD Assay 1 were more severely deteriorated than was the case with PPD Assay 4. On the other hand, C4 and the WT, which were the least deteriorated samples with Assay 1, now showed considerable PPD symptoms.

Scoring of PPD symptoms was done using PPD Symptom Score software. In this assay, B2 and D7 had lower PPD scores than the WT suggesting some tolerance to PPD, while C4 had a higher score than the WT suggesting weaker tolerance to PPD. However, this might not be correct because the scores in these samples were substantially reduced because one of the root sample replicates had PPD score about two times less than other replicates. Also, statistical analysis proved no significant differences in PPD resistance between the transgenics and the WT (WT vs all transgenics, t-test > 0.05). It is difficult to draw categorical conclusions from variable data derived from a small number of replicates; therefore, based on the data presented here, it can be concluded that overexpression with MecSOD2 did not alter tolerance to PPD.

6.3.6 Summary (Pat:SOD)

In summary, over-expression of MecSOD2 in cassava roots was successful where up to 5.3-fold more transcriptional level was achieved. However, the increase of transcriptional level occurred mostly from 24 hours, which is after the initial post-harvest burst of O_2^- was detected. Additionally, the increase of SOD enzyme activities was only achieved at 72 hours after harvest. While it was too late to prevent oxidative burst, the mechanism to detoxify harmful H_2O_2 was not activated causing it to accumulate in the root tissue. Collectively, the data gathered here explain why overexpression with MecSOD did not contribute tolerance to oxidative stress as well as to PPD.

6.4 Results - AtGCS

Transformation of cassava with AtGCS gene generated ten single-insert lines. Sequence analysis revealed that the gene was driven by the Patatin promoter, retained the correct length, and thus was expected to be functional. Phenotypic analysis of these lines found significant differences in some of the transgenic lines. Four lines (Pat:GCS C5, C6, C11 and C16) were significantly taller than the WT while one line (C19) was significantly shorter. The transformation with AtGCS also changed the performance of the plants in terms of yield. Four lines, including those that were significantly taller than the WT plant, produced lower yields than the WT plants. The lines were C5, C6, C16 and C19.

6.4.1 Cassava harbouring the pDEST:AtGCS cassette over-express the transgene in root tissue

Five single-insert lines were randomly selected for qPCR experiment. The extraction and quantification of RNA were carried out using the same methods used in Pat:SOD.

6.4.1.1 Validation of target gene and reference gene primers for qPCR

The AtGCS gene is foreign to cassava genome. Therefore, designing primers to amplify the AtGCS cDNA is straightforward. A forward primer flanking AtGCS sequence and a reverse primer flanking attB2 sequence was designed to amplify approximately 135 bp PCR product.

Figure 6.23 Primers designed for qPCR of AGCS gene. The position of attB2 sequence is shown.

To check the primer specificities, a BLAST search against cassava genome and a similarity search with T-DNA of pDEST:AtGCS were performed, and no similar sequences were found. The specificity of the primer pair was confirmed by conventional PCR using *Taq* polymerase.
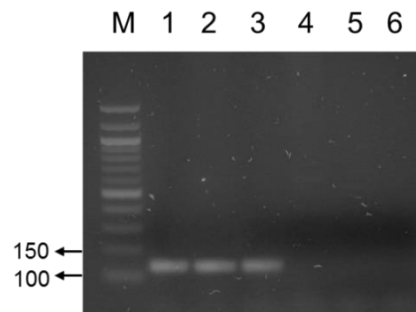
Figure 6.24 PCR of various DNA templates using primers GCStf and GCStr with Taq polymerase. Amplification from plasmid, genomic and cDNA derived from transgenic plants produced 135 bp PCR products. M = DNA marker, 1 = positive control (pDEST:GCS plasmid), 2 = transgenic genomic DNA, 3 = transgenic cDNA, 4 = WT DNA, 5 = WT cDNA, 6 = negative control (water).

Amplification with Pat:GCS cDNA produced a single PCR product of the correct size, as confirmed by the positive control (plasmid). A similar PCR product was also obtained from Pat:GCS genomic DNA. The absence of additional PCR products confirmed that other target sequences for the primers did not exist in cassava genome. This was validated by amplification of both the genomic DNA and cDNA of WT plants, which produced no PCR product (Figure 6.24). For a more rigorous verification, the PCR product was sequenced and it confirmed that it was the expected fragment (data not shown).

6.4.1.2 Melting curve analysis

As mentioned previously, melting curve analysis is essential in qPCR using SYBR-green in order to verify whether the amplification signals produced are the result of a single PCR product or from primer dimers. Primer dimer formation must be avoided because it also generates a signal that gives a false result.
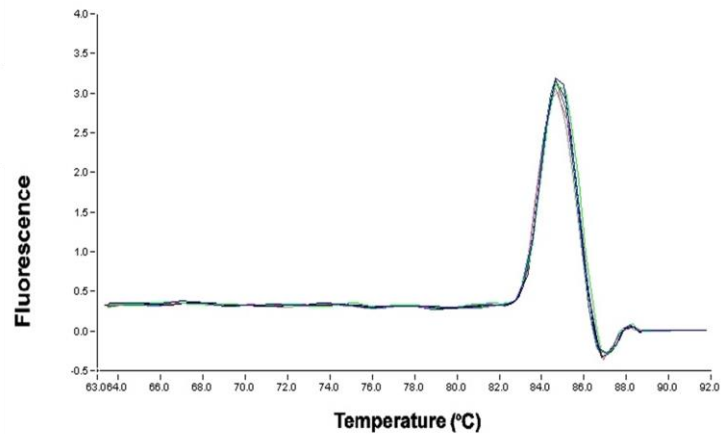
Figure 6.25 Fluorescence peak produced from amplification of Pat:GCS DNA with primers GCStf/GCStr. A single peak indicates specificity of the primers and absence of primer dimers.

The fluorescence profile generated from qPCR with Pat:GCS cDNA produced a single peak indicating high specificity of the primers. No primer dimer peak was detected. The melting curve analysis for reference gene primers 18s was shown earlier and it had also confirmed specific (Figure 6.25).

6.4.1.3 Determination of amplification efficiencies of target and reference gene

Amplification efficiency (AE) tends to vary between primers and materials; therefore, it is essential to take it into account when determining fold expression. Five cDNA dilutions prepared from Pat:GCS roots harvested at 0, 1 and 3 DAH were used as template in qPCR reaction with GCStf and GCStr primers (Figure 6.26) and 18s For/18s Rev. The CT values obtained from the reactions were plotted against the diluted cDNAs to construct a standard curve. The slope of the standard curve was used for calculating the AE for each material.
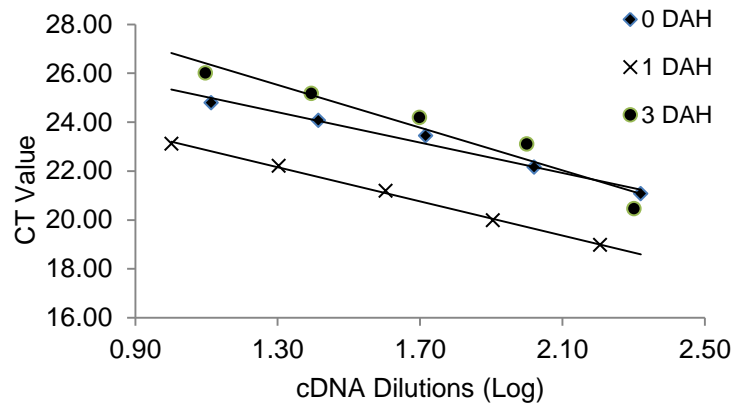
Figure 6.26 Standard curve analysis of real-time PCR amplification. Dilutions of transgenic-derived cDNA amplified with GCStf and GCStr primers. 0 DAH; y= -3.101x + 28.43 (R^2 = 0.980), 1 DAH; y = -3.491x + 26.69 (R^2 = 0.997), 3 DAH; y= -4.372x + 31.21 (R^2 = 0.934).
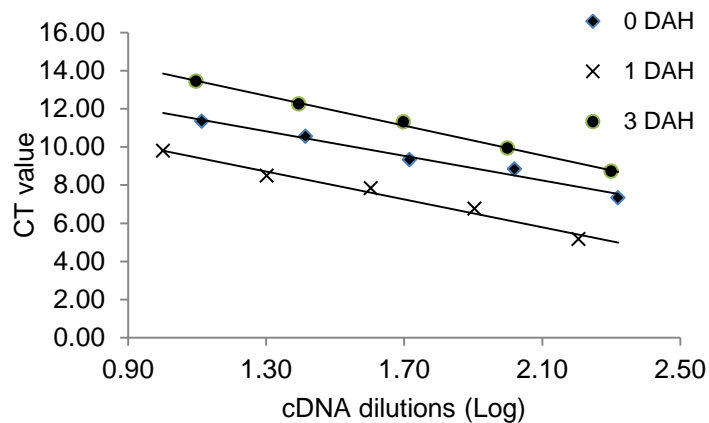
Figure 6.27 Standard curve analysis of real-time PCR amplification. Dilutions of transgenic-derived cDNA amplified with 18s For and 18s Rev primers. 0 DAH; y = -3.222x + 15.01 (R^2 = 0.979), 1 DAH; y = -3.656x + 13.46 (R^2 = 0.981), 3 DAH; y = -3.903x + 17.75 (R^2 = 0.997).

Table 6.3 Amplification efficiencies of Pat:GCS roots harvested at 0, 1 and 3 DAH.

	Reference gene		Target genes	
Materials	Slope	EA (%)	Slope	EA(%)
0 DAH	-3.222	104.3	-3.101	110
1 DAH	-3.656	87.7	-3.491	93
3 DAH	-3.903	80.4	-4.372	70

The recommended AE is close to 100% (90-110%) (Taylor et al., 2010). In both reference and target genes, high AEs were achieved with fresh materials but these were reduced by 10 to 20% in aged materials. The disparity in amplification efficiency might arise from an unavoidable consequence of the PPD process itself, which is the release of polyphenols and their oxidation. Despite applying the best RNA extraction method to get the highest quality RNA possible the presence of these unwanted compounds in RNA and cDNA preparations could disrupt the qPCR process itself, such as during the release of the SYBR green signal. Indeed, this highlights the need to determine amplification efficiency for each type of material.

6.4.1.4 At:GCS profile in deteriorating cassava roots

All independent single-insert lines were grown to mature plants (six months) but only roots from those with sufficient biological replicates were harvested and analysed. The roots were assayed for PPD with Assay 3 and were collected at 0, 1 and 3 DAH. RNA was extracted from the root samples and used for cDNA synthesis which later served as templates in qPCR.
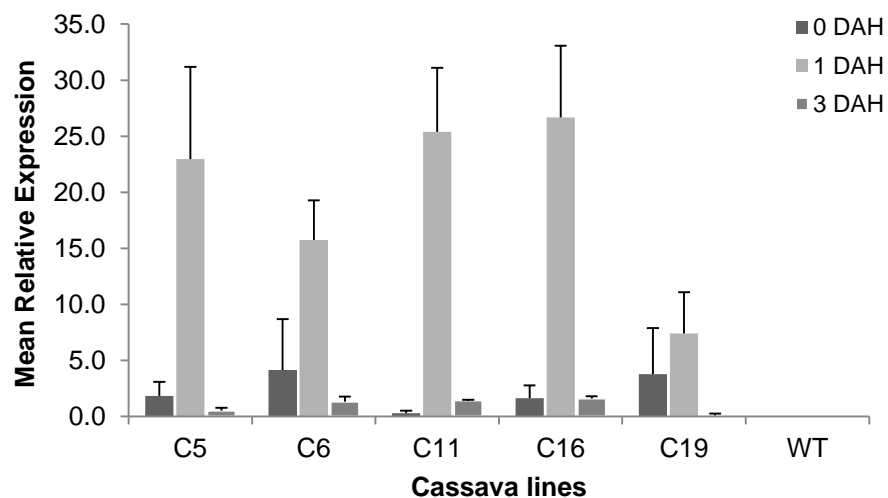
Figure 6.28   AtGCS transcriptional level relative to 18s transcriptional level during PPD. The transcriptional levels of each root samples are shown.

The transcriptional level of AtGCS was measured as the relative abundance of AtGCS gene to 18s gene. Since the primers would not work in the WT, because target sites for them are not present in the cassava genome, normalisation to WT transcriptional level could not be done. Figure 6.28 shows transcriptional level of AtGCS during the PPD time-course.

The mean relative expression between 0.3 to 4.1 was achieved in the Pat:GCS roots indicating transgene expression, with C6 having the highest fold increase than other transgenics. After 24 hours, the AtGCS transgene was very actively transcribed in the Pat:GCS roots where more than 20-fold increase were achieved in C5, C11 and C16. A lower level of 15- and 7-fold increase was achieved by C6 and C19 respectively but the increases were significant (t-test, 0 DAH vs 1 DAH, $p < 0.05$) except in C19. Nevertheless, the transcriptional level appears to be transient as it decreased significantly (t-test, 1 DAH vs 3 DAH $p < 0.05$) to mean relative expression between 0.1 to 1.6-fold. The clear-cut pattern of expression shown by AtGCS is exciting as it may indicate the novel response of the Patatin promoter which could not be determined using Gus gene. However, more importantly, it must be determined whether this pattern of expression altered the anti-oxidant status of the transgenic.

6.4.2 Does the increase in Pat:GCS expression increase the anti-oxidant status of cassava roots?

Due to the difficulty in obtaining meaningful data from the measurement of separate oxidative stress components as was found with the Pat:SOD samples, the effects of AtGCS transformation was evaluated based on overall anti-oxidant capacity of the transgenic roots. The anti-oxidant status of Pat:GCS plants were measured using the Oxygen Radical Absorbance Capacity (ORAC) assay (Section 2.5.8).

The ORAC assay is widely used in measuring the anti-oxidant capacity of biomolecules from a variety of samples. In this assay, the anti-oxidant capacity is expressed as Trolox equivalents, which measure the amount of anti-oxidant required to scavenge the free-radical diphenylpicrylhydrazyl (DPPH•) determined from area under curve (AUC). Trolox (6-hydroxy-2,5,7,8-tetramethylchroman-2-carboxylic acid) is a water-soluble analogue of α-tocopherol.
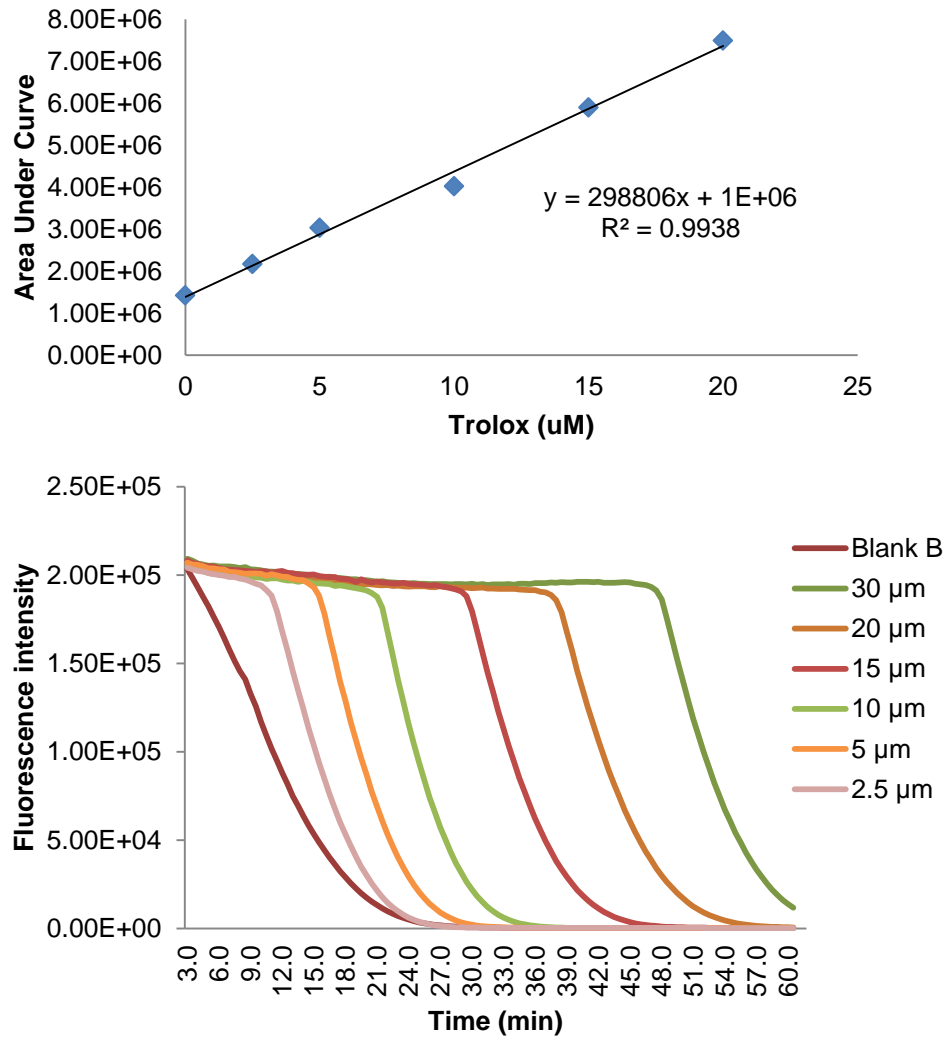
Figure 6.29 Trolox standard curve for the ORAC assay (upper panel). Typical fluorescence profile of trolox standard and blank (bottom panel). The ORAC activity of a sample is calculated by subtracting the area under the blank curve from the area under the sample curve to obtain the net area under the curve (Net AUC).
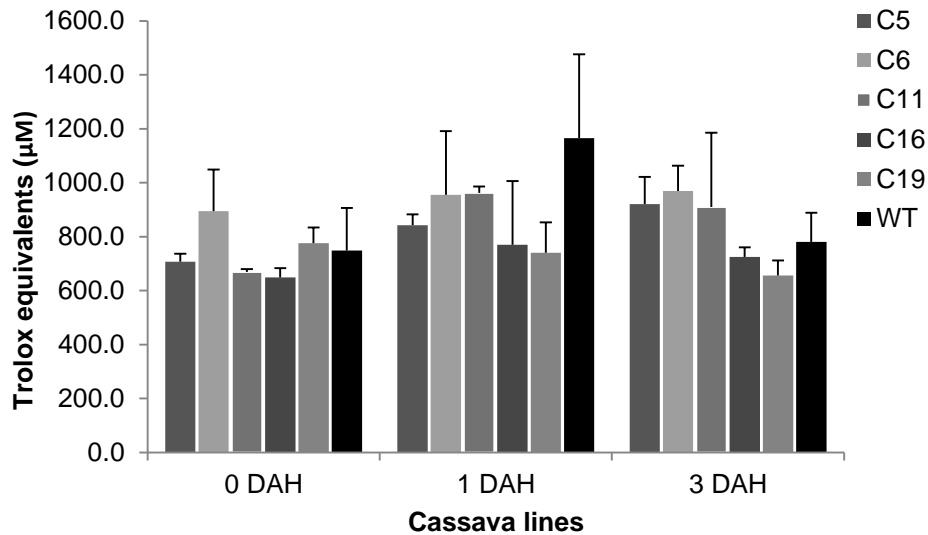
Figure 6.30 Comparative antioxidative capacity of Pat:GCS roots with the WT measured with ORAC assay. Measurement was taken at different PPD times from roots assayed with PPD Assay 3. n = 3, SD shown.

The anti-oxidant capacities of Pat:GCS roots were compared to those of WT to assess the behaviour of the AtGCS gene in cassava roots (Figure 6.30). In freshly harvested roots, the majority of Pat:GCS lines were found to have lower anti-oxidant capacities than the WT except in C6 and C19 which showed slightly, but non-significant, higher anti-oxidant capacities. After being harvested for 24 hours, though not significantly (t-test, 0 DAH vs 1 DAH, $p > 0.05$), the anti-oxidant capacities of the Pat:GCS roots increased slightly except for C19. The low anti-oxidant capacity shown by C10 corresponds to the low AtGCS transcriptional level but it must be noted that higher anti-oxidant capacities were shown by the WT roots at this time point despite not expressing the target gene AtGCS. Subsequently, there was a clear reduction in anti-oxidant activities shown by the WT from 1 to 3 DAH but no apparent changes of anti-oxidant capacities shown by the transgenic lines.

Based on the data presented here, it is clear that the expression of AtGCS did not contribute to the anti-oxidant capacity of the cassava roots. Despite being highly expressed, especially at 1 DAH, there was no significant increase in antioxidative capacity. This data indicate two possibilities. 1) The overexpression of AtGCS did not increase GSH/GSSG content significantly to cause a high anti-oxidant capacity 2) GSH/GSSG content itself did not contribute to better antioxidative capacities.

6.4.3 Do Pat:GCS transgenic plants confer tolerance to oxidative stress?

To test the tolerance to oxidative stress at the plant level, the plants were grown on Cassava Basic Medium (CBM) with added H_2O_2 at 100, 200 add 300 µM. After two weeks growth photographs of the plates were taken and the average root lengths of three replicates were measured using ImageJ. Since this did not require growth in the greenhouse, all single-insert independent lines were used.
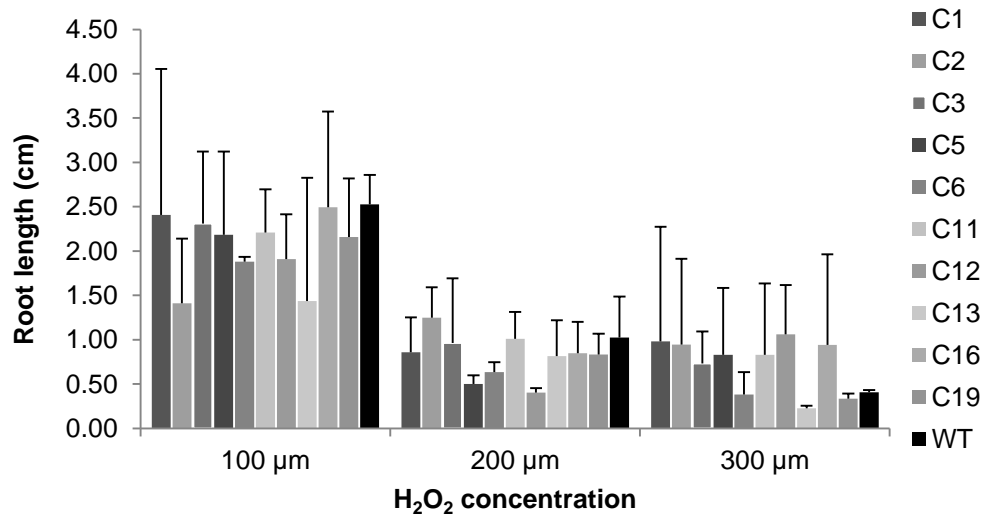
Figure 6.31   Pat:GCS roots measured following two weeks sub-culturing in H_2O_2-containing plates. The plantlets were grown in a growth room under the same conditions as normally grown plantlet libraries. n = 3, SD shown.

The result is shown in Figure 6.31. In general, the lengths of the roots decreased with H_2O_2 concentration. At 100 µM, nearly all plantlets produced highly variable data, so no significant difference between the lengths of the roots in transgenics and the WT measured at this concentration could be detected. When the H_2O_2 concentration was increased to 200 µM, the root lengths were reduced significantly (t-test, p <0.05) in the WT and most transgenic lines, except in C1, C2, C3 and C13. Interestingly, when the concentration was increased to 300 µM no significant reductions in root length were measured in all lines which also may suggest tolerance to high oxidative stress. However, since this was also observed in the WT, it is unlikely that the tolerance was conferred by the transgene. Moreover, there was no significant difference in the root length of the WT and the transgenics at this concentration although it might appear that the transgenics had greater root length. Based on the data gathered, it can be concluded that some degree of tolerance might be gained by a number transgenics such as C1, C2, C3 and C13 when exposed to medium H_2O_2-mediated oxidative stress.

6.4.4   Do the Pat:GCS transgenic plants develop tolerance to pH?

The effects of pH on glutathione has been shown previously (Ikebuchi et al., 1993) where acidic conditions was found to reduce GSH content and impair the glutathione redox cycle. To test this, *in vitro* plantlets of Pat:GCS plants were grown in CBM adjusted to pH 3.8, 5.8 and 7.8. Similar to the H_2O_2 test, above, the photographs of the plates were taken after two weeks and the average root lengths of three replicates were measured using ImageJ. The result is presented in Figure 6.32.
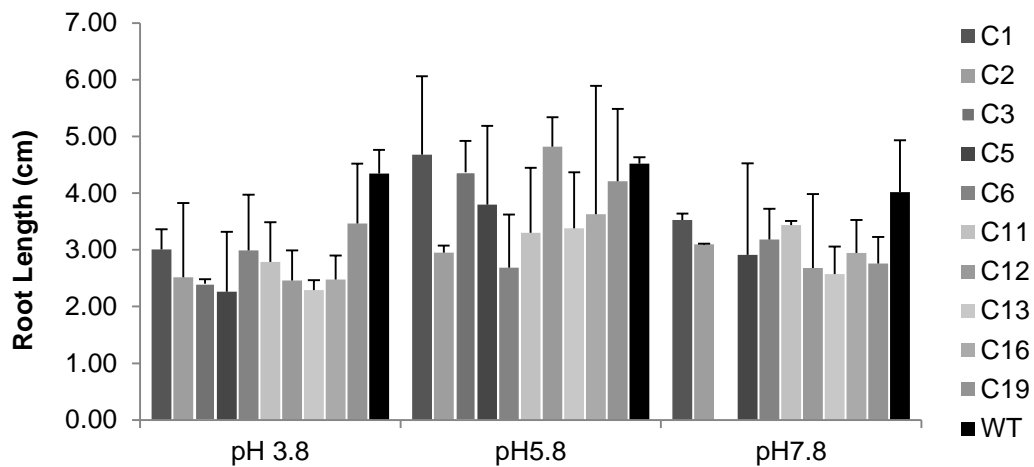
Figure 6.32   The response of Pat:GCS roots grown on CBM plates adjusted at various pHs. The plantlets were grown in growth room under the condition of normally grown plantlet libraries. C3 was not tested at pH 7.8 due to loss of plants. n=3, SD shown

Cassava plantlets are normally propagated on CBM medium at pH 5.8. There was no significant difference in the length of roots produced by the transgenics and the WT at this pH except in the case of C2, which was shorter (t-test, C2 vs. WT p <0.05). Lowering the pH to 3.8 seemed not to affect the root formation in these plants except in transgenic line C3, C11 and C12 which were reduced significantly (t-test, pH 3.8 vs pH 5.8, p<0.05). However, at this pH nearly all transgenics except C2 and C19 produced significantly shorter root lengths compared to the WT (t-test, WT vs transgenics, p <0.05). Although not conclusive, this might relate to the impairment of the glutathione redox cycle in the transgenics because cassava normally is tolerant to acidic pH. However, increasing the pH to 7.8 did not significantly affect the formation of roots in both the transgenics and the WT (t-test, pH 5.8 vs pH 7.8, p>0.05), although they may appear to be reduced at certain extent. Also there was no significant difference

between the lengths of roots formed by the transgenics and the WT at this pH. Overall, it can be concluded that expression of AtGCS did not enhance tolerance to pH change but it suggested that the transgenics plants are not suitable to acidic soil.

6.4.5   Does overexpression of AtGCS alter the response towards PPD?

The Pat:GCS plants were planted and harvested twice. The first batch of planting was assayed with PPD Assay 2 while the second was assayed with PPD Assay 3 (Section 4.3.2 & 4.3.3). PPD Assay 2 caused root samples at later PPD stages to become severely dehydrated, which prevented any biochemical activities from the samples from being evaluated reliably. On the other hand, PPD Assay 3 failed to produce PPD symptoms for valid comparison. Due to time constraints it was not possible to grow another batch of Pat:GCS and assay it with PPD Assay 4. While the data presented here were generated from analysis of roots assayed with PPD Assay 3 the symptoms showed by the roots in PPD assay 2, though with low certainties due to highly variable symptoms between replicates, might be useful to qualitatively assess the symptoms between WT and the transgenics.
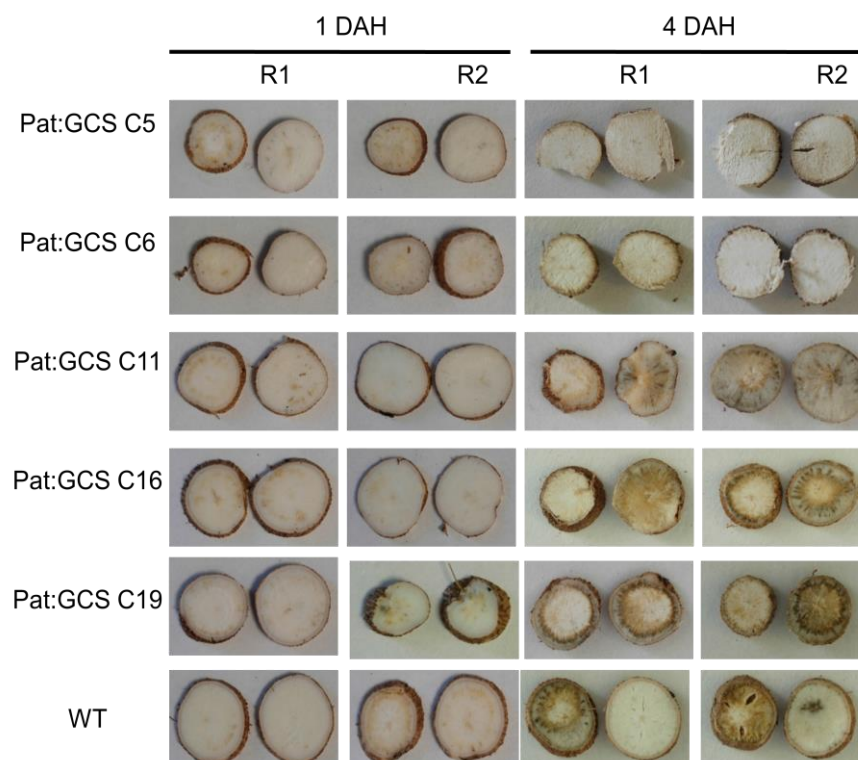
Figure 6.33   PPD Assay 2 of Pat:GCS roots. Two root samples representing each line are shown. Samples were collected from different plants and only photographs at 1 and 4 DAH were assessed.

In this assay at least two roots from separate plant replicates were used. The pictures of the roots were taken with automatic setting so computer scoring might not be valid. Instead, visual scoring was applied. Since PPD symptoms developed after one day after harvest, the pictures taken at this time-point were used for assessment. Attention was drawn to the 'high-expression' lines such as C5, C11 and C16.

Assessment at 4 DAH was done by excluding the C5 and C6 root samples because they were severely dehydrated. Figure 6.33 shows no apparent differences in the PPD symptoms shown by the rest of the transgenic roots, including the high-expression line, at this time-point. Observation of PPD symptoms was also done on root samples at 1 DAH, which is assumed to be more appropriate because dehydration had not taken place, but PPD symptoms had not developed at this early time, so detecting differences between the high- and low-expression lines among the transgenics and the WT root samples was unlikely. Essentially, a precise conclusion is not possible using these limited data, but they suggest that overexpression of AtGCS in cassava roots had no effect on PPD symptoms.

6.4.6   Putative GCS sequence in cassava

There is no information on the role of GSH in cassava PPD. Its biosynthesis in cassava has also not been studied. However, a BLAST search with AtGCS (*gshl*) used in this study found a putative GCS sequence homolog in cassava genome database (Phytozome).
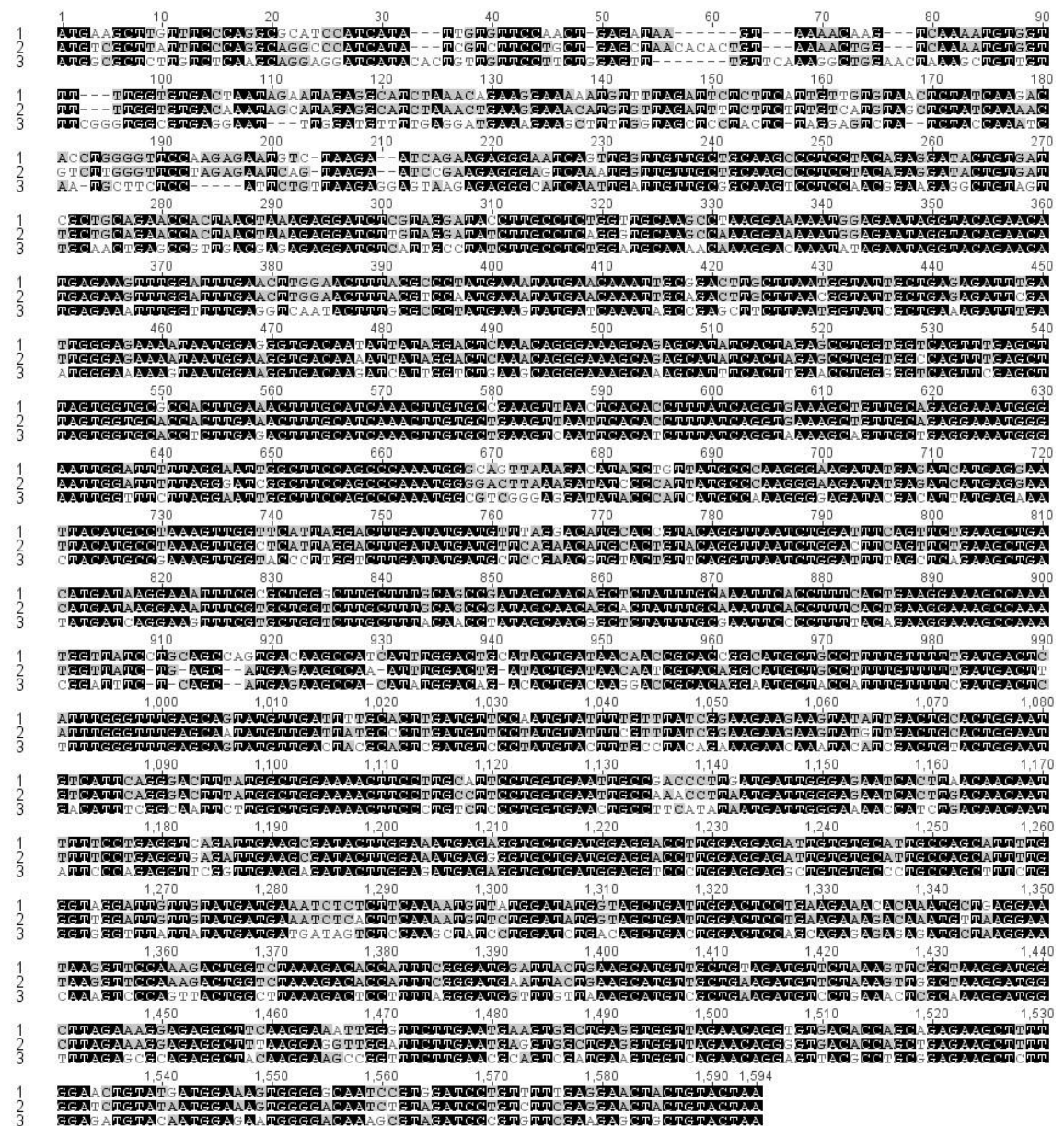
Figure 6.34 Nucleotide sequence alignment of 1: putative cassava GCS coding sequence (Phytozome accession: cassava4.1_005513m), 2: *Hevea brasiliensis* GCS coding sequence (Genbank accession: GU997638) and 3: *Arabidopsis* GCS coding sequence, *gshl* (Genbank accession: AF419576).

The sequence is 1572 bp and found to have 92% identity with *Hevea brasiliensis* (GU997638), a species close to cassava. Less percentage similarity was found with the *Arabidopsis* sequence. Nucleotide sequence alignment of these sequences found more divergence in the 5'-end rather than 3'-end (Figure 6.36). Identification of this sequence will facilitate the isolation of this gene and its role in defining the GSH anti-oxidant properties in cassava PPD.

6.5   Results – MecAPX3

Transformation with MecAPX3 produced seven independent single-insert lines. Sequencing revealed that Patatin and MecAPX3 coding sequence is integrated in the genome of Pat:APX plants.

6.5.1   Does MecAPX3 cause changes in APX activity?

Pat:APX roots were harvested from 6 months old plants and APX enzyme activity over the PPD time-course was measured according Section 2.4.4.The result is presented below.
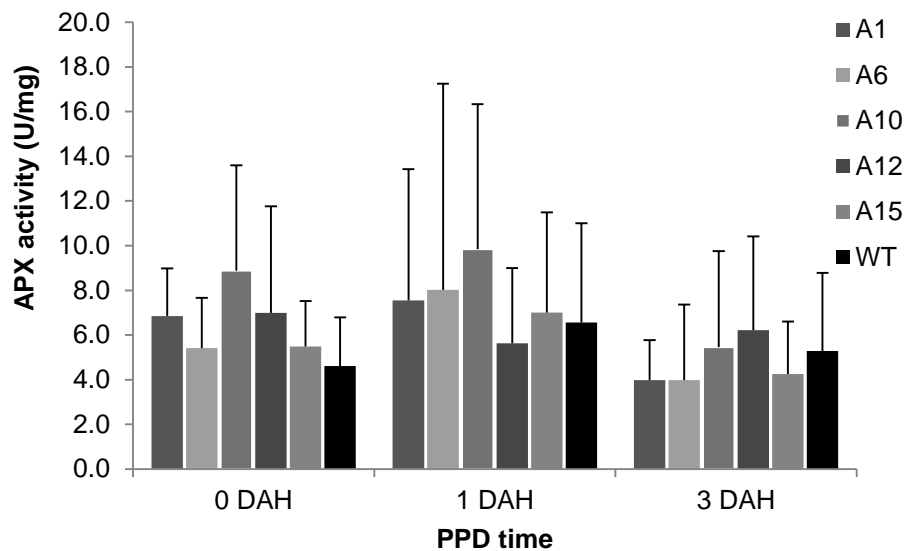
Figure 6.35 APX activities of transgenic lines following harvest. The activities were measured from root samples obtained from single-insert independent lines. n = 3, SD shown.

A general observation on the data presented in Figure 6.35 was that APX enzyme activities over the PPD time course did not appear to change. As with the expression levels, the APX enzyme activities were also variable. At 0 DAH, although the APX enzyme activity in the transgenics appear higher than those in the WT, this was not significant by statistical analysis. While the expression data for roots sampled at 1 and 3 DAH were not available, the enzyme activities at these time points showed that they were equally varied as the 0 DAH enzyme activities. Importantly, measurement of APX enzyme activities in the transgenic roots at all time points found that activities in these roots resemble those measured in the WT which were constant during the course of

deterioration. Therefore, it can be concluded that MecAPX3 did not increase APX activities at any PPD time point.

6.5.2   Do the Pat:APX transgenic plants confer tolerance to oxidative stress?

The tolerance to oxidative stress at the plant level was assessed by propagating Pat:APX plantlets on Cassava Basic Medium (CBM) plate containing H_2O_2. After two weeks, the photographs of the plates were taken and the average root lengths of three replicates were measured using ImageJ. Six single-insert independent lines were used for this experiment. The result of the experiment is presented in Figure 6.36.
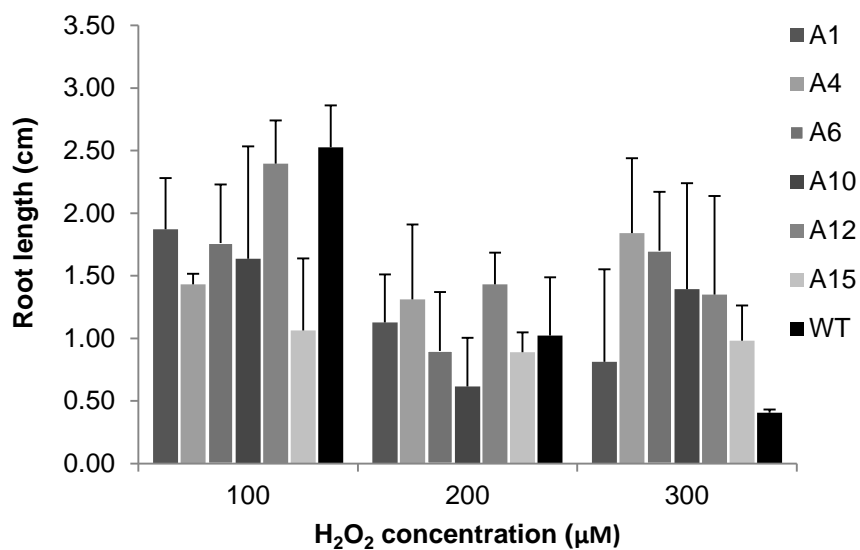
Figure 6.36 Average length of fibrous root measured from *in vitro* plants grown in CBM plate containing various concentration of H_2O_2. n = 3, SD shown.

Measurement of root length showed all transgenics produced shorter root lengths compared to the WT indicating weaker tolerance to H_2O_2 at 100 μM. However, due to highly variable data this was only statistically valid for A4, A6 and A15 (t-test, transgenics vs WT, p <0.05). Increasing the H_2O_2 concentration to 200 μM caused significant reduction in the root length of the WT, A6 and A12 (t-test, 100 μM vs 200 μM, p <0.05) but not in the rest of the transgenic lines. This result may suggest that a degree of tolerance was exhibited by the transgenics at this concentration. Moreover, when the concentration was increased to 300 μM, it is shown the transgenics produced greater lengths of roots while the WT produced shorter roots. While this may indicate high tolerance of the transgenics at high H_2O_2 concentration, statistically, there was no significant change of root length occurred either in the transgenic or the WT. Therefore,

it can be concluded that overexpression of MecAPX3 did not confer tolerance to H_2O_2-mediated oxidative stress.

6.5.3 Does the APX enzyme activity alter the PPD response?

Pat:APX plants were harvested at six months old and the roots were sampled at 0, 1 and 3 DAH. The roots were assayed with PPD Assay 1 in which they were allowed to deteriorate intact. Although it did not allow accurate scoring of PPD symptoms the representative roots for each line are shown here in Figure 6.37.
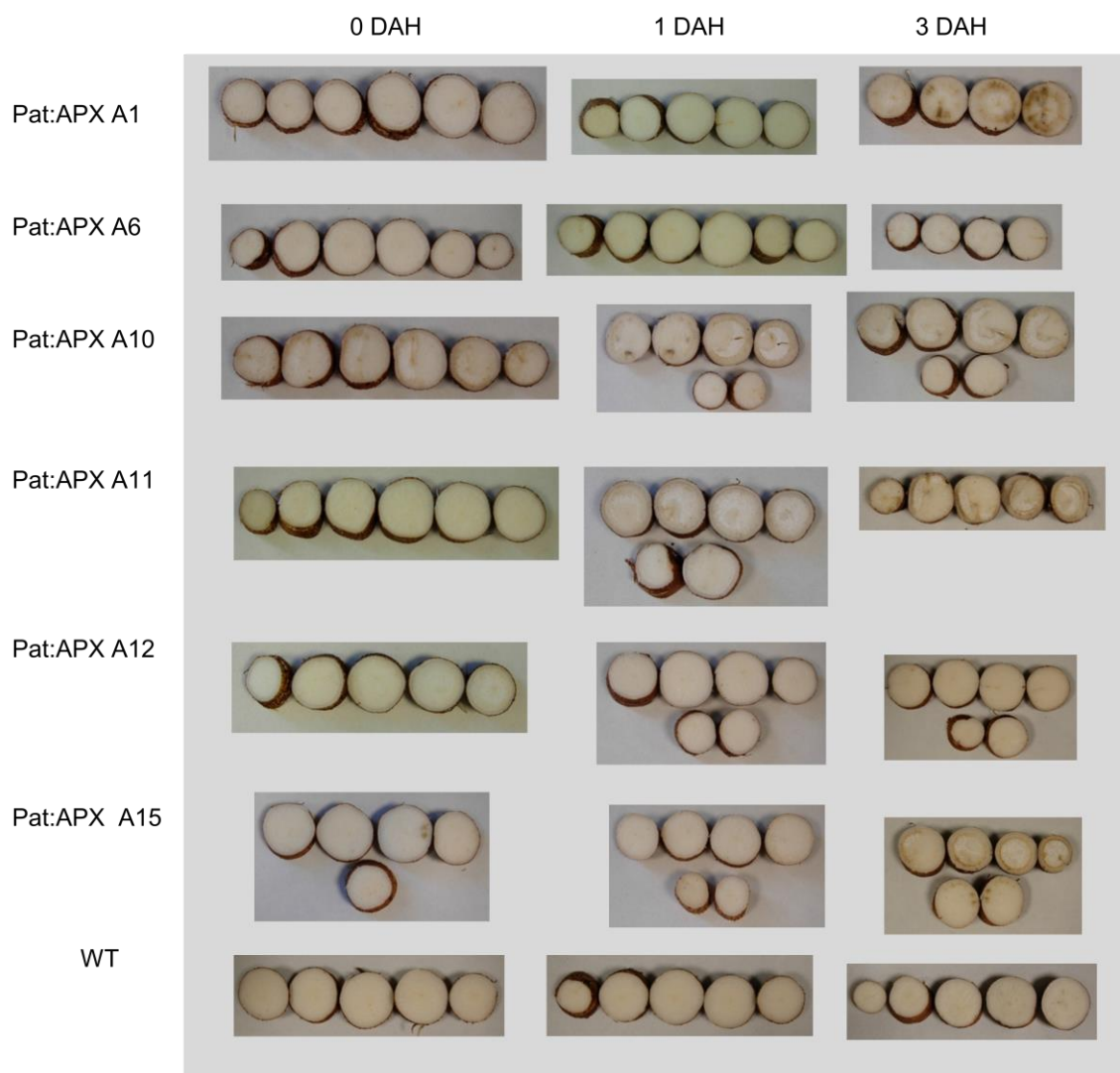
Figure 6.37 Representatives of Pat:SOD roots following harvest. The roots were assayed with PPD Assay 1 (Section 4.3.1).

In general, the roots lacked PPD symptoms at 0 and 1 DAH. PPD symptoms became visible at 3 DAH in most transgenic roots but no symptoms were shown by the WT roots. Interestingly the root samples from line A10 showed PPD symptoms on the day of harvest as indicated by brown staining. It was very unlikely for the roots to develop the symptoms immediately after harvesting of just before harvesting. Close examination suggests the symptoms were not the typical PPD symptoms. Instead, these plants probably were over-watered during their growth (J. Watling, *pers. comm.).*

6.5.4   Summary (Pat:APX)

In conclusion, the transformation with MecAPX3 did not cause tolerance to oxidative stress. It also did not successfully increase APX activities within the PPD assay period tested here, so the effects of APX activities could not be examined. It would be interesting to extend the assay to later PPD times, but were APX activities to increase they would probably be too late to delay or prevent PPD.

6.6   Results-FaGAR

Transformation with FaGAR had generated nine independent single-insert lines. The analysis of the phenotypes of Pat:GAR transgenic plants showed no significant differences in terms of the growth of the plant and yield except two lines (B29 and B33) that produced significantly lower yields of storage roots.

6.6.1   PPD assessment of Pat:GAR roots

The weakness of the existing PPD assay method and the limitation of its application with the greenhouse-grown materials have been identified and discussed thoroughly in Chapter 4. Finally, PPD Assay 4 that efficiently measured PPD within a convenient timeframe was established. Using this assay method, the cassava roots undergoing PPD developed typical symptoms of PPD such as vascular streaking and browning without drying the roots excessively. The transgenic groups that was fortunately assayed with this method include Pat:GAR. Here, the use of this method to measure PPD is demonstrated.

The effects of cassava transformation with Pat:GAR to PPD in roots were assessed based on the PPD scores which were calculated using the equation below

PPD score = ((Mean Greyness Score **Y** DAH – Mean Greyness Score at 0 DAH)/ Mean Greyness Score at **Y** DAH)) x 100%

Y = the time-point PPD scores intended to measure

Since the PPD symptoms in Pat:GAR roots were only highly visible at 3 and 4 DAH, using PPD scores derived from either time-point are valid. The PPD score of seven independent single-insert Pat:GAR lines are presented in Figure 6.39 and Table 6.4.
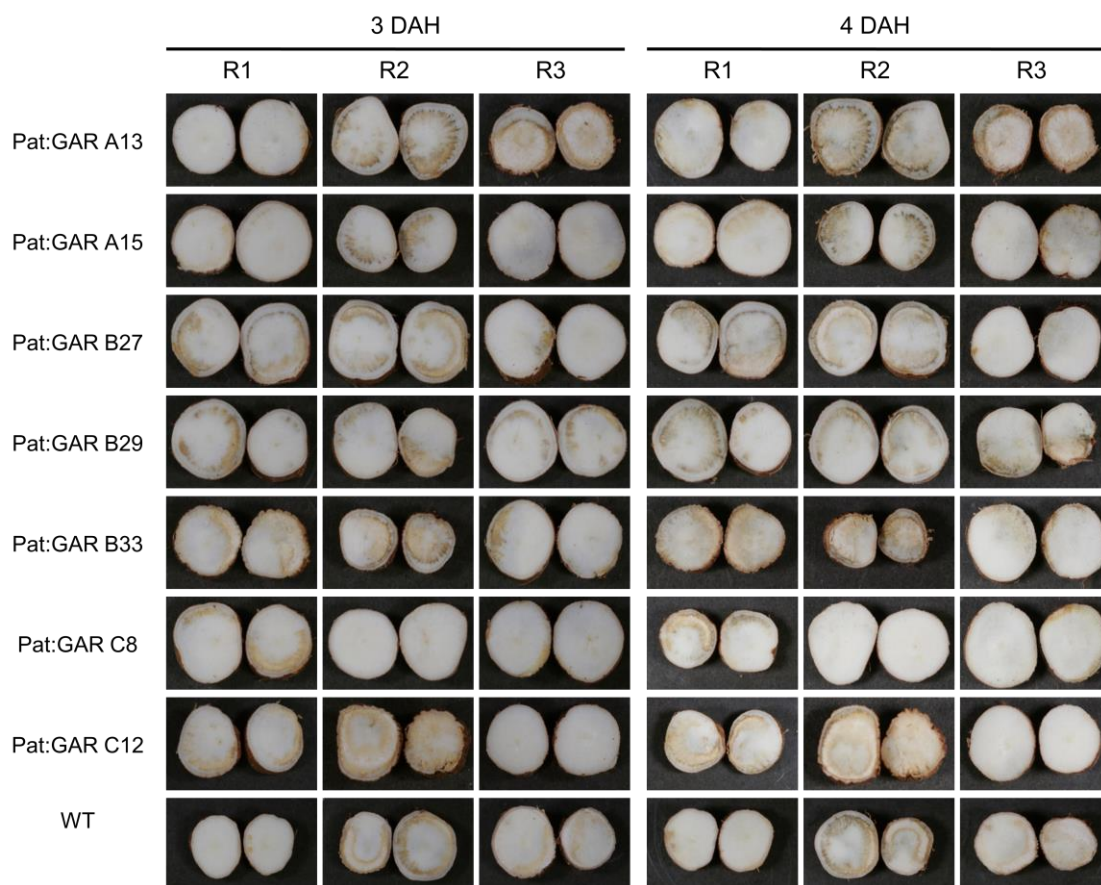
Figure 6.38 Pat:GAR root samples photographed at 3 and 4 DAH. The roots were assayed with PPD Assay 4.

As discussed in Chapter 4, it is simply impossible to avoid variations in PPD symptoms, either in the transgenics or the WT plants. In the Pat:GAR transgenic group this was observed at both 3 and 4 DAH, although the former relatively exhibited less (Figure 6.38). Using the mean PPD scores at 3 DAH for PPD assessment shows that all the Pat:GAR root samples were more severely deteriorated than the WT with PPD scores of up to 60 being calculated, whereas the WT had the mean PPD score of only 30 Figure (6.39). However, due to extremely high variation between PPD scores of the WT roots, as reflected by PPD symptoms in Figure 6.38 and score in Table 6.4 this difference was deemed not significant. Using the PPD scores at 4 DAH, where the symptoms generally more distinctive, also shows that the Pat:GAR were more deteriorated than the WT except in C8. Nevertheless, this was also not statistically significant. Therefore, it was not shown that the transformation altered PPD tolerance.
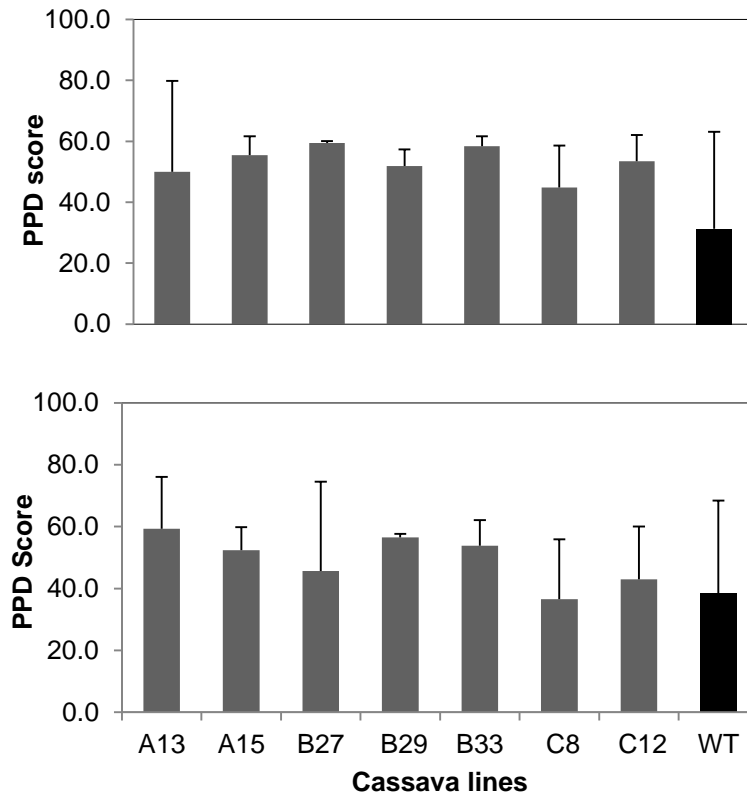
Figure 6.39 The mean PPD score of Pat:GAR transgenic lines measured at 3 DAH (upper panel) and 4 DAH (lower panel). n = 3 SD shown.

Table 6.4 PPD scoring of Pat:GAR root samples at 3 and 4 DAH. Student t-test was performed at p = 0.05, two-tailed level of significance to test whether transformation with FaGAR increased tolerance to PPD.

Plant lines	3 DAH		4 DAH	
	Mean score ± SD (max/min)	t-test	Mean score ± SD (max,min)	t-test
Pat:GAR A13	49.9 ± 29.8 (70.1 / 15.7)	p = 0.50	59.3 ± 16.8 (71.4 / 40.2)	p = 0.35
Pat:GAR A15	55.4 ± 6.2 (60.9 / 48.9)	p = 0.27	52.4 ± 7.5 (60.1 / 45.2)	p = 0.48
Pat:GAR B27	59.4 ± 0.6 (60.1 / 58.9)	p = 0.20	45.7 ± 28.9 (65.2 / 12.5)	p = 0.36
Pat:GAR B29	51.8 ± 5.5 (56.0 / 45.6)	p = 0.33	56.5 ± 1.2 (57.8 / 55.7)	p = 0.36
Pat:GAR B33	58.3 ± 3.3 (61.8 / 55.2)	p = 0.22	53.8 ± 8.3 (63.2 / 47.7)	p = 0.44
Pat:GAR C8	44.8 ± 13.8 (53.0 / 28.9)	p = 0.54	36.6 ± 19.4 (52.2 / 14.9)	p = 0.93
Pat:GAR C12	53.4 ± 8.6 (62.7 / 45.8)	p = 0.31	42.9 ± 17.1 (54.0 / 23.2)	p = 0.84
WT	31.3 ± 31.8 (66.5 / 4.6)	na	38.6 ± 29.9 (72.3 / 15.5)	na

6.6.2   PPD comparison of Pat:GAR and Pat:SOD samples

The main advantage of PPD Assay 4 is that it enabled cross comparison with samples from separate samplings. This is because the samples were allowed to deteriorate under controlled conditions, the pictures were taken with fixed camera settings and the PPD symptoms were scored with a computer program.

The PPD tolerance of Pat:GAR and Pat:SOD transgenics were assessed by comparing the scores in each group. Although it may be suggested that Pat:SOD tolerated PPD better, it could not be statistically proven due to highly variable data. Comparing the highest (t-test, Pat:GAR A13 vs Pat:SOD C4, $p > 0.05$) and the lowest score (t-test, Pat:GAR C8 vs Pat:SOD D7, $p > 0.05$) from each group also produced similar results. Therefore, based on the data gathered, it can be concluded that Pat:GAR and Pat:SOD had similar tolerance to PPD.

Table 6.5 The mean score of Pat:GAR and Pat:SOD root samples collected at 4 DAH.

Pat:GAR plant lines	Mean score	Pat:SOD plant lines	Mean score
Pat:GAR A13	59.3 ± 16.8	Pat:SOD B2	42.5 ± 11.6
Pat:GAR A15	52.4 ± 7.5	Pat:SOD C1	48.9 ± 1.4
Pat:GAR B27	45.7 ± 28.9	Pat:SOD C4	50.4 ± 4.0
Pat:GAR B29	56.5 ±1.2	Pat:SOD D7	40.7 ± 13.6
Pat:GAR B33	53.8 ± 8.3		
Pat:GAR C8	36.6 ± 19.4		
Pat:GAR C12	42.9 ± 17.1		
WT	38.6 ± 29.9	WT	48.9 ± 7.7

6.6.3 Putative GAR sequence in cassava

The GAR gene sequence had not been identified in cassava but a BLAST search with the target gene used in this work found a putative GAR sequence in the cassava genome. It shares approximately 81% similarity with putative GAR sequence in *Theobroma cacao* (cocoa plant) and 71% with that in *Papaver somniferum* (opium poppy). Collectively this suggests cassava may utilise the same pathway as the strawberry plants, which is the galacturonate pathway.
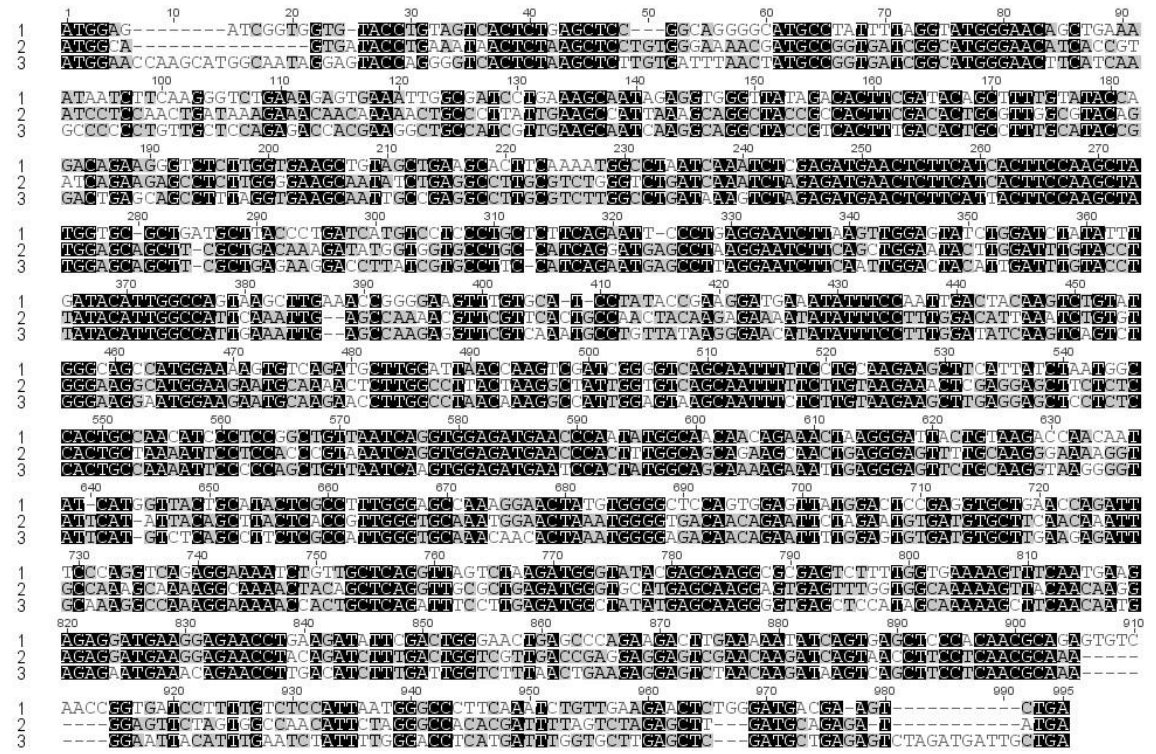
Figure 6.40 Nucleotide sequence alignment of 1: Opium poppy GAR coding sequence (Genbank accession: AF108438), 2: putative cassava GAR coding sequence (Phytozome accession: 4.1_012131.2, 3: putative cocoa GAR coding sequence (Genbank accession: XM 007045353).

6.7 Discussion

Unexpected expression pattern in transgenic cassava

The overexpression of the target genes of Pat:SOD and Pat:GCS transgenic groups have been confirmed in this experiment. MecSOD2 and AtGCS target genes showed enhanced transcriptional level in storage roots upon harvesting with the highest increase between 5- to 10-fold over the WT, respectively. The use of patatin as a gene promoter in cassava transformation is relatively new so there is limited information about its performance. Additionally, gene expression using this promoter in the existing studies has been qualitatively evaluated by others (Ihemere et al., 2006, Ihemere, 2003, Siritunga and Sayre, 2004, Zidenga et al., 2012). However, up to 20-fold increase has been reported in HNL gene expression using a longer version of class I patatin (Narayanan et al., 2011). Whereas, about the same fold expression was reported using a vascular-specific promoter (p45/1.0) in cassava roots (Xu et al., 2013a). Therefore, compared to these results, the expression enhancement achieved in the work presented here, though significant, is relatively low.

The initial aim of these transgenic experiments was to increase the accumulation of individual anti-oxidant enzymes in the cassava roots at, and immediately after harvest in order to elevate the anti-oxidative status at the point where the oxidative burst is triggered and the damage to the root from ROS starts. However, the overexpression of these transgenes was only observed from 24 hours after harvesting. Such increases were not observed in the WT either here or in previous work. In the case of MecSOD2, its transcriptional level was found steady but low from the day of harvest until five days after that; a consistent pattern that was found in cassava roots of various PPD tolerances (Reilly, 2001), although transient upregulation between 6 to 12 hours after wounding was reported in an unknown cultivar (Owiti, 2009). There has been no report on GCS transcription profile in the WT cassava so far but the boost in overexpression after 24 hours of harvesting either suggests that there was delay in Patatin response towards wounding or the biochemical changes in PPD process itself. It is unfortunate not to be able to show the expression pattern of Patatin in transgenic Gus-expressing cassava plants, but the evidence on sugar metabolism (Tanaka et al., 1983), ethylene accumulation (Hirose et al., 1984) and flavonoid biosynthesis (Uarrota et al., 2014) during PPD suggests that the motifs identified in the Patatin promoter could be activated by these compounds, as described in the previous chapter.

Overexpression of target genes did not confer tolerance to oxidative stress to the roots during PPD

The overall tolerance of transgenic plants to major ROS was evaluated in all transgenic groups. Less convincing data can be gathered from measurement of root length following propagation on hydrogen peroxide-containing medium due to high variation between replicates. However, the upregulation of the genes did not render the cassava roots less susceptible to oxidative stress. For example, the increase of MecSOD2 transcriptional level seemed not to affect its efficiency in reducing O_2^- content in the roots and it did not prevent accumulation of H_2O_2. It must be emphasised that the main consequence of increasing SOD activities is increasing production of H_2O_2, which then may present a new threat. Unless the mechanism to detoxify this by-product synchronises with the mechanism that produced it, using SOD alone is not a good strategy. In this work it is shown that, Pat:SOD transgenic roots lacked this synchronisation as the CAT and APX enzyme activities did not change over PPD. H_2O_2 toxicity due to overexpression of SOD has been rarely reported, but was observed in tobacco and tomato cells introduced with petunia SOD gene (Tepperman and Dunsmuir, 1990) and in winter survival alfalfa plants (McKersie et al., 2000).

Due to the threat of H_2O_2, coupled expression of SOD with other H_2O_2-detoxifying genes has been attempted and proved more efficient at increasing oxidative-stress related resistance. Potato plants transformed with the combination of SOD and APX were found to be highly tolerant to MV treatment and had increased photosynthetic activity (Tang et al., 2006). Similarly, it substantially improved the phytoremediative potential of tall fescue plants by increasing their tolerance to oxidative stress and various heavy metals. There was significant increased in SOD and APX activities as well as reduction in H_2O_2 formation in the transgenic plants when challenged with abiotic stress (Lee et al., 2007). Simultaneous expression with CAT gene also is promising. Transgenic Chinese cabbage plants over-expressing SOD and CAT were also found to be less affected by sulphur dioxide compared to those over-expressing SOD alone (Tseng et al., 2007). Recently, coupled expression of SOD and CAT genes driven by the vascular-specific promoter p54/1.0 in cassava roots caused PPD to delay for to up four days which correlates with a significant reduction of H_2O_2 at this time-point (Xu et al., 2013a).

The sudden increase in AtGCS transgene expression, an enzyme catalysing the first step of GSH biosynthesis, also did not confer resistance to oxidative stress to the Pat:GCS roots. Up to 30-fold increase of transgene expression was achieved

compared to only about 12-fold achieved in the Pat:SOD but it showed that the transgenics had less anti-oxidant capacities than the WT. These results are in agreement with a study that claims GCS might not be the best candidate for increasing GSH in poplar trees. Instead, glutathione reductase (GR) was suggested to be a better choice (Foyer et al., 1995). The anti-oxidant property of glutathione relies on its reduced form (GSH), which scavenges peroxide and oxidises it to GSSG. GSSG is reduced back to GSH by GR, thus GR is an alternative to GCS in increasing the antioxidative potential of GSH (Gill et al., 2013). Moreover, a number of experiments suggest that there is possible feedback inhibition of GSH on GCS itself, which limits its use (Jez et al., 2004, Richman and Meister, 1975, Huang et al., 1988). Nevertheless, increasing GSH content alone seemed not to improve the antioxidative potential of GSH because it disrupts the GSH/GSSG balance. For example, in tobacco, GSH levels were enhanced via GCS over-expression by three-fold, but the transgenic leaves became more susceptible to photo-oxidative stress compared to the WT. Impairment of redox sensing of the chloroplast due to an imbalance in GSH/GSSG was identified as the main reason for this (Creissen et al., 1999). Therefore, since the GSH content was not measured in this experiment, the unimproved oxidative stress shown by the root samples overexpressing AtGCS could arise from two possibilities: it could either caused by the inefficiency of AtGCS to increase GSH content or by disruption of the GSH/GSSG balance.

Transformation with the target genes may not be sufficient to delay PPD

Although the gene expression was not measured in all the transgenic groups, a large percentage of independent single-insert lines from each group were assessed for PPD symptoms. Transformation with MecSOD2 was evaluated using the best assay determined by the present study, which is PPD Assay 4. However, there were not enough data to support a relationship between the overexpression of this gene and delayed PPD. No significant differences in PPD scores were measured between the transgenic roots and the WT roots. Moreover, PPD assays found that the roots deteriorated in a random fashion. Some of the roots deteriorated more rapidly when stored intact but rather slowly in the form of sections and vice versa. Cassava plants transformed with FaGAR was also evaluated using PPD Assay 4, but statistical analysis found no significant difference between the WT and the transgenic roots in terms of the PPD symptoms they produced. On the other hand, it was not possible to determine with high confidence if overexpression in AtGCS overexpression and MecAPX2 transgenics caused a reduction in PPD symptoms, due to the weakness of the assays used for PPD assessment in these roots.

Given that PPD is a complex process, it is unlikely that overexpression of one gene could sufficiently ameliorate the response. Moreover, the genes used in this study are those involved in ROS defence network, which is itself a complex process with many interacting components. As substantiated by this study, the release of O_2- following wounding probably is the earliest indicator that PPD is oxidative stress-related, but the recent findings suggested that O_2^- can be preceded by cyanogenesis (Siritunga and Sayre, 2007). Cyanogenesis is triggered by wounding of the cassava roots releasing cyanide, which then interrupts electron transfer in mitochondrial cytochrome c oxidase leading to ROS formation. However, in addition to cytochrome c oxidase plant contains a cyanide insensitive alternative oxidase (AOX), which provides an alternative pathway for the electron transfer (Maxwell et al., 1999, Van Aken et al., 2009). Research focusing on AOX gene and PPD is currently ongoing.

CHAPTER 7

General Discussion

The aim of this research was to determine whether PPD is ROS-mediated. The strategy was to use transgenic cassava plants designed to have an increased ability to scavenge ROS through root-specific over-expression of target genes encoding ROS-scavenging enzymes or enzymes for the biosynthesis of anti-oxidant molecules. While altered patterns of gene expression were measured, these were not sufficient to confer significant alterations to ROS levels, nor to alter the PPD response of the roots.

7.1   ROS detoxification in plant cells is complex

The formation of ROS is a consequence of aerobic respiration and photosynthesis, which are processes to produce energy. Being present at a basal concentration, ROS functions as signalling molecules to maintain the integrity of the cells, but if this concentration is exceeded ROS can potentially damage the cells. Therefore, in a plant cell, ROS formation is expected but there is no benchmark to determine if ROS is formed excessively to levels that cause oxidative stress.

Oxidative stress occurs at the heart of PPD due to unsynchronised changes between ROS production and transcript abundance of genes associated with ROS-scavenging (Reilly et al., 2003). In the present study, SOD gene transcriptional levels were found to be low at the time of harvest despite dramatic cellular production of superoxide. It was possible that the changes in transcriptional activity of MecSOD and activity of SOD did not occur as anticipated because there is alternative pathway for its removal. Excess superoxide in cassava roots probably was neutralised by spontaneous dismutation instead of by the catalytic activity of SOD (Sawyer and Valentine, 1981). In contrast to spontaneous dismutation, SOD dismutation is a reversible process as it is inhibited by its by-product H_2O_2, thus it is favoured by cells only when there is a low superoxide concentration (Miwa et al., 2008). The preference for spontaneous dismutation is supported by the nature of SOD itself, particularly CuZnSOD, which is known to be cyanide–sensitive. While cyanide is abundant and progressively released upon wounding in cassava roots, it is possible that this enzyme may not be functioning as efficiently as it would in a cyanide-free environment. Cyanide is highly poisonous, exogenous application at micromolar concentrations has been shown to rapidly inhibit

the activity of CuZnSOD in mungbean (Reddy and Venkaiah, 1984). Also, cyanide in the form of KCN is a chemical routinely added to SOD enzyme assays intended to measure SOD activity of SOD isoforms other than CuZn.

The proposed model for ROS-scavenging network may seem to suggest an orchestrated process to ensure oxidative stress is avoided at any cost but the anti-oxidant enzymes may not change their activities in a linear fashion. For example, while SOD is expected to be transcribed first because MV is a superoxide-generating agent, MV-treated transgenic potato transformed with SOD and APX gene showed earlier overexpression of APX (at 12 hours) but rather late SOD transcript accumulation of (48 hours after treatment) (Tang et al., 2006). Moreover, plants show resistance to oxidative stress by manipulating anti-oxidant capacities of different ROS-scavenging components. In wheat, one stress tolerant genotype had high APX and ascorbate level while another genotype with similar tolerance had increased activity of SOD and CAT (Sairam et al., 2002). Additionally, an independent study on the role of CAT and SOD in norflurazon-induced oxidative stress in maize showed increased transcript levels of CAT and chloroplastic SOD (but not cytosolic or mitochondrial), indicating differential antioxidative responses by a similar type of enzyme is possible (Jung et al., 2001). That said, it is possible that PPD is controlled by activation of only several components of the system keeping others unaltered. It is critical to identify these components but the task is not going to be straightforward. There are numerous factors to add to the complexity of the plant ROS-scavenging system. For example, a stress inducer may act to suppress specific components of the system. In oxidative stress caused by cadmium in pea plants, treatment with the metal caused cellular glutathione and ascorbate to decrease severely, but it induced CAT and MDHAR transcript levels in a cadmium-dependent manner (Romero-Puertas et al., 2007). However, the metal might have indirectly caused this, since it has been shown that other components of the system can also act in the similar fashion. For instance, inhibition of GSH synthesis and APX activity by CuZnSOD over-expression has been reported (Ai et al., 2008, Kwon et al., 2002).

It was mentioned in Chapter 6 that sensitivity to PPD shown by Pat:GCS plants might relate to the inability of AtGCS to increase GSH content. However, increased activity of the biosynthetic enzyme does not guarantee increased GSH as it also is determined by many factors including its constituents availability, particularly cysteine (Ogawa et al., 2004). An independent study demonstrated that overexpression of serine acetyl transferase, which is involved in cysteine biosynthesis in transgenic potato, is critical for increased levels of GSH (Harms et al., 2000). Besides, there are many ways to

increase GSH concentration, including by enhancing GSH turnover by direct feeding with GSSG (Gomez et al., 2004) and overexpression of glutathione reductase (Gill et al., 2013). Nevertheless, although it is accepted that the redox potential of glutathione is attributed to GSH oxidation to GSSG that simultaneously catalyses the detoxification of H_2O_2 through ascorbate-glutathione cycle, GSH oxidation was recently found to be coupled to at least to four other reactions in four different pathways emphasising the complexity of GSH/GSSG modulation and plant ROS scavenging network in general (Rahantaniaina et al., 2013). Likewise, the goal to increase AA pool is not straightforward as both the turnover pathway and down-regulation of AA oxidation could also affect its accumulation (Ishikawa et al., 2006). Moreover, AA itself has the potential to generate the hydroxyl radical through interaction with a transition metal ion and H_2O_2via the Udenfriend reaction (Valko et al., 2005). However, rather than the above-mentioned problems, the existence of multiple biosynthesis pathways for ascorbate is seen as the main challenge that makes ascorbate accumulation difficult to engineer. Since cassava AA biosynthesis has not been studied in cassava, it was also possible that the wrong enzyme was targeted in the present study.

ROS production is the earliest response in wounded tissue, which also activates the stress hormones such as salicylic acid (SA), jasmonic acid and ethene as wound signalling molecules (León et al., 2001). Since these molecules are not exclusive to wounding, but also play roles in other physiological processes, it is necessary to measure them to see if their concentrations are affected by PPD. Importantly, many of these molecules are derived from the phenylpropanoid biosynthetic pathway, which has been shown to be activated during the onset of PPD (Tanaka et al., 1983, Rodriguez, 2001). In *Arabidopsis*, SA, despite being known as a signalling molecule in defence to pathogen-related stress, was shown to provoke production of H_2O_2 causing lipid peroxidation and oxidative damage due to impeded CAT and APX activities under continuous SA treatment (Rao et al., 1997). While in PPD, although some of these molecules and their precursors had been detected, it is not known if they may play a role in the occurrence of PPD (Hirose et al., 1984, Owiti et al., 2011)

7.2 Improvement of PPD assessment is crucial

The factors that accelerate PPD, such as dehydration and multiple wounding, were recognised and a reliable method to assay PPD was finally developed in the present study. Although developing a new PPD assay method was not perceived as required at the beginning of this project, problems arising from getting meaningful signals to differentiate subtle differences between samples from several rounds of harvesting highlighted the urgency to design a robust and useful assay. The difficulty in assessing PPD has been acknowledged by many researchers in cassava PPD, but has not been further investigated or even reported (Salcedo et al., 2010). Very recently, PPD scoring using the same software used in the present study (PPD Symptom Score Software) unambiguously showed statistically significant reduction of PPD symptoms in transgenic cassava roots (Vanderschuren et al., 2014).

Scoring PPD based on visual symptoms that develop on the surface of storage root sample may be simple and straightforward but it requires trained eyes to differentiate minor differences. The use of computer software and the need to calculate the PPD score for each sample, though it might be considered more laborious than visual assessment that only requires personal judgement, was proven the most practical in the present study because it generates objective descriptive data, thereby reducing human bias. With other plant produce, visual assessment is commonly used to inspect the external appearance and to grade post-harvest quality, but it often involves evaluation of many characteristics making it an easier task. For example, papaya is rated by firmness, peel colour, degree of shrivelling and decay severity (Emond and Brecht, 2005) while parsley post-harvest quality is graded by aroma, percentage of greenness, discoloration and decay (Loaiza and Cantwell, 1997). This was not the case with PPD of cassava, as the symptoms attributed to it are limited to the physical appearance of root surface so careful assessment of the symptoms is a must. Nowadays, computer vision has become a potential component in the quality control of various produce because it is hygienic, non-destructive and relatively robust (Brosnan and Sun, 2002).

There is need to find an alternative method to assess PPD other than a visual one (with or without software analysis), ideally by the use of a marker related to the variable symptoms shown by the roots. While scopoletin would appear a good candidate due to its abundance and fluorescence under UV, exploratory assays were not persuasive of its usefulness as a good marker. The method should either involve measurement of other biochemical markers or assessment of a molecular marker. The combined

analysis of physical appearance and a useful marker would be the ideal way forward in PPD assessment. In this respect, H_2O_2 is seen as a potential candidate. Not only it is detectable by *in situ* techniques but its concentration in the affected tissue can be determined easily. Compared to superoxide, H_2O_2 is not only relatively stable but more connected to the deterioration symptoms because it tends to appear later in the PPD stage. There is evidence from the present study that the accumulation of H_2O_2 in cassava root tissue is more likely to cause oxidative stress than the superoxide because the H_2O_2-scavenging enzymes did not increase their activities despite increases in the H_2O_2 cellular concentration (Section 6.3.2). Possible direct regulation of gene expression by H_2O_2 has also been proposed, but the exact mechanisms underlying this remain to be determined (Neill et al., 2002). H_2O_2 either oxidises transcription factors or interacts with signalling proteins, such as protein kinase or protein phosphatase in the cytoplasm or in the nucleus, in which protein s-nitrosylation by nitric oxide is said to be the mediator of the process (Lin et al., 2012, Wang et al., 2013).

7.3   Assessment of Pat:Gus cassava plants and Pat (-):Gus *Arabidopsis* will provide clearer insights in Patatin promoter

It was unfortunate not to be able to see Gus expression in cassava, because the plasmid containing Patatin-driven *GusPlus* gene was not transformed. However, some useful information was gathered from evaluating Gus expression in *Arabidopsis* seedlings, which allowed prediction of the general features of the promoter. The patatin used in the present study was confirmed to be root-specific and wound-inducible. Rapid induction by tissue damage is a characteristic never reported in any patatins before (Page, 2009).

The significant increase of transgene transcription of Pat:SOD and Pat:GCS, which occurred 24 hours after harvest is considered late when compared to Gus expression in *Arabidopsis*. Certainly, the wound-inducibility characteristic is the result of several interacting molecules that function as wound signals, both systemic and local (Zhou and Thornburg, 1999). Because this was not examined in either *Arabidopsis* or cassava it was possible that the unidentified molecules were produced at a slower rate in cassava roots so increased gene expression took longer to occur. Therefore, measurement of these molecules such as systemin, abscisic acid, ethene, jasmonic acid and oligogalacturonides (OGAs) may be the key to understanding the differences between the two plants. Species-specific wound response has been demonstrated in

tomato and *Arabidopsis* in which the former was activated by OGAs while the former was inhibited by the same substances (Schilmiller and Howe, 2005). It is also important to note that wounded cassava tissue releases considerable amount of cyanogens which may impair the process by blocking mitochondrial oxidative phosphorylation (Nzwalo and Cliff, 2011).

The strong Gus expression in promoterless cassava lines must also be investigated as it might suggest that the neighbouring CaMV35s promoter driving *hptII* gene could be able to co-regulate the expression of MecSOD2 and AtGCS gene in Pat:SOD and Pat:GCS transgenic plants respectively. Such a response is rare but CaMV35s interference with adjacent promoters have been reported before (Zheng et al., 2007, Yoo et al., 2005). Therefore, creating promoterless Gus plants in *Arabidopsis* and making comparative assessments between *Arabidopsis* Pat:Gus would be of interest as this could confirm whether or not the wound-inducible characteristic observed before is exclusively attributed to Patatin or influenced by the CaMV35s.

7.4   Future prospect for cassava PPD research

ROS production had been observed and measured in cassava roots immediately after harvest in the present study. Therefore, increasing the anti-oxidant status as the first line of protection, with the aim to avoid oxidative stress, is a viable strategy. However, as mentioned earlier, the associated physiological stress implicated with ROS and oxidative stress is equally important to be considered in understanding PPD.

There exists considerable evidence that shows that oxidative stress triggers the onset of programmed cell death (PCD). PCD which initially was considered as a degenerative process is a high metabolic activity and a consequence of severe injury. The regulation of PCD by redox activity in the cell has been proposed (De Pinto et al., 2012). PCD involving cytoplasmic male sterility in rice is associated with down-regulation of CAT and APX activities causing premature microspore loss, indicating that H_2O_2 is an essential component in this process through disrupting mitochondrial ETC function (Li et al., 2004). The mechanism for H_2O_2-induced PCD is not fully understood, but overexpression of human apoptotic suppressor *Bcl-2* and *Ced-9* enhanced oxidative tolerance in rice and tobacco respectively (Deng et al., 2011, Wang et al., 2009). These findings are encouraging and a co-expression of these genes with anti-oxidant genes could be a potential solution to delay PPD. A project research investigating PCD in

PPD by manipulating these genes is currently ongoing in this lab (K. Jones, *pers. comm.*).

Nevertheless, the success of this approach would critically hinge on the choice of promoter, the target genes and transformation method. While the method of transformation used in the present study had produced high percentage of independent single-insert lines, a wide range of tissue-specific promoters are available to be tested. However, given the highly variable data produced in the present study, the ability to produce a huge number of replicates which enable careful selection of materials is crucial. This is the goal that will only be achieved by collaboration with cassava growing countries.

8   REFERENCES

ABHARY, M., SIRITUNGA, D., STEVENS, G., TAYLOR, N. J. & FAUQUET, C. M. 2011. Transgenic biofortification of the starchy staple cassava (*Manihot esculenta*) generates a novel sink for protein. *PloS One,* 6**,** e16256.

AGIUS, F., GONZALEZ-LAMOTHE, R., CABALLERO, J. L., MUNOZ-BLANCO, J., BOTELLA, M. A. & VALPUESTA, V. 2003. Engineering increased vitamin C levels in plants by overexpression of a D-galacturonic acid reductase. *Nature Biotechnology,* 21**,** 177-181.

AI, Y.-Z., DU, Y.-J., ZU, Y.-G. & AN, Z.-G. 2008. Inhibition effect of expression of Cu/Zn superoxide dismutase from rice on synthesis of glutathione in *Saccharomyces cerevisiae. Journal of Forestry Research,* 19**,** 63-66.

AKSENOVA, N. P., KONSTANTINOVA, T. N., GOLYANOVSKAYA, S. A., SERGEEVA, L. I. & ROMANOV, G. A. 2012. Hormonal regulation of tuber formation in potato plants. *Russian Journal of Plant Physiology,* 59**,** 451-466.

ALLEM, A. C. 1999. The closest wild relatives of cassava (*Manihot esculenta* Crantz). *Euphytica,* 107**,** 123-133.

ALSCHER, R. G., ERTURK, N. & HEATH, L. S. 2002. Role of superoxide dismutases (SODs) in controlling oxidative stress in plants. *Journal of Experimental Botany,* 53**,** 1331-1341.

ALVES, A. A. C. 2002. Cassava botany and physiology. *In:* HILLCOCKS, R. J., THRESH, J. M. & BELLOTTI, A. (eds.) *Cassava: Biology, Production and Utilisation.* Wallingford: CABI.

AN, D., YANG, J. & ZHANG, P. 2012. Transcriptome profiling of low temperature-treated cassava apical shoots showed dynamic responses of tropical plant to cold stress. *BMC Genomics,* 13**,** 1-25.

AN, G., COSTA, M. A. & HA, S.-B. 1990. Nopaline synthase promoter is wound inducible and auxin inducible. *The Plant Cell Online,* 2**,** 225-233.

ANDREWS, D. L., BEAMES, B., SUMMERS, M. & PARK, W. 1988. Characterization of the lipid acyl hydrolase activity of the major potato (*Solanum tuberosum*) tuber protein, patatin, by cloning and abundant expression in a baculovirus vector. *Biochemical Journal,* 252**,** 199-206.

APEL, K. & HIRT, H. 2004. Reactive oxygen species: Metabolism, oxidative stress, and signal transduction. *Annual Review of Plant Biology,* 55**,** 373-399.

ARANGO, J., SALAZAR, B., WELSCH, R., SARMIENTO, F., BEYER, P. & AL-BABILI, S. 2010. Putative storage root specific promoters from cassava and yam: cloning and evaluation in transgenic carrots as a model system. *Plant Cell Reports,* 29**,** 651-659.

AVERRE, C. W. Year. Vascular streaking of stored cassava roots. *In:* Proceedings of the 1st Symposium of the International Society for Tropical Root Crops, 1967 St Augustine, Trinidad. 31-35.

BACHEM, C., VAN DER HOEVEN, R., LUCKER, J., OOMEN, R., CASARINI, E., JACOBSEN, E. & VISSER, R. 2000. Functional genomic analysis of potato tuber life-cycle. *Potato Research,* 43**,** 297-312.

BACHEM, C. W. B., VAN DER HOEVEN, R. S., DE BRUIJN, S. M., VREUGDENHIL, D., ZABEAU, M. & VISSER, R. G. F. 1996. Visualization of differential gene expression using a novel method of RNA fingerprinting based on AFLP:

analysis of gene expression during potato tuber development. *Plant Journal,* 9**,** 745-753.

BADAWI, G. H., KAWANO, N., YAMAUCHI, Y., SHIMADA, E., SASAKI, R., KUBO, A. & TANAKA, K. 2004. Over-expression of ascorbate peroxidase in tobacco chloroplasts enhances the tolerance to salt stress and water deficit. *Physiologia Plantarum,* 121**,** 231-238.

BAS, A., FORSBERG, G., HAMMARSTRÖM, S. & HAMMARSTRÖM, M. L. 2004. Utility of the housekeeping genes 18s rRna, β-actin and glyceraldehyde-3-phosphate-dehydrogenase for normalization in real-time quantitative reverse transcriptase-polymerase chain reaction analysis of gene expression in human T lymphocytes. *Scandinavian Journal of Immunology,* 59**,** 566-573.

BAUMANN, K., DE PAOLIS, A., COSTANTINO, P. & GUALBERTI, G. 1999. The DNA binding site of the Dof protein NtBBF1 is essential for tissue-specific and auxin-regulated expression of the rolB oncogene in plants. *The Plant Cell Online,* 11**,** 323-333.

BAYOUMI, S. A. L., ROWAN, M. G., BLAGBROUGH, I. S. & BEECHING, J. R. 2008. Investigation of scopoletin biosynthesis during post-harvest physiological deterioration in cassava roots using stable isotopic labelling. *Journal of Pharmacy and Pharmacology,* 60**,** 10.

BEAUCHAMP, C. & FRIDOVICH, I. 1971. Superoxide dismutase: improved assays and an assay applicable to acrylamide gels. *Analytical Biochemistry,* 44**,** 276-287.

BEDON, F., BOMAL, C., CARON, S., LEVASSEUR, C., BOYLE, B., MANSFIELD, S. D., SCHMIDT, A., GERSHENZON, J., GRIMA-PETTENATI, J., SÉGUIN, A. & MACKAY, J. 2010. Subgroup 4 R2R3-MYBs in conifer trees: gene family expansion and contribution to the isoprenoid- and flavonoid-oriented responses. *Journal of Experimental Botany,* 61**,** 3847-3864.

BEECHING, J. R. 2001. Strategies for the modulation of post-harvest physiological deterioration in cassava for the benefit of poor people. *Commissioned report for DFID's Crop Post-Harvest Programme.*

BEECHING, J. R., BUSCHMANN, H., GÓMEZ-VÁSQUEZ, R., HAN, Y., IGLESIAS, C., LI, H., REILLY, K. & RODRIGUEZ, M. X. 1999. An abiotic stress response in cassava: Post-harvest physiological deterioration. *In:* SMALLWOOD, M. F., CALVERT, C. M. & BOWLES, D. J. (eds.) *Plant Responses to Environmental Stress.* Oxford: BIOS.

BEECHING, J. R., DODGE, A. D., MOORE, K. G. & WENHAM, J. E. Year. Physiological deterioration in cassava: An incomplete wound response? *In:* THRO, A. M. & ROCA, W., eds. The Cassava Biotechnology Network: Proceedings of the Second International Scientific Meeting, 1994 Bogor, Indonesia. CIAT, Cali, Colombia, 729-736.

BEECHING, J. R., HAN, Y., GÓMEZ-VÁSQUEZ, R., DAY, R. C. & COOPER, R. M. 1998. Wound and defense responses in cassava as related to post-harvest physiological deterioration. *Recent Advances in Phytochemistry,* 32**,** 231-248.

BEERS, R. F. & SIZER, I. W. 1952. A spectrophotometric method for measuring the breakdown of hydrogen peroxide by catalase. *The Journal of Biological Chemistry,* 195**,** 133-140.

BELLOTTI, A. C., SMITH, L. & LAPOINTE, S. L. 1999. Recent Advances in Cassava Pest Management. *Annual Review of Entomology,* 44**,** 343-370.

BENESI, I. R. M., LABUSCHAGNE, M. T., HERSELMAN, L. & MAHUNGU, N. 2010. Ethnobotany, Morphology and Genotyping of Cassava Germplasm from Malawi. *Journal of Biological Sciences,* 10**,** 616-623.

BEVAN, M., BARKER, R., GOLDSBROUGH, A., JARVIS, M., KAVANAGH, T. & ITURRIAGA, G. 1986. The structure and transcription start site of a major potato tuber protein gene. *Nucleic Acids Research,* 14**,** 4625-4638.

BOOTH, R. H. 1976. Storage of fresh cassava (*Manihot esculenta*). I. Post-harvest deterioration and its control. *Experimental Agriculture,* 12**,** 103-111.

BOWLER, C., VAN CAMP, W., VAN MONTAGU, M. & INZE, D. 1994. Superoxide-dismutase in plants. *Critical Reviews in Plant Sciences,* 13**,** 199-218.

BROSNAN, T. & SUN, D.-W. 2002. Inspection and grading of agricultural and food products by computer vision systems—a review. *Computers and Electronics in Agriculture,* 36**,** 193-213.

BULL, S. E. 2011. *Study of post-harvest physiological deterioration in transgenic cassava.* PhD, University of Bath.

BUSCHMANN, H., REILLY, K., RODRIGUEZ, M. X., TOHME, J. & BEECHING, J. R. 2000a. Hydrogen peroxide and flavan-3-ols in storage roots of cassava (*Manihot esculenta* Crantz) during postharvest deterioration. *Journal of Agricultural and Food Chemistry,* 48**,** 5522-5529.

BUSCHMANN, H., RODRIGUEZ, M. X., TOHME, J. & BEECHING, J. R. 2000b. Accumulation of hydroxycoumarins during post-harvest deterioration of tuberous roots of cassava (*Manihot esculenta* Crantz). *Annals of Botany,* 86**,** 1153-1160.

CAIRNS, N. G., PASTERNAK, M., WACHTER, A., COBBETT, C. S. & MEYER, A. J. 2006. Maturation of *Arabidopsis* seeds is dependent on glutathione biosynthesis within the embryo. *Plant Physiology,* 141**,** 446-455.

CEBALLOS, H., IGLESIAS, C. A., PEREZ, J. C. & DIXON, A. G. O. 2004. Cassava breeding: opportunities and challenges. *Plant Molecular Biology,* 56**,** 503-516.

CHANG, S., PURYEAR, J. & CAIRNEY, J. 1993. A simple and efficient method for isolating RNA from pine trees. *Plant Molecular Biology Reporter,* 11**,** 113-116.

CHAVEZ, A. L., BEDOYA, J. M., SANCHEZ, T., IGLESIAS, C., CEBALLOS, H. & ROCA, W. 2000. Iron, carotene, and ascorbic acid in cassava roots and leaves. *Food and Nutrition Bulletin,* 21**,** 410-413.

COCK, J., FRANKLIN, D., SANDOVAL, G. & JURI, P. 1979. The ideal cassava plant for maximum yield. *Crop Science,* 19**,** 271-279.

COCK, J. H. 1982. Cassava - a basic energy-source in the tropics. *Science,* 218**,** 755-762.

COCK, J. H. 1985. New Potential for a Neglected Crop. *IADS, Development Oriented Literature Series, Westview Press, Colorado, USA p192*.

CREISSEN, G., FIRMIN, J., FRYER, M., KULAR, B., LEYLAND, N., REYNOLDS, H., PASTORI, G., WELLBURN, F., BAKER, N., WELLBURN, A. & MULLINEAUX, P. 1999. Elevated glutathione biosynthetic capacity in the chloroplasts of transgenic tobacco plants paradoxically causes increased oxidative stress. *The Plant Cell Online,* 11**,** 1277-1291.

DA SILVA VIEIRA, M. R., SANTOS, C. M. G., DE SOUZA, A. V., DE ALENCAR PAES, R. & DA SILVA, L. F. 2013. Physiological blockage in plants in response to postharvest stress. *African Journal of Biotechnology,* 12**,** 1168-1170.

DATA, E. S., QUEVEDO, M. A. & GLORIA, L. A. 1984. Pruning techniques affecting the root quality of cassava at harvest and subsequent storage. *In Tropical Root Crops: Postharvest Physiology and Processing. Eds. Uritani & Reyes. JSSP: Tokyo.*, 127-143.

DAVIES, M. J. 2004. Reactive species formed on proteins exposed to singlet oxygen. *Photochemical & Photobiological Sciences,* 3, 17-25.

DE PINTO, M. C., LOCATO, V. & DE GARA, L. 2012. Redox regulation in plant programmed cell death. *Plant Cell and Environment,* 35, 234-244.

DE SOUZA, C. R., ARAGAO, F. J., MOREIRA, E. C. O., COSTA, C. N. M., NASCIMENTO, S. B. & CARVALHO, L. J. 2009. Isolation and characterization of the promoter sequence of a cassava gene coding for Pt2L4, a glutamic acid-rich protein differentially expressed in storage roots. *Genetics and Molecular Research,* 8, 334-344.

DE SOUZA, C. R. B., CARVALHO, L., DE ALMEIDA, E. R. P. & GANDER, E. S. 2006. A cDNA sequence coding for a glutamic acid-rich protein is differentially expressed in cassava storage roots. *Protein and Peptide Letters,* 13, 453-457.

DENG, M. J., BIAN, H. W., XIE, Y. K., KIM, Y., WANG, W. Z., LIN, E. P., ZENG, Z. H., GUO, F., PAN, J. W., HAN, N., WANG, J. H., QIAN, Q. & ZHU, M. Y. 2011. Bcl-2 suppresses hydrogen peroxide-induced programmed cell death via OsVPE2 and OsVPE3, but not via OsVPE1 and OsVPE4, in rice. *Febs Journal,* 278, 4797-4810.

DIOP, A. & CALVERLEY, D. J. B. 1998. Storage and Processing of Roots and Tubers in the Tropics. *FAO Report.* Rome.

DRUMMOND, A., ASHTON, B., CHEUNG, M., HELED, J., KEARSE, M., MOIR, R., STONES-HAVAS, S., THIERER, T. & WILSON, A. 2009. Geneious v4.7. *URL http://www.geneious.com/ [accessed on 27 August 2014]*.

ELMAYAN, T. & TEPFER, M. 1995. Evaluation in tobacco of the organ specificity and strength of the *rolD* promoter, domain A of the 35S promoter and the 35S2 promoter. *Transgenic Research,* 4, 388-396.

EMOND, J. & BRECHT, J. K. Year. Quality attributes limiting papaya postharvest life at chilling and non-chilling temperatures. *In: Proceedings of the Florida State Horticultural Society*, 2005. 389-395.

FAUQUET, C. & FARGETTE, D. 1990. African cassava mosaic virus: etiology, epidemiology and control. *Plant Disease,* 74, 404-411.

FAWAL, N., LI, Q., SAVELLI, B., BRETTE, M., PASSAIA, G., FABRE, M., MATHÉ, C. & DUNAND, C. 2013. PeroxiBase: a database for large-scale evolutionary analysis of peroxidases. *Nucleic Acids Research,* 41, D441-D444.

FERNÁNDEZ-OCAÑA, A., CHAKI, M., LUQUE, F., GÓMEZ-RODRÍGUEZ, M. V., CARRERAS, A., VALDERRAMA, R., BEGARA-MORALES, J. C., HERNÁNDEZ, L. E., CORPAS, F. J. & BARROSO, J. B. 2011. Functional analysis of superoxide dismutases (SODs) in sunflower under biotic and abiotic stress conditions. Identification of two new genes of mitochondrial Mn-SOD. *Journal of Plant Physiology,* 168, 1303-1308.

FOYER, C. & HALLIWELL, B. 1976. The presence of glutathione and glutathione reductase in chloroplasts: A proposed role in ascorbic acid metabolism. *Planta,* 133, 21-25.

FOYER, C. H. & NOCTOR, G. 2000. Tansley Review No. 112. *New Phytologist,* 146, 359-388.

FOYER, C. H. & NOCTOR, G. 2005. Oxidant and antioxidant signalling in plants: a re-evaluation of the concept of oxidative stress in a physiological context. *Plant Cell and Environment,* 28**,** 1056-1071.

FOYER, C. H., SOURIAU, N., PERRET, S., LELANDAIS, M., KUNERT, K. J., PRUVOST, C. & JOUANIN, L. 1995. Overexpression of glutathione-reductase but not glutathione synthetase leads to increases in antioxidant capacity and resistance to photoinhibition in poplar trees. *Plant Physiology,* 109**,** 1047-1057.

FRANCHE, C., BOGUSZ, D., SCHÖPKE, C., FAUQUET, C. & BEACHY, R. 1991. Transient gene expression in cassava using high-velocity microprojectiles. *Plant Molecular Biology,* 17**,** 493-498.

FRY, S. 1998. Oxidative scission of plant cell wall polysaccharides by ascorbate-induced hydroxyl radicals. *Biochemical Journal,* 332**,** 507-515.

FUJIMOTO, S. Y., OHTA, M., USUI, A., SHINSHI, H. & OHME-TAKAGI, M. 2000. *Arabidopsis* ethylene-responsive element binding factors act as transcriptional activators or repressors of GCC box–mediated gene expression. *The Plant Cell Online,* 12**,** 393-404.

GECHEV, T., GADJEV, I., VAN BREUSEGEM, F., INZE, D., DUKIANDJIEV, S., TONEVA, V. & MINKOV, I. 2002. Hydrogen peroxide protects tobacco from oxidative stress by inducing a set of antioxidant enzymes. *Cellular and Molecular Life Sciences,* 59**,** 708-714.

GEIGENBERGER, P. 2003. Regulation of sucrose to starch conversion in growing potato tubers. *Journal of Experimental Botany,* 54**,** 457-465.

GILL, S. S., ANJUM, N. A., HASANUZZAMAN, M., GILL, R., TRIVEDI, D. K., AHMAD, I., PEREIRA, E. & TUTEJA, N. 2013. Glutathione and glutathione reductase: A boon in disguise for plant abiotic stress defense operations. *Plant Physiology and Biochemistry,* 70**,** 204-212.

GIRAUD, E., GOSSELIN, L. & RAIMBAULT, M. 1992. Degradation of cassava linamarin by lactic acid bacteria. *Biotechnology Letters,* 14**,** 593-598.

GODA, H., SAWA, S., ASAMI, T., FUJIOKA, S., SHIMADA, Y. & YOSHIDA, S. 2004. Comprehensive comparison of auxin-regulated and brassinosteroid-regulated genes in *Arabidopsis*. *Plant Physiology,* 134**,** 1555-1573.

GÓMEZ-VÁSQUEZ, R., DAY, R., BUSCHMANN, H., RANDLES, S., BEECHING, J. R. & COOPER, R. M. 2004. Phenylpropanoids, phenylalanine ammonia lyase and peroxidases in elicitor-challenged cassava (*Manihot esculenta*) suspension cells and leaves. *Annals of Botany,* 94**,** 87-97.

GOMEZ, L., NOCTOR, G., KNIGHT, M. & FOYER, C. 2004. Regulation of calcium signalling and gene expression by glutathione. *Journal of Experimental Botany,* 55**,** 1851-1859.

GONZALEZ, A. E., SCHOPKE, C., TAYLOR, N. J., BEACHY, R. N. & FAUQUET, C. M. 1998. Regeneration of transgenic cassava plants (*Manihot esculenta* Crantz) through *Agrobacterium*-mediated transformation of embryogenic suspension cultures. *Plant Cell Reports,* 17**,** 827-831.

GRIERSON, C., DU, J. S., ZABALA, M. D., BEGGS, K., SMITH, C., HOLDSWORTH, M. & BEVAN, M. 1994. Separate cis sequences and trans factors direct metabolic and developmental regulation of a potato-tuber storage protein gene. *Plant Journal,* 5**,** 815-826.

GUKASYAN, I., GOLYANOVSKAYA, S., GRISHUNINA, E., KONSTANTINOVA, T., AKSENOVA, N. & ROMANOV, G. 2005. Effect of rol transgenes, IAA, and

kinetin on starch content and the size of starch granules in tubers of *in vitro* potato plants. *Russian Journal of Plant Physiology,* 52**,** 809-813.

GUSTA, L. V., BENNING, N. T., WU, G. H., LUO, X. M., LIU, X. J., GUSTA, M. L. & MCHUGHEN, A. 2009. Superoxide dismutase: an all-purpose gene for agri-biotechnology. *Molecular Breeding,* 24**,** 103-115.

HARMS, K., VON BALLMOOS, P., BRUNOLD, C., HÖFGEN, R. & HESSE, H. 2000. Expression of a bacterial serine acetyltransferase in transgenic potato plants leads to increased levels of cysteine and glutathione. *The Plant Journal,* 22**,** 335-343.

HATTORI, T., FUKUMOTO, H., NAKAGAWA, S. & NAKAMURA, K. 1991. Sucrose-induced expression of genes coding for the tuberous root storage protein, sporamin, of sweet potato in leaves and petioles. *Plant and Cell Physiology,* 32**,** 79-86.

HEMAVATHI, UPADHYAYA, C. P., YOUNG, K. E., AKULA, N., KIM, H. S., HEUNG, J. J., OH, O. M., ASWATH, C. R., CHUN, S. C., KIM, D. H. & PARK, S. W. 2009. Over-expression of strawberry d-galacturonic acid reductase in potato leads to accumulation of vitamin C with enhanced abiotic stress tolerance. *Plant Science,* 177**,** 659-667.

HIGO, K., UGAWA, Y., IWAMOTO, M. & KORENAGA, T. 1999. Plant cis-acting regulatory DNA elements (PLACE) database: 1999. *Nucleic Acids Research,* 27**,** 297-300.

HILLOCKS, R. J. & JENNINGS, D. L. 2003. Cassava brown streak disease: a review of present knowledge and research needs. *International Journal of Pest Management,* 49**,** 225-234.

HIROSE, S. & DATA, E. S. 1984. Physiology of postharvest deterioration of cassava roots. *In:* URITANI, I. & REYES, E. D. (eds.) *Tropical Root Crops: Postharvest Physiology and Processing.* Tokyo: Japan Scientific Societies Press.

HIROSE, S., DATA, E. S. & QUEVEDO, M. A. 1984. Changes in respiration and ethylene production in cassava roots in relation to postharvest deterioration. *In:* URITANI, I. & REYES, E. D. (eds.) *Tropical Root Crops: Postharvest Physiology and Processing.* Tokyo: Japan Scientific Societies Press.

HIROSE, S., DATA, E. S. & URITANI, I. 1983. Some observations on post-harvest deterioration of cassava (*Manihot esculenta* Crantz) roots. *Japanese Journal of Tropical Agriculture,* 27**,** 149-157.

HIRSCHBERG, H. J. H. B., SIMONS, J.-W. F. A., DEKKER, N. & EGMOND, M. R. 2001. Cloning, expression, purification and characterization of patatin, a novel phospholipase A. *European Journal of Biochemistry,* 268**,** 5037-5044.

HOLT, N. E., ZIGMANTAS, D., VALKUNAS, L., LI, X.-P., NIYOGI, K. K. & FLEMING, G. R. 2005. Carotenoid cation formation and the regulation of photosynthetic light harvesting. *Science,* 307**,** 433-436.

HUANG, C.-S., MOORE, W. R. & MEISTER, A. 1988. On the active site thiol of gamma-glutamylcysteine synthetase: relationships to catalysis, inhibition, and regulation. *Proceedings of the National Academy of Sciences,* 85**,** 2464-2468.

IHEMERE, U. 2003. *Somatic Embryogenesis and Transformation of Cassava for Enhanced Starch Production.* PhD, The Ohio State University.

IHEMERE, U., ARIAS-GARZON, D., LAWRENCE, S. & SAYRE, R. 2006. Genetic modification of cassava for enhanced starch production. *Plant Biotechnology Journal,* 4**,** 453-465.

IKEBUCHI, M., KASHIWAGI, A., ASAHINA, T., TANAKA, Y., TAKAGI, Y., NISHIO, Y., HIDAKA, H., KIKKAWA, R. & SHIGETA, Y. 1993. Effect of medium pH on glutathione redox cycle in cultured human umbilical vein endothelial cells. *Metabolism,* 42**,** 1121-1126.

ISAMAH, G. K. 2004. ATPase, peroxidase and lipoxygenase activity during post-harvest deterioration of cassava (*Manihot esculenta* Crantz) root tubers. *International Biodeterioration & Biodegradation,* 54**,** 319-323.

ISAMAH, G. K., ASAGBA, S. O. & EKAKITIE, A. O. 2003. Lipid peroxidation, activities of superoxide dismutase and catalase during post-harvest deterioration of cassava (*Manihot esculenta* Crantz) root tubers. *International Biodeterioration & Biodegradation,* 52**,** 129-133.

ISHIKAWA, T., DOWDLE, J. & SMIRNOFF, N. 2006. Progress in manipulating ascorbic acid biosynthesis and accumulation in plants. *Physiologia Plantarum,* 126**,** 343-355.

JANSSON, C., WESTERBERGH, A., ZHANG, J. M., HU, X. W. & SUN, C. X. 2009. Cassava, a potential biofuel crop in (the) People's Republic of China. *Applied Energy,* 86**,** S95-S99.

JEZ, J. M., CAHOON, R. E. & CHEN, S. 2004. *Arabidopsis thaliana* glutamate-cysteine ligase functional properties, kinetic mecanism and regulation of activity. *Journal of Biological Chemistry,* 279**,** 33463-33470.

JIANG, M. & ZHANG, J. 2001. Effect of abscisic acid on active oxygen species, antioxidative defence system and oxidative damage in leaves of maize seedlings. *Plant and Cell Physiology,* 42**,** 1265-1273.

JORGE, M. A. 2008. Regeneration guidelines: Cassava. *In:* DULLOO, M. E., THORMANN, I., JORGE, M. A. & HANSON, J. (eds.) *Crop specific regeneration guidelines.* Rome, Italy: CGIAR System-wide Genetic Resource Programm.

JUNG, S., KERNODLE, S. P. & SCANDALIOS, J. G. 2001. Differential antioxidant responses to norflurazon-induced oxidative stress in maize. *Redox Report,* 6**,** 311-317.

KAGAYA, Y., OHMIYA, K. & HATTORI, T. 1999. RAV1, a novel DNA-binding protein, binds to bipartite recognition sequence through two distinct DNA-binding domains uniquely found in higher plants. *Nucleic Acids Research,* 27**,** 470-478.

KATO, M. D. A., DECARVALHO, V. D. & CORREA, H. 1991. Effects of pruning on physiological deterioration, enzymatic activity and phenolic compound levels in cassava roots. *Pesquisa Agropecuaria Brasileira,* 26**,** 237-245.

KEMP, B. P., BEECHING, J. R. & COOPER, R. M. 2005. cDNA-AFLP reveals genes differentially expressed during the hypersensitive response of cassava. *Molecular Plant Pathology,* 6**,** 113-123.

KIM, S., MAY, G. & PARK, W. 1994. Nuclear protein factors binding to a class I patatin promoter region are tuber-specific and sucrose-inducible. *Plant Molecular Biology,* 26**,** 603-615.

KOEHORST-VAN PUTTEN, H. J., WOLTERS, A.-M., PEREIRA-BERTRAM, I., BERG, H. J., KROL, A. & VISSER, R. F. 2012. Cloning and characterization of a tuberous root-specific promoter from cassava (*Manihot esculenta* Crantz). *Planta,* 236**,** 1955-1965.

KOSTER-TOPFER, M., FROMMER, W. B., ROCHA-SOSA, M., ROSAHL, S., SCHELL, J. & WILLMITZER, L. 1989. A class-II patatin promoter is under

developmental control in both transgenic potato and tobacco plants *Molecular and General Genetics,* 219**,** 390-396.

KWON, S. Y., JEONG, Y. J., LEE, H. S., KIM, J. S., CHO, K. Y., ALLEN, R. D. & KWAK, S. S. 2002. Enhanced tolerances of transgenic tobacco plants expressing both superoxide dismutase and ascorbate peroxidase in chloroplasts against methyl viologen-mediated oxidative stress. *Plant, Cell & Environment,* 25**,** 873-882.

LEBOT, V. 2009. *Tropical Root and Tuber Crops: Cassava, Sweet Potato, Yams and Aroids*, CABI.

LEE, H. S., KIM, K. Y., YOU, S. H., KWON, S. Y. & KWAK, S. S. 1999. Molecular characterization and expression of a cDNA encoding copper/zinc superoxide dismutase from cultured cells of cassava (*Manihot esculenta* Crantz). *Molecular and General Genetics,* 262**,** 807-814.

LEE, S.-H., AHSAN, N., LEE, K.-W., KIM, D.-H., LEE, D.-G., KWAK, S.-S., KWON, S.-Y., KIM, T.-H. & LEE, B.-H. 2007. Simultaneous overexpression of both CuZn superoxide dismutase and ascorbate peroxidase in transgenic tall fescue plants confers increased tolerance to a wide range of abiotic stresses. *Journal of Plant Physiology,* 164**,** 1626-1638.

LEGG, J. P. & FAUQUET, C. M. 2004. Cassava mosaic geminiviruses in Africa. *Plant Molecular Biology,* 56**,** 585-599.

LEÓN, J., ROJO, E. & SÁNCHEZ-SERRANO, J. J. 2001. Wound signalling in plants. *Journal of Experimental Botany,* 52**,** 1-9.

LEOTARD, G., DUPUTIE, A., KJELLBERG, F., DOUZERY, E. J. P., DEBAIN, C., DE GRANVILLE, J. J. & MCKEY, D. 2009. Phylogeography and the origin of cassava: New insights from the northern rim of the Amazonian basin. *Molecular Phylogenetics and Evolution,* 53**,** 329-334.

LI, S., WAN, C., KONG, J., ZHANG, Z., LI, Y. & ZHU, Y. 2004. Programmed cell death during microgenesis in a Honglian CMS line of rice is correlated with oxidative stress in mitochondria. *Functional Plant Biology,* 31**,** 369-376.

LI, Y., DANKHER, O. P., CARREIRA, L., SMITH, A. P. & MEAGHER, R. B. 2006. The shoot-specific expression of gamma-glutamylcysteine synthetase directs the long-distance transport of thiol-peptides to roots conferring tolerance to mercury and arsenic. *Plant Physiology,* 141**,** 288-298.

LI, Y. & SCHELLHORN, H. E. 2007. Rapid kinetic microassay for catalase activity. *Journal of Biomolecular Techniques,* 18**,** 185.

LIN, A., WANG, Y., TANG, J., XUE, P., LI, C., LIU, L., HU, B., YANG, F., LOAKE, G. J. & CHU, C. 2012. Nitric oxide and protein S-nitrosylation are integral to hydrogen peroxide-induced leaf cell death in rice. *Plant Physiology,* 158**,** 451-464.

LINSTER, C. L. & CLARKE, S. G. 2008. L-Ascorbate biosynthesis in higher plants: the role of VTC2. *Trends in Plant Science,* 13**,** 567-573.

LIU, X. J., PRAT, S., WILLMITZER, L. & FROMMER, W. B. 1990. Cis regulatory elements directing tuber-specific and sucrose-inducible expression of a chimeric class-I patatin promoter GUS-gene fusion. *Molecular and General Genetics,* 223**,** 401-403.

LIU, Y.-W., HAN, C.-H., LEE, M.-H., HSU, F.-L. & HOU, W.-C. 2003. Patatin, the tuber storage protein of potato (*Solanum tuberosum* l.), exhibits antioxidant activity *in vitro*. *Journal of Agricultural and Food Chemistry,* 51**,** 4389-4393.

LOAIZA, J. & CANTWELL, M. 1997. Postharvest physiology and quality of cilantro (*Coriandrum sativum L.*). *Horticultural Science,* 32**,** 104-107.

LOEW, O. 1900. A new enzyme of general occurrence in organisms. *Science,* 11**,** 701-702.

LUONG, H. T., SHEWRY, P. R. & LAZZERI, P. A. 1995. Transient expression in cassava somatic embryos by tissue electroporation. *Plant Science,* 107**,** 105-115.

MACRAE, A., VISICCHIO, J. & LANOT, A. 1998. Application of potato lipid acyl hydrolase for the synthesis of monoacylglycerols. *Journal of the American Oil Chemists' Society,* 75**,** 1489-1494.

MARFO, E. K., SIMPSON, B. K., IDOWU, J. S. & OKE, O. L. 1990. Effect of local food processing on phytate levels in cassava, cocoyam, yam, maize, sorghum, rice, cowpea, and soybean. *Journal of Agricultural and Food Chemistry,* 38**,** 1580-1585.

MARRIOTT, J., BEEN, B. O. & PERKINS, C. 1978. The aetiology of vascular discoloration in cassava roots after harvesting: association with water loss from wounds. *Physiologia Plantarum,* 44**,** 38-42.

MARRIOTT, J., BEEN, B. O. & PERKINS, C. 1979. The aetiology of vascular discoloration in cassava roots after harvesting: development of endogenous resistance in stored roots. *Physiologia Plantarum,* 45**,** 51-56.

MARRIOTT, J., PLUMBLEY, R., RICKARD, J., HURD, R., BISCOE, P. & DENNIS, C. 1980. Opportunities for Increasing Crop Yields. *In:* HURD, R. B., P. DENNIS, C. (ed.) *Physiological aspects of the storage of cassava and other tropical crops.* London: Pitman.

MARTIN, T., HELLMANN, H., SCHMIDT, R., WILLMITZER, L. & FROMMER, W. B. 1997. Identification of mutants in metabolically regulated gene expression. *Plant Journal,* 11**,** 53-62.

MATARASSO, N., SCHUSTER, S. & AVNI, A. 2005. A novel plant cysteine protease has a dual function as a regulator of 1-aminocyclopropane-1-carboxylic acid synthase gene expression. *The Plant Cell Online,* 17**,** 1205-1216.

MAXWELL, D. P., WANG, Y. & MCINTOSH, L. 1999. The alternative oxidase lowers mitochondrial reactive oxygen production in plant cells. *Proceedings of the National Academy of Sciences of the United States of America,* 96**,** 8271-8276.

MAY, M. J., VERNOUX, T., LEAVER, C., MONTAGU, M. V. & INZÉ, D. 1998. Glutathione homeostasis in plants: implications for environmental sensing and plant development. *Journal of Experimental Botany,* 49**,** 649-667.

MBANZIBWA, D. R., TIAN, Y. P., TUGUME, A. K., PATIL, B. L., YADAV, J. S., BAGEWADI, B., ABARSHI, M. M., ALICAI, T., CHANGADEYA, W., MKUMBIRA, J., MULI, M. B., MUKASA, S. B., TAIRO, F., BAGUMA, Y., KYAMANYWA, S., KULLAYA, A., MARUTHI, M. N., FAUQUET, C. M. & VALKONEN, J. P. T. 2011. Evolution of cassava brown streak disease-associated viruses. *Journal of General Virology,* 92**,** 974-987.

MCKERSIE, B. D., MURNAGHAN, J., JONES, K. S. & BOWLEY, S. R. 2000. Iron-superoxide dismutase expression in transgenic alfalfa increases winter survival without a detectable increase in photosynthetic oxidative stress tolerance. *Plant Physiology,* 122**,** 1427-1438.

MEDINA, R. D., FALOCI, M. M., GONZALEZ, A. M. & MROGINSKI, L. A. 2007. *In vitro* cultured primary roots derived from stem segments of cassava (*Manihot esculenta*) can behave like storage organs. *Annals of Botany,* 99**,** 409-423.

MELCHIORRE, M., ROBERT, G., TRIPPI, V., RACCA, R. & LASCANO, H. R. 2009. Superoxide dismutase and glutathione reductase overexpression in wheat protoplast: photooxidative stress tolerance and changes in cellular redox state. *Plant Growth Regulation,* 57**,** 57-68.

MIGNERY, G. A., PIKAARD, C. S., HANNAPEL, D. J. & PARK, W. D. 1984. Isolation and sequence analysis of cDNAs for the major potato tuber protein, patatin. *Nucleic Acids Research* 12**,** 7987-8000.

MIGNERY, G. A., PIKAARD, C. S. & PARK, W. D. 1988. Molecular characterization of the patatin multigene family of potato. *Gene,* 62**,** 27-44.

MIWA, S., MULLER, F. & BECKMAN, K. 2008. The Basics of Oxidative Biochemistry. *In:* MIWA, S., BECKMAN, K. & MULLER, F. (eds.) *Oxidative Stress in Aging.* Humana Press.

MLINGI, N. L. & BAINBRIDGE, Z. Year. Reduction of cyanogen levels during sun-drying of cassava in Tanzania. *In:* International Workshop on Cassava Safety 375, 1994. 233-240.

MOLLER, I. M., JENSEN, P. E. & HANSSON, A. 2007. Oxidative modifications to cellular components in plants. *Annual Review of Plant Biology,* 58**,** 459-481.

MORANTE, N., SANCHEZ, T., CEBALLOS, H., CALLE, F., PEREZ, J. C., EGESI, C., CUAMBE, C. E., ESCOBAR, A. F., ORTIZ, D., CHAVEZ, A. L. & FREGENE, M. 2010. Tolerance to postharvest physiological deterioration in cassava roots. *Crop Science,* 50**,** 1333-1338.

MURGIA, I., TARANTINO, D., VANNINI, C., BRACALE, M., CARRAVIERI, S. & SOAVE, C. 2004. *Arabidopsis thaliana* plants overexpressing thylakoidal ascorbate peroxidase show increased resistance to Paraquat- induced photooxidative stress and to nitric oxide-induced cell death. *Plant Journal,* 38**,** 940-953.

MURSHED, R., LOPEZ-LAURI, F. & SALLANON, H. 2008. Microplate quantification of enzymes of the plant ascorbate-glutathione cycle. *Analytical Biochemistry,* 383**,** 320-322.

NARAYANAN, N. N., IHEMERE, U., ELLERY, C. & SAYRE, R. T. 2011. Overexpression of hydroxynitrile lyase in cassava roots elevates protein and free amino acids while reducing residual cyanogen levels. *PloS One,* 6**,** e21996.

NASSAR, N. & ORTIZ, R. 2010. Breeding cassava to feed the poor. *Scientific American,* 302**,** 78-84.

NAUMKINA, E., BOLYAKINA, Y. P. & ROMANOV, G. 2007. Organ-specificity and inducibility of patatin class I promoter from potato in transgenic *Arabidopsis* plants. *Russian Journal of Plant Physiology,* 54**,** 350-359.

NAVROT, N., ROUHIER, N., GELHAYE, E. & JACQUOT, J. P. 2007. Reactive oxygen species generation and antioxidant systems in plant mitochondria. *Physiologia Plantarum,* 129**,** 185-195.

NEILL, S., DESIKAN, R. & HANCOCK, J. 2002. Hydrogen peroxide signalling. *Current Opinion in Plant Biology,* 5**,** 388-395.

NJOKU, D. N., VERNON, G., EGESI, C. N., ASANTE, I., OFFEI, S. K., OKOGBENIN, E., KULAKOW, P., EKE-OKORO, O. N. & CEBALLOS, H. 2011. Breeding for

Enhanced β-Carotene Content in Cassava: Constraints and Accomplishments. *Journal of Crop Improvement,* 25**,** 560-571.

NOCTOR, G. & FOYER, C. H. 1998. Ascorbate and glutathione: keeping active oxygen under control. *Annual Review of Plant Physiology and Plant Molecular Biology,* 49**,** 249-279.

NOCTOR, G., GOMEZ, L., VANACKER, H. & FOYER, C. H. 2002. Interactions between biosynthesis, compartmentation and transport in the control of glutathione homeostasis and signalling. *Journal of Experimental Botany,* 53**,** 1283-1304.

NOON, R. A. & BOOTH, R. H. 1977. Nature of post-harvest deterioration of cassava roots. *Transactions of the British Mycological Society,* 69**,** 287-290.

NZWALO, H. & CLIFF, J. 2011. Konzo: from poverty, cassava, and cyanogen intake to toxico-nutritional neurological disease. *Plos Neglected Tropical Diseases,* 5**,** e1051.

OGAWA, K. I., HATANO-IWASAKI, A., YANAGIDA, M. & IWABUCHI, M. 2004. Level of glutathione is regulated by ATP-dependent ligation of glutamate and cysteine through photosynthesis in *Arabidopsis thaliana*: mechanism of strong interaction of light intensity with flowering. *Plant and Cell Physiology,* 45**,** 1-8.

OKE, O. L. Year. Eliminating cyanogens from cassava through processing: technology and tradition. *In:* International Workshop on Cassava Safety 375, 1994. 163-174.

OLLER, A. L. W., AGOSTINI, E., MILRAD, S. R. & MEDINA, M. I. 2009. *In situ* and *de novo* biosynthesis of vitamin C in wild type and transgenic tomato hairy roots: A precursor feeding study. *Plant Science,* 177**,** 28-34.

OLSEN, K. M. 2004. SNPs, SSRs and inferences on cassava's origin. *Plant Molecular Biology,* 56**,** 517-526.

ORRENIUS, S. 2007. Reactive oxygen species in mitochondria-mediated cell death. *Drug Metabolism Reviews,* 39**,** 443-455.

OWITI, J., GROSSMANN, J., GEHRIG, P., DESSIMOZ, C., LALOI, C., HANSEN, M. B., GRUISSEM, W. & VANDERSCHUREN, H. 2011. iTRAQ-based analysis of changes in the cassava root proteome reveals pathways associated with post-harvest physiological deterioration. *The Plant Journal,* 67**,** 145-156.

OWITI, J. A. 2009. *Molecular and Biochemical Understanding of Post-harvest Physiological Deterioration in Cassava Roots and Approaches for its Modulation.* PhD, Swiss Federal Institute of Technology.

PAGE, M. 2009. *Modulation of root antioxidant status to delay cassava post-harvest physiological deterioration.* PhD, University of Bath.

PARK, J.-S., KIM, J.-B., CHO, K.-J., CHEON, C.-I., SUNG, M.-K., CHOUNG, M.-G. & ROH, K.-H. 2008. *Arabidopsis* R2R3-MYB transcription factor AtMYB60 functions as a transcriptional repressor of anthocyanin biosynthesis in lettuce (*Lactuca sativa*). *Plant Cell Reports,* 27**,** 985-994.

PASTUGLIA, M., ROBY, D., DUMAS, C. & COCK, J. M. 1997. Rapid induction by wounding and bacterial infection of an S gene family receptor-like kinase gene in *Brassica oleracea*. *The Plant Cell Online,* 9**,** 49-60.

PEÑA-CORTÉS, H., LIU, X., SERRANO, J. S., SCHMID, R. & WILLMITZER, L. 1992. Factors affecting gene expression of patatin and proteinase-inhibitor-II gene families in detached potato leaves. *Planta,* 186**,** 495-502.

PFAFFL, M. W. 2001. A new mathematical model for relative quantification in real-time RT–PCR. *Nucleic Acids Research,* 29**,** e45.

PRASHANTH, S. R., SADHASIVAM, V. & PARIDA, A. 2008. Over expression of cytosolic copper/zinc superoxide dismutase from a mangrove plant *Avicennia marina* in indica Rice var Pusa Basmati-1 confers abiotic stress tolerance. *Transgenic Research,* 17**,** 281-291.

PRESTRIDGE, D. S. 1991. SIGNAL SCAN: a computer program that scans DNA sequences for eukaryotic transcriptional elements. *Computer Applications in the Biosciences: CABIOS,* 7**,** 203-206.

QUEVAL, G., THOMINET, D., VANACKER, H., MIGINIAC-MASLOW, M., GAKIÈRE, B. & NOCTOR, G. 2009. H_2O_2-activated up-regulation of glutathione in *Arabidopsis* involves induction of genes encoding enzymes involved in cysteine synthesis in the chloroplast. *Molecular Plant,* 2**,** 344-356.

RAEMAKERS, C. J. J. M., SOFIARI, E., TAYLOR, N., HENSHAW, G., JACOBSEN, E. & VISSER, R. G. F. 1996. Production of transgenic cassava (*Manihot esculenta* Crantz) plants by particle bombardment using luciferase activity as selection marker. *Molecular Breeding,* 2**,** 339-349.

RAHANTANIAINA, M.-S., TUZET, A., MHAMDI, A. & NOCTOR, G. 2013. Missing links in understanding redox signaling via thiol/disulfide modulation: How is glutathione oxidized in plants? *Frontiers in Plant Science,* 4.

RAO, M. V., PALIYATH, G., ORMROD, D. P., MURR, D. P. & WATKINS, C. B. 1997. Influence of salicylic acid on H_2O_2 production, oxidative stress, and H_2O_2-metabolizing enzymes (salicylic acid-mediated oxidative damage requires H_2O_2). *Plant Physiology,* 115**,** 137-149.

REDDY, C. D. & VENKAIAH, B. 1984. Purification and characterization of Cu-Zn superoxide dismutases from mungbean (*Vigna radiata*) seedlings. *Journal of Biosciences,* 6**,** 115-123.

REES, D., WESTBY, A., TOMLINS, K.,VAN OIRSHOT, Q.,CHEEMA, M., CORNELIUS, E., AMJAD M. (ed.) 2012. *Crop Post-harvest Science and Technology*: Blackwell Publishing Ltd.

REILLY, K. 2001. *Oxidative stress related genes in cassava post-harvest physiological deterioration.* PhD, University of Bath.

REILLY, K., BERNAL, D., CORTES, D. F., GOMEZ-VASQUEZ, R., TOHME, J. & BEECHING, J. R. 2007. Towards identifying the full set of genes expressed during cassava post-harvest physiological deterioration. *Plant Molecular Biology,* 64**,** 187-203.

REILLY, K., GÓMEZ-VÁSQUEZ, R., BUSCHMANN, H., TOHME, J. & BEECHING, J. R. 2003. Oxidative stress responses during cassava post-harvest physiological deterioration. *Plant Molecular Biology,* 53**,** 669-685.

REILLY, K., GÓMEZ-VÁSQUEZ, R., BUSCHMANN, H., TOHME, J. & BEECHING, J. R. 2004. Oxidative stress responses during cassava post-harvest physiological deterioration. *Plant Molecular Biology,* 56, 625-641.

RICHMAN, P. G. & MEISTER, A. 1975. Regulation of gamma-glutamyl-cysteine synthetase by nonallosteric feedback inhibition by glutathione. *Journal of Biological Chemistry,* 250**,** 1422-1426.

RICKARD, J. E. & COURSEY, D. G. 1981. Cassava storage. Part 1: Storage of fresh cassava roots. *Tropical Science,* 23**,** 1-32.

RICKARD, J. E. & GAHAN, P. B. 1983. The development of occlusions in cassava (*Manihot esculenta* Crantz) root xylem vessels. *Annals of Botany,* 52**,** 811-821.

RICKARD, J. E., MARRIOTT, J. & GAHAN, P. B. 1979. Occlusions in cassava xylem vessels associated with vascular discoloration. *Annals of Botany,* 43**,** 523-526.

RO, D. K. & DOUGLAS, C. J. 2004. Reconstitution of the entry point of plant phenylpropanoid metabolism in yeast *(Saccharomyces cerevisiae)* - Implications for control of metabolic flux into the phenylpropanoid pathway. *Journal of Biological Chemistry,* 279**,** 2600-2607.

ROA, A. C., CHAVARRIAGA-AGUIRRE, P., DUQUE, M. C., MAYA, M. M., BONIERBALE, M. W., IGLESIAS, C. & TOHME, J. 2000. Cross-species amplification of cassava (*Manihot esculenta*) (Euphorbiaceae) microsatellites: allelic polymorphism and degree of relationship. *American Journal of Botany,* 87**,** 1647-1655.

ROCHA-SOSA, M., SONNEWALD, U., FROMMER, W., STRATMANN, M., SCHELL, J. & WILLMITZER, L. 1989. Both developmental and metabolic signals activate the promoter of a class I patatin gene. *The EMBO Journal,* 8**,** 23.

RODRÍGUEZ-FALCÓN, M., BOU, J. & PRAT, S. 2006. Seasonal control of tuberization in potato: conserved elements with the flowering response. *Annual Review of Plant Biology,* 57**,** 151-180.

RODRIGUEZ, M. X. 2001. *Towards identifying markers for post-harvest physiological deterioration in cassava.* PhD, University of Bath.

ROMANOV, G. 2009. How do cytokinins affect the cell? *Russian Journal Of Plant Physiology,* 56**,** 268-290.

ROMBAUTS, S., DÉHAIS, P., VAN MONTAGU, M. & ROUZÉ, P. 1999. PlantCARE, a plant cis-acting regulatory element database. *Nucleic Acids Research,* 27**,** 295-296.

ROMERO-PUERTAS, M. C., CORPAS, F. J., RODRÍGUEZ-SERRANO, M., GÓMEZ, M., DEL RÍO, L. A. & SANDALIO, L. M. 2007. Differential expression and regulation of antioxidative enzymes by cadmium in pea plants. *Journal of Plant Physiology,* 164**,** 1346-1357.

RYDEL, T. J., WILLIAMS, J. M., KRIEGER, E., MOSHIRI, F., STALLINGS, W. C., BROWN, S. M., PERSHING, J. C., PURCELL, J. P. & ALIBHAI, M. F. 2003. The crystal structure, mutagenesis, and activity studies reveal that patatin is a lipid acyl hydrolase with a Ser-Asp catalytic dyad. *Biochemistry,* 42**,** 6696-6708.

SAELIM, L., PHANSIRI, S., SUKSANGPANOMRUNG, M., NETRPHAN, S. & NARANGAJAVANA, J. 2009. Evaluation of a morphological marker selection and excision system to generate marker-free transgenic cassava plants. *Plant Cell Reports,* 28**,** 445-455.

SAIRAM, R. K., RAO, K. V. & SRIVASTAVA, G. 2002. Differential response of wheat genotypes to long term salinity stress in relation to oxidative stress, antioxidant activity and osmolyte concentration. *Plant Science,* 163**,** 1037-1046.

SALCEDO, A., DEL VALLE, A., SANCHEZ, B., OCASIO, V., ORTIZ, A., MARQUEZ, P. & SIRITUNGA, D. 2010. Comparative evaluation of physiological post-harvest root deterioration of 25 cassava (Manihot esculenta) accessions: visual vs. hydroxycoumarins fluorescent accumulation analysis. *African Journal of Agricultural Research,* 5**,** 3138-3144.

SALCEDO, A. & SIRITUNGA, D. 2011. Insights into the physiological, biochemical and molecular basis of postharvest deterioration in cassava (*Manihot esculenta*) roots. *American Journal of Experimental Agriculture,* 1**,** 414-431.

SANCHEZ, T., CHAVEZ, A. L., CEBALLOS, H., RODRIGUEZ-AMAYA, D., NESTEL, P. & ISHITANI, M. 2006. Reduction or delay of post-harvest physiological deterioration in cassava roots with higher carotenoid content. *Journal of the Science of Food and Agriculture,* 86**,** 634-639.

SAROWAR, S., KIM, E. N., KIM, Y. J., OK, S. H., KIM, K. D. & HWANG, B. K. S. J. S. 2005. Overexpression of a pepper ascorbate peroxidase-like 1 gene in tobacco plants enhances tolerance to oxidative stress and pathogens. *Plant Science,* 169**,** 55-63.

SARRIA, R. A., BALCAZAR, N., DESTEFANO BELTRAN, L. & ROCA, W. M. 1995. Progress in Agrobacterium-mediated transformation of cassava (*Manihot esculenta* Crantz). *Working document (CBN; CRIFC; AARD; CIAT).*

SAWYER, D. T. & VALENTINE, J. S. 1981. How super is superoxide? *Accounts of Chemical Research,* 14**,** 393-400.

SCHILMILLER, A. L. & HOWE, G. A. 2005. Systemic signaling in the wound response. *Current Opinion in Plant Biology,* 8**,** 369-377.

SCHNEIDER, C. A., RASBAND, W. S. & ELICEIRI, K. W. 2012. NIH Image to ImageJ: 25 years of image analysis. *Nature Methods,* 9**,** 671-675.

SCHOMBURG, I., CHANG, A., PLACZEK, S., SÖHNGEN, C., ROTHER, M., LANG, M., MUNARETTO, C., ULAS, S., STELZER, M., GROTE, A., SCHEER, M. & SCHOMBURG, D. 2013. BRENDA in 2013: integrated reactions, kinetic data, enzyme function data, improved disease classification: new options and contents in BRENDA. *Nucleic Acids Research,* 41**,** D764-D772.

SCHOPKE, C., TAYLOR, N. J., CARCAMO, R., BEACHY, R. N. & FAUQUET, C. 1997. Optimization of parameters for particle bombardment of embryogenic suspension cultures of cassava (*Manihot esculenta* Crantz) using computer image analysis. *Plant Cell Reports,* 16**,** 526-530.

SHIN, S. Y., LEE, H. S., KWON, S. Y., KWON, S. T. & KWAK, S. S. 2005. Molecular characterization of a cDNA encoding copper/zinc superoxide dismutase from cultured cells of *Manihot esculenta. Plant Physiology and Biochemistry,* 43**,** 55-60.

SIRITUNGA, D. & SAYRE, R. 2004. Engineering cyanogen synthesis and turnover in cassava (*Manihot esculenta*). *Plant Molecular Biology,* 56**,** 661-669.

SIRITUNGA, D. & SAYRE, R. 2007. Transgenic approaches for cyanogen reduction in cassava. *Journal of AOAC International,* 90**,** 1450-1455.

SIRITUNGA, D. & SAYRE, R. T. 2003. Generation of cyanogen-free transgenic cassava. *Planta,* 217**,** 367-373.

SONG, X. S., HU, W. H., MAO, W. H., OGWENO, J. O., ZHOU, Y. H. & YU, J. Q. 2005. Response of ascorbate peroxidase isoenzymes and ascorbate regeneration system to abiotic stresses in *Cucumis sativus* L. *Plant Physiology and Biochemistry,* 43**,** 1082-1088.

SRINIVASAN, T., KUMAR, K. R. R., MEUR, G. & KIRTI, P. B. 2009. Heterologous expression of *Arabidopsis* NPR1 (AtNPR1) enhances oxidative stress tolerance in transgenic tobacco plants. *Biotechnology Letters,* 31**,** 1343-1351.

SRIVASTAVA, S., PATHAK, A. D., GUPTA, P. S., SHRIVASTAVA, A. K. & SRIVASTAVA, A. K. 2012. Hydrogen peroxide-scavenging enzymes impart

tolerance to high temperature induced oxidative stress in sugarcane. *Journal of Environmental Biology* 33**,** 657-661.

STRICKLAND, J. A., ORR, G. L. & WALSH, T. A. 1995. Inhibition of Diabrotica larval growth by patatin, the lipid acyl hydrolase from potato tubers. *Plant Physiology,* 109**,** 667-674.

STUPAR, R. M., BEAUBIEN, K. A., JIN, W. W., SONG, J. Q., LEE, M. K., WU, C. C., ZHANG, H. B., HAN, B. & JIANG, J. M. 2006. Structural diversity and differential transcription of the patatin multicopy gene family during potato tuber development. *Genetics,* 172**,** 1263-1275.

SUGIMOTO, K., TAKEDA, S. & HIROCHIKA, H. 2003. Transcriptional activation mediated by binding of a plant GATA-type zinc finger protein AGP1 to the AG-motif (AGATCCAA) of the wound-inducible Myb gene NtMyb2. *The Plant Journal,* 36**,** 550-564.

SUN, Q., ROST, T. L. & MATTHEWS, M. A. 2008. Wound-induced vascular occlusions in *Vitis vinifera* (Vitaceae): Tyloses in summer and gels in winter1. *American Journal of Botany,* 95**,** 1498-1505.

SZALAI, G., KELLOS, T., GALIBA, G. & KOCSY, G. 2009. Glutathione as an antioxidant and regulatory molecule in plants under abiotic stress conditions. *Journal of Plant Growth Regulation,* 28**,** 66-80.

TAMAGNONE, L., MERIDA, A., PARR, A., MACKAY, S., CULIANEZ-MACIA, F. A., ROBERTS, K. & MARTIN, C. 1998. The AmMYB308 and AmMYB330 transcription factors from Antirrhinum regulate phenylpropanoid and lignin biosynthesis in transgenic tobacco. *The Plant Cell Online,* 10**,** 135-154.

TANAKA, Y., DATA, E. S., HIROSE, S., TANIGUCHI, T. & URITANI, I. 1983. Biochemical changes in secondary metabolites in wounded and deteriorated cassava roots. *Agricultural Biological Chemistry,* 47**,** 693-700.

TANAKA, Y., DATA, E. S., LAPE, V. G., VILLEGAS, C. D., GORGONIO, M., HIROSE, S. & URITANI, I. 1984. Effect of pruning treatment on physiological deterioration in cassava roots. *Agricultural Biological Chemistry,* 48**,** 739-743.

TANG, L., KWON, S. Y., KIM, S. H., KIM, J. S., CHOI, J. S., CHO, K. Y., SUNG, C. K., KWAK, S. S. & LEE, H. S. 2006. Enhanced tolerance of transgenic potato plants expressing both superoxide dismutase and ascorbate peroxidase in chloroplasts against oxidative stress and high temperature. *Plant Cell Reports,* 25**,** 1380-1386.

TAYLOR, S., WAKEM, M., DIJKMAN, G., ALSARRAJ, M. & NGUYEN, M. 2010. A practical approach to RT-qPCR—publishing data that conform to the MIQE guidelines. *Methods,* 50**,** S1-S5.

TEPPERMAN, J. M. & DUNSMUIR, P. 1990. Transformed plants with elevated levels of chloroplastic SOD are not more resistant to superoxide toxicity. *Plant Molecular Biology,* 14**,** 501-511.

TERTIVANIDIS, K., GOUDOULA, C., VASILIKIOTIS, C., HASSIOTOU, E., PERL-TREVES, R. & TSAFTARIS, A. 2004. Superoxide dismutase transgenes in sugarbeets confer resistance to oxidative agents and the fungus *C. beticola. Transgenic Research,* 13**,** 225-233.

TONÓN, C., DALEO, G. & OLIVA, C. 2001. An acidic β-1, 3 glucanase from potato tubers appears to be patatin. *Plant Physiology and Biochemistry,* 39**,** 849-854.

TRIANTAPHYLIDÈS, C., KRISCHKE, M., HOEBERICHTS, F. A., KSAS, B., GRESSER, G., HAVAUX, M., VAN BREUSEGEM, F. & MUELLER, M. J. 2008.

Singlet oxygen is the major reactive oxygen species involved in photooxidative damage to plants. *Plant Physiology,* 148**,** 960-968.

TSENG, M. J., LIU, C.-W. & YIU, J.-C. 2007. Enhanced tolerance to sulfur dioxide and salt stress of transgenic Chinese cabbage plants expressing both superoxide dismutase and catalase in chloroplasts. *Plant Physiology and Biochemistry,* 45**,** 822-833.

UARROTA, V. G., MORESCO, R., COELHO, B., NUNES, E. D. C., PERUCH, L. A. M., NEUBERT, E. D. O., ROCHA, M. & MARASCHIN, M. 2014. Metabolomics combined with chemometric tools (PCA, HCA, PLS-DA and SVM) for screening cassava (*Manihot esculenta* Crantz) roots during postharvest physiological deterioration. *Food Chemistry,* 161**,** 67-78.

ULUKAN, H. 2009. The evolution of cultivated plant species: classical plant breeding versus genetic engineering. *Plant Systematics and Evolution,* 280**,** 133-142.

UNTERGASSER, A., CUTCUTACHE, I., KORESSAAR, T., YE, J., FAIRCLOTH, B. C., REMM, M. & ROZEN, S. G. 2012. Primer3—new capabilities and interfaces. *Nucleic Acids Research,* 40**,** e115-e115.

URITANI, I. 1999. Biochemistry on postharvest metabolism and deterioration of some tropical tuberous crops. *Botanical Bulletin of Academia Sinica,* 40**,** 177-183.

URITANI, I., DATA, E. S. & TANAKA, Y. 1984. Biochemistry of postharvest deterioration of cassava and sweet potato roots. *In:* URITANI, I. & REYES, E. D. (eds.) *Tropical Root Crops: Postharvest Physiology and Processing.* Tokyo: JSSP.

VALKO, M., MORRIS, H. & CRONIN, M. 2005. Metals, toxicity and oxidative stress. *Current Medicinal Chemistry,* 12**,** 1161-1208.

VAN AKEN, O., GIRAUD, E., CLIFTON, R. & WHELAN, J. 2009. Alternative oxidase: a target and regulator of stress responses. *Physiologia Plantarum,* 137**,** 354-361.

VAN OIRSCHOT, Q. E. A., O'BRIEN, G. M., DUFOUR, D., EL-SHARKAWY, M. A. & MESA, E. 2000. The effect of pre-harvest pruning of cassava upon root deterioration and quality characteristics. *Journal of the Science of Food and Agriculture,* 80**,** 1866-1873.

VANDERSCHUREN, H., AKBERGENOV, R., POOGGIN, M. M., HOHN, T., GRUISSEM, W. & ZHANG, P. 2007. Transgenic cassava resistance to African cassava mosaic virus is enhanced by viral DNA-A bidirectional promoter-derived siRNAs. *Plant Molecular Biology,* 64**,** 549-557.

VANDERSCHUREN, H., NYABOGA, E., POON, J. S., BAERENFALLER, K., GROSSMANN, J., HIRSCH-HOFFMANN, M., KIRCHGESSNER, N., NANNI, P. & GRUISSEM, W. 2014. Large-scale proteomics of the cassava storage root and identification of a target gene to reduce postharvest deterioration. *The Plant Cell Online***,** tpc. 114.123927.

VELIKOVA, V., YORDANOV, I. & EDREVA, A. 2000. Oxidative stress and some antioxidant systems in acid rain-treated bean plants: protective role of exogenous polyamines. *Plant Science,* 151**,** 59-66.

VIEWEG, M. F., FRÜHLING, M., QUANDT, H.-J., HEIM, U., BÄUMLEIN, H., PÜHLER, A., KÜSTER, H. & PERLICK, A. M. 2004. The promoter of the *Vicia faba* L. leghemoglobin gene VfLb29 is specifically activated in the infected cells of root nodules and in the arbuscule-containing cells of mycorrhizal roots from different legume and nonlegume plants. *Molecular Plant-Microbe Interactions,* 17**,** 62-69.

VOGT, T. 2010. Phenylpropanoid biosynthesis. *Molecular Plant,* 3**,** 2-20.

WANG, F.-Z., WANG, Q.-B., KWON, S.-Y., KWAK, S.-S. & SU, W.-A. 2005. Enhanced drought tolerance of transgenic rice plants expressing a pea manganese superoxide dismutase. *Journal of Plant Physiology,* 162**,** 465-472.

WANG, W. Year. Cassava production for industrial utilization in China–present and future perspective. *In:* Cassava research and development in Asia: exploring new opportunities for an ancient crop 2002 Bangkok, Thailand. 33-38.

WANG, W. Z., PAN, J. W., ZHENG, K., CHEN, H., SHAO, H. H., GUO, Y. J., BIAN, H. W., HAN, N., WANG, J. H. & ZHU, M. Y. 2009. Ced-9 inhibits Al-induced programmed cell death and promotes Al tolerance in tobacco. *Biochemical and Biophysical Research Communications,* 383**,** 141-145.

WANG, Y., LOAKE, G. J. & CHU, C. 2013. Cross-talk of nitric oxide and reactive oxygen species in plant programed cell death. *Frontiers in Plant Science,* 4.

WANG, Y., QU, G., LI, H., WU, Y., WANG, C., LIU, G. & YANG, C. 2010. Enhanced salt tolerance of transgenic poplar plants expressing a manganese superoxide dismutase from *Tamarix androssowii. Molecular Biology Reports,* 37**,** 1119-1124.

WENHAM, J. E. 1995. *Post-harvest Deterioration of Cassava. A Biotechnological Perspective,* Rome, FAO.

WENZLER, H. C., MIGNERY, G. A., FISHER, L. M. & PARK, W. D. 1989. Analysis of a chimeric class-I patatin-GUS gene in transgenic potato plants: high-level expression in tubers and sucrose-inducible expression in cultured leaf and stem explants. *Plant Molecular Biology,* 12**,** 41-50.

WESTBY, A. 2002. Cassava utilization, storage and small-scale processing. *In:* HILLOCKS, R. J., THRESH, J. M. & BELLOTTI, A. C. (eds.) *Cassava: Biology, Production and Utilization.* Wallingford: CABI.

WHEATLEY, C., LOZANO, C. & GOMEZ, G. 1985. Post-harvest deterioration of cassava roots. *In:* COCK, J. H. & REYES, J. A. (eds.) *Cassava Research, Production and Utilization.* Cali, Colombia: UNDP-CIAT.

WHEATLEY, C. C. & SCHWABE, W. W. 1985. Scopoletin involvement in post-harvest physiological deterioration of cassava root (*Manihot esculenta* Crantz). *Journal of Experimental Botany,* 36**,** 783-791.

WHEELER, G. L., JONES, M. A. & SMIRNOFF, N. 1998. The biosynthetic pathway of vitamin C in higher plants. *Nature,* 393**,** 365-369.

WILLEKENS, H., CHAMNONGPOL, S., DAVEY, M., SCHRAUDNER, M., LANGEBARTELS, C., VAN MONTAGU, M., INZÉ, D. & VAN CAMP, W. 1997. Catalase is a sink for H_2O_2 and is indispensable for stress defence in C3 plants. *The EMBO Journal,* 16**,** 4806-4816.

WOBETO, C., CORRÊA, A. D., ABREU, C. M. P. D., SANTOS, C. D. D. & ABREU, J. R. D. 2006. Nutrients in the cassava (*Manihot esculenta* Crantz) leaf meal at three ages of the plant. *Food Science and Technology (Campinas),* 26**,** 865-869.

WOJTASZEK, P. 1997. Oxidative burst: An early plant response to pathogen infection. *Biochemical Journal,* 322**,** 681-692.

WOLUCKA, B. A. & VAN MONTAGU, M. 2003. GDP-mannose 3′,5′-epimerase forms GDP-L-gulose, a putative intermediate for the *de novo* biosynthesis of vitamin C in plants. *Journal of Biological Chemistry,* 278**,** 47483-47490.

WOLUCKA, B. A. & VAN MONTAGU, M. 2007. The VTC2 cycle and the *de novo* biosynthesis pathways for vitamin C in plants: An opinion. *Phytochemistry,* 68**,** 2602-2613.

XU, J., DUAN, X., YANG, J., BEECHING, J. R. & ZHANG, P. 2013a. Coupled expression of Cu/Zn-superoxide dismutase and catalase in cassava improves tolerance against cold and drought stresses. *Plant Signaling and Behavior,* 8**,** e24525.

XU, J., DUAN, X. G., YANG, J., BEECHING, J. R. & ZHANG, P. 2013b. Enhanced reactive oxygen species scavenging by overproduction of superoxide dismutase and catalase delays postharvest physiological deterioration of cassava storage roots. *Plant Physiology,* 161**,** 1517-1528.

XU, X., PAN, S. K., CHENG, S. F., ZHANG, B., MU, D. S., NI, P. X., ZHANG, G. Y., YANG, S., LI, R. Q., WANG, J., ORJEDA, G., GUZMAN, F., TORRES, M., LOZANO, R., PONCE, O., MARTINEZ, D., DE LA CRUZ, G., CHAKRABARTI, S. K., PATIL, V. U., SKRYABIN, K. G., KUZNETSOV, B. B., RAVIN, N. V., KOLGANOVA, T. V., BELETSKY, A. V., MARDANOV, A. V., DI GENOVA, A., BOLSER, D. M., MARTIN, D. M. A., LI, G. C., YANG, Y., KUANG, H. H., HU, Q., XIONG, X. Y., BISHOP, G. J., SAGREDO, B., MEJIA, N., ZAGORSKI, W., GROMADKA, R., GAWOR, J., SZCZESNY, P., HUANG, S. W., ZHANG, Z. H., LIANG, C. B., HE, J., LI, Y., HE, Y., XU, J. F., ZHANG, Y. J., XIE, B. Y., DU, Y. C., QU, D. Y., BONIERBALE, M., GHISLAIN, M., HERRERA, M. D., GIULIANO, G., PIETRELLA, M., PERROTTA, G., FACELLA, P., O'BRIEN, K., FEINGOLD, S. E., BARREIRO, L. E., MASSA, G. A., DIAMBRA, L., WHITTY, B. R., VAILLANCOURT, B., LIN, H. N., MASSA, A., GEOFFROY, M., LUNDBACK, S., DELLAPENNA, D., BUELL, C. R., SHARMA, S. K., MARSHALL, D. F., WAUGH, R., BRYAN, G. J., DESTEFANIS, M., NAGY, I., MILBOURNE, D., THOMSON, S. J., FIERS, M., JACOBS, J. M. E., NIELSEN, K. L., SONDERKAER, M., IOVENE, M., TORRES, G. A., JIANG, J. M., VEILLEUX, R. E., BACHEM, C. W. B., DE BOER, J., BORM, T., KLOOSTERMAN, B., VAN ECK, H., DATEMA, E., HEKKERT, B. T. L., GOVERSE, A., VAN HAM, R. C. H. J., VISSER, R. G. F. & CONSORTIU, P. G. S. 2011. Genome sequence and analysis of the tuber crop potato. *Nature,* 475**,** 189-U94.

XU, X., VAN LAMMEREN, A. A., VERMEER, E. & VREUGDENHIL, D. 1998. The role of gibberellin, abscisic acid, and sucrose in the regulation of potato tuber formation in vitro. *Plant Physiology,* 117**,** 575-584.

XU, Y., ZHU, X., CHEN, Y., GONG, Y. & LIU, L. 2013c. Expression profiling of genes involved in ascorbate biosynthesis and recycling during fleshy root development in radish. *Plant Physiology and Biochemistry,* 70**,** 269-277.

YOKOTANI, N., TAMURA, S., NAKANO, R., INABA, A., MCGLASSON, W. B. & KUBO, Y. 2004. Comparison of ethylene-and wound-induced responses in fruit of wild-type*,rin* and *nor* tomatoes. *Postharvest Biology and Technology,* 32**,** 247-252.

YOO, S. Y., BOMBLIES, K., YOO, S. K., YANG, J. W., CHOI, M. S., LEE, J. S., WEIGEL, D. & AHN, J. H. 2005. The 35S promoter used in a selectable marker gene of a plant transformation vector affects the expression of the transgene. *Planta,* 221**,** 523-530.

YOU, S. H., KIM, S.W., KIM,S.H., LIU,J.R., KWAK S.S. 1996. Selection and isoenzyme analysis of plant cell lines for high yields of superoxide dismutase. *Korean Journal Plant Tissue Culture,* 23**,** 103-106.

ZEIDA, A., BABBUSH, R., GONZÁLEZ LEBRERO, M. C., TRUJILLO, M., RADI, R. & ESTRIN, D. A. 2012. Molecular basis of the mechanism of thiol oxidation by hydrogen peroxide in aqueous solution: challenging the SN2 paradigm. *Chemical Research in Toxicology,* 25**,** 741-746.

ZHANG, C., HAN, W. J., JING, X. D., PU, G. Q. & WANG, C. T. 2003a. Life cycle economic analysis of fuel ethanol derived from cassava in southwest China. *Renewable and Sustainable Energy Reviews,* 7**,** 353-366.

ZHANG, P., BOHL-ZENGER, S., PUONTI-KAERLAS, J., POTRYKUS, I. & GRUISSEM, W. 2003b. Two cassava promoters related to vascular expression and storage root formation. *Planta,* 218**,** 192-203.

ZHANG, P., POTRYKUS, I. & PUONTI-KAERLAS, J. 2000. Efficient production of transgenic cassava using negative and positive selection. *Transgenic Research,* 9**,** 405-415.

ZHANG, P., VANDERSCHUREN, H., FUTTERER, J. & GRUISSEM, W. 2005. Resistance to cassava mosaic disease in transgenic cassava expressing antisense RNAs targeting virus replication genes. *Plant Biotechnology Journal,* 3**,** 385-397.

ZHENG, X., DENG, W., LUO, K., DUAN, H., CHEN, Y., MCAVOY, R., SONG, S., PEI, Y. & LI, Y. 2007. The cauliflower mosaic virus (CaMV) 35S promoter sequence alters the level and patterns of activity of adjacent tissue-and organ-specific gene promoters. *Plant Cell Reports,* 26**,** 1195-1203.

ZHOU, L. & THORNBURG, R. 1999. Wound-inducible genes in plants. *Inducible Gene Expression in Plants***,** 127-58.

ZIDENGA, T., LEYVA-GUERRERO, E., MOON, H., SIRITUNGA, D. & SAYRE, R. 2012. Extending cassava root shelf life via reduction of reactive oxygen species production. *Plant Physiology,* 159**,** 1396-1407.

ZOURELIDOU, M., DE TORRES-ZABALA, M., SMITH, C. & BEVAN, M. W. 2002. Storekeeper defines a new class of plant-specific DNA-binding proteins and is a putative regulator of patatin expression. *Plant Journal,* 30**,** 489-497.

9   APPENDIX

Table 9.1 Mean height of cassava plants and storage root mean weight of Pat:CAT plants. Asterisk (*) denotes significant differences at the 95% level using the Student's t-test. na= not applicable.

Cited in Chapter 3, page 60

Plant lines	Height (cm)	Height (SD)	t-test height	Weight (g)	Weight (SD)	t-test weight
Pat:CAT B2	70.3	5.3	0.81	60.8	7.6	0.07
Pat:CAT B3	66.1	4.5	0.68	56.0	6.6	0.69
Pat:CAT C1	62.3	3.7	0.18	51.5	8.9	0.63
Pat:CAT C2	73.0	4.9	0.25	55.2	5.0	0.91
Pat:CAT C3	68.1	4.1	0.29	54.3	5.3	0.52
Pat:CAT C4	69.3	9.5	0.91	50.5	5.7	0.88
Pat:CAT D1	73.4	6.9	0.21	40.0	8.9	0.46
Pat:CAT D3	77.1	9.8	0.08	21.1	5.3	0.03*
WT	67.3	6.7	na	51.3	14.1	na

Table 9.2 Mean height of cassava plants and storage root mean weight of Pat:GAR plants. Asterisk (*) denotes significant differences at the 95% level using the Student's t-test. na= not applicable.

Cited in Chapter 3, page 60

Plant lines	Height (cm)	Height (SD)	t-test height	Weight (g)	Weight (SD)	t-test weight
Pat:GAR A13	81.3	11.9	0.56	116.8	10.6	0.07
Pat:GAR A15	72.7	8.1	0.22	105.9	13.6	0.62
Pat:GAR B27	87.0	7.0	0.34	88.9	18.8	0.33
Pat:GAR B29	89.3	3.8	0.41	75.7	8.1	0.05*
Pat:GAR B33	82.7	13.6	0.79	62.1	13.1	0.02*
Pat:GAR C8	94.3	10.2	0.30	79.4	8.7	0.09
Pat:GAR C12	94.3	5.1	0.18	95.1	9.3	0.37
WT	84.7	4.0	na	100.0	4.0	na

Table 9.3 Mean height of cassava plants and storage root mean weight of Pat:GCS plants. Asterisk (*) denotes significant differences at the 95% level using the Student's t-test. na= not applicable.

Cited in Chapter 3, page 60

Plant lines	Height (cm)	Height (SD)	t-test height	Weight (g)	Weight (SD)	t-test weight
Pat:GCS C5	66.7	3.4	0.00*	66.5	12.6	0.05*
Pat:GCS C6	70.5	3.6	0.00*	56.2	10.4	0.00*
Pat:GCS C11	67.8	3.2	0.01*	69.6	8.4	0.07
Pat:GCS C12	54.3	9.1	0.02*	50.4	23.4	0.02*
Pat:GCS C13	60.3	5.5	0.26	60.0	12.1	0.00*
Pat:GCS C16	68.6	4.4	0.01*	61.7	13.1	0.01*
Pat:GCS C19	59.3	4.2	0.05*	54.0	11.0	0.00*
WT	62.7	3.8	na	81.3	16.6	na

Table 9.4 Mean height of cassava plants and storage root mean weight of Pat:Gus plants.

Cited in Chapter 3, page 60

Plant lines	Height (cm)	Height (SD)	t-test height	Weight (g)	Weight (SD)	t-test weight
Pat:Gus A4	67.7	2.3	0.71	86.9	7.8	0.26
Pat:Gus A6	66.0	3.0	0.46	85.1	18.2	0.30
Pat:Gus A15	68.0	3.5	0.86	95.5	7.3	0.35
Pat:Gus B1	70.5	6.4	0.66	104.3	5.6	0.74
Pat:Gus B2	72.5	2.1	0.16	83.2	2.1	0.29
Pat:Gus B4	77.0	3.0	0.62	119.8	11.8	0.73
WT	68.7	2.3	na	112.6	30.9	na

```
CTGCAGTTGTAGTTAATGCGTATTAGTTTTAGCGACGAAGCACTAAATCGTCTTTGTATACTTTGAGTGA
CACATGTTTAGTGACGACTGATTGACGAAATTTTTTTCGTCTCACAAAATTTTTAGTGACGAAACATGAT
TTATAGATGACGAAATTATTTGTCCCTCATAATCTAATTTGTTGTAGTGATCATTACTCCTTTGTTTGTT
TTATTTGTCATGTTAGTTCATTAAAAAAAAAATCTCTCTTCTTATCAATCCTGACGTGTTTAATATCATA
AGATTAAAAAATATTTTAATATATCTTTAATTTAAACTCACAAAGTTTAATTTTCTTCGTTAACTTAATT
TGTCAAATCAGGCTCAAAGATCGTTTTTCATATCGGAATGAGGATTTTATTTATTCTTTTAAAAATAAAG
AGGTGTTGAGCTAAACAATTTCAAATCTCATCACACATATGGGGTCAGCCACAAAAATAAAGAACGGTTG
GAACGGATCTATTATATAATACTAATAAAGAATAGAAAAAGGAAAGTGAGTGAGGTGCGAGGGAGAGAAT
CTGTTTAATATCAGAGTCGATCATGTGTCAGTTTTATCGATATGACTTTGACTTCAACTGAGTTTAAGCA
ATTCTGATAAGGCGAGGAAAATCACAGTGCTGAATCTAGAAAAATCTTATACAATGTGAGATAAATCTCA
ACAAAAACGTTGAGTCCATAGAGGGGGTGTATGTGACACCCCAACCTCAGCAAAAGAAAACCTCCCCTCA
AGAAGGACATTTGCGGTGCTAAACAATTTCAAGTCTCATCACACATATATATTATATAATACTAATAAAG
AATAGAAAAAGGAAAGGTAAACATCACTAATGACAGTTGCGGTGCAAAGTGAGTGAGATAATAAACATCA
GTAATAGACATCACTAACTTTTATTGGTTATGTCAAACTCAAAATAAAATTTCTCAACTTGTTTACGTGC
CTATATATACCATGCTTGTTATATGCCATGGTAGATCATCACAAGTTTGTACAAAAAAGCAGGCTCGGTC
ATGGATCCTTGCAAGTTCCGTCCATCAAGCTCAAACAATACCCCCTTCTGGACCACCGATGCTGGTGCTC
CAGTATGGAACAACAATTCCTCCATGACTGTTGGAACCAGAGGTCCAATCCTTTTGGAGGACTATCATAT
GATAGAGAAACTTGCCAACTTTACCAGAGAGAGGATTCCAGAGCGTGTCGTCCATGCTAGGGGAATGAGT
GCAAAGGGCTTCTTTGAAGTCACCCACGATGTCTCTCACCTTACTTGTGCTGATTTCCTTCGAGCCCCTG
GAGTTCAAACCCCTGTCATCGTCCGTTTCTCCACTGTTATCCACGAGCGTGGCAGCCCTGAAACACTCAG
GGATCCTCGAGGTTTTGCGACTAAGTTCTACACCAGAGAGGGCAACTTTGATATTGTGGGAAACAACTTC
CCTGTCTTCTTCATCCGTGATGGAATAAAATTCCCAGATGTGATACACGCTTTTAAGCCCAATCCCAAGT
CTCACATCCAAGAATACTGGAGGATCTTTGACTTCTTATCACACCATCCTGAGAGCTTGAGCACCTTCGC
CTGGTTCTTCGATGATGTTGGAATTCCCCAAGATTACAGACACATGGAAGGTTTCGGTGTTCACACCTTT
ACTTTCATCAACAAGGCTGGAAAAGTAACCTACGTGAAATTTCACTGGAAACCCACTTGCGGGGTCAAGT
GTTTGATGGATGATGAGGCACTTAAGATCGGAGGTGCCAACCACAGCCATGCTACGCAGGATTTATACGA
CTCCATTGCCGCTGGCAACTATCCTGAGTGGAGACTCTTCATCCAGACAATGGATCCAGCTGATGAAGAC
AAATTCGACTTTGATCCACTTGATATGACCAAGATCTGGCCTGAGGATATTTTTCCTCTACAGCAAATTG
GCCGTTTGGTCTTGAACAGGAACATCGATAACTGGTTTGCTGAGAATGAAATGCTCGCATTCGACCCTGG
TCATATTGTTCCTGGCATTCACTATTCAAACGACAAGTTGTTTCAGCTCAGAACCTTTGCATATGCTGAC
ACTCAGAGGCACCGTCTCGGACCCAACTATAAGATGCTCCCTGTTAATGCTCCCAAGTGTGCTTATCACA
ACAATCATTACGATGGTTTCATGAATTTCATGCACAGGGATGAGGAGGTGGATTACTTCCCATCCAGGTA
TGATCCAGTTCGCCATGCTGAGAGAAGCCCCATTCCTAACGCTATCTGTAGTGGAAGGCGTGAAAAGTGC
GTCATTGAAAAGGAGAACAATTTCAAGCAACCTGGAGAGAGATATCGATCCTGGGCACCTGATAGACAAG
AAAGATTCCTGTGCAGATTGGTTAACGCCTTATCAGAGCCACGTATCACCTTTGAGATTCGCAGTATCTG
GGTCTCTTACTGGTCTAAGTGCGACGCGTCTCTGGGTCAAAAGCTGGCTTCTCGTCTCAACGTGAGGCCA
AATATATGA
```

Figure 9.1 Pat:MecCAT1 sequence obtained from sequencing *Arabidopsis* Pat:CAT line (At3.8). The Patatin sequence is highlighted in turquoise, MecCAT1 is highlighted in grey. Sequence in red font and underlined indicates restriction site for *Pst*I and sequence in red font indicates restriction site for *Nco*I. The attB1 sequence is underlined, Kozak sequence which introduce for efficient gene translation is highlighted in yellow.

Cited in Chapter 5, page 124.

```
CTGCAGTTGTAGTTAATGCGTATTAGTTTTAGCGACGAAGCACTAAATCGTCTTTGTATACTTTGAGTGA
CACATGTTTAGTGACGACTGATTGACGAAATTTTTTTCGTCTCACAAAATTTTTAGTGACGAAACATGAT
TTATAGATGACGAAATTATTTGTCCCTCATAATCTAATTTGTTGTAGTGATCATTACTCCTTTGTTTGTT
TTATTTGTCATGTTAGTTCATTAAAAAAAAAATCTCTCTTCTTATCAATCCTGACGTGTTTAATATCATA
AGATTAAAAAATATTTTAATATATCTTTAATTTAAACTCACAAAGTTTAATTTTCTTCGTTAACTTAATT
TGTCAAATCAGGCTCAAAGATCGTTTTTCATATCGGAATGAGGATTTTATTTATTCTTTTAAAAATAAAG
AGGTGTTGAGCTAAACAATTTCAAATCTCATCACACATATGGGGTCAGCCACAAAAATAAAGAACGGTTG
GAACGGATCTATTATATAATACTAATAAAGAATAGAAAAAGGAAAGTGAGTGAGGTGCGAGGGAGAGAAT
CTGTTTAATATCAGAGTCGATCATGTGTCAGTTTTATCGATATGACTTTGACTTCAACTGAGTTTAAGCA
ATTCTGATAAGGCGAGGAAAATCACAGTGCTGAATCTAGAAAAATCTTATACAATGTGAGATAAATCTCA
ACAAAAACGTTGAGTCCATAGAGGGGGTGTATGTGACACCCCAACCTCAGCAAAAGAAAACCTCCCCTCA
AGAAGGACATTTGCGGTGCTAAACAATTTCAAGTCTCATCACACATATATATTATATAATACTAATAAAG
AATAGAAAAAGGAAAGGTAAACATCACTAATGACAGTTGCGGTGCAAAGTGAGTGAGATAATAAACATCA
GTAATAGACATCACTAACTTTTATTGGTTATGTCAAACTCAAAATAAAATTTCTCAACTTGTTTACGTGC
CTATATATACCATGCTTGTTATATGCCATGGTAGATCATCACAAGTTTGTACAAAAAAGCAGGCTCGACA
ATGGTGAAGGCCGTTGCTGTTCTTAACAGTAGTGAGGGTGTTGCTGGGACAATCTTCTTCACCCAAGAAG
GAGATGGTCCAACCACCGTCACTGGAAGTGTTTCTGGCCTTAAGCCAGGGCTTCATGGATTCCATGTTCA
TGCCCTTGGAGACACAACAAATGGTTGCATGTCAACTGGGCCACATTTCAACCCTGGTGGCAAAGAGCAT
GGTGCCCCTGAGGACGACATTCGTCATGCTGGTGATCTGGGAAATGTCACTGCTGGTGATGATGGCACTG
CTAGTTTCACAATCGTTGACAAGGATATTCCTCTTTCTGGTCCGCATTCCATTGTAGGAAGGGCAGTCGT
TGTTCACGCAGATCCTGATGATCTTGGAAAGGGGGGACATGAACTTAGCAAAACCACTGGAAATGCTGGT
GGCAGGGTAGCATGTGGTGTTATTGGTTTGCAAGGATAG
```

Figure 9.2 Pat:MecSOD2 sequence obtained from sequencing cassava Pat:SOD line. The Patatin sequence is highlighted in turquoise, MecSOD2 is highlighted in grey. Sequence in red font and underlined indicates restriction site for *Pst*I and sequence in red font indicates restriction site for *Nco*I. The attB1 sequence is underlined, Kozak sequence which introduce for efficient gene translation is highlighted in yellow.

Cited in Chapter 5, page 128.

```
CTGCAGTTGTAGTTAATGCGTATTAGTTTTAGCGACGAAGCACTAAATCGTCTTTGTATACTTTGAGTGA
CACATGTTTAGTGACGACTGATTGACGAAATTTTTTTCGTCTCACAAAATTTTTAGTGACGAAACATGAT
TTATAGATGACGAAATTATTTGTCCCTCATAATCTAATTTGTTGTAGTGATCATTACTCCTTTGTTTGTT
TTATTTGTCATGTTAGTTCATTAAAAAAAAAATCTCTCTTCTTATCAATCCTGACGTGTTTAATATCATA
AGATTAAAAAATATTTTAATATATCTTTAATTTAAACTCACAAAGTTTAATTTTCTTCGTTAACTTAATT
TGTCAAATCAGGCTCAAAGATCGTTTTTCATATCGGAATGAGGATTTTATTTATTCTTTTAAAAATAAAG
AGGTGTTGAGCTAAACAATTTCAAATCTCATCACACATATGGGGTCAGCCACAAAAATAAAGAACGGTTG
GAACGGATCTATTATATAATACTAATAAAGAATAGAAAAAGGAAAGTGAGTGAGGTGCGAGGGAGAGAAT
CTGTTTAATATCAGAGTCGATCATGTGTCAGTTTTATCGATATGACTTTGACTTCAACTGAGTTTAAGCA
ATTCTGATAAGGCGAGGAAAATCACAGTGCTGAATCTAGAAAAATCTTATACAATGTGAGATAAATCTCA
ACAAAAACGTTGAGTCCATAGAGGGGGTGTATGTGACACCCCAACCTCAGCAAAAGAAAACCTCCCCTCA
AGAAGGACATTTGCGGTGCTAAACAATTTCAAGTCTCATCACACATATATATTATATAATACTAATAAAG
AATAGAAAAAGGAAAGGTAAACATCACTAATGACAGTTGCGGTGCAAAGTGAGTGAGATAATAAACATCA
GTAATAGACATCACTAACTTTTATTGGTTATGTCAAACTCAAAATAAAATTTCTCAACTTGTTTACGTGC
CTATATATACCATGCTTGTTATATGCCATGGTAGATCATCACAAGTTTGTACAAAAAAGCAGGCTACACC
ATGGCAAAGGTTCCTTCAGTAACCCTCAGCTCCTGCGGTGATGACATCCAGACCATGCCTGTAATCGGCA
TGGGAACTTCATCGTACCCTCGGGCCGACCCTGAAACCGCCAAGGCTGCTATTCTCGAAGCAATTAGAGC
TGGTTACCGACATTTCGACACCGCCGCTGCTTACGGCTCGGAGAAAGATCTCGGTGAAGCCATAGCCGAG
GCTCTCCGTCTCCAACTCATCAAGTCTAGGGACGAGCTCTTCATCACAACCAAACTTTGGGCCAGTTTCG
CCGAGAAAGACCTTGTGCTGCCCTCCATCAAAGCCAGTTTAAGCAATCTTCAAGTAGAATACATTGACAT
GTACATCATACACTGGCCATTCAAATTGGGAAAAGAGGTGAGAACCATGCCTGTTGAGAGAGATCTGGTG
CAGCCCCTTGATATCAAATCTGTTTGGGAAGCCATGGAAGAGTGCAAGAAACTTGGGCTTGCTAGAGGTA
TTGGTGTCAGTAACTTCACTAGCAGCATGCTTGAGGAGCTTCTTTCCTTCGCCGAAATCCCTCCGGCCGT
AAACCAATTGGAGATGAACCCAGCTTGGCAGCTGAAGAAATTGAGGGACTTCTGCAAGGCAAAGGGAATT
CATGTCACGGCTTACTCTCCGCTCGGAGCAGCTAGGACTAAATGGGGTGACGATAGGGTTTTGGGATCAG
ATATCATCGAAGAGATTGCCCAAGCCAAAGGAAAATCAACTGCTCAGATATCATTGAGATGGGTGTACGA
ACAAGGTGTGAGCATAGTAACAAAAAGTTACAACAAAGAAAGAATGAGGCAGAACCTTGACATCTTCGAC
TTCTGCTTGACCGAGGAGGAACTGGAGAAGATGAGTCATCTTCCACAGCGGAAAGGGGTTACCTTTGCTT
CAATTCTAGGACCCCATGATATTGTTCTGGAAGTTGACGAAGAATTATGA
```

Figure 9.3 Pat:FaGAR sequence obtained from sequencing cassava Pat:GAR line. The Patatin sequence is highlighted in turquoise, FaGAR is highlighted in grey. Sequence in red font and underlined indicates restriction site for *Pst*I and sequence in red font indicates restriction site for *Nco*I. The attB1 sequence is underlined, Kozak sequence which introduce for efficient gene translation is highlighted in yellow.

Cited in Chapter 5, page 128.

```
CTGCAGTTGTAGTTAATGCGTATTAGTTTTAGCGACGAAGCACTAAATCGTCTTTGTATACTTTGAGTGA
CACATGTTTAGTGACGACTGATTGACGAAATTTTTTTCGTCTCACAAAATTTTTAGTGACGAAACATGAT
TTATAGATGACGAAATTATTTGTCCCTCATAATCTAATTTGTTGTAGTGATCATTACTCCTTTGTTTGTT
TTATTTGTCATGTTAGTTCATTAAAAAAAAAATCTCTCTTCTTATCAATCCTGACGTGTTTAATATCATA
AGATTAAAAAATATTTTAATATATCTTTAATTTAAACTCACAAAGTTTAATTTTCTTCGTTAACTTAATT
TGTCAAATCAGGCTCAAAGATCGTTTTTCATATCGGAATGAGGATTTTATTTATTCTTTTAAAAATAAAG
AGGTGTTGAGCTAAACAATTTCAAATCTCATCACACATATGGGGTCAGCCACAAAAATAAAGAACGGTTG
GAACGGATCTATTATATAATACTAATAAAGAATAGAAAAAGGAAAGTGAGTGAGGTGCGAGGGAGAGAAT
CTGTTTAATATCAGAGTCGATCATGTGTCAGTTTTATCGATATGACTTTGACTTCAACTGAGTTTAAGCA
ATTCTGATAAGGCGAGGAAAATCACAGTGCTGAATCTAGAAAAATCTTATACAATGTGAGATAAATCTCA
ACAAAAACGTTGAGTCCATAGAGGGGGTGTATGTGACACCCCAACCTCAGCAAAAGAAAACCTCCCCTCA
AGAAGGACATTTGCGGTGCTAAACAATTTCAAGTCTCATCACACATATATATTATATAATACTAATAAAG
AATAGAAAAAGGAAAGGTAAACATCACTAATGACAGTTGCGGTGCAAAGTGAGTGAGATAATAAACATCA
GTAATAGACATCACTAACTTTTATTGGTTATGTCAAACTCAAAATAAAATTTCTCAACTTGTTTACGTGC
CTATATATACCATGCTTGTTATATGCCATGGTAGATCATCACAAGTTTGTACAAAAAAGCAGGCTCTACC
ATGGCGCTCTTGTCTCAAGCAGGAGGATCATACACTGTTGTTCCTTCTGGAGTTTGTTCAAAGGCTGGAA
CTAAAGCTGTTGTTTCGGGTGGCGTGAGGAATTTGGATGTTTTGAGGATGAAAGAAGCTTTTGGTAGCTC
CTACTCTAGGAGTCTATCTACCAAATCAATGCTTCTCCATTCTGTTAAGAGGAGTAAGAGAGGGCATCAA
TTGATTGTTGCGGCAAGTCCTCCAACGGAAGAGGCTGTAGTTGCAACTGAGCCGTTGACGAGAGAGGATC
TCATTGCCTATCTTGCCTCTGGATGCAAAACAAAGGACAAATATAGAATAGGTACAGAACATGAGAAATT
TGGTTTTGAGGTCAATACTTTGCGCCCTATGAAGTATGATCAAATAGCCGAGCTTCTTAATGGTATCGCT
GAAAGATTTGAATGGGAAAAAGTAATGGAAGGTGACAAGATCATTGGTCTGAAGCAGGGAAAGCAAAGCA
TTTCACTTGAACCTGGGGGTCAGTTCGAGCTTAGTGGTGCACCTCTTGAGACTTTGCATCAAACTTGTGC
TGAAGTCAATTCACATCTTTATCAGGTAAAAGCAGTTGCTGAGGAAATGGGAATTGGTTTCTTAGGAATT
GGCTTCCAGCCCAAATGGCGTCGGGAGGATATACCCATCATGCCAAAGGGGAGATACGACATTATGAGAA
ACTACATGCCGAAAGTTGGTACCCTTGGTCTTGATATGATGCTCCGAACGTGTACTGTTCAGGTTAATCT
GGATTTTAGCTCAGAAGCTGATATGATCAGGAAGTTTCGTGCTGGTCTTGCTTTACAACCTATAGCAACG
GCTCTATTTGCGAATTCCCCTTTTACAGAAGGAAAGCCAAACGGATTTCTCAGCATGAGAAGCCACATAT
GGACAGACACTGACAAGGACCGCACAGGAATGCTACCATTTGTTTTCGATGACTCTTTTGGGTTTGAGCA
GTATGTTGACTACGCACTCGATGTCCCTATGTACTTTGCCTACAGAAAGAACAAATACATCGACTGTACT
GGAATGACATTTCGGCAATTCTTGGCTGGAAAACTTCCCTGTCTCCCTGGTGAACTGCCTTCATATAATG
ATTGGGAAAACCATCTGACAACAATATTCCCAGAGGTTCGGTTGAAGAGATACTTGGAGATGAGAGGTGC
TGATGGAGGTCCCTGGAGGAGGCTGTGTGCCCTGCCAGCTTTCTGGGTGGGTTTATTATATGATGATGAT
AGTCTCCAAGCTATCCTGGATCTGACAGCTGACTGGACTCCAGCAGAGAGAGAGATGCTAAGGAACAAAG
TCCCAGTTACTGGCTTAAAGACTCCTTTTAGGGATGGTTTGTTAAAGCATGTCGCTGAAGATGTCCTGAA
ACTCGCAAAGGATGGTTTAGAGCGCAGAGGCTACAAGGAAGCCGGTTTCTTGAACGCAGTCGATGAAGTG
GTCAGAACAGGAGTTACGCCTGCGGAGAAGCTCTTGGAGATGTACAATGGAGAATGGGGACAAAGCGTAG
ATCCCGTGTTCGAAGAGCTGCTGTACTAA
```

Figure 9.4 Pat:*gsh*I sequence obtained from sequencing cassava Pat:GCS line. The Patatin sequence is highlighted in turquoise, *gsh*I is highlighted in grey. Sequence in red font and underlined indicates restriction site for *Pst*I and sequence in red font indicates restriction site for *Nco*I. The attB1 sequence is underlined, Kozak sequence which introduce for efficient gene translation is highlighted in yellow.

Cited in Chapter 5, page 128.

```
CTGCAGTTGTAGTTAATGCGTATTAGTTTTAGCGACGAAGCACTAAATCGTCTTTGTATACTTTGAGTGA
CACATGTTTAGTGACGACTGATTGACGAAATTTTTTTCGTCTCACAAAATTTTTAGTGACGAAACATGAT
TTATAGATGACGAAATTATTTGTCCCTCATAATCTAATTTGTTGTAGTGATCATTACTCCTTTGTTTGTT
TTATTTGTCATGTTAGTTCATTAAAAAAAAAATCTCTCTTCTTATCAATCCTGACGTGTTTAATATCATA
AGATTAAAAAATATTTTAATATATCTTTAATTTAAACTCACAAAGTTTAATTTTCTTCGTTAACTTAATT
TGTCAAATCAGGCTCAAAGATCGTTTTTCATATCGGAATGAGGATTTTATTTATTCTTTTAAAAATAAAG
AGGTGTTGAGCTAAACAATTTCAAATCTCATCACACATATGGGGTCAGCCACAAAAATAAAGAACGGTTG
GAACGGATCTATTATATAATACTAATAAAGAATAGAAAAAGGAAAGTGAGTGAGGTGCGAGGGAGAGAAT
CTGTTTAATATCAGAGTCGATCATGTGTCAGTTTTATCGATATGACTTTGACTTCAACTGAGTTTAAGCA
ATTCTGATAAGGCGAGGAAAATCACAGTGCTGAATCTAGAAAAATCTTATACAATGTGAGATAAATCTCA
ACAAAAACGTTGAGTCCATAGAGGGGGTGTATGTGACACCCCAACCTCAGCAAAAGAAAACCTCCCCTCA
AGAAGGACATTTGCGGTGCTAAACAATTTCAAGTCTCATCACACATATATATTATATAATACTAATAAAG
AATAGAAAAAGGAAAGGTAAACATCACTAATGACAGTTGCGGTGCAAAGTGAGTGAGATAATAAACATCA
GTAATAGACATCACTAACTTTTATTGGTTATGTCAAACTCAAAATAAAATTTCTCAACTTGTTTACGTGC
CTATATATACCATGCTTGTTATATGCCATGGTAGATCATCACAAGTTTGTACAAAAAAGCAGGCTCAAAA
ATGCCGAAGAACTACCCAAAAGTTAGTGAAGAGTACCAGAAAGCCATTGATAAGGCCAGGAGGAAGCTCA
GAGGTTTCATCGCTGAGAAAGGCTGCGCTCCTCTCATGCTCCGTATCGCATGGCACTCAGCTGGAACTTA
CGACGTGAAGACGAACACTGGAGGTCCTTTTGGAACCATGAGGCACGCAGCGGAGCAGGGTCATGCTGCT
AACAATGGGTTAGATATTGCTGTTAGACTCCTTGAGCCCATCAAGGAGCAGTTCCCTATCCTCTCCTACG
CCGACTTCTATCAGCTCGCTGGTGTTGTTGCCGTTGAGATCACTGGTGGGCCTGATATCCCATTCCACCC
AGGAAGAGAGGACAAGCCTGAACCGCCTCCAGAAGGTCGTCTCCCTAATGCTACTAAAGGTGCTGATCAC
TTGAGAGAGGTCTTTGGGAAAACCATGGGTCTCACCGACAAGGATATTGTTGTCCTTTCTGGTGGCCACA
CCTTGGGAAGGTGCCACAAGGAACGCTCTGGTTTTGAAGGTCCCTGGACTCCTAATCCTCTCATCTTTGA
CAATTCCTTCTTCCAGGTGCTCTTGGACGAACCGACAGAAGATCTTCTACAATTGCCGACTGACAGTGTT
CTTGTCACGGATCCTGTCTTCCGCCCATATGTTGAAAAATATGCTGCTGATGAAGAGGCATTCTTTGCTG
ATTATGCTGAGTCCCATATGAAGCTCTCTGAGCTCGGATTTGCTGAGGCGTAA
```

Figure 9.5 Pat:MecAPX3 sequence obtained from sequencing cassava Pat:APX line. The Patatin sequence is highlighted in turquoise, MecAPX3 highlighted in grey. Sequence in red font and underlined indicates restriction site for *Pst*I and sequence in red font indicates restriction site for *Nco*I. The attB1 sequence is underlined, Kozak sequence which introduce for efficient gene translation is highlighted in yellow.

Cited in Chapter 5, page 128.

CCATGGTAGATCATCACAAGTTTGTACAAAAAAGCAGGCT**CG**ATGGTAGATCTGAGGGTAAATTTCTAGT
TTTTCTCCTTCATTTTCTTGGTTAGGACCCTTTTCTCTTTTTATTTTTTTGAGCTTTGATCTTTCTTTAA
ACTGATCTATTTTTTAATTGATTGGTTATGGTGTAAATATTACATAGCTTTAACTGATAATCTGATTACT
TTATTTCGTGTGTCTATGATGATGATGATAGTTACAGAACCGACGAACTAGTCTGTACCCGATCAACACC
GAGACCCGTGGCGTCTTCGACCTCAATGGCGTCTGGAACTTCAAGCTGGACTACGGGAAAGGACTGGAAG
AGAAGTGGTACGAAAGCAAGCTGACCGACACTATTAGTATGGCCGTCCCAAGCAGTTACAATGACATTGG
CGTGACCAAGGAAATCCGCAACCATATCGGATATGTCTGGTACGAACGTGAGTTCACGGTGCCGGCCTAT
CTGAAGGATCAGCGTATCGTGCTCCGCTTCGGCTCTGCAACTCACAAAGCAATTGTCTATGTCAATGGTG
AGCTGGTCGTGGAGCACAAGGGCGGATTCCTGCCATTCGAAGCGGAAATCAACAACTCGCTGCGTGATGG
CATGAATCGCGTCACCGTCGCCGTGGACAACATCCTCGACGATAGCACCCTCCCGGTGGGGCTGTACAGC
GAGCGCCACGAAGAGGGCCTCGGAAAAGTCATTCGTAACAAGCCGAACTTCGACTTCTTCAACTATGCAG
GCCTGCACCGTCCGGTGAAAATCTACACGACCCCGTTTACGTACGTCGAGGACATCTCGGTTGTGACCGA
CTTCAATGGCCCAACCGGGACTGTGACCTATACGGTGGACTTTCAAGGCAAAGCCGAGACCGTGAAAGTG
TCGGTCGTGGATGAGGAAGGCAAAGTGGTCGCAAGCACCGAGGGCCTGAGCGGTAACGTGGAGATTCCGA
ATGTCATCCTCTGGGAACCACTGAACACGTATCTCTACCAGATCAAAGTGGAACTGGTGAACGACGGACT
GACCATCGATGTCTATGAAGAGCCGTTCGGCGTGCGGACCGTGGAAGTCAACGACGGCAAGTTCCTCATC
AACAACAAACCGTTCTACTTCAAGGGCTTTGGCAAACATGAGGACACTCCTATCAACGGCCGTGGCTTTA
ACGAAGCGAGCAATGTGATGGATTTCAATATCCTCAAATGGATCGGCGCCAACAGCTTCCGGACCGCACA
CTATCCGTACTCTGAAGAGTTGATGCGTCTTGCGGATCGCGAGGGTCTGGTCGTGATCGACGAGACTCCG
GCAGTTGGCGTGCACCTCAACTTCATGGCCACCACGGGACTCGGCGAAGGCAGCGAGCGCGTCAGTACCT
GGGAGAAGATTCGGACGTTTGAGCACCATCAAGACGTTCTCCGTGAACTGGTGTCTCGTGACAAGAACCA
TCCAAGCGTCGTGATGTGGAGCATCGCCAACGAGGCGGCGACTGAGGAAGAGGGCGCGTACGAGTACTTC
AAGCCGTTGGTGGAGCTGACCAAGGAACTCGACCCACAGAAGCGTCCGGTCACGATCGTGCTGTTTGTGA
TGGCTACCCCGGAGACGGACAAAGTCGCCGAACTGATTGACGTCATCGCGCTCAATCGCTATAACGGATG
GTACTTCGATGGCGGTGATCTCGAAGCGGCCAAAGTCCATCTCCGCCAGGAATTTCACGCGTGGAACAAG
CGTTGCCCAGGAAAGCCGATCATGATCACTGAGTACGGCGCAGACACCGTTGCGGGCTTTCACGACATTG
ATCCAGTGATGTTCACCGAGGAATATCAAGTCGAGTACTACCAGGCGAACCACGTCGTGTTCGATGAGTT
TGAGAACTTCGTGGGTGAGCAAGCGTGGAACTTCGCGGACTTCGCGACCTCTCAGGGCGTGATGCGCGTC
CAAGGAAACAAGAAGGGCGTGTTCACTCGTGACCGCAAGCCGAAGCTCGCCGCGCACGTCTTTCGCGAGC
GCTGGACCAACATTCCAGATTTCGGCTACAAGAACGCTAGCCATCACCATCACCATCACGTGTGA

Figure 9.6 Pat(-):*GusPlus* sequence obtained from sequencing cassava Pat(-):Gus line. The *GusPlus* is highlighted in grey. Sequence in red font indicates restriction site for *Nco*I. The attB1 sequence is underlined, Kozak sequence which introduce for efficient gene translation is highlighted in yellow.

Cited in Chapter 5, page 129.

CTGCAGTTGTAGTTAATGCGTATTAGTTTTAGCGACGAAGCACTAAATCGTCTTTGTATACTTTGAGTGA
CACATGTTTAGTGACGACTGATTGACGAAATTTTTTTCGTCTCACAAAATTTTTAGTGACGAAACATGAT
TTATAGATGACGAAATTATTTGTCCCTCATAATCTAATTTGTTGTAGTGATCATTACTCCTTTGTTTGTT
TTATTTGTCATGTTAGTTCATTAAAAAAAAAATCTCTCTTCTTATCAATCCTGACGTGTTTAATATCATA
AGATTAAAAAATATTTTAATATATCTTTAATTTAAACTCACAAAGTTTAATTTTCTTCGTTAACTTAATT
TGTCAAATCAGGCTCAAAGATCGTTTTTCATATCGGAATGAGGATTTTATTTATTCTTTTAAAAATAAAG
AGGTGTTGAGCTAAACAATTTCAAATCTCATCACACATATGGGGTCAGCCACAAAAATAAAGAACGGTTG
GAACGGATCTATTATATAATACTAATAAAGAATAGAAAAAGGAAAGTGAGTGAGGTGCGAGGGAGAGAAT
CTGTTTAATATCAGAGTCGATCATGTGTCAGTTTTATCGATATGACTTTGACTTCAACTGAGTTTAAGCA
ATTCTGATAAGGCGAGGAAAATCACAGTGCTGAATCTAGAAAAATCTTATACAATGTGAGATAAATCTCA
ACAAAAACGTTGAGTCCATAGAGGGGGTGTATGTGACACCCCAACCTCAGCAAAAGAAAACCTCCCCTCA
AGAAGGACATTTGCGGTGCTAAACAATTTCAAGTCTCATCACACATATATATTATATAATACTAATAAAG
AATAGAAAAAGGAAAGGTAAACATCACTAATGACAGTTGCGGTGCAAAGTGAGTGAGATAATAAACATCA
GTAATAGACATCACTAACTTTTATTGGTTATGTCAAACTCAAAATAAAATTTCTCAACTTGTTTACGTGC
CTATATATACCATGCTTGTTATATGCCATGGTAGATCATCACAAGTTTGTACAAAAAAGCAGGCTCGATG
GTAGATCTGAGGGTAAATTTCTAGTTTTTCTCCTTCATTTTCTTGGTTAGGACCCTTTTCTCTTTTTATT
TTTTTGAGCTTTGATCTTTCTTTAAACTGATCTATTTTTTAATTGATTGGTTATGGTGTAAATATTACAT
AGCTTTAACTGATAATCTGATTACTTTATTTCGTGTGTCTATGATGATGATGATAGTTACAGAACCGACG
AACTAGTCTGTACCCGATCAACACCGAGACCCGTGGCGTCTTCGACCTCAATGGCGTCTGGAACTTCAAG
CTGGACTACGGGAAAGGACTGGAAGAGAAGTGGTACGAAGCAAGCTGACCGACACTATTAGTATGGCCG
TCCCAAGCAGTTACAATGACATTGGCGTGACCAAGGAAATCCGCAACCATATCGGATATGTCTGGTACGA
ACGTGAGTTCACGGTGCCGGCCTATCTGAAGGATCAGCGTATCGTGCTCCGCTTCGGCTCTGCAACTCAC
AAAGCAATTGTCTATGTCAATGGTGAGCTGGTCGTGGAGCACAAGGGCGGATTCCTGCCATTCGAAGCGG
AAATCAACAACTCGCTGCGTGATGGCATGAATCGCGTCACCGTCGCCGTGGACAACATCCTCGACGATAG
CACCCTCCCGGTGGGGCTGTACAGCGAGCGCCACGAAGAGGGCCTCGGAAAAGTCATTCGTAACAAGCCG
AACTTCGACTTCTTCAACTATGCAGGCCTGCACCGTCCGGTGAAAATCTACACGACCCCGTTTACGTACG
TCGAGGACATCTCGGTTGTGACCGACTTCAATGGCCCAACCGGGACTGTGACCTATACGGTGGACTTTCA
AGGCAAAGCCGAGACCGTGAAAGTGTCGGTCGTGGATGAGGAAGGCAAAGTGGTCGCAAGCACCGAGGGC
CTGAGCGGTAACGTGGAGATTCCGAATGTCATCCTCTGGGAACCACTGAACACGTATCTCTACCAGATCA
AAGTGGAACTGGTGAACGACGGACTGACCATCGATGTCTATGAAGAGCCGTTCGGCGTGCGGACCGTGGA
AGTCAACGACGGCAAGTTCCTCATCAACAACAAACCGTTCTACTTCAAGGGCTTTGGCAAACATGAGGAC
ACTCCTATCAACGGCCGTGGCTTTAACGAAGCGAGCAATGTGATGGATTTCAATATCCTCAAATGGATCG
GCGCCAACAGCTTCCGGACCGCACACTATCCGTACTCTGAAGAGTTGATGCGTCTTGCGGATCGCGAGGG
TCTGGTCGTGATCGACGAGACTCCGGCAGTTGGCGTGCACCTCAACTTCATGGCCACCACGGGACTCGGC
GAAGGCAGCGAGCGCGTCAGTACCTGGGAGAAGATTCGGACGTTTGAGCACCATCAAGACGTTCTCCGTG
AACTGGTGTCTCGTGACAAGAACCATCCAAGCGTCGTGATGTGGAGCATCGCCAACGAGGCGGCGACTGA
GGAAGAGGGCGCGTACGAGTACTTCAAGCCGTTGGTGGAGCTGACCAAGGAACTCGACCCACAGAAGCGT
CCGGTCACGATCGTGCTGTTTGTGATGGCTACCCCGGAGACGGACAAAGTCGCCGAACTGATTGACGTCA
TCGCGCTCAATCGCTATAACGGATGGTACTTCGATGGCGGTGATCTCGAAGCGGCCAAAGTCCATCTCCG
CCAGGAATTTCACGCGTGGAACAAGCGTTGCCCAGGAAAGCCGATCATGATCACTGAGTACGGCGCAGAC
ACCGTTGCGGGCTTTCACGACATTGATCCAGTGATGTTCACCGAGGAATATCAAGTCGAGTACTACCAGG
CGAACCACGTCGTGTTCGATGAGTTTGAGAACTTCGTGGGTGAGCAAGCGTGGAACTTCGCGGACTTCGC
GACCTCTCAGGGCGTGATGCGCGTCCAAGGAAACAAGAAGGGCGTGTTCACTCGTGACCGCAAGCCGAAG
CTCGCCGCGCACGTCTTTCGCGAGCGCTGGACCAACATTCCAGATTTCGGCTACAAGAACGCTAGCCATC
ACCATCACCATCACGTGTGA

Figure 9.7 Pat:*GusPlus* sequence obtained from sequencing *Arabidopsis* Pat:*GusPlus* line. The Patatin sequence is highlighted in turquoise, *GusPlus* is highlighted in grey. Sequence in red font and underlined indicates restriction site for *Pst*I and sequence in red font indicates restriction site for *Nco*I*.* The attB1 sequence is underlined, Kozak sequence which introduce for efficient gene translation is highlighted in yellow.

Cited in Chapter 5, page 130.